Automatic Forward Modelling Of Two-Dimensional Problems In Electromagnetic Induction

by
Helena E. Poll
B.Sc., University of Guelph, 1985
M.Sc., University of Victoria, 1987

A Dissertation Submitted in Partial Fulfillment of the Requirements for the Degree of
DOCTOR OF PHILOSOPHY
in the Department of Physics and Astronomy

We accept this dissertation as conforming to the required standard

---

Dr. J.T. Weaver, Supervisor (Department of Physics and Astronomy)

Dr. H.W. Dosso, Departmental Member (Department of Physics and Astronomy)

Dr. R.E. Horita, Departmental Member (Department of Physics and Astronomy)

Dr. E. van der Flier-Keller, Outside Member (Department of Earth and Ocean Sciences)

Dr. A. Zielinski, Outside Member (Department of Electrical and Computer Engineering)

Dr. T.W. Dawson, External Examiner (Defence Research Establishment Pacific)

Name Helena L. Fall

Dissertation Abstracts International is arranged by broad, general subject categories. Please select the one subject which most nearly describes the content of your dissertation. Enter the corresponding four-digit code in the spaces provided.

(Geophysics)
SUBJECT TERM

0373
SUBJECT CODE

U·M·I

Subject Categories

THE HUMANITIES AND SOCIAL SCIENCES

COMMUNICATIONS AND THE ARTS
Architecture 0729
Art History 0377
Cinema 0900
Dance 0378
Fine Arts 0357
Information Science 0723
Journalism 0391
Library Science 0399
Mass Communications 0708
Music 0413
Speech Communication 0459
Theater 0465

EDUCATION
General 0515
Administration 0514
Adult and Continuing 0516
Agricultural 0517
Art 0273
Bilingual and Multicultural 0282
Business 0688
Community College 0275
Curriculum and Instruction 0727
Early Childhood 0518
Elementary 0524
Finance 0277
Guidance and Counseling 0519
Health 0680
Higher 0745
History of 0520
Home Economics 0278
Industrial 0521
Language and Literature 0279
Mathematics 0280
Music 0522
Philosophy of 0998
Physical 0523
Psychology 0525
Reading 0535
Religious 0527
Sciences 0714
Secondary 0533
Social Sciences 0534
Sociology of 0340
Special 0529
Teacher Training 0530
Technology 0710
Tests and Measurements 0288
Vocational 0747

LANGUAGE, LITERATURE AND LINGUISTICS
Language
- General 0679
- Ancient 0289
- Linguistics 0290
- Modern 0291

Literature
- General 0401
- Classical 0294
- Comparative 0295
- Medieval 0297
- Modern 0298
- African 0316
- American 0591
- Asian 0305
- Canadian (English) 0352
- Canadian (French) 0355
- English 0593
- Germanic 0311
- Latin American 0312
- Middle Eastern 0315
- Romance 0313
- Slavic and East European 0314

PHILOSOPHY, RELIGION AND THEOLOGY
Philosophy 0422
Religion
- General 0318
- Biblical Studies 0321
- Clergy 0319
- History of 0320
- Philosophy of 0322
- Theology 0469

SOCIAL SCIENCES
American Studies 0323
Anthropology
- Archaeology 0324
- Cultural 0326
- Physical 0327

Business Administration
- General 0310
- Accounting 0272
- Banking 0770
- Management 0454
- Marketing 0338

Canadian Studies 0385
Economics
- General 0501
- Agricultural 0503
- Commerce Business 0505
- Finance 0508
- History 0509
- Labor 0510
- Theory 0511

Folklore 0358
Geography 0366
Gerontology 0351
History
- General 0578
- Ancient 0579
- Medieval 0581
- Modern 0582
- Black 0328
- African 0331
- Asia, Australia and Oceania 0332
- Canadian 0334
- European 0335
- Latin American 0336
- Middle Eastern 0333
- United States 0337

History of Science 0585
Law 0398
Political Science
- General 0615
- International Law and Relations 0616
- Public Administration 0617

Recreation 0814
Social Work 0452
Sociology
- General 0626
- Criminology and Penology 0627
- Demography 0938
- Ethnic and Racial Studies 0631
- Individual and Family Studies 0628
- Industrial and Labor Relations 0629
- Public and Social Welfare 0630
- Social Structure and Development 0700
- Theory and Methods 0344

Transportation 0709
Urban and Regional Planning 0999
Women's Studies 0453

THE SCIENCES AND ENGINEERING

BIOLOGICAL SCIENCES
Agriculture
- General 0473
- Agronomy 0285
- Animal Culture and Nutrition 0475
- Animal Pathology 0476
- Food Science and Technology 0359
- Forestry and Wildlife 0478
- Plant Culture 0479
- Plant Pathology 0480
- Plant Physiology 0817
- Range Management 0777
- Wood Technology 0746

Biology
- General 0306
- Anatomy 0287
- Biostatistics 0308
- Botany 0309
- Cell 0379
- Ecology 0329
- Entomology 0353
- Genetics 0369
- Limnology 0793
- Microbiology 0410
- Molecular 0307
- Neuroscience 0317
- Oceanography 0416
- Physiology 0433
- Radiation 0821
- Veterinary Science 0778
- Zoology 0472

Biophysics
- General 0786
- Medical 0760

EARTH SCIENCES
Biogeochemistry 0425
Geochemistry 0996
Geodesy 0370
Geology 0372
Geophysics 0373
Hydrology 0388
Mineralogy 0411
Paleobotany 0345
Paleoecology 0426
Paleontology 0418
Paleozoology 0985
Palynology 0427
Physical Geography 0368
Physical Oceanography 0415

HEALTH AND ENVIRONMENTAL SCIENCES
Environmental Sciences 0768
Health Sciences
- General 0566
- Audiology 0300
- Chemotherapy 0992
- Dentistry 0567
- Education 0350
- Hospital Management 0769
- Human Development 0758
- Immunology 0982
- Medicine and Surgery 0564
- Mental Health 0347
- Nursing 0569
- Nutrition 0570
- Obstetrics and Gynecology 0380
- Occupational Health and Therapy 0354
- Ophthalmology 0381
- Pathology 0571
- Pharmacology 0419
- Pharmacy 0572
- Physical Therapy 0382
- Public Health 0573
- Radiology 0574
- Recreation 0575
- Speech Pathology 0460
- Toxicology 0383

Home Economics 0386

PHYSICAL SCIENCES
Pure Sciences
Chemistry
- General 0485
- Agricultural 0749
- Analytical 0486
- Biochemistry 0487
- Inorganic 0488
- Nuclear 0738
- Organic 0490
- Pharmaceutical 0491
- Physical 0494
- Polymer 0495
- Radiation 0754

Mathematics 0405
Physics
- General 0605
- Acoustics 0986
- Astronomy and Astrophysics 0606
- Atmospheric Science 0608
- Atomic 0748
- Electronics and Electricity 0607
- Elementary Particles and High Energy 0798
- Fluid and Plasma 0759
- Molecular 0609
- Nuclear 0610
- Optics 0752
- Radiation 0756
- Solid State 0611

Statistics 0463

Applied Sciences
Applied Mechanics 0346
Computer Science 0984

Engineering
- General 0537
- Aerospace 0538
- Agricultural 0539
- Automotive 0540
- Biomedical 0541
- Chemical 0542
- Civil 0543
- Electronics and Electrical 0544
- Heat and Thermodynamics 0348
- Hydraulic 0545
- Industrial 0546
- Marine 0547
- Materials Science 0794
- Mechanical 0548
- Metallurgy 0743
- Mining 0551
- Nuclear 0552
- Packaging 0549
- Petroleum 0765
- Sanitary and Municipal 0554
- System Science 0790

Geotechnology 0428
Operations Research 0796
Plastics Technology 0795
Textile Technology 0994

PSYCHOLOGY
General 0621
Behavioral 0384
Clinical 0622
Developmental 0620
Experimental 0623
Industrial 0624
Personality 0625
Physiological 0989
Psychobiology 0349
Psychometrics 0632
Social 0451

ABSTRACT

A finite difference algorithm for solving the forward modelling problem of geoelectromagnetic induction in two-dimensional (2D) structures has been developed in this thesis. The governing equations have been modified to solve for the anomalous field by separating out the 'host' field which is assumed to be the field generated by the one-dimensional (1D) conductivity distribution on the left hand side of the model. This was done to prevent the small anomalous fields being masked by the much larger host field due to the finite length of the computer word. One of the most important features of this program is an automatic gridding subroutine which greatly reduces the amount of time required to design a suitable grid for a model and removes the human element from such grid design. Up to 20 periods can be submitted to the model at one time and specific locations (e.g. the locations at which field data are available) can be added to the automatically generated grid. Integral boundary conditions at the surface and bottom ($z = d$) of the model eliminate the need to extend the grid above the earth's surface or down into the half-space underlying the model.

The program has been used to perform a 2D inversion of magnetotelluric data from a NS profile in Sardinia. The magnetotelluric responses from two sites along this profile indicated that the structure underneath them could not be considered to be solely 2D. To examine the conductivity anomalies perpendicular to the profile

that are affecting the results at these two sites, 2D inversions were performed on the data to obtain their EW conductivity models. The apparent resistivity curves from the models fit the data fairly well at both sites especially at short periods. Many features of the models were in agreement with the 2D model along the profile obtained by Peruzza et al. (1990) and they also provided insight into the geological structure of the area.

A study was made of the behaviour of 2D induction arrows over a buried conductivity contrast. Although the general trend of in-phase arrows is to point towards the regions of high electrical conductivity, some investigators have found small amplitude in-phase arrows that point away from these same regions. Reversals such as these, which do not behave according to the general trend, can cause confusion and erroneous interpretation of the in-phase induction arrows. Using a model with two semi-infinite conducting plates, one at the surface and one buried at a depth d in a layered half space, it was found that the period at which a reversal in the in-phase induction arrow direction occurs was a function of the apparent resistivity of the layered host. Anomalous behaviour was found in the short period in-phase arrows from which the coast effect had been removed. The problems in interpretation of such arrows was discussed.

Finally a 2D inversion scheme was discussed in which a 2D forward modelling program was incorporated with a minimization routine MINDEF. First an investigation was made into the relative merits of using the impedances Z_{TE}, Z_{TM}, Z_{ave} and Z_{eff} to calculate the 1D inversions that are combined to form starting models

for the 2D inversions. A subsequent 2D inversion of the North American Central Plains (NACP) anomaly results in a best fit model whose responses show good agreement with the field data from 20 sites. Tests have been performed to ensure that an oversimplification of the starting model is not responsible for the lack of certain features found by other authors. It is concluded that the incorporation of these features in the model is not required in order to obtain a good fit to the field data.

Examiners:

Dr. J.T. Weaver, Supervisor (Department of Physics and Astronomy)

Dr. H.W. Dosso, Departmental Member (Department of Physics and Astronomy)

Dr. R.E. Horita, Departmental Member (Department of Physics and Astronomy)

Dr. E. van der Flier-Keller, Outside Member (Department of Earth and Ocean Sciences)

Dr. A. Zielinski, Outside Member (Department of Electrical and Computer Engineering)

Dr. T.W. Dawson, External Examiner (Defence Research Establishment Pacific)

Contents

List of Figures

List of Tables

ACKNOWLEDGEMENTS

I would like to thank my supervisor Dr. John Weaver for his unfailing patience and encouragement during the past years. Words are not enough; without his help and generous financial support this project could not have been completed. I would also like to thank Dr. Gaston Fischer of the Observatoire Cantonal, Neuchâtel, who suggested the Sardinian project and furnished many helpful suggestions along with his field data.

For many enlightening discussions and many years of friendship I would like to acknowledge my 'office mates' Ashok Agarwal and Xing-Hua Pu. I must give special thanks to Ashok who devoted much time to checking and rechecking my program and who was always willing to help me with any problems I had. I would also like to thank Ashok's family who gave me many memorable dinners and turned my liking for East Indian food into a love.

Credit must also go to my friends and family who kicked me into completing this thesis and offered much support throughout. To Rick Coles who delayed a ski vacation to photocopy my thesis and my friends at the Environmental Sciences Group at Royal Roads Military College who picked up the slack when I took time off to finish this — thanks!

DEDICATION

To my husband Andrew

---

who put up with me all these years

and has promised to call me 'Dr.' Darling from now on.

Chapter 1

INTRODUCTION

1.1 Historical Review

The conductivity of the rocks and minerals that make up the earth have long been studied for the information they provide about the structure and evolution of the crust and mantle. The electromagnetic field at the surface of the earth is the sum of the external field due to sources in the ionosphere and magnetosphere and the internal field generated by currents induced in a conducting earth. These fields are called primary and secondary and their ratios and phase relations provide valuable information on the earth's conductivity structure.

Studies have been performed both globally, when the overall conductivity structure at great depth (i.e. ~1000km) is of interest, and regionally, when the emphasis is on finer details of the crust and upper mantle (i.e. ~100km). The geometry of the source and the region determines whether the problem is considered to be one, two or three-dimensional. Global studies, reviewed by Rikitake (1973) and Roberts(1986), will not be discussed further as this thesis is concerned only with electromagnetic problems of a local nature in which lateral conductivity inhomo-

geneities occur.

There are two techniques for determining the conductivity in the earth; "inversion" and "forward modelling". The former is dependent on the latter. In the inversion technique the conductivity distribution of the region under study is deduced from observed surface results which have been fed into an algorithm. Although, theoretically, a unique solution can be derived from exact data for a dense set of frequencies or an infinite set of exact data for a small frequency range, this is never possible in practice. A solid foundation for two-dimensional linearized iterative inversion is provided by the classic papers of Weidelt (1975) and Jupp and Vozoff (1977). Recent summaries of inverse techniques have been presented by Parker (1983), Hohmann and Raiche (1987) and Oldenburg (1990).

"Forward modelling" is the opposite of inversion in the sense that a model for the local conductivity distribution is assumed and the secondary field that would result from a given primary (source) field is calculated. These two techniques can be effectively combined to probe the conductivity structure of the earth. Forward modelling produces calculated results which are compared with the observed response for the region. The adjustments needed to improve the fit of the data are calculated by some form of inversion. This procedure is then repeated until the results agree to within some acceptable limit of error. The technique that uses the ratio of electric to magnetic fields to make the required comparisons is known as the magnetotelluric (MT) method. First introduced by Tikhonov (1950) and Cagniard (1953) this method is now in common use. Forward modelling is still

the most commonly used method for determining the conductivity distributions of two and three-dimensional models, although much work is currently being done in the field of two-dimensional inversions.

Local electromagnetic induction studies have been reviewed by Filloux (1979), Hermance (1983) and Chave and Booker (1987). For regional studies the area under examination is limited in size (typically to several hundred kilometers in depth and horizontal range) and can therefore be considered flat. In a now classic paper by Price (1950), a general treatment of electromagnetic induction problems for such a flat earth is discussed. Price analyzed the problem of a homogeneous conducting half-space (an approximation for the earth) acted upon by an arbitrary known source field above it. Weaver (1971) simplified Price's theory by using integral transforms and by the introduction of electric and magnetic Hertz vectors. This has since been generalized to the case of electromagnetic induction in an n-layered conducting half-space, the principal features of which have been reviewed by Weaver (1973).

Lateral variations in conductivity have been studied analytically, numerically and through the use of analogue models. Because of the mathematical difficulties encountered, analytic solutions are only practical for problems of simple geometry. Yet, although analytic solutions are limited to a few simple models, they are extremely useful as accuracy checks on the various numerical techniques in use. The first analytic solution of electromagnetic induction in an earth with lateral conductivity variations was obtained by d'Erceville and Kunetz (1962) who

considered the effect of a vertical contact between two homogeneous media with contrasting conductivity. Rankin (1962) extended their solution to treat a vertical dike embedded in a homogeneous structure. In solutions of this type the magnetic vector is polarized parallel to the strike and the basement region is idealized as a perfect electric (or perfect magnetic) conductor. It should be noted that nearly all successful analytic solutions are for the B-polarization problems where the horizontal magnetic field of the source is polarized parallel to the strike. E-polarization problems, where the horizontal magnetic field of the source is perpendicular to the strike, are much harder to analyse. Weaver (1963) extended the vertical contact to an infinite basement depth. More recently, Geyer (1972) considered the effect of a dipping contact between two homogeneous regions. Solutions have also been obtained for models with more than one vertical contact (i.e. the "segmented overburden" model of Wait and Spies (1974), also discussed by Wait (1982), and the similar model of Weaver, Le Quang and Fischer (1985, 1986).

Various numerical techniques have been used to analyse problems involving more complex structures — finite differences, finite elements, integral equations and transmission line analogy for example. A review of some numerical methods is found in the treatment by Ward et al. (1973) and Kaikkonen (1986). These methods generally involve superimposing a mesh of grid points over the model of the conductivity distribution so that it is represented by number of cells with homogeneous conductvity. The construction of an efficient mesh, if done by hand, is often one of the most time consuming steps in a forward calculation. Many modelling

programs have been developed which employ numerical techniques (sometimes combined with analytic methods to speed computation) such as the finite element program of Wannamaker (1987) and the finite difference program of Brewitt-Taylor and Weaver (1976). The finite element method of solution for electromagnetic problems has been described by Coggon (1971) and numerous works based on this method have been published (e.g. Reddy and Rankin, 1973; Pridmore et al., 1981; Rodi, 1976; Kaikkonen, 1977, 1980; Reddy et al., 1977). Finite differences were first used for electromagnetic problems by Neves (1957) and later by many others such as Jones and Vozoff (1978) and Zhdanov et al. (1982). Both the finite element and finite difference methods are capable of solving very general electromagnetic induction problems but for the more complex of these, large amounts of computer time and computer storage space are required. It has been noted (Coggon,1971; Wannamaker et al.,1987) that numerical techniques which solve for the total field are prone to errors caused by the finite length of the computer word. To prevent this problem, which is especially prominent at low frequencies, programs can solve directly for the much smaller anomalous field variations. This technique may also allow the use of single precision arithmetic which would result in a substantial saving of CPU time.

Analogue models (see review by Dosso, 1973) have proved useful for the study of very complex three-dimensional conductivity structures which cannot be treated by numerical modelling because of the limitations imposed by the coarseness of the numerical grid. These include bays, capes, channels, islands, irregular coastlines

and seamounts (Nienaber et al., 1976, 1977; Chan et al., 1981; Dosso et al., 1986; Hu et al., 1984, 1986, 1989), the effect of various source fields (Ramaswamy and Dosso, 1973, 1975) and tectonic subduction zones (Dosso et al., 1989, 1990; Chen et al., 1989, 1990). Unfortunately analogue models are themselves limited by the scarcity of materials with appropriate laboratory scale conductivities and also by the size of the facility required to model complex structures in realistic detail.

The study of near-surface lateral inhomogeneities was greatly simplified by Price (1949) who introduced the "thin-sheet" approximation. In this aproach the earth is represented mathematically by an infinitely thin sheet of variable integrated conductivity underlain by a non-conducting region. Rikitake (1966) took into account the effect of a highly conducting mantle by adding a conducting half-space under the non-conducting region. The "coast-effect" has been extensively studied by incorporation of discontinuities into the integrated conductivity of the thin sheet (see e.g. Roden, 1964; Ashour 1971). An important observation from these studies is that the vertical magnetic field is enhanced at the coastline (or continental shelf) dropping off rapidly seawards and more slowly inland.

In strictly two-dimensional flat earth models with electrically isolated thin sheets, only the E-polarization mode is of importance for electromagnetic induction. A second type of model has the thin sheet in contact with the underlying layered structure, permitting vertical current flow into and out of the sheet. For strictly two-dimensional problems only the B-polarization mode admits vertical current loops (i.e. the "poloidal" mode). Weidelt (1971) obtained an analytic

E-polarization solution for the case of one plane, situated in free space, consisting of two half-sheets of differing (finite) integrated conductivities and more recently Raval et al. (1981) and Dawson (1983) have solved the complete problem with a conducting half-space beneath the thin sheet. The corresponding B-polarization problem has been treated analytically by Nicoll and Weaver (1977), Dawson and Weaver (1979) and Dawson et al. (1982). A numerical method for the solution of a two-dimensional thin sheet layered medium model was developed by McKirdy and Weaver (1984) and then generalized for the three-dimensional case by McKirdy et al. (1985). The thin sheet method has also been used numerically to study the three-dimensional electromagnetic field distortion due to near-surface inhomogeneities. This technique was first developed by Vasseur and Weidelt (1977) with more recent work being done by Weaver (1982), Agarwal and Weaver (1989) and Weaver and Agarwal (1991).

Some progress has been made in the numerical analysis of three-dimensional problems although the major stumbling blocks of computer speed and storage space limit the complexity of the models under study. The numerical techniques used for this purpose include the difference equation method (Lines and Jones, 1973; Dey and Morrison, 1979; Pridmore et al., 1981; Chen and Fung, 1985), and the integral equation method (Raiche, 1974; Weidelt, 1975; Hohmann, 1975, 1983; Wannamaker et al., 1984). Various hybrid methods have also been developed based on a combination of the difference equation and integral equation solutions. Lee et al. (1981) and Best et al. (1985) have studied this approach and, based on this,

Gupta et al. (1987, 1989) have developed a corresponding hybrid finite element procedure.

Part of the interest in the study of layered half-spaces lies in the magnetotelluric method of inferring underlying conductivities from surface field measurements at a point. Since the classic paper of Cagniard (1953), who discussed plane waves incident on a layered conductor, numerous papers have been published on this subject (see e.g. the review by Wait (1962) and the bibliography in Kaufman and Keller (1981)). Wait (1954) discussed the case of more general sources by extending this to complex angles of incidence.

In the magnetotelluric method of geophysical prospecting, natural source fields over a broad frequency band are used to examine the conductivity of the earth via surface measurements of the horizontal electric and magnetic fields. Cagniard (1953) showed that if the region under study is assumed to have a laterally homogeneous conductivity structure and the inducing field is uniform then the apparent resistivity is defined as

$$\rho_a = \frac{\mu_0}{\omega}\frac{|E|^2}{|B|^2}. \tag{1.1}$$

where μ_0 is the permeability and ω is the frequency. If there is a horizontal gradient in conductivity then ρ_a will depend on the direction of $\mathbf{E}$ and $\mathbf{B}$ so that the two possible apparent resistivities will be

$$(\rho_a)_x = \frac{\mu_0}{\omega}\frac{|E_x|^2}{|B_y|^2}, \quad \text{and} \quad (\rho_a)_y = \frac{\mu_0}{\omega}\frac{|E_y|^2}{|B_x|^2}. \tag{1.2}$$

If the frequency ω is given in rad s^{-1}, E in mV/km and B in nanoteslas then ρ_a

will have units of resistivity ohm-m. It has been appreciated for some time that lateral variations of the electric and geometrical characteristics will complicate any interpretation of apparent resistivity data. Many apparent resistivity curves (ρ_a versus T) for two-dimensional and three-dimensional conductivity distributions have been generated in order to examine the distortion caused by such lateral variations (e.g. Park, 1985).

Another method of studying conductivity anomalies uses geomagnetic depth sounding (GDS) which is based on the ratio of vertical (Z) to horizontal (X, Y) magnetic field responses. Most of the anomalies of short period geomagnetic variation are of the "directional variation" type (Uyeda and Rikitake, 1970). In general the vertical field amplitude observed at mid-latitudes should be much smaller than the horizontal but in directional variations the vertical field amplitude is large. In such cases there are good correlations between the vertical and horizontal magnetic fields which were first noticed by Parkinson (1959). This correlation can be written as

$$\Delta Z = A\Delta X + B\Delta Y \tag{1.3}$$

where ΔZ, ΔX and ΔY are variations of the downward, geographically northward and eastward components and A and B are frequency or period-dependent coefficients. In most cases (1.3) is used in the frequency domain where A and B are complex functions of frequency (transfer functions) and the field variations are replaced by Fourier transformations of the vertical and horizontal components. The pairs $\Re(A, B)$ and $\Im(A, B)$ are called the in-phase (real) and quadrature (imagi-

nary) induction arrows for a field site.

Equation (1.3) can also be interpreted as representing a plane in which the vector of geomagnetic field variation is confined. This is called the "preferred plane" and the projection of the normal of this plane onto the earth's surface is called the Parkinson arrow (Parkinson, 1959,1962). These arrows are commonly used in the graphical representation of the electromagnetic responses of anomalous conductors in the earth. Different arrow conventions have been dicussed by Gregori and Lanzerotti (1980,1982), Jones (1981) and Wolf (1982).

Convention states that if the time dependence of the field is represented by $\exp(i\omega t)$ then the sign of the transfer functions should be reversed in order to satisfy the criteria that both the in-phase and quadrature arrow should point towards the current concentration in a conductive body (as does the Parkinson arrow). If, however, the time dependence is $\exp(-i\omega t)$ then only the sign of the in-phase transfer function should be reversed (Lilley and Arora, 1982). The in-phase arrow has been observed by most authors to point towards the areas of high conductivity where the current concentration is greatest and its amplitude increases with increasing current strength. Hu et al. (1989) and Jones (1986) have found small amplitude in-phase arrows that point away from the conductive zones for cases where the depth to the conductor is less than one skin depth (δ) in the more resistive host where a skin depth is defined as

$$\delta = (2/\omega\mu_0\sigma_h)^{1/2} \tag{1.4}$$

and σ_h is the host conductivity. The behaviour of the quadrature arrow is not as

easily understood. Analogue model results (e.g. Nienaber et al., 1983: Dosso et al., 1985: Hu et al., 1989) and analytic and numerical calculations (e.g. Weaver., 1987; Agarwal and Dosso, 1990) have reported sign reversals of the quadrature arrow. The two-dimensional results of Agarwal and Dosso (1990) show the quadrature arrow pointing away from the conductive zones at short periods and then reversing direction at the characteristic period. The characteristic period T_c (Rokityansky, 1982) is the period at which the amplitude for the in-phase arrow is a maximum and that for the quadrature arrow is a minimum.

1.2 Review of work in this thesis

In this thesis a two-dimensional (2D) finite difference program (see Appendix B) is developed that solves directly for the anomalous electromagnetic fields due to a two-dimensional conductivity model. The source is assumed to be a uniform magnetic field. The model consists of a two-dimensional conductivity structure $\sigma(y, z)$ with no sloping boundaries (i.e. all boundaries are either vertical or horizontal). This two-dimensional structure is bounded on the left and right hand sides by separate, possibly different, one-dimensional conductivity profiles. The underlying structure is a half-space of uniform conductivity. The method of solution is by a hybrid finite difference approach with integral boundary conditions at the earth's surface (E-polarization only) and at the top of the underlying half-space and asymptotic boundary conditions at the sides (E-polarization only). The resulting matrix is solved directly to provide values for either the horizontal elec-

tric field U (in the E-polarization case) or the horizontal magnetic field X (in the B-polarization case).

Chapter 2 provides a general background for the thesis by presenting the mathematical development of some important equations of electromagnetic induction. The E and B-polarization induction equations are derived and are written in terms of the single field components $E_x = U$ (E-polarization) and $B_x = X$ (B-polarization). The forward problem is solved for these components. Expressions for the remaining components (Y and Z for E-polarization and V and W for B-polarization) are developed in Chapter 6. Chapter 2 also introduces the surface, side and bottom boundary conditions.

In Chapter 3 the governing equations introduced in Chapter 2 are modified so that they are expressed in terms of the anomalous parts of U or X. This increases the accuracy of the solution and should allow the program to be used in single precision if necessary to run on less powerful personal computers.

In Chapter 4 the finite difference method is introduced. Recursion relations are developed that are used in solving the 1D problems at the edges of the 2D model. Although these equations were known previously (see e.g. Weaver 1994) they have been written in a form which contains only negative exponentials. This was done to avoid the problems that can occur if the argument of an exponential attains a very large, positive value. The finite difference forms of the governing equations, including the boundary conditions, are developed for all points in a numerical grid that covers the 2D area under study. The method of solution of

the resulting matrix of coefficients is discussed. A comparison of the results of the forward modelling program to results from an analytical solution of a simple model are presented in Appendix A.

Chapter 5 explains the principles of good grid design and explains the procedure used to generate such a grid automatically. The development of the automatic gridding procedure was crucial to the successfull application of the program to the geophysical problems investigated in Chapters 7, 8 and 9 which required the solution of many forward problems with different model parameters.

The equations used in evaluating the remaining components of the electromagnetic field (the derivative fields) are developed in Chapter 6. A more accurate method of calculating the horizontal electric field (in the B-polarization case) at the surface of the earth above a vertical fault is developed in this chapter. This ensures that the phases calculated on either side of the vertical boundary match well. The program uses these components of the field to calculate apparent resistivity and phase. A complete listing of the program is given in Appendix B.

Chapters 7, 8 and 9 explore separate geophysical problems to which the forward modelling program has been applied. First (in Chapter 7) the forward modelling program is used in conjunction with an optimization program to investigate data from a magnetotelluric profile on the island of Sardinia. The apparent resistivity and phase data were inverted at two sites along the profile to obtain two-dimensional models perpendicular to the profile. This was done to probe the underlying geological structures in these areas which are considered to be three-

dimensional in nature.

Secondly (in Chapter 8) studies were performed on the behaviour of induction arrows over a two-dimensional model representing an ocean overlying a deeply buried conductivity contrast. The E-polarization induction arrows were calculated using the two-dimensional forward program and the relationship (1.3) and the effect on these arrows of varying model parameters was observed.

Finally (in Chapter 9) the forward model was used in a two-dimensional inversion study. The calculation of suitable starting models was discussed and the relative merits of using different impedances to calculate these starting models was explored. The basic method behind the 2D inversion was described and, as an example, a 2D inversion was performed on the North American Central Plains anomaly using magnetotelluric data from an international comparison study of 2D inversion techniques called COPROD2.

Chapter 10 provides conclusions and suggestions for further work.

Chapter 2

BASIC EQUATIONS OF ELECTROMAGNETIC INDUCTION

2.1 Introduction

This chapter provides a general background for the thesis by presenting the mathematical development of some important equations of electromagnetic induction and the derivation of two-dimensional surface, side and bottom boundary conditions. The work in this chapter is based on the earlier work of Green (1978), Jones (1964), Kertz(1954), Siebert and Kertz (1957), Schmucker (1971) and Green and Weaver (1978).

2.2 Maxwell's Equations

Maxwell's equations are a mathematical expression of the properties of time dependent electromagnetic fields. Let $\mathbf{E}$ and $\mathbf{H}$ represent the electric and magnetic field intensities and $\mathbf{D}$ and $\mathbf{B}$ the electric and magnetic flux densities. These quantities define the field, are dependent on the space variables (x, y, z) and on time t,

and are related by Maxwell's equations which, in SI units, are

$$\nabla \times \mathbf{E} + \partial \mathbf{B}/\partial t = 0 \tag{2.1}$$

$$\nabla \times \mathbf{H} - \partial \mathbf{D}/\partial t = \mathbf{J} \tag{2.2}$$

$$\nabla \cdot \mathbf{D} = \rho \tag{2.3}$$

$$\nabla \cdot \mathbf{B} = 0, \tag{2.4}$$

where $\mathbf{J}$ and ρ are respectively the volume densities of current and charge. These equations can be simplified so that they depend only on $\mathbf{E}$ and $\mathbf{B}$ which we will loosely refer to as the electric and magnetic fields.

In geophysical induction problems all regions below the earth's surface are assumed to be linear and isotropic. In such cases

$$\mathbf{D} = \epsilon \mathbf{E}, \quad \mathbf{H} = \mathbf{B}/\mu, \quad \mathbf{J} = \sigma \mathbf{E}, \tag{2.5}$$

hold true where ϵ is the permittivity, μ the permeability and σ the conductivity of the medium. It is also assumed that these regions have a permeability of $\mu \approx \mu_0 = 4\pi \times 10^{-7}$ H/m (Weaver 1994). This is approximately true for most material except ferromagnetic materials which have $\mu \gg \mu_0$. Large differences in magnitude between μ and μ_0 are, however, uncommon and occur in the earth only rarely. It is also assumed that any sources have a common harmonic time dependence with angular frequency ω so that

$$\mathbf{E} = \mathbf{E}(x, y, z)e^{i\omega t}, \quad \mathbf{B} = \mathbf{B}(x, y, z)e^{i\omega t}, \tag{2.6}$$

where it is usual to write the (complex) spatial part of the electric and magnetic fields in component form as $\mathbf{E}=(U,V,W)$ and $\mathbf{B}=(X,Y,Z)$.

Using the assumptions represented by equations (2.5) and (2.6) the Maxwell equations (2.1) – (2.4) can be rewritten in the simplified form

$$\nabla \times \mathbf{E} + i\omega\mathbf{B} = 0 \tag{2.7}$$

$$\nabla \times \mathbf{B} - i\omega\epsilon\mu_0\mathbf{E} = \mu_0\sigma\mathbf{E} \tag{2.8}$$

$$\nabla \cdot \mathbf{E} = \rho/\epsilon \tag{2.9}$$

$$\nabla \cdot \mathbf{B} = 0. \tag{2.10}$$

For geomagnetic induction st... ies the displacement current term $i\omega\epsilon\mu_0\mathbf{E}$ in (2.8) can be shown to be negligible with respect to the other terms in the relevant ...ation. For this to be true in the earth it is required that

$$\omega \ll \sigma/\epsilon \tag{2.11}$$

Since most materials within the earth have conductivities ranging from 10^{-6} – -10^{-4} S/m for crustal rocks to 4 S/m for seawater and $1 \leq \epsilon/\epsilon_0 \leq 110$ kHz (Jackson 1975, p.16) the above equation (2.11) demands only that $\sigma/\epsilon < 110$ kHz (ie that frequency $f \ll 110$ kHz so $\omega = 2\pi f \ll 509$ rad/s). One further constraint that must be satisfied in order to allow the neglect of displacement current in free space where $\sigma = 0$ is that

$$\omega^2 \ll 1/l^2\epsilon\mu_0 \tag{2.12}$$

(see e.g. Green, 1978) where l is the characteristic length in the region under study. For global studies l is of the order of one earth radius ($\approx$ 6400 km) so that (2.12) is valid for $f \ll 47$ Hz. For this case the upper limit of f is usually said to be 10 Hz. If l is smaller, as it is for local studies, the bound on ω will be correspondingly higher. Since the values of f important in geomagnetic induction studies are generally bounded by $f < 1$ Hz the neglect of displacement currents is justified both in the earth and in free-space regions. Exclusion of the displacement current in (2.8) leaves the simpler form $\nabla \times \mathbf{B} = \mu_0 \sigma \mathbf{E}$.

If it is assumed that the earth is made up of homogeneous conducting regions we can take the volume charge density to be zero, since if any volume charge density did initially exist it would quickly disperse to the boundaries of the region, independent of any applied field (Jones 1964, p.12). In air, the volume charge density is also assumed zero so $\rho = 0$ everywhere. This fact makes (2.9), $\nabla \cdot \mathbf{E} = \rho/\epsilon$, redundant ($\rho$=0, hence $\nabla \cdot \mathbf{E} = 0$). Using the vector identity $\nabla \cdot (\nabla \times \ ) \equiv 0$ on (2.8) results in $\nabla \cdot (\mu_0 \sigma \mathbf{E}) = 0$. In the homogeneous regions under consideration μ_0 and σ are both constant so $\nabla \cdot \mathbf{E} = 0$ is obtained without the need for equation (2.9). (*At* the boundaries between the homogeneous regions the discontinuous conductivity leads to discontinuities in the field associated with surface charge densities and $\nabla \cdot \mathbf{E} \neq 0$. This is not a problem in this thesis since the finite difference method used (see section 4.4) approximates the sharp boundaries with a conductivity that changes smoothly from one value to the next in a roughly linear manner.)

Another redundant equation is (2.10) which can be obtained from (2.7) and the vector identity $\nabla \cdot (\nabla \times \ ) \equiv 0$. Elimination of these redundancies leaves the two basic equations of electromagnetic induction:

$$\nabla \times \mathbf{E} = -i\omega\mathbf{B} \tag{2.13}$$

$$\nabla \times \mathbf{B} = \mu_0\sigma\mathbf{E}. \tag{2.14}$$

Some components of the field vectors change discontinuously on the boundaries between regions which have different conductivities and, therefore, there exist boundary conditions which connect the field components in neighbouring regions 1 and 2 (Rokityansky 1982):

$$\hat{\mathbf{n}} \times (\mathbf{E}_2 - \mathbf{E}_1) = 0, \tag{2.15}$$

$$\hat{\mathbf{n}} \times (\mathbf{B}_2 - \mathbf{B}_1) = \mu_0\mathbf{J}_s, \tag{2.16}$$

$$\hat{\mathbf{n}} \cdot (\mathbf{D}_2 - \mathbf{D}_1) = \rho_s, \tag{2.17}$$

$$\hat{\mathbf{n}} \cdot (\mathbf{J}_2 - \mathbf{J}_1) = -\frac{\partial\rho_s}{\partial t}, \tag{2.18}$$

$$\hat{\mathbf{n}} \cdot (\mathbf{B}_2 - \mathbf{B}_1) = 0 \tag{2.19}$$

where $\hat{\mathbf{n}}$ is the unit vector normal to the boundary between the regions and directed from region 1 to region 2. The tangential component of the magnetic field is discontinuous only in the presence of the surface currents $\mathbf{J}_s$ flowing in a thin conducting film or sheet. If there is no thin sheet in the model then the surface currents are assumed zero and the tangential components of both the magnetic and the electric field become continuous.

2.3 General Two-Dimensional Equations

For this two-dimensional problem there is assumed to be a uniform magnetic source field generated by a uniform sheet current above the surface of the earth. An induction problem is two-dimensional if σ and the field vectors ($\mathbf{E}$ and $\mathbf{B}$) are independent of one of the horizontal coordinates, typically chosen to be the x direction. The rectangular components of $\mathbf{E}$ and $\mathbf{B}$ can be written in the form

$$E_x = U(y,z), \quad E_y = V(y,z), \quad E_z = W(y,z), \tag{2.20}$$

$$B_x = X(y,z), \quad B_y = Y(y,z), \quad B_z = Z(y,z). \tag{2.21}$$

Using these components and the vector induction equations (2.13) and (2.14) we obtain six well-known scalar equations (see e.g. Weaver, 1994)

$$\partial W/\partial y - \partial V/\partial z = -i\omega X \tag{2.22}$$

$$\partial X/\partial z = \mu_0 \sigma V \tag{2.23}$$

$$\partial X/\partial y = -\mu_0 \sigma W \tag{2.24}$$

and

$$\partial Z/\partial y - \partial Y/\partial z = \mu_0 \sigma U \tag{2.25}$$

$$\partial U/\partial z = -i\omega Y \tag{2.26}$$

$$\partial U/\partial y = i\omega Z. \tag{2.27}$$

It can be seen that these equations fall into two independent groups. The field has decoupled into the B-polarization (B-pol) or transverse magnetic (TM) mode associated with (2.22), (2.23) and (2.24) and the E-polarization (E-pol) or transverse electric (TE) mode associated with (2.25), (2.26) and (2.27). The B-polarization problem involves only the X, V and W components and the field in this case can be written as

$$\mathbf{B} = (X, 0, 0), \quad \mathbf{E} = (0, V, W). \tag{2.28}$$

Similarly the E-polarization problem involves only the Y, Z and U components and its field is given by

$$\mathbf{B} = (0, Y, Z), \quad \mathbf{E} = (U, 0, 0) \tag{2.29}$$

(see Fig. 2.1). For any two-dimensional (2D) problem these modes can be treated separately and the overall fields found by linear superposition.

The differential equation for X can be readily obtained by differentiating (2.23) with respect to z, (2.24) with respect to y and substituting the results into (2.22). This produces

$$\frac{\partial^2 X}{\partial y^2} + \frac{\partial^2 X}{\partial z^2} = i\omega\mu_0\sigma X, \tag{2.30}$$

where we recall that we are dealing with regions where σ is constant. The more general form of this differential equation, with σ not necessarily a constant, is

$$\frac{\partial^2 X}{\partial y^2} + \frac{\partial^2 X}{\partial z^2} - \frac{1}{\sigma}\frac{\partial \sigma}{\partial y}\frac{\partial X}{\partial y} - \frac{1}{\sigma}\frac{\partial \sigma}{\partial z}\frac{\partial X}{\partial z} = i\omega\mu_0\sigma X. \tag{2.31}$$

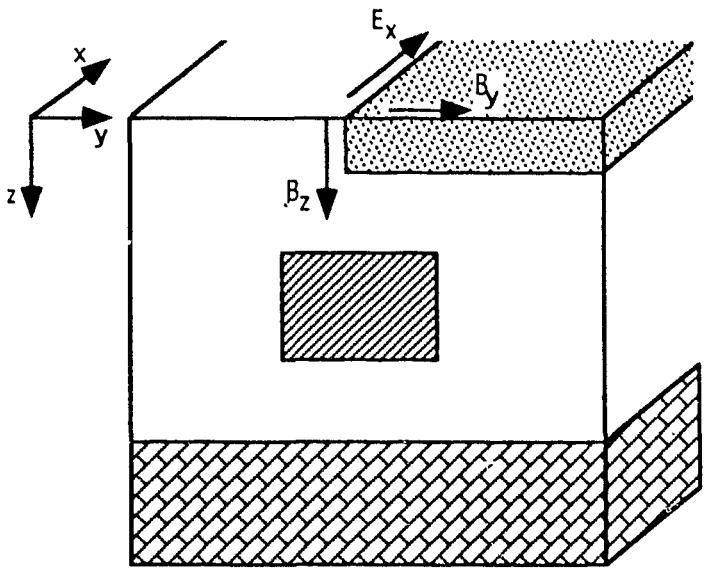

(a) The E-polarization case.

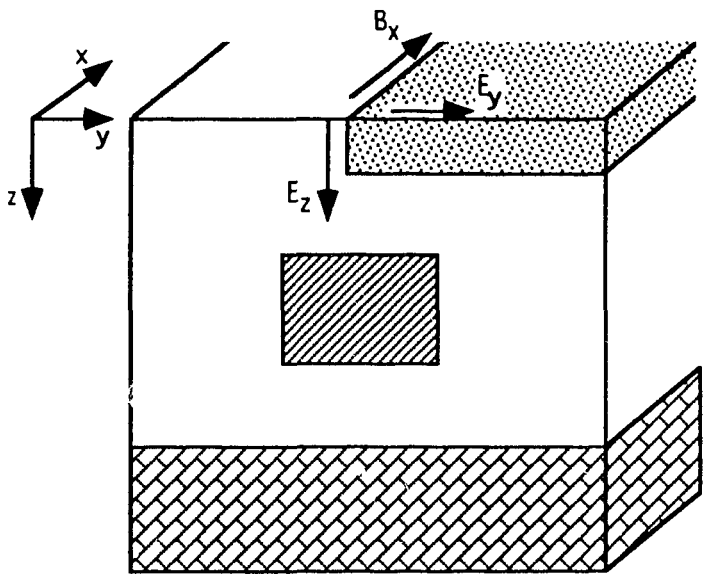

(b) The B-polarization case.

Figure 2.1: The orientation of the axes and the fields in the E-polarization case (a) and the B-polarization case (b) for a general two-dimensional model. The model has a two-dimensional conductivity structure $\sigma(x, y)$ (i.e. the conductivity is constant in the x-direction). The differently shaded areas represent regions with different conductivities. The surface of the earth is at $z = 0$ and z is negative above the surface of the earth.

In a similar way (2.26) can be differentiated by z and (2.27) by y and both substituted into (2.25) which straight away gives the differential equation satisfied by U:

$$\frac{\partial^2 U}{\partial y^2} + \frac{\partial^2 U}{\partial z^2} = i\omega\mu_0\sigma U \tag{2.32}$$

The equations (2.30) and (2.32) can both be written in the general form

$$\nabla^2 F = i\kappa F \tag{2.33}$$

where $\nabla^2 = \partial/\partial y^2 + \partial/\partial z^2$ is the scalar Laplacian operator, $\kappa = \omega\mu_0\sigma$ and F is a general component (X or U) of the electromagnetic field.

2.4 Surface Boundary Conditions

For the surface boundary conditions, as well as for the bottom boundary conditions, careful note must be taken of the side of the boundary on which the horizontal magnetic field is evaluated. If a surface current flows along the boundary plane then this field component can be discontinuous (see (2.16)), unlike the tangential electric field which is continuous (see (2.15)). So, for example, writing $X(y, 0-)$ indicates that it is evaluated above the $z = 0$ boundary and $X(y, d+)$ indicates that it is evaluated below the $z = d$ boundary.

For B-polarization it is obvious from (2.23) and (2.24) that in a non-conducting region or above the surface of the earth ($\sigma = 0$) $\partial X/\partial y = 0$ and $\partial X/\partial z = 0$ so that

$$X(y, 0-) = X_0 \tag{2.34}$$

where X_0 is a constant. For a uniform horizontal primary magnetic field of B_0 the total field above a one-dimensional (1D) earth is $2B_0$ (see e.g. Weaver, 1994). Since a 2D problem becomes 1D as $|y| \to \infty$ the constant $X_0 = 2B_0$ (ie: twice the primary field).

The E-polarization problem also reduces to a 1D problem as $|y| \to \infty$. For a uniform horizontal primary field this situation is identical to the B-polarization 1D limit as $|y| \to \infty$ if we imagine interchanging the x and y axes. From this it follows that $Y \to Y_0$ where Y_0 is also a constant with a magnitude equal to twice the primary magnetic field in the y direction. Differentiation of (2.26) by y and (2.27) by z results in

$$\partial Y/\partial y = -\partial Z/\partial z \tag{2.35}$$

and in the nonconducting region above the surface of the earth ($\sigma = 0$) equation (2.25) reduces to

$$\partial Y/\partial z = \partial Z/\partial y. \tag{2.36}$$

Since Z is associated with conductivity anomalies it will vanish in regions infinitely far removed from those anomalies. This implies that $Z \to 0$ as $|y| \to \infty$ and $z \to -\infty$ and consequently (2.35) and (2.36) require $\partial Y/\partial y$ and $\partial Y/\partial z$ to vanish as well. So as $z \to -\infty$, Y becomes a constant which must have the value Y_0 in order to match up with the solution $Y = Y_0$ at $y = \pm\infty$.

By introducing the anomalous field $\tilde{Y} = Y - Y_0$, where Y is the sum of the 1D solution at $y = \pm\infty$ and the anomalous field (ie: Y is the total field), (2.35) and

(2.36) can be written as

$$\partial\tilde{Y}/\partial y = \partial Z/\partial\tilde{z}, \quad \partial\tilde{Y}/\partial\tilde{z} = -\partial Z/\partial y, \tag{2.37}$$

where the new variable $\tilde{z} = -z$. The equations (2.37) take the form of the Cauchy-Riemann equations. So given that the first partial derivatives of $\tilde{Y}$ and Z exist, are continuous and satisfy (2.37) in the region $\tilde{z} > 0$, then $f(s) \equiv \tilde{Y} + iZ$ where $s = y + i\tilde{z}$, is analytic in the upper half-plane $\tilde{z} > 0$ of complex space. It is neccessary to integrate around the closed contour comprising the real axes with an indentation upwards around the pole $y = u$ and a return at infinity in the upper half-plane (Fig. 2.2). What follows is a description of the well-known method for dealing with such an integration. In the half circle C_R $f(s) \to 0$ as $s \to \infty$ since $\tilde{Y}$ and Z are both due to anomalies and their effect vanishes here. Using this fact together with Cauchy's Integral Formula coupled with the theory of residues and poles of indented contours it can be found that

$$⨍_{-\infty}^{\infty} \frac{f(u)}{u-y}\,du = \pi i f(y). \tag{2.38}$$

where y is a simple pole on the u axis and the bar on the integral sign indicates the principal value of the integral. Since the function $f(u)/(u-y)$ is continuous over the whole real line except at y, the principal value of its integral is defined as

$$⨍_{-\infty}^{\infty} \frac{f(u)}{u-y}\,du = \lim_{\substack{R\to\infty \\ r\to 0+}} \left(\int_{-R}^{y-r} \frac{f(u)}{u-y}\,du + \int_{y+r}^{R} \frac{f(u)}{u-y}\,du \right) \tag{2.39}$$

where R and r are shown in Fig. 2.1. Writing the imaginary part of (2.38)

$$⨍_{-\infty}^{\infty} \frac{Z(u)}{u-y}\,du = \pi\tilde{Y}(y) \tag{2.40}$$

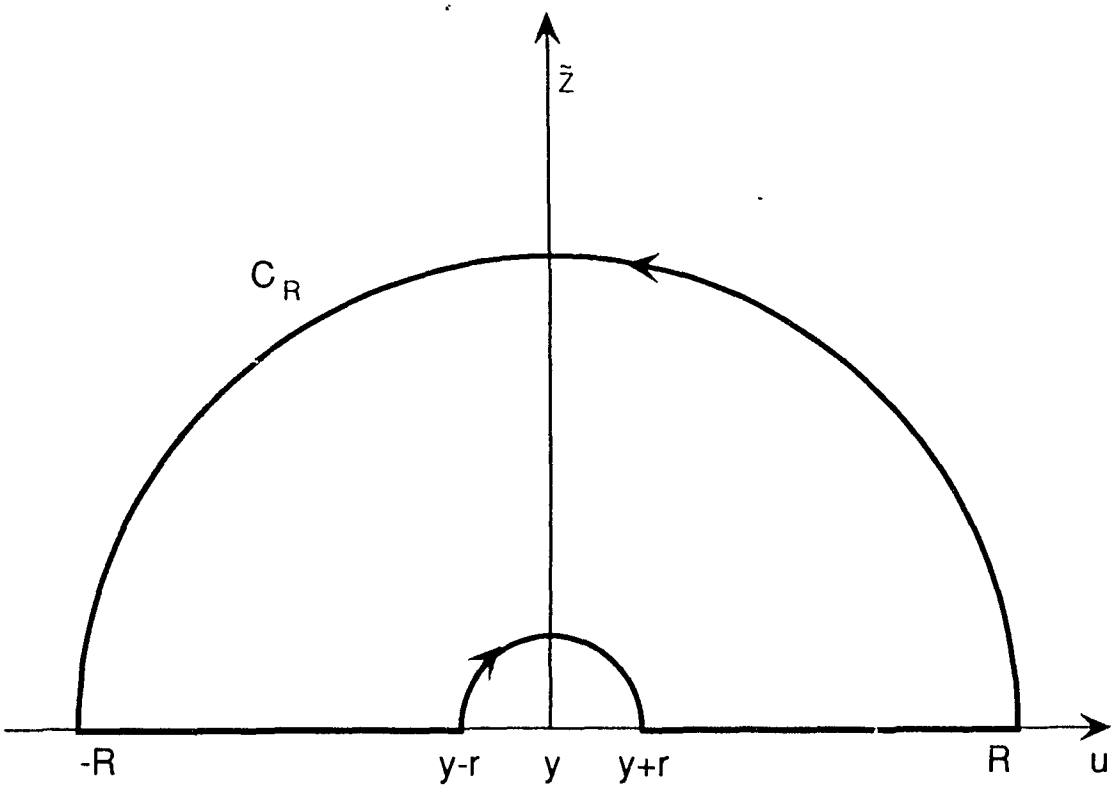

Figure 2.2: The upper half-plane of complex space showing the closed contour C_R with an indentation upwards around the pole $y = u$.

and writing the result in terms of Y, yields

$$Y(y,0-) = Y_0 + \mathcal{H}Z(y,0). \tag{2.41}$$

$\mathcal{H}$ is the Hilbert transform and from (2.40) it can be seen that

$$\mathcal{H}f(y) = \frac{1}{\pi} \fint_{-\infty}^{\infty} \frac{f(u)}{u-y}\, du. \tag{2.42}$$

Converting (2.41) to terms of U by (2.26) and (2.27) produces

$$U'(y,0-) = -i\omega Y_0 - \mathcal{H}\left(\frac{\partial U(y,0)}{\partial y}\right) \tag{2.43}$$

where the prime on U denotes a derivative in z (ie: $U'(y,0-) = \partial U(y,0-)/\partial z$). This notation for $\partial/\partial z$ will be used often throughout this thesis. The first appearence of formulae of the form (2.41) was in work by Kertz (1954) and Siebert and Kertz (1957) on the separation of the internal and external parts of the geomagnetic field. The above equation (2.43) is equivalent to the integral boundary condition obtained by Schmucker (1971) where he uses the Kertz operator $\mathcal{K} = -\mathcal{H}$ introduced by Kertz (1954). To evaluate (2.43) the Hilbert transform is expanded using the definition of the principal value which, written out in full, is

$$U'(y,0-) = -i\omega Y_0 - \frac{1}{\pi} \lim_{\substack{R\to\infty \\ r\to 0+}} \left(\int_{-R}^{y-r} + \int_{y+r}^{R} \right) \frac{\partial}{\partial v}[U(v,0) - U(y,0)] \frac{dv}{v-y} \tag{2.44}$$

where the constant $U(y,0)$ has been included so that an integration by parts will be possible. Integrating by parts results in

$$\begin{aligned} U'(y,0-) = -i\omega Y_0 - \frac{1}{\pi} \Bigg[& \lim_{\substack{R\to\infty \\ r\to 0+}} \left(\frac{U(v,0)-U(y,0)}{v-y} \Big|_{-R}^{y-r} + \frac{U(v,0)-U(y,0)}{v-y} \Big|_{y+r}^{R} \right) \\ & + \lim_{\substack{R\to\infty \\ r\to 0+}} \left(\int_{-R}^{y-r} + \int_{y+r}^{R} \right) \frac{U(v,0)-U(y,0)}{(v-y)^2}\, dv \Bigg] \end{aligned} \tag{2.45}$$

which simplifies to

$$\begin{aligned} U'(y,0-) &= -i\omega Y_0 - \frac{1}{\pi}\left[\frac{\partial U(y,0)}{\partial y} - \frac{\partial U(y,0)}{\partial y} + \int_{-\infty}^{\infty} \frac{U(v,0)-U(y,0)}{(v-y)^2}\,dv\right] \\ &= -i\omega Y_0 - \frac{1}{\pi}\int_{-\infty}^{\infty} \frac{U(v,0)-U(y,0)}{(v-y)^2}\,dv \end{aligned} \tag{2.46}$$

This equation (2.46) is the E-polarization surface boundary condition.

2.5 Side Boundary Conditions

As $|y| \to \infty$ the problem becomes 1D, so that the y-derivatives of the fields X and U and the parameter σ all vanish. So at some z, the side boundary conditions for X and U are

$$X(\pm\infty, z) = X^{\pm}(z) \tag{2.47}$$

$$U(\pm\infty, z) = U^{\pm}(z) \tag{2.48}$$

Imposing the conditions above on the differential equations (2.30) and (2.32) it can be seen that $X^{\pm}$ and $U^{\pm}$ satisfy

$$X''^{\pm}(z) = i\omega\mu_0\sigma^{\pm}(z)X^{\pm}(z) \tag{2.49}$$

$$U''^{\pm}(z) = i\omega\mu_0\sigma^{\pm}(z)U^{\pm}(z) \tag{2.50}$$

for all values of $z > 0$ where $\sigma^{\pm}(z)$ are the 1D conductivity distributions at the extreme left and right edges of the model. The boundary conditions derived in the previous section apply to the above equations, $X^{\pm}(0) = X_0$ for the B-polarization equation and $U'^{\pm}(0-) = -i\omega Y_0$ for the E-polarization equation. The solutions for (2.49) and (2.50) are the 1D solutions discussed in §4.2.

2.6 Bottom Boundary Conditions

While it is true that $X \to 0$ and $U \to 0$ as $z \to \infty$ due to attenuation of the field by the earth it is less time consuming to solve only down to a depth $z = d$ below which there lies a homogeneous half-space of conductivity σ_0. This is often the case in 2D models and it is relatively easy to replace the solution in $d < z < \infty$ with a boundary condition at $z = d$. If, in general, there are two regions with differing conductivities we recall that the boundary condition (2.15) that connects the tangential electric field components is

$$\hat{\mathbf{n}} \times (\mathbf{E}_2 - \mathbf{E}_1) = 0 \tag{2.51}$$

where $\hat{\mathbf{n}}$ is the unit vector normal to the boundary between the regions. If region 1 is a perfect conductor then $\mathbf{E}_1 = 0$ and one is left with $\hat{\mathbf{n}} \times \mathbf{E}_2 = 0$. This in turn requires that $U_2 = 0$ and $V_2 = 0$. It follows that our boundary conditions for the case where our underlying half-space is a perfect conductor, $\sigma_0 = \infty$, are

$$X'(y, d) = 0, \quad U(y, d) = 0. \tag{2.52}$$

For the more general case where σ_0 is not a perfect conductor it is possible to derive an integral boundary condition for $z = d$. What follows is the method of Green and Weaver (1978) who begin by taking the Fourier transform

$$\hat{f}(\eta) = \frac{1}{\sqrt{2\pi}} \int_{-\infty}^{\infty} f(y) \mathrm{e}^{i\eta y}\, dy, \tag{2.53}$$

of the general differential equation (2.33) satisfied by both X and U. In $z > d$ and with $\sigma = \sigma_0$ a constant they obtained

$$-\eta^2 \hat{F}(\eta, z) + \hat{F}''(\eta, z) = i\omega\mu_0\sigma_0 \hat{F}(\eta, z), \tag{2.54}$$

and by rearranging slightly

$$\hat{F}''(\eta, z) = (\eta^2 + i\alpha_0^2)\hat{F}(\eta, z) \tag{2.55}$$

where $\alpha_0^2 = \kappa_0 = \omega\mu_0\sigma_0$. The solution of the above equation is

$$\hat{F}(\eta, z) = \hat{F}(\eta, d+)\mathrm{e}^{-(z-d)\gamma_0(\eta)} \tag{2.56}$$

where $\gamma_0(\eta) = \sqrt{\eta^2 + i\alpha_0^2}$. The known transform (Erdélyi, 1954 1.4(26))

$$\frac{1}{\sqrt{2\pi}} \int_{-\infty}^{\infty} P(y, z)\mathrm{e}^{i\eta y}\, dy = \sqrt{\frac{\pi}{2}} \frac{\mathrm{e}^{-z\gamma_0(\eta)}}{z\alpha_0\sqrt{i}} \tag{2.57}$$

where

$$P(y, z) = \frac{K_1[(y^2 + z^2)^{\frac{1}{2}}\alpha_0\sqrt{i}]}{(y^2 + z^2)^{\frac{1}{2}}}, \tag{2.58}$$

and K_1 is the 1^{st} order modified Bessel function can be used to obtain the Fourier inverse of (2.56). Except for the function $\hat{F}(\eta, d+)$, referred to as $\hat{f}(\eta)$, (2.56) can be changed to resemble the right hand side of (2.57) referred to as $\hat{g}(\eta)$. The convolution theorem for Fourier transforms states that

$$f \star g(y) = \frac{1}{\sqrt{2\pi}} \int_{-\infty}^{\infty} \hat{f}(\eta)\hat{g}(\eta)\mathrm{e}^{-i\eta y}\, d\eta \tag{2.59}$$

where

$$f \star g(y) \equiv \frac{1}{\sqrt{2\pi}} \int_{-\infty}^{\infty} f(v)g(y - v)\, dv. \tag{2.60}$$

Starting with $\hat{f}(\eta)$ and $\hat{g}(\eta)$ in the form (2.59) and using (2.57) the inverse transform can be written in the form (2.60):

$$\begin{aligned} F(y,z) &= \frac{1}{2\pi}\int_{-\infty}^{\infty} F(v,d+)\left[(z-d)\alpha_0\sqrt{i}\sqrt{\frac{2}{\pi}}P(y-v,z-d)\right]dv \\ &= \frac{(z-d)\alpha_0\sqrt{i}}{\pi}\int_{-\infty}^{\infty} F(v,d+)P(y-v,z-d)\,dv. \end{aligned} \tag{2.61}$$

Now if (2.57) is rewritten using $\eta = 0$, $y = y - v$ and $z = z - d$ with v as the new variable the result is

$$\frac{(z-d)\alpha_0\sqrt{i}}{\pi}\int_{-\infty}^{\infty} P(y-v,z-d)\,dv = \mathrm{e}^{-(z-d)\alpha_0\sqrt{i}}. \tag{2.62}$$

Multiplying this by $F(y,d+)$ and subtracting it from both sides of (2.61) removes the non-integrable singularity in P at $v = y$ when $z = d+$ and leaves us with

$$\begin{aligned} &F(y,z) - F(y,d+)\mathrm{e}^{-(z-d)\alpha_0\sqrt{i}} = \\ &\qquad \frac{(z-d)\alpha_0\sqrt{i}}{\pi}\int_{-\infty}^{\infty}[F(v,d+) - F(y,d+)]P(y-v,z-d)\,dv. \end{aligned} \tag{2.63}$$

which, if the integral is taken as a Cauchy principal value, is convergent on $z = d+$. Differentiation in z and evaluation on $z = d+$ results in

$$\begin{aligned} &F'(y,d+) + \alpha_0\sqrt{i}F(y,d+) = \\ &\qquad \frac{\alpha_0\sqrt{i}}{\pi}\int_{-\infty}^{\infty}[F(v,d+) - F(y,d+)]\frac{K_1(|y-v|\alpha_0\sqrt{i})}{|y-v|}\,dv \end{aligned} \tag{2.64}$$

which is the integral boundary condition on $z = d$ for both X and U.

Chapter 3

EQUATIONS FOR THE ANOMALOUS ELECTROMAGNETIC FIELD

3.1 General Equations

It has been noted (Coggon,1971; Wannamaker et al.,1987) that numerical techniques which solve for the total field are prone to errors caused by the finite length of the computer word especially when single precision arithmetic is used in the calculations. To prevent this problem, which is especially prominent at low frequencies, the program presented in this thesis will solve directly for the much smaller anomalous field variations. This technique is most useful for those cases where the one-dimenstional conductivity structures at the left and right-hand sides of the model are identical or at least similar. In most real geophysical situations this is the case. If the 1D structures at the edges of the model are completely different then using the anomalous fields will not provide any additional accuracy but in the worst case the solution will be as accurate as that which would be obtained by solving for the total field. Wannamaker et al. (1987) have shown that

solving for the anomalous field using single precision computations results in accuracy comparable to solving for the total field using double precision computations. This means that a program that solves for the anomalous field could be converted to run using single precision calculations which would enable it to run faster or be used on less powerful personal computers such as those that are often used on location during field work. The program in this thesis was, however, written in double precision. In this chapter the governing equations introduced in the previous chapter have been modified to solve for the anomalous field by separating out the 'host' field, which is defined to be the field generated by the 1D conductivity distribution on the left-hand side of the model. This was accomplished by a simple substitution

$$F = F^{-} + \tilde{F} \tag{3.1}$$

where we have defined F as any component of the total electromagnetic field, F^{-} as the 1D host field and $\tilde{F}$ as the anomalous field. Following this notation we also have $\sigma = \sigma^{-} + \tilde{\sigma}$ where the host conductivity is the 1D conductivity distribution on the left side of the model and the anomalous conductivity is the difference between this and the total conductivity. From the definition of F^{-} it is obvious that X^{-} and U^{-} will be independent of the variable y and so $F^{-}(y,z)$ will be written as $F^{-}(z)$ and, likewise, $\sigma^{-}(y,z)$ will be written as $\sigma^{-}(z)$.

The B-polarization equation (2.23) (which can be written $\partial X/\partial z = \mu_0\sigma V$) becomes

$$\partial(X^- + \tilde{X})/\partial z = \mu_0\sigma(V^- + \tilde{V}). \tag{3.2}$$

Since the 1D host field also satisfies (2.23) (i.e. $\partial X^-/\partial z = \mu_0\sigma^- V^-$) we have

$$\partial\tilde{X}/\partial z = \mu_0\sigma\tilde{V} + \mu_0\tilde{\sigma}V^-. \tag{3.3}$$

Similarly (2.22) and (2.24) transform to

$$\partial\tilde{W}/\partial y - \partial\tilde{V}/\partial z = -i\omega\tilde{X}, \tag{3.4}$$

and (since $W^- = \partial X^-/\partial y \equiv 0$)

$$\partial\tilde{X}/\partial y = -\mu_0\sigma\tilde{W} \tag{3.5}$$

respectively. The E-polarization equations (2.25), (2.26) and (2.27) become

$$\partial\tilde{Z}/\partial y - \partial\tilde{Y}/\partial z = \mu_0\sigma\tilde{U} + \mu_0\tilde{\sigma}U^-, \tag{3.6}$$

$$\partial\tilde{U}/\partial z = -i\omega\tilde{Y}, \tag{3.7}$$

$$\partial\tilde{U}/\partial y = i\omega\tilde{Z}. \tag{3.8}$$

The differential equation (2.33) satisfied by both X and U can be transformed to

$$\nabla^2\tilde{F} = i\kappa\tilde{F} + i\omega\mu_0\tilde{\sigma}F^- \tag{3.9}$$

where we recall $\kappa = \omega\mu_0\sigma$.

If σ is not a constant in the area under study then we must use the anomalous form of (2.31)

$$\frac{\partial^2 \tilde{X}}{\partial y^2} + \frac{\partial^2 \tilde{X}}{\partial z^2} - \frac{1}{\sigma}\frac{\partial \sigma}{\partial y}\frac{\partial \tilde{X}}{\partial y} - \frac{1}{\sigma}\frac{\partial \sigma}{\partial z}\frac{\partial \tilde{X}}{\partial z} = i\kappa\tilde{X} + i\omega\mu_0\tilde{\sigma}X^- + \left(\frac{1}{\sigma}\frac{\partial \sigma}{\partial z} - \frac{1}{\sigma^-}\frac{\partial \sigma^-}{\partial z}\right)\frac{\partial X^-}{\partial z} \tag{3.10}$$

for the B-polarization case.

3.2 Surface Boundary Conditions

The surface condition for the B-polarization case given in (2.34) can be written as

$$X^-(0-) + \tilde{X}(y, 0-) = X_0 \tag{3.11}$$

where, for a uniform primary magnetic field B_0, $X_0 = 2B_0$. As $y \to -\infty$, $\sigma(y, z) \to \sigma^-(z)$ and it follows that $\tilde{X}(y, 0-) \to 0$ reducing (3.10) to

$$X^-(0-) = X_0. \tag{3.12}$$

Since $X^-(0-)$ is constant and, from (2.34), $X(y, 0-)$ is constant the anomalous field must also be constant and is given by

$$\tilde{X}(y, 0-) = 0 \tag{3.13}$$

which serves as the surface boundary condition for the B-polarization case. This simple equation can be used in this form in the finite difference program.

Substitution of (3.1) in the surface boundary condition for the E-polarization case (2.46) results in

$$(U')^-(0-) + \tilde{U}'(y, 0-) = -i\omega Y_0$$

$$-\frac{1}{\pi}\fint_{-\infty}^{\infty}\frac{U^-(0)+\tilde{U}(v,0)-U^-(0)-\tilde{U}(y,0)}{(v-y)^2}\,dv \tag{3.14}$$

where $U^-(v,0) = U^-(y,0) = U^-(0)$. Using the host field solution of (2.26), $(U')^-(0-) = -i\omega Y_0$, we can simplify the above equation to

$$\tilde{U}'(y,0-) = -\frac{1}{\pi}\fint_{-\infty}^{\infty}\frac{\tilde{U}(v,0)-\tilde{U}(y,0)}{(v-y)^2}\,dv \tag{3.15}$$

which is the surface boundary condition for the E-polarization case. This equation must be converted into a form than can be programmed into the finite difference equation. This is done in Chapter 4.

3.3 Side Boundary Conditions

Starting with (2.47) and (2.48) and recalling that the anomalous field vanishes as $y \to -\infty$ we have

$$\tilde{X}(-\infty,z) = \tilde{X}^-(z) = 0 \tag{3.16}$$

$$\tilde{U}(-\infty,z) = \tilde{U}^-(z) = 0 \tag{3.17}$$

$$\tilde{X}(+\infty,z) = \tilde{X}^+(z) = X^+(z) - X^-(z) \tag{3.18}$$

$$\tilde{U}(+\infty,z) = \tilde{U}^+(z) = U^+(z) - U^-(z) \tag{3.19}$$

where $X^-(z) = X^-(-\infty,z)$ and $U^-(z) = U^-(-\infty,z)$ since the host fields are independent of y and the host field *is* the total field at $y \to -\infty$.

3.4 Bottom Boundary Conditions

The boundary conditions for the case where the model's underlying half-space is a perfect conductor (2.52) are satisfied by both the total fields (X and U) and the 1D host fields (X^- and U^-). Therefore, equation (3.1) implies that

$$\tilde{X}'(y,d) = 0, \quad \tilde{U}(y,d) = 0 \tag{3.20}$$

which are the boundary conditions on $z = d$ for this case.

For the more general case ($\sigma_0 \neq \infty$) we use (3.1) together with (2.64) to obtain

$$\tilde{F}'(y,d+) + \alpha_0\sqrt{i}\tilde{F}(y,d+)$$
$$= \frac{\alpha_0\sqrt{i}}{\pi} \int_{-\infty}^{\infty} [\tilde{F}(v,d+) - \tilde{F}(y,d+)] \frac{K_1(|y-v|\alpha_0\sqrt{i})}{|y-v|}\, dv \tag{3.21}$$

where the $F^-(d+)$ terms in the integrand cancel each other. This equation is developed further in Chapter 4. In $z > d$ equations (2.49) and (2.50) give the general 1D equation

$$(F'')^- = i\omega\mu_0\sigma_0 F^- \tag{3.22}$$

whose solution is

$$F^-(z) = F(d+)\mathrm{e}^{-(z-d)\alpha_0\sqrt{i}}. \tag{3.23}$$

From this it is obvious that

$$(F')^-(d+) = -\alpha_0\sqrt{i}F^-(d+). \tag{3.24}$$

This property of the 1D (host) solution was used to cancel the host field terms that were generated on the left side of (3.22). Note that α_0 has no minus sign

superscript since in $z > d$ we are dealing with a homogeneous half space implying that $\sigma = \sigma_0 = \sigma^-$ while $\tilde{\sigma} = 0$.

Chapter 4

EQUATIONS FOR NUMERICAL SOLUTION OF THE TWO-DIMENSIONAL INDUCTION PROBLEM

4.1 Introduction

The work done in this chapter is, for the most part, based on earlier work done chiefly by Schmucker (1970), Wait (1953), Brewitt-Taylor and Weaver (1976), Weaver and Brewitt-Taylor (1978) and Weaver (1994). All calculations performed with the anomalous fields are original although the solution methods are not. Finite difference forms for the solution of the anomalous fields at a general point in the grid are developed as well as finite difference forms of the anomalous boundary conditions. These equations make up a set of simultaneous linear equations that govern the field values at the nodes of the grid. The resulting sparse matrix of coefficients is solved by the computer program to give U or X at each point in the grid.

4.2 Finite Difference Methods

To solve the 2D problem numerically we must first discretize the model (see Fig. 4.1). We set up a grid that covers all anomalies and extends out far enough away from them that it is valid to say that the 2D problem degenerates to a 1D problem at the sides.

The region $z > 0$ is covered by $M \times N$ nodes (y_m, z_n) where $z_1 = 0$ with separations $k_n = z_{n+1} - z_n$, $(n = 1, 2, \ldots, N-1)$ and $h_m = y_{m+1} - y_m$, $(m = 1, 2, \ldots, M-1)$. The conductivity between z_n and z_{n+1} in z and y_m and y_{m+1} in y is $\sigma_{m,n}$. The region $z > z_N$ is an underlying half space with uniform conductivity σ_N.

If the grid is set up properly then the fields at y_1 and y_M can be related to the values of the 1D solutions at $-\infty$ and $+\infty$ respectively. For this reason the field values at y_1 and y_M which make the transition between the normal 2D grid equations and the 1D edges require the special treatment discussed in §4.4. The surface boundary conditions govern all field values at $z = z_1$ and the bottom boundary conditions govern all those at $z = z_N$. The interior nodes (y_m, z_n) are those with $m = 2, 3, \ldots, M-1$ and $n = 2, 3, \ldots, N-1$.

The finite difference method (see, for instance, Press et al. 1992) approximates first and second derivatives of the field by central difference formulae obtained by expanding the field in a Taylor series. For example if $F(y, z_n) = F(y)$ is a general component of the electromagnetic field with continuous derivatives then the Taylor

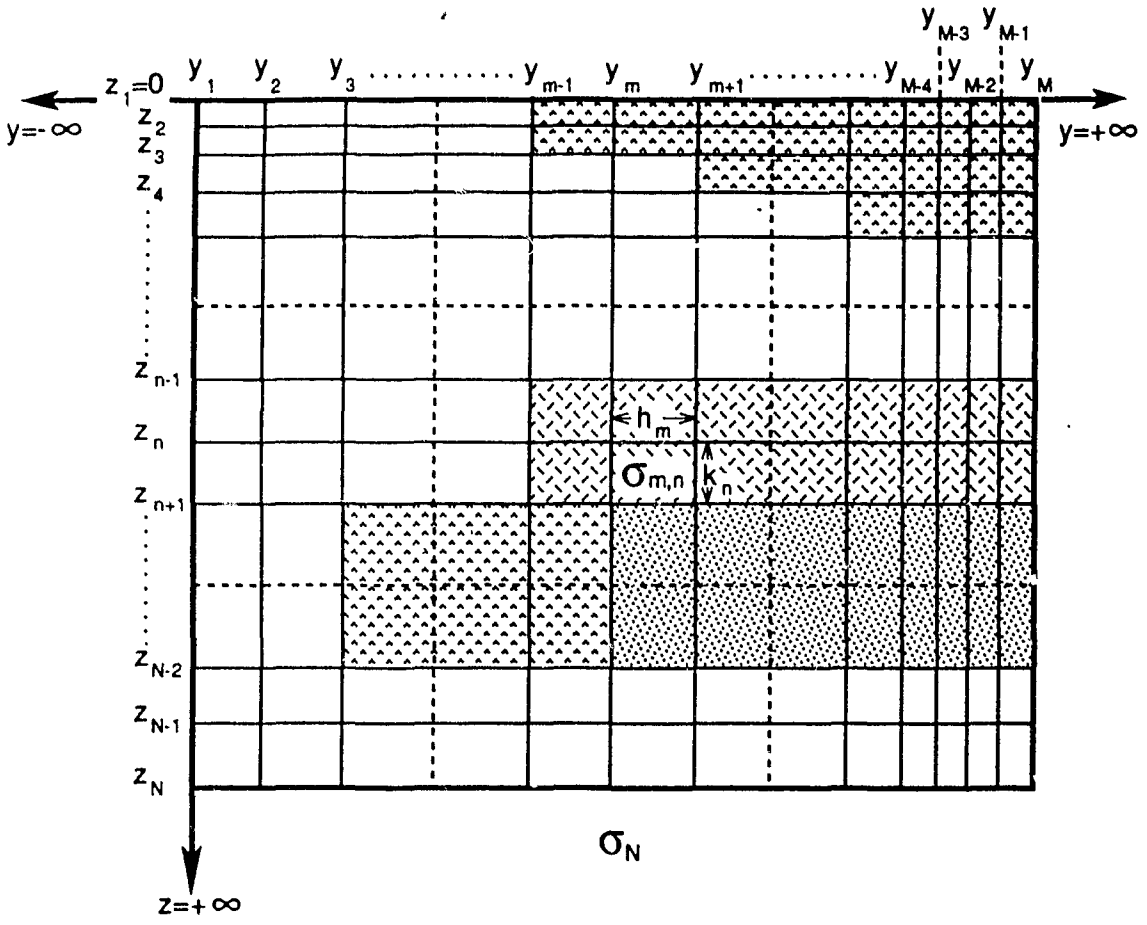

Figure 4.1: The two-dimensional numerical grid showing the notation used to descibe to positions of the grid lines and cell lengths, widths and conductivities.

expansions about $y = y_m$ yield

$$F(y_{m+1}) = F(y_m) + h_m \frac{\partial F(y_m)}{\partial y} + \frac{1}{2} h_m^2 \frac{\partial^2 F(y_m)}{\partial y^2} \tag{4.1}$$

$$F(y_{m-1}) = F(y_m) - h_{m-1} \frac{\partial F(y_m)}{\partial y} + \frac{1}{2} h_{m-1}^2 \frac{\partial^2 F(y_m)}{\partial y^2} \tag{4.2}$$

where terms higher than second order have been ignored. Multiplying the first equation by h_{m-1} and the second by h_m enables us to eliminate the first derivative by adding the equations together. Similarly multiplying the first equation by h_{m-1}^2 and the second by h_m^2 allows the elimination of the second derivative so that we are left with the approximations

$$\frac{\partial F(y_m)}{\partial y} = \frac{h_{m-1}}{h_m h_m^+} F(y_{m+1}) + \frac{h_m^-}{h_m h_{m-1}} F(y_m) - \frac{h_m}{h_{m-1} h_m^+} F(y_{m-1}) \tag{4.3}$$

$$\frac{\partial^2 F(y_m)}{\partial y^2} = \frac{2}{h_m h_m^+} F(y_{m+1}) - \frac{2}{h_m h_{m-1}} F(y_m) + \frac{2}{h_{m-1} h_m^+} F(y_{m-1}) \tag{4.4}$$

where $h_m^+ = h_m + h_{m-1}$ and $h_m^- = h_m - h_{m-1}$. These are the well known central difference formulae for the first and second derivatives (see e.g. Weaver 1994). In contrast a less accurate one-sided difference formula would involve only $F(y_m)$ and one other field value (i.e. either $F(y_{m-1})$ or $F(y_{m+1})$).

For a Taylor expansion, and hence these formulae, to be valid the node separation must be kept small. The exact size will depend on the size of the higher order derivatives but is usually a fraction of the skin depth of the region which contains the nodes in question. It is obvious that near conductivity boundaries, where the derivatives are larger, grid spacing must be finer. Details of the gridding procedure are discussed in chapter 5.

4.3 One-Dimensional Solution at Grid Edges

At $y \rightarrow \pm\infty$ the solutions for the E-polarization and B-polarization problems are $X^{\pm}$ and $U^{\pm}$ as discussed in §2.4. These are the solutions to the one-dimensional conductivity distributions at the right and left hand edges of the grid. All that is required are the total field solutions since (3.16) – (3.19) easily provide $\tilde{X}^{\pm}$ and $\tilde{U}^{\pm}$ in terms of $X^{\pm}$ and $U^{\pm}$. For a uniform field and a 1D layered earth as shown in Fig. 4.2 the solutions are known to be

$$X^{\pm}(z) = -X_0 c(\omega) e'_{\pm}(z) \tag{4.5}$$

$$U^{\pm}(z) = i\omega Y_0 c(\omega) e_{\pm}(z) \tag{4.6}$$

where, dropping the $\pm$,

$$e(z) = e_{n+1}\cosh\left[\gamma_n(z_{n+1}-z)\right] - \frac{e'_{n+1}}{\gamma_n}\sinh\left[\gamma_n(z_{n+1}-z)\right] \tag{4.7}$$

in the n^{th} layer (i.e. $z_n < z < z_{n+1}$) and the transfer function $c(\omega)$ is obtained through the recursion relations

$$c_n = \frac{1 + c_{n+1}\gamma_n - (1 - c_{n+1}\gamma_n)e^{-2\gamma_n d_n}}{\gamma_n[1 + c_{n+1}\gamma_n + (1 - c_{n+1}\gamma_n)e^{-2\gamma_n d_n}]} \tag{4.8}$$

$$c_N = \frac{1}{\gamma_N}. \tag{4.9}$$

In the above equations $\gamma_n = \sqrt{i}\alpha_n = \sqrt{i\omega\mu_0\sigma_n}$ and $d_n = z_{n+1} - z_n$ with $z_1 = 0$ and $z_{N+1} = \infty$. Unlike the nodes of the grid z_n mentioned in §4.1 the z_n in Fig. 4.2 separate areas of different conductivity σ_n. So the above formulae are not used

on grid nodes inside the layers but only on those at boundaries between them. The d_n used are then the distances between these boundaries.

Starting with (4.9) and knowing the 1D conductivity distribution c_N can be found. If the underlying half space is a perfect conductor then, from (4.9), $c_N = 0$. Using (4.8) and stepping upwards through the layers results in a value for the transfer function $c(\omega) = c_1$. Then, starting with $e(z_1) = e(0) = 1$ and $e'(0) = -1/c(\omega)$, and using the recursion formulae

$$e_{n+1} = e_n \cosh \gamma_n d_n + \frac{e_n'}{\gamma_n} \sinh \gamma_n d_n \tag{4.10}$$

$$e_{n+1}' = \gamma_n e_n \sinh \gamma_n d_n + e_n' \cosh \gamma_n d_n \tag{4.11}$$

and (4.7) $e(z)$ and $e'(z)$ can be calculated at any depth z. In the N^{th} layer the fields must vanish as $z \rightarrow \infty$ so that

$$e(z) = e_N e^{-\gamma_N (z - z_N)}. \tag{4.12}$$

Knowing $c(\omega)$, $e(z)$ and $e'(z)$ equations (4.5) and (4.6) can be used to find X and U for the 1D conductivity distribution. This procedure was developed by Schmucker (1970, §5.3) and others using the recursion formula (4.8) first obtained by Wait (1953) for the propagation of radio waves.

In fact (4.8) is essentially Schmucker's equation (5.44) using different notation and the tanh function instead of the exponential. Other references are Summers and Weaver (1973) and a review by Weaver(1973).

The recursion relations (4.10) and (4.11) contain positive exponentials in the cosh and sinh functions which could cause problems if $\gamma_n d_n$ becomes large. To

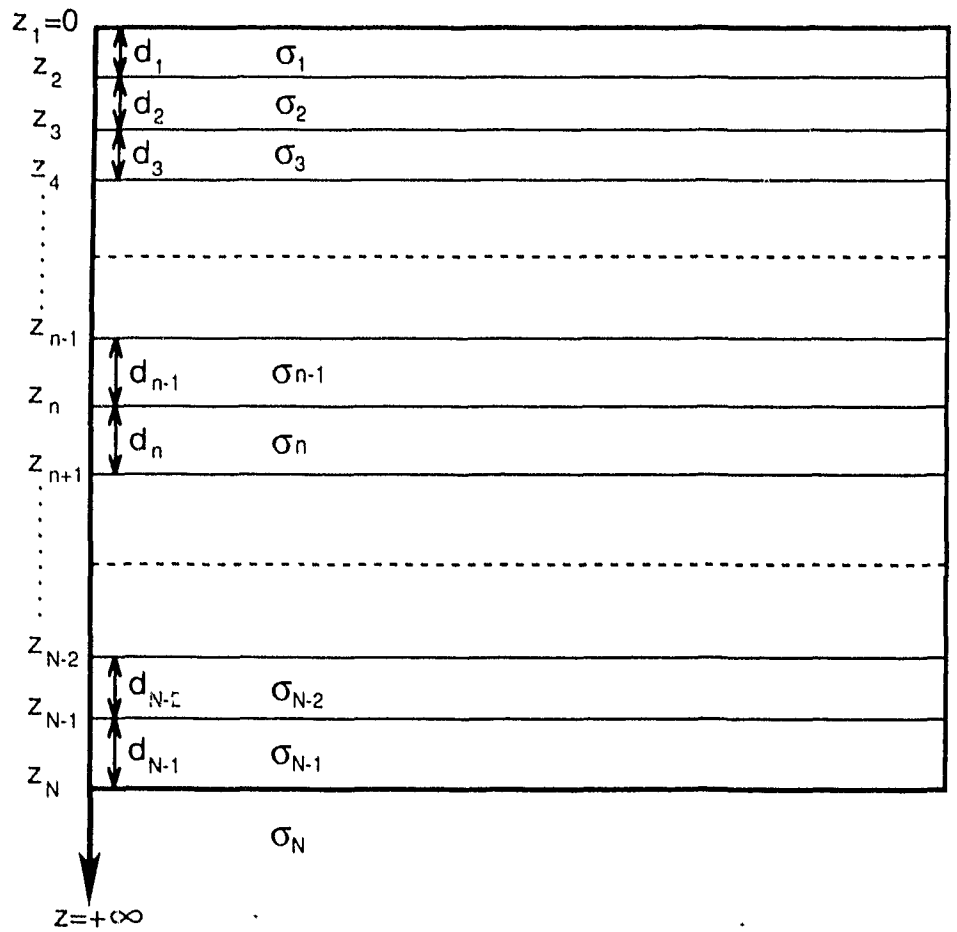

Figure 4.2: A one-dimensional layered earth model. Unlike the nodes of the grid z_n seen in Fig. 4.1 the z_n in this figure *all* separate areas of different conductivity.

avoid possible errors during computation we modify the equations to eliminate all positive exponentials. Separating the positive and negative exponential terms causes (4.10) and (4.11) to become

$$e_{n+1} = (\frac{e_n}{2} + \frac{e_n^{'}}{2\gamma_n})e^{\gamma_n d_n} + (\frac{e_n}{2} - \frac{e_n^{'}}{2\gamma_n})e^{-\gamma_n d_n} \tag{4.13}$$

$$e_{n+1}^{'} = (\frac{\gamma_n e_n}{2} + \frac{e_n^{'}}{2})e^{\gamma_n d_n} + (\frac{-\gamma_n e_n}{2} + \frac{e_n^{'}}{2})e^{-\gamma_n d_n}. \tag{4.14}$$

From (4.10),(4.11) and (4.8) it can be verified that

$$c_n = -\frac{e_n}{e_n^{'}} \tag{4.15}$$

and this can be used to rewrite the two equations as

$$e_{n+1} = \frac{e_n}{2}(\frac{c_n\gamma_n - 1}{c_n\gamma_n})e^{\gamma_n d_n} + \frac{e_n}{2}(\frac{c_n\gamma_n + 1}{c_n\gamma_n})e^{-\gamma_n d_n} \tag{4.16}$$

$$-\frac{e_{n+1}}{c_{n+1}\gamma_n} = \frac{e_n}{2}(\frac{c_n\gamma_n - 1}{c_n\gamma_n})e^{\gamma_n d_n} + \frac{e_n}{2}(\frac{-c_n\gamma_n - 1}{c_n\gamma_n})e^{-\gamma_n d_n} \tag{4.17}$$

where (4.15) has been used on the left hand side of (4.14) and the result divided by γ_n. Subtracting the above equations and rearranging slightly leaves

$$e_{n+1} = \frac{c_{n+1}e_n(1 + c_n\gamma_n)e^{-\gamma_n d_n}}{c_n(1 + c_{n+1}\gamma_n)}. \tag{4.18}$$

If the c_n values have been stored during the calculation of $c(\omega)$, (4.18) and (4.15) will yield all the required values of e_n and $e_n^{'}$ using a starting value of $e_1 = 1$. The field in the n^{th} layer ($n = 1, 2, \ldots, N-1$) is then

$$\begin{aligned} e(z) \;=\; & \frac{e_n c_{n+1}(1 + c_n\gamma_n)}{2c_n(1 + c_{n+1}\gamma_n)}\left[e^{-\gamma_n(z - z_n)} + e^{-\gamma_n(2d_n + z_n - z)}\right] \\ & + \frac{e_n(1 + c_n\gamma_n)}{2c_n\gamma_n(1 + c_{n+1}\gamma_n)}\left[e^{-\gamma_n(z - z_n)} - e^{-\gamma_n(2d_n + z_n - z)}\right] \end{aligned} \tag{4.19}$$

which further reduces to

$$e(z) = \frac{e_n(1 + c_n\gamma_n)}{2c_n\gamma_n}\left[e^{-\gamma_n(z-z_n)} - r_n e^{-\gamma_n(2d_n+z_n-z)}\right] \tag{4.20}$$

where

$$r_n = \frac{1 - c_{n+1}\gamma_n}{1 + c_{n+1}\gamma_n}. \tag{4.21}$$

From (4.20) it is obvious that

$$e'(z) = -\frac{e_n(1 + c_n\gamma_n)}{2c_n}\left[e^{-\gamma_n(z-z_n)} + r_n e^{-\gamma_n(2d_n+z_n-z)}\right]. \tag{4.22}$$

These equations, together with (4.5), (4.6) and (4.8) provide us with the 1D solutions used in solving the 2D problem. These were programmed into the subroutine ONED in Appendix A to obtain the 1D solutions at the for the fields at $y = -\infty$ and $y = +\infty$.

4.4 Solution for Interior Nodes

The solution for the interior nodes is derived using a method based on that used by Brewitt-Taylor and Weaver (1976). In the E-polarization problem the electric field component U satisfies the differential equation (2.32)

$$i\omega\mu_0\sigma U = \frac{\partial^2 U}{\partial y^2} + \frac{\partial^2 U}{\partial z^2}. \tag{4.23}$$

Since U is a scalar the above equation can be rewritten as

$$i\omega\mu_0\sigma U = \mathrm{div}(\mathrm{grad}U). \tag{4.24}$$

Next a set of grid points on the grid Fig. 4.3 is chosen and elements with boundaries midway between the points are defined. Integrating (4.24) over the area of the dotted rectangle and applying the divergence theorem to the right hand side leaves

$$i\omega\mu_0 \int \sigma U dA = \oint_C \frac{\partial U}{\partial n} dl \tag{4.25}$$

where $\partial U/\partial n$ is the normal derivative at the boundary of the enclosed area. The integral on the left hand side of (4.25) can be written as the sum of the integrals of the four subrectangles of different σ. Inside the dotted rectangle we assume $U(y,z) = U_{m,n}$ so (4.25) can take the form

$$\begin{aligned} &i\omega\mu_0 U_{m,n}\left(\sigma_{m,n-1}\int dA_1 + \sigma_{m,n}\int dA_2 + \sigma_{m-1,n}\int dA_3 + \sigma_{m-1,n-1}\int dA_4\right) \\ &= \frac{U_{m+1,n}-U_{m,n}}{h_m}\int dl_1 + \frac{U_{m,n+1}-U_{m,n}}{k_n}\int dl_2 + \frac{U_{m-1,n}-U_{m,n}}{h_{m-1}}\int dl_3 \\ &+ \frac{U_{m,n-1}-U_{m,n}}{k_{n-1}}\int dl_4 \end{aligned} \tag{4.26}$$

where the derivative on the right hand side of (4.25) has been replaced by its finite difference approximation and the areas A_1, A_2, A_3, A_4 and the lengths l_1, l_2, l_3, l_4 are shown in Fig. 4.3. Evaluating the integrals in (4.26) and writing the areas and lengths in terms of k_{n-1}, k_n, h_{m-1} and h_m gives

$$\begin{aligned} &i\omega\mu_0 U_{m,n}\left(\sigma_{m,n-1}\frac{h_m k_{n-1}}{4} + \sigma_{m,n}\frac{h_m k_n}{4} + \sigma_{m-1,n}\frac{h_{m-1}k_n}{4} + \sigma_{m-1,n-1}\frac{h_{m-1}k_{n-1}}{4}\right) \\ &= \frac{k_n^+}{2}\frac{U_{m+1,n}-U_{m,n}}{h_m} + \frac{h_m^+}{2}\frac{U_{m,n+1}-U_{m,n}}{k_n} + \frac{k_n^+}{2}\frac{U_{m-1,n}-U_{m,n}}{h_{m-1}} \\ &+ \frac{h_m^+}{2}\frac{U_{m,n-1}-U_{m,n}}{k_{n-1}} \end{aligned} \tag{4.27}$$

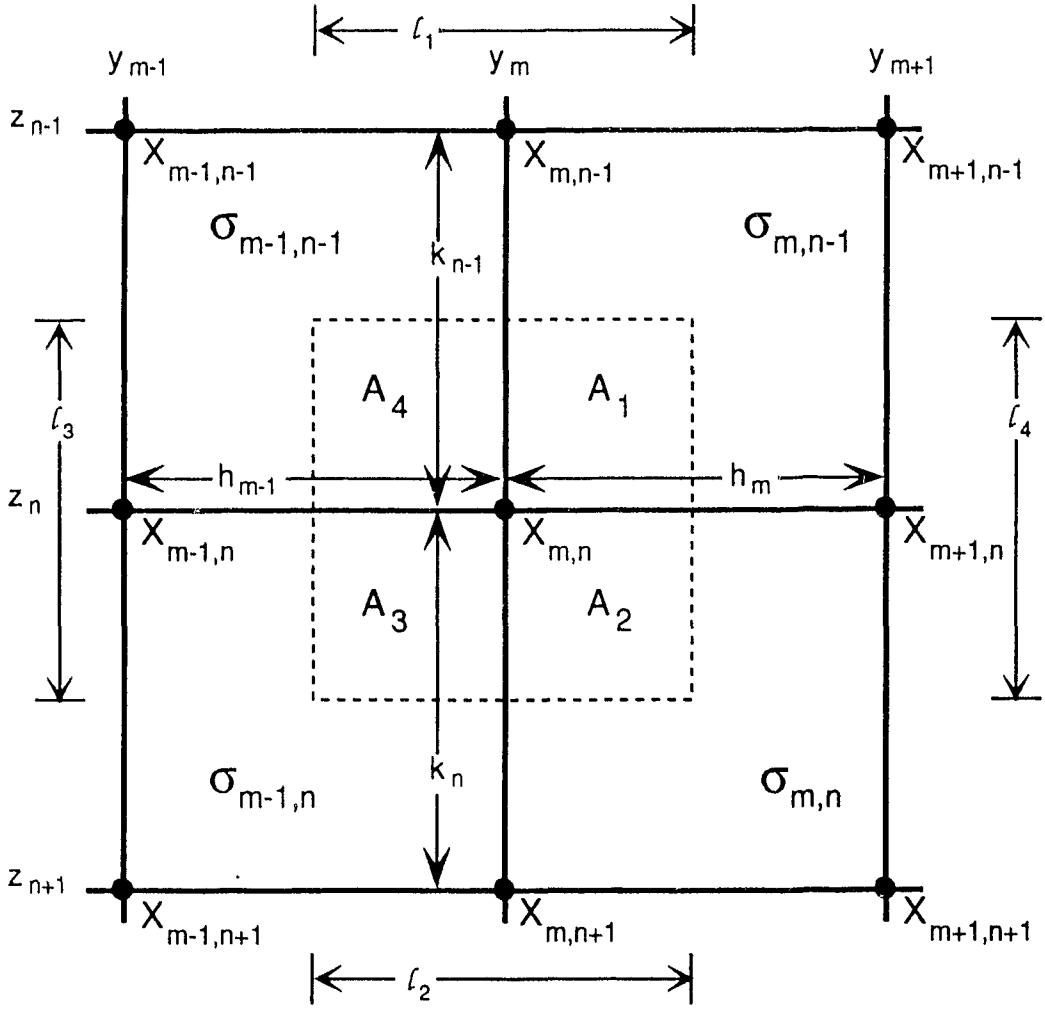

Figure 4.3: A general node (m, n) in the numerical grid showing the notation for magnetic fields at each grid point as well as some commonly used parameters such as cell sizes in y and z (h and k respectively).

where $k_n^+ = k_{n-1} + k_n$ and $h_m^+ = h_{m-1} + h_m$. Dividing through by $\frac{1}{2}h_m^+ k_n^+$ and rearranging yields

$$\left(\frac{1}{h_{m-1}h_m} + \frac{1}{k_{n-1}k_n} + \frac{i\omega\mu_0}{2}\overline{\sigma}_{m,n}\right) U_{m,n} = \frac{U_{m,n-1}}{k_{n-1}k_n^+} + \frac{U_{m+1,n}}{h_m h_m^+} + \frac{U_{m,n+1}}{k_n k_n^+} + \frac{U_{m-1,n}}{h_{m-1}h_m^+} \tag{4.28}$$

where

$$\overline{\sigma}_{m,n} = \frac{h_m k_{n-1}\sigma_{m,n-1} + h_m k_n \sigma_{m,n} + h_{m-1}k_n\sigma_{m-1,n} + h_{m-1}k_{n-1}\sigma_{m-1,n-1}}{h_m^+ k_n^+}. \tag{4.29}$$

This previously known equation (see e.g. Weaver 1994) is now modified by substituting for the total fields with the anomalous and host fields as in chapter 3. We note that the host field U_n^- must also satisfy (4.28) with (4.29) simplifying to

$$\overline{\sigma}_n^- = \frac{k_{n-1}}{k_n^+}\sigma_{n-1}^- + \frac{k_n}{k_n^+}\sigma_n^-. \tag{4.30}$$

We transform (4.28) to the equation for the anomalous $\tilde{U}_{m,n}$

$$\frac{\tilde{U}_{m,n-1}}{k_{n-1}k_n^+} + \frac{\tilde{U}_{m+1,n}}{h_m h_m^+} + \frac{\tilde{U}_{m,n+1}}{k_n k_n^+} + \frac{\tilde{U}_{m-1,n}}{h_{m-1}h_m^+} = \left(\frac{1}{h_{m-1}h_m} + \frac{1}{k_{n-1}k_n} + \frac{i\omega\mu_0}{2}\overline{\sigma}_{m,n}\right)\tilde{U}_{m,n} + \frac{i\omega\mu_0}{2}[\overline{\sigma}_{m,n} - \overline{\sigma}_n^-]U_n^-. \tag{4.31}$$

This, in turn, can be written in a manner that somewhat simplifies the calculation of the coefficients.

$$C_1\tilde{U}_{m,n-1} + C_2\tilde{U}_{m+1,n} + C_3\tilde{U}_{m,n+1} + C_4\tilde{U}_{m-1,n} = (C_5 + i)\tilde{U}_{m,n} + i\left(1 - \frac{\overline{\sigma}_n^-}{\overline{\sigma}_{m,n}}\right)U_n^- \tag{4.32}$$

where

$$C_0 = \omega\mu_0\overline{\sigma}_{m,n}h_m^+ k_n^+ \tag{4.33}$$

$$C_1 = \frac{h_m^+}{k_{n-1}C_0} \tag{4.34}$$

$$C_2 = \frac{k_n^+}{h_m C_0} \tag{4.35}$$

$$C_3 = \frac{h_m^+}{k_n C_0} \tag{4.36}$$

$$C_4 = \frac{k_n^+}{h_{m-1}C_0} \tag{4.37}$$

and

$$C_5 = C_1 + C_2 + C_3 + C_4. \tag{4.38}$$

which is similar to the equation used by Brewitt-Taylor and Weaver (1976) for the solution of the total field. The equation (4.38) is the finite difference expression used in the numerical solution for all interior nodes $m = 2, 3, \ldots, M-1$, $n = 2, 3, \ldots, N-1$.

In the B-polarization case we use the general differential equation (2.31) satisfied by the magnetic field component X where no assumptions are made about the value of σ (i.e. it need not be constant). Using, once again, the method of Brewitt-Taylor and Weaver (1976) it can be seen that by rearranging slightly and simplifying the form of the equation by using resistivities instead of conductivities (2.31) becomes

$$i\omega\mu_0 X = \frac{\partial}{\partial y}\left(\rho\frac{\partial X}{\partial y}\right) + \frac{\partial}{\partial z}\left(\rho\frac{\partial X}{\partial z}\right) \tag{4.39}$$

and since X is a scalar

$$i\omega\mu_0 X = \mathrm{div}\,(\rho\,\mathrm{grad}X). \tag{4.40}$$

After using a similar set of grid points and notation as shown in Fig. 4.3, integrating once again over the area of the rectangle and applying the divergence theorem as before it is found that

$$i\omega\mu_0 \int X dA = \oint_C \rho \frac{\partial X}{\partial n} dl \tag{4.41}$$

where $\partial X/\partial n$ is the derivative normal to the boundary of the rectangle. The left hand side integral is easy to evaluate since $X(y,z) = X_{m,n}$ is a constant inside the dotted rectangle. Because of the presence of ρ inside the integral on the right hand side of (4.41) the integral must be split into a sum of eight others instead of four as was done for E-polarization. This is written as

$$\begin{aligned} i\omega\mu_0 X_{m,n} \int dA = & \frac{X_{m,n-1} - X_{m,n}}{k_{n-1}} \left(\rho_{m-1,n-1} \int dl + \rho_{m,n-1} \int dl \right) \\ & + \frac{X_{m+1,n} - X_{m,n}}{h_m} \left(\rho_{m,n-1} \int dl + \rho_{m,n} \int dl \right) \\ & + \frac{X_{m,n+1} - X_{m,n}}{k_n} \left(\rho_{m,n} \int dl + \rho_{m-1,n} \int dl \right) \\ & + \frac{X_{m-1,n} - X_{m,n}}{h_{m-1}} \left(\rho_{m-1,n} \int dl + \rho_{m-1,n-1} \int dl \right) \end{aligned} \tag{4.42}$$

where the normal derivatives for the subintegrals have been expressed in their finite difference form. The integrated area on the left is just the area of the dotted rectangle and the lengths on the right are the lengths l_1, l_2, l_3, l_4 where each has been divided into two at the boundary between regions of different ρ. So expressing (4.42) in terms of h_{m-1}, h_m, k_{n-1} and k_n we obtain

$$\begin{aligned} i\omega\mu_0 X_{m,n} \frac{h_m^+ k_n^+}{4} = & \left(\frac{h_{m-1}\rho_{m-1,n-1}}{2} + \frac{h_m \rho_{m,n-1}}{2} \right) \frac{X_{m,n-1} - X_{m,n}}{k_{n-1}} \\ & + \left(\frac{k_{n-1}\rho_{m,n-1}}{2} + \frac{k_n \rho_{m,n}}{2} \right) \frac{X_{m+1,n} - X_{m,n}}{h_m} \end{aligned}$$

$$+\left(\frac{h_m\rho_{m,n}}{2}+\frac{h_{m-1}\rho_{m-1,n}}{2}\right)\frac{X_{m,n+1}-X_{m,n}}{k_n}$$
$$+\left(\frac{k_n\rho_{m-1,n}}{2}+\frac{k_{n-1}\rho_{m-1,n-1}}{2}\right)\frac{X_{m-1,n}-X_{m,n}}{h_{m-1}} \tag{4.43}$$

where h_m^+ and k_n^+ are defined as before. After some rearrangement the above equation becomes

$$\left[\frac{h_m^2+k_{n-1}^2}{h_m k_{n-1}}\rho_{m,n-1}+\frac{h_m^2+k_n^2}{h_m k_n}\rho_{m,n}+\frac{h_{m-1}^2+k_n^2}{h_{m-1}k_n}\rho_{m-1,n}\right.$$
$$\left.+\frac{h_{m-1}^2+k_{n-1}^2}{h_{m-1}k_{n-1}}\rho_{m-1,n-1}+\frac{i\omega\mu_0 h_m^+ k_n^+}{2}\right]X_{m,n}$$
$$=\frac{h_{m-1}\rho_{m-1,n-1}+h_m\rho_{m,n-1}}{k_{n-1}}X_{m,n-1}+\frac{k_{n-1}\rho_{m,n-1}+k_n\rho_{m,n}}{h_m}X_{m+1,n}$$
$$+\frac{h_{m-1}\rho_{m-1,n}+h_m\rho_{m,n}}{k_n}X_{m,n+1}+\frac{k_{n-1}\rho_{m-1,n-1}+k_n\rho_{m-1,n}}{h_{m-1}}X_{m-1,n}. \tag{4.44}$$

Next we once again convert the equations to solve for the anomalous fields. In order to make the conversion to the anomalous form of (4.44) easier to follow we can write the above equation as

$$C_1X_{m,n-1}+C_2X_{m+1,n}+C_3X_{m,n+1}+C_4X_{m-1,n}=(C_5+i)X_{m,n} \tag{4.45}$$

where

$$C_0=\frac{1}{2}\omega\mu_0 h_m^+ k_n^+ \tag{4.46}$$

$$C_1=\frac{h_{m-1}\rho_{m-1,n-1}+h_m\rho_{m,n-1}}{k_{n-1}C_0} \tag{4.47}$$

$$C_2=\frac{k_{n-1}\rho_{m,n-1}+k_n\rho_{m,n}}{h_m C_0} \tag{4.48}$$

$$C_3=\frac{h_{m-1}\rho_{m-1,n}+h_m\rho_{m,n}}{k_n C_0} \tag{4.49}$$

$$C_4=\frac{k_{n-1}\rho_{m-1,n-1}+k_n\rho_{m-1,n}}{h_{m-1}C_0} \tag{4.50}$$

and

$$C_5 = C_1 + C_2 + C_3 + C_4. \tag{4.51}$$

Note that C_0 is independent of ρ while C_1 to C_5 are dependent on ρ unlike the E-polarization case where the reverse was true. It is because of this that the transformation to the anomalous field results in more terms involving the host field than it did in the E-polarization problem. Substituting the anomalous and host fields into equation (4.45) and using the fact that the host field is constant in y to simplify the result, we have

$$C_1\tilde{X}_{m,n-1} + C_2\tilde{X}_{m+1,n} + C_3\tilde{X}_{m,n+1} + C_4\tilde{X}_{m-1,n} =$$

$$= (C_5 + i)\tilde{X}_{m,n} - C_1X^-_{n-1} - (C_2 + C_4 - C_5 - i)X^-_n - C_3X^-_{n+1}. \tag{4.52}$$

This equation is the B-polarization finite difference expression that was used in the numerical solution for all interior nodes (y_m, z_n) with $m = 2, 3, \ldots, M-1$ and $n = 2, 3, \ldots, N-1$.

4.5 Side Boundary Conditions

The solution for the side nodes is presented first since the equations given here are used later in the top and bottom boundary conditions.

In the E-polarization problem we use the asymptotic boundary conditions developed by Weaver and Brewitt-Taylor (1978) which allow us to reduce the overall size of the grid. On the surface $z = 0$ they showed that

$$\left(1 + y\frac{\partial}{\partial y}\right) U(y,0) \simeq U^{\pm} \tag{4.53}$$

where $U^+ = U(+\infty, 0)$ and $U^- = U(-\infty, 0)$. In $y \geq y_M$ the solution of (4.53) subject to the boundary condition $U(y_M, 0) = U_M$ is

$$U(y,0) = U^+ - y_M \frac{U^+ - U_M}{y} \tag{4.54}$$

which is also the finite difference form of (4.53). This equation is derived from equation (8) in Weaver and Brewitt-Taylor (1978) by neglecting terms of order $1/y^2$ and by solving it at $y = y_M$ to find a value for their $g'(0)$ term. In order to make the neglect of terms of the order of $1/y^2$ valid it is necessary to locate the origin of the grid in the approximate centre of the anomalous area. By doing this $|y_1|$ and $|y_M|$ will both be large enough to make this procedure valid (and y_1 will always be negative). What is needed is an equation connecting U_M with U_{M-1}. Using the central difference formula

$$\left(\frac{\partial U}{\partial y}\right)_M = \frac{U_{M+1} - U_{M-1}}{2h_{M-1}} \tag{4.55}$$

where U_{M+1} is the field value at $y_{M+1} = y_M + h_{M-1}$ and from (4.53)

$$\left(\frac{\partial U}{\partial y}\right)_M = \frac{U^+ - U_M}{y_M}. \tag{4.56}$$

We can equate the two values for the derivative so that

$$\frac{U_{M+1} - U_{M-1}}{2h_{M-1}} = \frac{U^+ - U_M}{y_M}. \tag{4.57}$$

Now since $y_{M+1} > y_M$ (4.54) can be used to write

$$U_{M+1} = U^+ - y_M \frac{U^+ - U_M}{y_M + h_{M-1}} \tag{4.58}$$

and by substitution for U_{M+1} using (4.57) the above equation becomes

$$2h_{M-1}\frac{U^+ - U_M}{y_M} + U_{M-1} = U^+ - y_M\frac{U^+ - U_M}{y_M + h_{M-1}}. \tag{4.59}$$

After some rearrangement (4.59) can be written as

$$\left(\frac{2h_{M-1}}{y_M} + \frac{y_M}{y_M + h_{M-1}}\right)U_M - U_{M-1} = \left(\frac{2h_{M-1}}{y_M} + \frac{y_M}{y_M + h_{M-1}} - 1\right)U^+ \tag{4.60}$$

Using the definition $\frac{h_{M-1}}{y_M} = \varepsilon_M$ the above equation can be written in a simpler form

$$\left(2\varepsilon_M + \frac{1}{1+\varepsilon_M}\right)U_M - U_{M-1} = \left(2\varepsilon_M + \frac{1}{1+\varepsilon_M} - 1\right)U^+ \tag{4.61}$$

or

$$\Gamma_M U_M - U_{M-1} = (\Gamma_M - 1)U^+ \tag{4.62}$$

where

$$\Gamma_M = 2\varepsilon_M + \frac{1}{1+\varepsilon_M}. \tag{4.63}$$

Following a similar procedure for the left-hand side of the grid where the equivalent of (4.54) is

$$U(y,0) = U^- + y_1\frac{U_1 - U^-}{y} \tag{4.64}$$

we obtain

$$\left(\frac{1}{1-\varepsilon_1} - 2\varepsilon_1\right)U_1 - U_2 = \left(\frac{1}{1-\varepsilon_1} - 2\varepsilon_1 - 1\right)U^- \tag{4.65}$$

where $\varepsilon_1 = \frac{h_1}{y_1}$ or

$$\Gamma_1 U_1 - U_2 = (\Gamma_1 - 1)U^- \tag{4.66}$$

where

$$\Gamma_1 = \frac{1}{1-\varepsilon_1} - 2\varepsilon_1. \tag{4.67}$$

The anomalous forms of (4.62) and (4.66) are

$$\Gamma_M \tilde{U}_M - \tilde{U}_{M-1} = (\Gamma_M - 1)(U^+ - U^-) \tag{4.68}$$

and

$$\Gamma_1 \tilde{U}_1 - \tilde{U}_2 = 0 \tag{4.69}$$

respectively where we recall that $\tilde{U}^+ = U^+ - U^-$. These two E-polarization equations were used in the program for the edges of the grid at $z = 0$.

For large $|y|$ in the region $z > 0$, Weaver and Brewitt-Taylor (1978) obtained an approximate expression for the electric field by neglecting second derivatives of y in the differential equation satisfied by U. Their solution was

$$U(y,z) = U(y,0)\frac{U^{\pm}(z)}{U^{\pm}(0)}, \tag{4.70}$$

which, on the left boundary of the grid gives

$$U_{1,n} = U_{1,n-1}\frac{U^-(z_n)}{U^-(z_{n-1})} \tag{4.71}$$

in finite difference form and on the right boundary it is

$$U_{M,n} = U_{M,n-1}\frac{U^+(z_n)}{U^+(z_{n-1})}. \tag{4.72}$$

Using (3.1) we obtain the anomalous forms of (4.71) and (4.72)

$$U^-(z_{n-1})\tilde{U}_{1,n} - U^-(z_n)\tilde{U}_{1,n-1} = 0 \tag{4.73}$$

$$U^+(z_{n-1})\tilde{U}_{M,n} - U^+(z_n)\tilde{U}_{M,n-1} = U^+(z_n)U^-(z_{n-1}) - U'^+(z_{n-1})U^-(z_n). \quad (4.74)$$

These E-polarization equations were used in the program at the edges of the grid in the region $z > 0$.

For the B-polarization problem the anomalous field decreases more rapidly as we move away from the boundaries of the anomaly. Thus, if $y1$ and y_M are far enough away from all anomalies then the fields there can be approximated by the fields at $\pm\infty$. Hence the simple side conditions

$$X_1(z) = X^-(z) \quad (4.75)$$

$$X_M(z) = X^+(z) \quad (4.76)$$

are used for all $z \geq 0$. For the anomalous field these are

$$\tilde{X}_1(z) = 0 \quad (4.77)$$

$$\tilde{X}_M(z) = X^+(z) - X^-(z). \quad (4.78)$$

The above two equations were used in the finite difference program as left and right boundary conditions for the B-polarization case.

4.6 Surface Boundary Conditions

The anomalous boundary condition for the E-polarization (3.15) evaluated at $m = p$, $p \neq 1, M$ is

$$\tilde{U}'(y_p, 0-) = -\frac{1}{\pi}\int_{-\infty}^{\infty} \frac{\tilde{U}(v,0) - \tilde{U}(y_p,0)}{(v-y_p)^2}\, dv. \quad (4.79)$$

The integral can be expanded as follows (see e.g. Weaver (1994) Chapter 5)

$$\oint_{-\infty}^{\infty} = \int_{-\infty}^{y_1} + \int_{y_M}^{\infty} + \oint_{y_{p-1}}^{y_{p+1}} + \left(\sum_{m=1}^{p-2} + \sum_{m=p+1}^{M-1} \right) \int_{y_m}^{y_{m+1}} \tag{4.80}$$

where y_p is the point at which the kernal of the third integral becomes singular. In (4.80) y_1 is the leftmost grid point and y_M is the rightmost grid point.

The mathematics that follows parallels work done by Weaver (1994) for the numerical solution of thin sheet problems. The anomalous fields, however, cause the coefficients obtained to be rather different and generate some extra terms. Looking first at the third integral in (4.80) we approximate around the singular point $y = y_p$ with a parabola

$$\tilde{U}(y,0) = \tilde{U}_p + A_p(y - y_p) + B_p(y - y_p)^2 \tag{4.81}$$

that passes through $\tilde{U}_{p-1}$, $\tilde{U}_p$ and $\tilde{U}_{p+1}$. Solving for A_p and B_p we have

$$A_p = \frac{h_{p-1}}{h_p h_p^+}\tilde{U}_{p+1} + \frac{h_p^-}{h_p h_{p-1}}\tilde{U}_p - \frac{h_p}{h_{p-1} h_p^+}\tilde{U}_{p-1} \tag{4.82}$$

$$B_p = \frac{1}{h_p h_p^+}\tilde{U}_{p+1} - \frac{1}{h_p h_{p-1}}\tilde{U}_p + \frac{1}{h_{p-1} h_p^+}\tilde{U}_{p-1}. \tag{4.83}$$

From comparison with (4.3) and (4.4) we can see that the coefficients A_p and B_p are the finite difference expressions of $\frac{\partial \tilde{U}}{\partial y}$ and $\frac{1}{2}\frac{\partial^2 \tilde{U}}{\partial y^2}$ which is consistent with (4.82) representing a Taylor expansion to second order. Rearranging (4.82) we have

$$\frac{\tilde{U}(y,0) - \tilde{U}_p}{(y - y_p)^2} = \frac{A_p}{y - y_p} + B_p \tag{4.84}$$

which we can substitute into the third integral resulting in

$$\begin{aligned} \oint_{y_{p-1}}^{y_{p+1}} \frac{\tilde{U}(v,0) - \tilde{U}_p}{(v - y_p)^2}\, dv &= A_p \oint_{y_{p-1}}^{y_{p+1}} \frac{dv}{v - y_p} + B_p \oint_{y_{p-1}}^{y_{p+1}} dv \\ &= A_p \ln \frac{h_p}{h_{p-1}} + B_p h_p^+. \end{aligned} \tag{4.85}$$

For the last integral in (4.80) we assume the electric field has a linear variation in $y_m < y < y_{m+1}$:

$$\tilde{U}(y,0) = \tilde{U}_m + (y - y_m)\frac{\tilde{U}_{m+1} - \tilde{U}_m}{h_m}. \tag{4.86}$$

Using (4.86) to substitute for $\frac{\tilde{U}(v,0)-\tilde{U}_p}{(v-y_p)^2}$ in the last integral we have

$$\left(\sum_{m=1}^{p-2} + \sum_{m=p+1}^{M-1}\right)\int_{y_m}^{y_{m+1}} \frac{\tilde{U}(v,0) - \tilde{U}_p}{(v-y_p)^2}\,dv = \left(\sum_{m=1}^{p-2} + \sum_{m=p+1}^{M-1}\right)\left[\frac{\tilde{U}_{m+1} - \tilde{U}_m}{h_m}\ln\left|\frac{y_{m+1}-y_p}{y_m - y_p}\right| + \frac{\tilde{U}_m}{y_m - y_p} - \frac{\tilde{U}_{m+1}}{y_{m+1}-y_p} + \frac{\tilde{U}_p}{y_{m+1}-y_p} - \frac{\tilde{U}_p}{y_m - y_p}\right]. \tag{4.87}$$

This can be written in the form

$$\begin{aligned}
\left(\sum_{m=1}^{p-2} + \sum_{m=p+1}^{M-1}\right)\int_{y_m}^{y_{m+1}} \frac{\tilde{U}(v,0) - \tilde{U}_p}{(v-y_p)^2}\,dv &= \left(\sum_{m=2}^{p-2} + \sum_{m=p+2}^{M-1}\right) R_p^m \tilde{U}_m \\
&+ \left[\tfrac{1}{y_1 - y_p} - \tfrac{1}{h_1}\ln\left(\tfrac{y_p - y_2}{y_p - y_1}\right)\right]\tilde{U}_1 && p \neq 2 \\
&+ \left[\tfrac{1}{h_{p-1}} - \tfrac{1}{h_{p-2}}\ln\tfrac{h_{p-1}}{h_{p-1}^+}\right]\tilde{U}_{p-1} && p \neq 2 \\
&+ \left[\overbrace{\frac{1}{y_p - y_1} - \frac{1}{h_{p-1}}}^{p\neq 2} \underbrace{- \frac{1}{h_p} + \frac{1}{y_M - y_p}}_{p\neq M-1}\right]\tilde{U}_p \\
&+ \left[\tfrac{1}{h_p} - \tfrac{1}{h_{p+1}}\ln\tfrac{h_{p+1}^+}{h_p}\right]\tilde{U}_{p+1} && p \neq M-1 \\
&- \left[\tfrac{1}{y_M - y_p} - \tfrac{1}{h_{M-1}}\ln\left(\tfrac{y_M - y_p}{y_{M-1} - y_p}\right)\right]\tilde{U}_M && p \neq M-1
\end{aligned} \tag{4.88}$$

where

$$R_p^m = \frac{1}{h_{m-1}}\ln\left|\frac{y_p - y_m}{y_p - y_{m-1}}\right| - \frac{1}{h_m}\ln\left|\frac{y_p - y_{m+1}}{y_p - y_m}\right|. \tag{4.89}$$

Note that the starting positions of the summations have changed which is how the five extra terms in (4.88) arose. The restrictions appearing with the extra terms

are necessary since if $p = 2$ the first summation on the left side of (4.88) would vanish and if $p = M - 1$ the second summation would vanish and the relevant terms would not exist.

For the first and second integrals we use the asymptotic boundary conditions from the previous section (4.68) and (4.69). In $y < y_1$ the side boundary condition (4.64) has the form

$$\tilde{U}(y,0) = \tilde{U}_1 \frac{y_1}{y}. \tag{4.90}$$

Substitution into the first integral leads to

$$\int_{-\infty}^{y_1} \frac{\tilde{U}(v,0) - \tilde{U}_p}{(v-y_p)^2}\, dv = \tilde{U}_1 y_1 \int_{-\infty}^{y_1} \frac{1}{v(v-y_p)^2}\, dv - \tilde{U}_p \int_{-\infty}^{y_1} \frac{1}{(v-y_p)^2}\, dv \tag{4.91}$$

which becomes

$$\begin{aligned} &\int_{-\infty}^{y_1} \frac{\tilde{U}(v,0) - \tilde{U}_p}{(v-y_p)^2}\, dv \\ &\quad = \begin{cases} \tilde{U}_1 \left[\frac{y_1}{y_p^2} \ln \left| \frac{y_1}{y_p - y_1} \right| + \frac{y_1}{y_p(y_p - y_1)} \right] - \tilde{U}_p \left[\frac{1}{y_p - y_1} \right] & y_p \neq 0 \\ \frac{\tilde{U}_p}{y_1} - \frac{\tilde{U}_1}{2y_1} & y_p = 0. \end{cases} \end{aligned} \tag{4.92}$$

In $y > y_M$ the side boundary condition (4.54) has the form

$$\tilde{U}(y,0) = (U^+ - U^-)\left(1 - \frac{y_M}{y}\right) + \tilde{U}_M \frac{y_M}{y}. \tag{4.93}$$

Substitution into the second integral of (4.80) gives

$$\begin{aligned} \int_{y_M}^{+\infty} \frac{\tilde{U}(v,0) - \tilde{U}_p}{(v-y_p)^2}\, dv &= \left[\tilde{U}_M y_M - (U^+ - U^-) y_M\right] \int_{y_M}^{+\infty} \frac{1}{v(v-y_p)^2}\, dv \\ &+ (U^+ - U^- - \tilde{U}_p) \int_{y_M}^{+\infty} \frac{1}{(v-y_p)^2}\, dv \end{aligned} \tag{4.94}$$

which becomes

$$\int_{y_M}^{+\infty} \frac{\tilde{U}(v,0) - \tilde{U}_p}{(v-y_p)^2}\, dv$$

$$= \begin{cases} [U^+ - U^- - \tilde{U}_M]\left[\frac{y_M}{y_p^2}\ln\left|\frac{y_M}{y_M - y_p}\right| - \frac{y_M}{y_p(y_M - y_p)}\right] & \\ \quad + \frac{U^+ - U^- - \tilde{U}_p}{y_M - y_p} & y_p \neq 0 \\ \frac{\tilde{U}_M - U^+ + U^-}{2y_M} + \frac{U^+ - U^- - \tilde{U}_p}{y_M} & y_p = 0. \end{cases} \tag{4.95}$$

Now we expand the left-hand side of (4.79) in forward difference form

$$\tilde{U}_{p,2} = \tilde{U}_{p,1} + \tilde{U}'_{p,1}k_1 + \frac{k_1^2}{2}\tilde{U}''_{p,1} \tag{4.96}$$

where we recall $k_1 = z_2 - z_1$. From (3.9) we have a value for the second derivative

$$\tilde{U}''_{p,1} = i\kappa_{p,1}\tilde{U}_{p,1} - \left(\frac{\partial^2\tilde{U}}{\partial y^2}\right)_{p,1} + i\omega\mu_0[\sigma_{p,1} - \sigma_1^-]U_1^- \tag{4.97}$$

and substitution of this into (4.96) allows us to write the left-hand side of (4.79) as

$$\tilde{U}'_p = \frac{\tilde{U}_{p,2} - \tilde{U}_p}{k_1} - \frac{k_1}{2}\left(i\kappa_{p,1}\tilde{U}_p - 2B_p + i\omega\mu_0(\sigma_{p,1} - \sigma_1^-)U^-\right) \tag{4.98}$$

where all fields are at $z = 0$ except for $\tilde{U}_{p,2}$ at $z = z_2$ and where B_p is given in (4.83).

After gathering all the coefficients together and simplifying we obtain a discrete form of (4.79)

$$L_p\tilde{U}_1 + M_p\tilde{U}_M + N_p\tilde{U}_{p-1} + P_p\tilde{U}_p + Q_p\tilde{U}_{p+1} + \left(\sum_{m=2}^{p-2} + \sum_{m=p+2}^{M-1}\right) R_p^m\tilde{U}_m$$
$$+ \frac{\pi}{k_1}\tilde{U}_{p,2} = S_pU^- + T_pU^+ \tag{4.99}$$

for $p = 2, 3, \ldots, M-1$ where we have defined

$$L_p = \frac{1}{h_1} \ln \frac{y_p - y_1}{y_p - y_2} + \frac{y_1}{y_p^2} \ln \frac{|y_1|}{y_p - y_1} - \frac{1}{y_p}, \qquad p \neq 2,\ y_p \neq 0 \tag{4.100}$$

$$M_p = \frac{1}{h_{M-1}} \ln \frac{y_M - y_p}{y_{M-1} - y_p} - \frac{y_M}{y_p^2} \ln \frac{|y_M|}{y_M - y_p} + \frac{1}{y_p}, \qquad p \neq M-1,\ y_p \neq 0 \tag{4.101}$$

$$N_p = \frac{1}{h_{p-2}} \ln \frac{h_{p-1}}{h_{p-1}^+} + \frac{2}{h_{p-1}} + \frac{h_p}{h_{p-1} h_p^+} \ln \frac{h_{p-1}}{h_p} + \frac{\pi k_1}{h_{p-1} h_p^+}, \qquad p \neq 2 \tag{4.102}$$

$$Q_p = \frac{1}{h_{p+1}} \ln \frac{h_p}{h_{p+1}^+} + \frac{2}{h_p} + \frac{h_{p-1}}{h_p h_p^+} \ln \frac{h_p}{h_{p-1}} + \frac{\pi k_1}{h_p h_p^+}, \qquad p \neq M-1 \tag{4.103}$$

$$P_p = \frac{h_p^-}{h_p h_{p-1}} \ln \frac{h_p}{h_{p-1}} - \frac{2h_p^+}{h_p h_{p-1}} - \frac{\pi}{k_1} - \pi k_1 \left(\frac{i\kappa_{p,1}}{2} + \frac{1}{h_p h_{p-1}} \right) \tag{4.104}$$

$$R_p^m = \frac{1}{h_{m-1}} \ln \left| \frac{y_p - y_m}{y_p - y_{m-1}} \right| - \frac{1}{h_m} \ln \left| \frac{y_p - y_{m+1}}{y_p - y_m} \right| \tag{4.105}$$

$$S_p = -\frac{1}{y_p} + \frac{y_M}{y_p^2} \ln \left| \frac{y_M}{y_p - y_M} \right| + \frac{i\omega\mu_0 \pi k_1}{2} (\sigma_{p,1} - \sigma_p^-) \tag{4.106}$$

$$T_p = \frac{1}{y_p} - \frac{y_M}{y_p^2} \ln \left| \frac{y_M}{y_p - y_M} \right|. \tag{4.107}$$

These equations hold for $y_p \neq 0$. If $y_p = 0$ then L_p, M_p, S_p and T_p are

$$L_p = \frac{1}{h_1} \ln \left| \frac{y_1}{y_2} \right| + \frac{1}{2y_1}, \quad p \neq 2 \tag{4.108}$$

$$M_p = \frac{1}{h_{M-1}} \ln \left| \frac{y_M}{y_{M-1}} \right| - \frac{1}{2y_M}, \quad p \neq M-1 \tag{4.109}$$

$$S_p = \frac{1}{2y_M} + \frac{i\omega\mu_0 \pi k_1}{2} (\sigma_{p,1} - \sigma_p^-) \tag{4.110}$$

$$T_p = -\frac{1}{2y_M}. \tag{4.111}$$

If $p = 2$ the terms in L_p and N_p that came from (4.88) vanish since the summation that generated them vanishes. The leftover terms of L_p and N_p will merge because $\tilde{U}_1 = \tilde{U}_{p-1}$ when $p = 2$. The new coefficient for $\tilde{U}_1$ is

$$L_2 = \frac{y_1}{y_2^2} \ln \frac{|y_1|}{h_1} + \frac{h_2}{h_1 h_2^+} \ln \frac{h_1}{h_2} + \frac{y_1 + y_2}{y_2 h_1} + \frac{\pi k_1}{h_1 h_2^+} \tag{4.112}$$

with $N_2 = 0$ to avoid duplicating terms in $\tilde{U}_1$.

If $p = M - 1$ a similar situation arises with vanishing first terms in M_p and Q_p, leaving

$$M_{M-1} = -\frac{y_M}{y_{M-1}^2} \ln \frac{|y_M|}{h_{M-1}} + \frac{h_{M-2}}{h_{M-1} h_{M-1}^+} \ln \frac{h_{M-1}}{h_{M-2}} + \frac{y_M + y_{M-1}}{y_{M-1} h_{M-1}} + \frac{\pi k_1}{h_{M-1} h_{M-1}^+} \tag{4.113}$$

and $Q_p = 0$. When $p = 2$ or $p = 3$ the first summation in (4.99) vanishes and when $p = M - 1$ or $p = M - 2$ the second summation vanishes.

The end values $\tilde{U}_1$ and $\tilde{U}_M$ are given by the asymptotic boundary conditions (4.69) and (4.68) respectively. So the solution of the problem requires the solution of $M - 2$ linear equations of the form (4.99) for $\tilde{U}_p$ $(p = 2, 3, \ldots, M - 1)$. Equations (4.99)–(4.113) were used in the program to calculate the matrix coefficients associated with the anomalous electric fields at the surface of the earth.

4.7 Bottom Boundary Conditions

The anomalous boundary condition for both the E-polarization and B-polarization case is

$$\begin{aligned} &\tilde{F}'(y, d+) + \alpha_0 \sqrt{i}\, \tilde{F}(y, d+) \\ &\quad = \frac{\alpha_0 \sqrt{i}}{\pi} \int_{-\infty}^{\infty} \left[\tilde{F}(v, d+) - \tilde{F}(y_p, d+) \right] P(v - y_p)\, dv \end{aligned} \tag{4.114}$$

where $P(v-y_p) = K_1(|v-y_p|\alpha_0\sqrt{i})/|v-y_p|$ and we recall that $d+ = z_N$, the depth to the underlying half space. Once again we follow the solution method of Weaver (1994) by expanding the integral as in (4.80). The development of the third and fourth integrals in (4.80) are identical for both E-polarization and B-polarization cases so they will be outlined first.

For the third integral we approximate around the singular point $y = y_p$ with a parabola

$$\tilde{F}(y, d+) = \tilde{F}_{p,N} + A_p(y - y_p) + B_p(y - y_p)^2 \tag{4.115}$$

that passes through $\tilde{F}_{p-1,N}, \tilde{F}_{p,N}$ and $\tilde{F}_{p+1,N}$. Solving for A_p and B_p we obtain equations identical to (4.82) and (4.83) for the E-polarization surface condition with $\tilde{F}$ in place of $\tilde{U}$. These are likewise equal to $\frac{\partial \tilde{F}}{\partial y}$ and $\frac{1}{2}\frac{\partial^2 \tilde{F}}{\partial y^2}$ respectively. Substitution of (4.115) into the third integral results in

$$\begin{aligned}
&\int_{y_{p-1}}^{y_{p+1}} \left[\tilde{F}(v, d+) - \tilde{F}(y_p, d+)\right] P(v - y_p)\, dv \\
&\quad = A_p \int_{y_{p-1}}^{y_{p+1}} (v - y_p) P(v - y_p)\, dv + B_p \int_{y_{p-1}}^{y_{p+1}} (v - y_p)^2 P(v - y_p)\, dv \qquad (4.116) \\
&\quad = A_p \left(\frac{1}{\alpha_0\sqrt{i}} \left[K_0(\alpha_0\sqrt{i}\, h_{p-1}) - K_0(\alpha_0\sqrt{i}\, h_p) \right] \right) \\
&\qquad - B_p \left(\frac{H(\alpha_0\sqrt{i}\, h_p) + H(\alpha_0\sqrt{i}\, h_{p-1})}{\alpha_0^2} \right. \\
&\qquad \left. + \frac{h_p K_0(\alpha_0\sqrt{i}\, h_p) + h_{p-1} K_0(\alpha_0\sqrt{i}\, h_{p-1})}{\alpha_0\sqrt{i}} \right) \qquad (4.117)
\end{aligned}$$

where we have used $K_0' = -K_1$, $H(z) = \int_0^z K_0(\eta) d\eta$ and a combination of the integrals $\int_{y_{p-1}}^{y_p}$ and $\int_{y_p}^{y_{p+1}}$ to evaluate the first integral above and a combination of

$\int_0^{y_{p+1}}$ and $\int_0^{y_{p-1}}$ to evaluate the second. This can be expanded to

$$\int_{y_{p-1}}^{y_{p+1}} \left[\tilde{F}(v,d+) - \tilde{F}(y_p,d+)\right] P(v-y_p)\,dv = -\left[\frac{H^{p+1}+H^{p-1}}{\alpha_0^2 h_p h_p^+} + \frac{K_0^{p+1}}{\alpha_0\sqrt{i}\,h_p}\right]\tilde{F}_{p+1,N}$$
$$-\left[\frac{H^{p+1}+H^{p-1}}{\alpha_0^2 h_{p-1} h_p^+} + \frac{K_0^{p-1}}{\alpha_0\sqrt{i}\,h_{p-1}}\right]\tilde{F}_{p-1,N}$$
$$+\left[\frac{H^{p+1}+H^{p-1}}{\alpha_0^2 h_p h_{p-1}} + \frac{K_0^{p-1}}{\alpha_0\sqrt{i}\,h_{p-1}} + \frac{K_0^{p+1}}{\alpha_0\sqrt{i}\,h_p}\right]\tilde{F}_{p,N} \tag{4.118}$$

where we have defined $H^m = H(\alpha_0\sqrt{i}\,|y_m - y_p|)$ and $K_0^m = K_0(\alpha_0\sqrt{i}\,|y_m - y_p|)$.

For the fourth integral of (4.80) we assume the field has a linear variation in $y_m < y < y_{m+1}$ such that

$$\tilde{F}(y,d+) = \tilde{F}_{m,N} + (y-y_m)\frac{\tilde{F}_{m+1,N} - \tilde{F}_{m,N}}{h_m}. \tag{4.119}$$

Using the above equation to substitute for $\tilde{F}(y,d+)$ in this integral we have

$$\left(\sum_{m=1}^{p-2} + \sum_{m=p+1}^{M-1}\right)\int_{y_m}^{y_{m+1}} [\tilde{F}(y,d+) - \tilde{F}_{p,N}]P(v-y_p)\,dv$$
$$= \left(\sum_{m=1}^{p-2} + \sum_{m=p+1}^{M-1}\right)\left[(\tilde{F}_{m,N} - \tilde{F}_{p,N})\int_{y_m}^{y_{m+1}} P(v-y_p)\,dv\right.$$
$$\left. + \frac{\tilde{F}_{m+1,N} - \tilde{F}_{m,N}}{h_m}\int_{y_m}^{y_{m+1}} (v-y_m)P(v-y_p)\,dv\right] \tag{4.120}$$
$$= \left(\sum_{m=1}^{p-2} + \sum_{m=p+1}^{M-1}\right)\left[(\tilde{F}_{m,N} - \tilde{F}_{p,N})\frac{|y_m - y_p|}{(y_m - y_p)}(H^m + K_1^m - H^{m+1} - K_1^{m+1})\right.$$
$$+ \frac{\tilde{F}_{m+1,N} - \tilde{F}_{m,N}}{h_m}\left\{\frac{1}{\alpha_0\sqrt{i}}(K_0^m - K_0^{m+1})\right.$$
$$\left.\left. - |y_m - y_p|(H^m + K_1^m - H^{m+1} - K_1^{m+1})\right\}\right] \tag{4.121}$$

where $K_1^m = K_1(\alpha_0\sqrt{i}\,|y_m - y_p|)$ and the second integral was evaluated by splitting it into two:

$$\int_{y_m}^{y_{m+1}} (v-y_m)P(v-y_p)\,dv$$

$$= \int_{y_m}^{y_{m+1}} (v - y_p) P(v - y_p)\, dv - (y_m - y_p) \int_{y_m}^{y_{m+1}} P(v - y_p)\, dv \tag{4.122}$$

Writing (4.121) out term by term results in

$$\begin{aligned}
&\left(\sum_{m=1}^{p-2} + \sum_{m=p+1}^{M-1} \right) \int_{y_m}^{y_{m+1}} [\tilde{F}(y, d+) - \tilde{F}_{p,N}] P(v - y_p)\, dv = \left(\sum_{m=2}^{p-2} + \sum_{m=p+2}^{M-1} \right) R_p^m \tilde{F}_{m,N} \\
&+ \tilde{F}_{1,N} \left\{ -H^1 - K_1^1 - \frac{K_0^1 - \alpha_0\sqrt{i}\,(y_p - y_1)H^1 - \alpha_0\sqrt{i}\,(y_p - y_1)K_1^1}{\alpha_0\sqrt{i}\,h_1} \right. \\
&\left. + \frac{K_0^2 - \alpha_0\sqrt{i}\,(y_p - y_2)H^2 - \alpha_0\sqrt{i}\,(y_p - y_2)K_1^2}{\alpha_0\sqrt{i}\,h_1} \right\} \qquad {\scriptstyle m=1, p\neq 2} \\
&+ \tilde{F}_{p-1,N} \left\{ \frac{K_0^{p-1}}{\alpha_0\sqrt{i}\,h_{p-1}} + \frac{K_0^{p-2} - \alpha_0\sqrt{i}\,(y_p - y_{p-2})H^{p-2} - \alpha_0\sqrt{i}\,(y_p - y_{p-2})K_1^{p-2}}{\alpha_0\sqrt{i}\,h_{p-2}} \right. \\
&\left. - h_{p-1}^+ \frac{K_0^{p-1} - \alpha_0\sqrt{i}\,(y_p - y_{p-1})H^{p-1} - \alpha_0\sqrt{i}\,(y_p - y_{p-1})K_1^{p-1}}{\alpha_0\sqrt{i}\,h_{p-2}h_{p-1}} \right\} \qquad {\scriptstyle m=p-2, p\neq 2} \\
&+ \tilde{F}_{p,N} \left\{ \overbrace{H^1 + K_1^1 - H^{p-1} - K_1^{p-1}}^{p\neq 2} \underbrace{- H^{p+1} - K_1^{p+1} + H^M + K_1^M}_{p\neq M-1} \right\} \qquad (4.123) \\
&+ \tilde{F}_{p+1,N} \left\{ \frac{K_0^{p+1}}{\alpha_0\sqrt{i}\,h_p} + \frac{K_0^{p} - \alpha_0\sqrt{i}\,(y_{p+2} - y_p)H^{p+2} - \alpha_0\sqrt{i}\,(y_{p+2} - y_p)K_1^{p+2}}{\alpha_0\sqrt{i}\,h_{p+1}} \right. \\
&\left. - h_{p+1}^+ \frac{K_0^{p+1} - \alpha_0\sqrt{i}\,(y_{p+1} - y_p)H^{p+1} - \alpha_0\sqrt{i}\,(y_{p+1} - y_p)K_1^{p+1}}{\alpha_0\sqrt{i}\,h_p h_{p+1}} \right\} \qquad {\scriptstyle m=p+1, p\neq M-1} \\
&+ \tilde{F}_{M,N} \left\{ -H^M - K_1^M - \frac{K_0^M - \alpha_0\sqrt{i}\,(y_M - y_p)H^M - \alpha_0\sqrt{i}\,(y_M - y_p)K_1^M}{\alpha_0\sqrt{i}\,h_{M-1}} \right. \\
&\left. + \frac{K_0^{M-1} - \alpha_0\sqrt{i}\,(y_{M-1} - y_p)H^{M-1} - \alpha_0\sqrt{i}\,(y_{M-1} - y_p)K_1^{M-1}}{\alpha_0\sqrt{i}\,h_{M-1}} \right\} \qquad {\scriptstyle m=M-1, p\neq M-1}
\end{aligned}$$

where

$$\begin{aligned}
R_p^m &= \frac{K_0^{m-1} - \alpha_0\sqrt{i}\,|y_{m-1} - y_p|H^{m-1} - \alpha_0\sqrt{i}\,|y_{m-1} - y_p|K_1^{m-1}}{\alpha_0\sqrt{i}\,h_{m-1}} \\
&- h_m^+ \frac{K_0^m - \alpha_0\sqrt{i}\,|y_m - y_p|H^m - \alpha_0\sqrt{i}\,(y_m - y_p)K_1^m}{\alpha_0\sqrt{i}\,h_{m-1}h_m} \\
&+ \frac{K_0^{m+1} - \alpha_0\sqrt{i}\,|y_{m+1} - y_p|H^{m+1} - \alpha_0\sqrt{i}\,|y_{m+1} - y_p|K_1^{m+1}}{\alpha_0\sqrt{i}\,h_m}.
\end{aligned} \tag{4.124}$$

As for the E-polarization surface condition the five extra terms arise as a result of changing the starting positions of the summations.

4.8 The B-polarization bottom boundary condition.

The remaining terms of the bottom boundary condition for the E-polarization and B-polarization case are different. To complete the development of the B-polarization case boundary condition we start by substitution of the side boundary condition (4.77)

$$\tilde{X}(y, d+) = 0, \qquad y \leq y_1 \tag{4.125}$$

into the first integral of (4.80) :

$$\begin{aligned} \int_{-\infty}^{y_1} [\tilde{X}(v, d+) - \tilde{X}(y_p, d+)] P(v - y_p)\, dv &= -\tilde{X}_{p,N} \int_{-\infty}^{y_1} P(v - y_p)\, dv \\ &= -\tilde{X}_{p,N}(H^1 + K_1^1 - \frac{\pi}{2}). \end{aligned} \tag{4.126}$$

For the second integral we use the left side boundary condition (4.78)

$$\tilde{X}(y, d+) = X^+(d+) - X^-(d+), \qquad y \geq y_M \tag{4.127}$$

to obtain

$$\begin{aligned} &\int_{y_M}^{+\infty} [\tilde{X}(v, d+) - \tilde{X}(y_p, d+)] P(v - y_p)\, dv \\ &\quad = (X_N^+ - X_N^- - \tilde{X}_{p,N}) \int_{y_M}^{+\infty} P(v - y_p)\, dv \\ &\quad = (X_N^+ - X_N^- - \tilde{X}_{p,N})(H^M + K_1^M - \frac{\pi}{2}). \end{aligned} \tag{4.128}$$

Since $\tilde{X}'(y, d+)$ is discontinuous at $z = d+ = z_N$ we use (3.3) to write the left-hand side of the boundary conditions (4.114) as

$$\begin{aligned} &\tilde{X}'(y, d+) + \alpha\sqrt{i}\,\tilde{X}(y, d+) = \sigma_0 r_{p,N-1} \tilde{X}'(y, d-) \\ &\quad + \mu_0(\sigma_0 r_{p,N-1} \sigma_{N-1}^- - \sigma_N^-) V_N^- + \alpha_0 \sqrt{i}\,\tilde{X}(y, d+) \end{aligned} \tag{4.129}$$

where

$$r_{p,N-1} = \frac{h_p \rho_{p,N-1} + h_{p-1}\rho_{p-1,N-1}}{h_p^+}. \tag{4.130}$$

We must use $r_{p,N-1}$ since we are evaluating $\tilde{X}(y, d-)$ *at* the node (p, N) where the conductivity is neither $\rho_{p,N-1}$ nor $\rho_{p-1,N-1}$ but some avera e of the two. In this case we can no longer assume that ρ is constant in the y direction in the region of interest.

A Taylor expansion upwards from the node (p, N) and substitution from the general differential equation for $\tilde{X}$ (3.10) written in terms of ρ with $\frac{\partial \rho}{\partial z} = 0$ results in

$$\begin{aligned}\tilde{X}'(y, d+) + \alpha_0\sqrt{i}\,\tilde{X}(y, d+) &= \sigma_0 r_{p,N-1}\left(\frac{\tilde{X}_{p,N} - \tilde{X}_{p,N-1}}{k_{N-1}}\right) \\ &+ \frac{\sigma_0 r_{p,N-1} k_{N-1}}{2}\left(i\kappa_{p,N-1}\tilde{X}_{p,N} + i(\kappa_{p,N-1} - \bar{\kappa}_{N-1})\bar{X}_N - \left(\frac{\partial^2 \tilde{X}}{\partial y^2}\right)_{p,N}\right. \\ &\left. - \frac{1}{r_{p,N-1}}\left(\frac{\partial \rho}{\partial y}\right)_{p,N-1}\left(\frac{\partial \tilde{X}}{\partial y}\right)_{p,N}\right) \\ &+ \mu_0(\sigma_0 r_{p,N-1}\bar{\sigma}_{N-1} - \bar{\sigma}_N)\bar{V}_N + \alpha_0\sqrt{i}\,\tilde{X}_{p,N}\end{aligned} \tag{4.131}$$

with

$$\left(\frac{\partial \rho}{\partial y}\right)_{p,N-1} = \frac{2(\rho_{p,N-1} - \rho_{p-1,N-1})}{h_p^+} \tag{4.132}$$

$$\bar{V}_N = \frac{1}{\mu_0 \bar{\sigma}_{N-1}}\left(\frac{\bar{X}_N - \bar{X}_{N-1}}{k_{N-1}} + \frac{i\bar{\kappa}_{N-1}k_{N-1}}{2}\bar{X}_N\right) \tag{4.133}$$

where $k_{N-1} = z_N - z_{N-1}$, $\kappa_{p,N-1} = \omega\mu_0/r_{p,N-1}$ and $\partial\tilde{X}/\partial y$ and $\partial^2\tilde{X}/\partial y^2$ are given by A_p and $2B_p$ respectively.

After gathering all coefficients together and simplifying we obtain

$$N_p\tilde{X}_{p-1,N} + P_p\tilde{X}_{p,N} + Q_p\tilde{X}_{p+1,N} + \left(\sum_{m=2}^{p-2} + \sum_{m=p+2}^{M-1}\right) R_p^m \tilde{X}_{m,N} + \frac{\pi\sigma_0 r_{p,N-1}}{k_{N-1}}\tilde{X}_{p,N-1}$$
$$= S_p X_N^- + T_p X_N^+ + \mu_0\pi(\sigma_0 r_{p,N-1}\sigma_{N-1}^- - \sigma_N^-)V_N^- \tag{4.134}$$

where the left-hand boundary condition (4.77) requires L_p, the $\tilde{X}_{1,N}$ coefficient, to be zero and the right-hand side boundary condition (4.78) combines M_p, the $\tilde{X}_{M,N}$ coefficient, with S_p and T_p. Using $d_m = \alpha_0\sqrt{i}|y_m - y_p|$ the coefficients are

$$N_p = \frac{K_0^{p-2} - d_{p-2}H^{p-2} - d_{p-2}K_1^{p-2}}{h_{p-2}} - h_{p-1}^+\frac{K_0^{p-1} - d_{p-1}H^{p-1} - d_{p-1}K_1^{p-1}}{h_{p-2}h_{p-1}}$$
$$+\frac{\pi\sigma_0 r_{p,N-1}k_{N-1}}{2}\left[\frac{-h_p}{r_{p,N-1}h_{p-1}h_p^+}\left(\frac{\partial\rho}{\partial y}\right)_{p,N-1} + \frac{2}{h_{p-1}h_p^+}\right]$$
$$+\frac{H^{p+1} + H^{p-1}}{\alpha_0\sqrt{i}\,h_{p-1}h_p^+}, \quad p \neq 2 \tag{4.135}$$

$$Q_p = \frac{K_0^{p+2} - d_{p+2}H^{p+2} - d_{p+2}K_1^{p+2}}{h_{p+1}} - h_{p+1}^+\frac{K_0^{p+1} - d_{p+1}H^{p+1} - d_{p+1}K_1^{p+1}}{h_p h_{p+1}}$$
$$+\frac{\pi\sigma_0 r_{p,N-1}k_{N-1}}{2}\left[\frac{h_{p-1}}{r_{p,N-1}h_p h_p^+}\left(\frac{\partial\rho}{\partial y}\right)_{p,N-1} + \frac{2}{h_p h_p^+}\right]$$
$$+\frac{H^{p+1} + H^{p-1}}{\alpha_0\sqrt{i}\,h_p h_p^+}, \quad p \neq M-1 \tag{4.136}$$

$$P_p = \frac{K_0^{p-1} - d_{p-1}H^{p-1} - d_{p-1}K_1^{p-1}}{h_{p-1}} + \frac{K_0^{p+1} - d_{p+1}H^{p+1} - d_{p+1}K_1^{p+1}}{h_p}$$
$$-\frac{\pi\sigma_0 r_{p,N-1}k_{N-1}}{2}\left[i\kappa_{p,N-1} - \frac{h_p^-}{r_{p,N-1}h_{p-1}h_p}\left(\frac{\partial\rho}{\partial y}\right)_{p,N-1} + \frac{2}{h_{p-1}h_p}\right]$$
$$-\frac{\pi\sigma_0 r_{p,N-1}}{k_{N-1}} - \frac{H^{p+1} + H^{p-1}}{\alpha_0\sqrt{i}\,h_{p-1}h_p} \tag{4.137}$$

$$R_p^m = \frac{K_0^{m-1} - d_{m-1}H^{m-1} - d_{m-1}K_1^{m-1}}{h_{m-1}} + \frac{K_0^{m+1} - d_{m+1}H^{m+1} - d_{m+1}K_1^{m+1}}{h_m}$$
$$-h_m^+\frac{K_0^m - d_m H^m - d_m K_1^m}{h_{m-1}h_m} \tag{4.138}$$

$$T_p = \frac{K_0^M - d_M H^M - d_M K_1^M}{h_{M-1}} - \frac{K_0^{M-1} - d_{M-1} H^{M-1} - d_{M-1} K_1^{M-1}}{h_{M-1}}$$
$$+\frac{\alpha_0 \sqrt{i}\,\pi}{2}, \quad p \neq M-1 \tag{4.139}$$

$$S_p = -T_p + \frac{i\pi\sigma_0 r_{p,N-1} k_{N-1}(\kappa_{p,N-1} - \kappa_{N-1}^-)}{2}. \tag{4.140}$$

When $p = 2$ the left-hand side boundary condition (4.77) requires

$$N_2 = 0 \tag{4.141}$$

and when $p = M-1$, Q_p merges with T_p with the aid of the right-hand side boundary condition (4.78) so that

$$T_{M-1} = -\frac{\pi\sigma_0 r_{M-1,N-1} k_{N-1}}{2}\left[\frac{h_{M-2}}{r_{M-1,N-1} h_{M-1} h_{M-1}^+}\left(\frac{\partial\rho}{\partial y}\right)_{M-1,N-1} + \frac{2}{h_{M-1} h_{M-1}^+}\right]$$
$$+\frac{\alpha_0\sqrt{i}\,\pi}{2} - \frac{H^M + H^{M-2}}{\alpha_0\sqrt{i}\, h_{M-1} h_{M-1}^+} + \frac{K_0^M - d_M H^M - d_M K_1^M}{h_{M-1}} \tag{4.142}$$

$$Q_{M-1} = 0. \tag{4.143}$$

Note that S_{M-1} will also change due to its dependence on T_{M-1}. The equations (4.134)–(4.143) were used in the program to calculate the matrix coefficients associated with the anomalous magnetic field at the surface c e underlying half-space.

4.9 The E-polarization bottom boundary condition.

To complet the development of the E-polarization boundary condition we start by substituting the anomalous form of the side boundary condition (4.70)

$$\tilde{U}(y,z) = \tilde{U}(y,0)\frac{U^-(z)}{U^-(0)}, \qquad y < y_1,\ z > 0 \tag{4.144}$$

together with the surface condition (see (4.90))

$$\tilde{U}(y,0) = \tilde{U}_{1,1}\frac{y_1}{y}, \qquad y < y_1,\ z = 0 \tag{4.145}$$

into the first integral of (4.80) applied to (4.114). This results in

$$\begin{aligned}
&\int_{-\infty}^{y_1} [\tilde{U}(v,d+) - \tilde{U}(y_p,d+)]P(v-y_p)\,dv \\
&\quad = \tilde{U}_{1,N}y_1 \int_{-\infty}^{y_1} \frac{P(v-y_p)}{v}dv - \tilde{U}_{p,N}\int_{-\infty}^{y_1} P(v-y_p)\,dz \qquad (4.146)\\
&\quad = \begin{cases}
\tilde{U}_{1,N}y_1\left[\frac{K_0^1}{\alpha_0\sqrt{i}\,y_p y_1} + \frac{H^1+K_1^1}{y_p} - \frac{\pi}{2y_p} + \frac{\Theta^1}{y_p}\right] & \\
\quad -\tilde{U}_{p,N}(H^1 + K_1^1 - \frac{\pi}{2}) & y_p \neq 0 \\
\tilde{U}_{1,N}y_1\left[-\frac{K_0[\alpha_0\sqrt{i}(-y_1)]}{\alpha_0\sqrt{i}\,y_1^2} + 2\alpha_0\sqrt{i}\,\Upsilon[\alpha_0\sqrt{i}(-y_1)]\right] & \\
\quad -\tilde{U}_{p,N}\left[H[\alpha_0\sqrt{i}(-y_1)] + K_1[\alpha_0\sqrt{i}(-y_1)] - \frac{\pi}{2}\right] & y_p = 0
\end{cases} \qquad (4.147)
\end{aligned}$$

where

$$\Theta^1 = \Theta[\alpha_0\sqrt{i}(y_p - y_1)] = \int_{\alpha_0\sqrt{i}(y_p-y_1)}^{\infty} \frac{K_0(u)}{(u-\alpha_0\sqrt{i}\,y_p)^2}\,du \tag{4.148}$$

and

$$\Upsilon[\alpha_0\sqrt{i}(-y_1)] = \int_{\alpha_0\sqrt{i}(-y_1)}^{\infty} \frac{K_0(u)}{u^3}\,du. \tag{4.149}$$

If we expand the above integrals as

$$\int_{a_1}^{\infty} = \int_{a_1}^{b_1} + \sum_{j=1}^{N-1}\int_{b_j}^{b_{j+1}} + \int_{b_p}^{\infty} \tag{4.150}$$

where b_p is chosen so that $\int_{b_p}^{\infty} \frac{K_0(u)}{(u-\alpha_0\sqrt{i}\,y_p)^2}\,du$ $\left(\text{or } \int_{b_p}^{\infty} \frac{K_0(u)}{u^3}\,du\right)$ are negligible and $b_j = a_1 + \frac{j(b_p-a_1)}{N}$, $j = 0,\ldots,N$ with $a_1 = \alpha_0\sqrt{i}(y_p - y_1)$ $\left(\text{or } a_1 = \alpha_0\sqrt{i}(-y_1)\right)$ then we can write

$$\begin{aligned}
\Theta[\alpha_0\sqrt{i}(y_p - y_1)] &\simeq \frac{1}{2}\sum_{j=0}^{N-1}\left[\frac{1}{(b_j - \alpha_0\sqrt{i}y_p)^2}\right. \\
&\left. + \frac{1}{(b_{j+1} - \alpha_0\sqrt{i}y_p)^2}\right][H(b_{j+1}) - H(b_j)] \qquad (4.151)
\end{aligned}$$

where we have used

$$\frac{1}{(u-\alpha_0\sqrt{i}y_p)^2} \simeq \frac{1}{2}\left[\frac{1}{(b_j-\alpha_0\sqrt{i}y_p)^2}+\frac{1}{(b_{j+1}-\alpha_0\sqrt{i}y_p)^2}\right] \tag{4.152}$$

and

$$\Upsilon[\alpha_0\sqrt{i}(-y_1)] \simeq \frac{1}{2}\sum_{j=0}^{N-1}\left[\frac{1}{b_j^3}+\frac{1}{b_{j+1}^3}\right][H(b_{j+1})-H(b_j)] \tag{4.153}$$

where we have used

$$\frac{1}{u^3} \simeq \frac{1}{2}\left[\frac{1}{b_j^3}+\frac{1}{b_{j+1}^3}\right]. \tag{4.154}$$

In $y > y_M$ the anomalous form of the side boundary condition (4.70)

$$\tilde{U}(y,z) = \tilde{U}(y,0)\frac{U^+(z)}{U^+(0)} + U^-(0)\frac{U^+(z)}{U^+(0)} - U^-(z) \tag{4.155}$$

together with the surface condition

$$\tilde{U}(y,0) = \left[U^+(0)-U^-(0)\right]\left(1-\frac{y_M}{y}\right) + \tilde{U}_{M,1}\frac{y_M}{y} \tag{4.156}$$

can be used to write the second integral as

$$\begin{aligned}
&\int_{y_M}^{\infty}\left[\tilde{U}(v,d+)-\tilde{U}(y_p,d+)\right]P(v-y_p)\,dv \\
&\quad = y_M\left(U_N^- - U_N^+ + \tilde{U}_{M,N}\right)\int_{y_M}^{\infty}\frac{P(v-y_p)}{v}dv \\
&\qquad\qquad + \left(U_N^+ - U_N^- - \tilde{U}_{p,N}\right)\int_{y_M}^{\infty}P(v-y_p)dv
\end{aligned} \tag{4.157}$$

$$= \begin{cases}
y_M\left(U_N^- - U_N^+ + \tilde{U}_{M,N}\right)\left[\frac{-K_0[\alpha_0\sqrt{i}(y_M-y_p)]}{\alpha_0\sqrt{i}\,y_M y_p} + \frac{H^M+K_1^M}{y_p} - \frac{\pi}{2y_p} + \frac{\Theta^M}{y_p}\right] \\
\quad + \left(U_N^+ - U_N^- - \tilde{U}_{p,N}\right)\left[H^M + K_1^M - \frac{\pi}{2}\right] & y_p \neq 0 \\
y_M\left(U_N^- - U_N^+ + \tilde{U}_{M,N}\right)\left[\frac{K_0(\alpha_0\sqrt{i}\,y_M)}{\alpha_0\sqrt{i}\,y_M^2} - 2\alpha_0\sqrt{i}\,\Upsilon(\alpha_0\sqrt{i}y_M)\right] & \\
\quad + \left(U_N^+ - U_N^- - \tilde{U}_{p,N}\right)\left[H(\alpha_0\sqrt{i}y_M) + K_1(\alpha_0\sqrt{i}\,y_M) - \frac{\pi}{2}\right] & y_p = 0.
\end{cases} \tag{4.158}$$

Now we Taylor expand the left-hand side of (4.114) to obtain

$$\tilde{U}'(y,d+)+\alpha_0\sqrt{i}\,\tilde{U}(y,d+)=\frac{\tilde{U}_{p,N}-\tilde{U}_{p,N-1}}{k_{N-1}}+\frac{k_{N-1}}{2}\left[i\kappa_{p,N-1}\tilde{U}'_{p,N}\right.$$
$$\left.-\left(\frac{\partial^2\tilde{U}}{\partial y^2}\right)_{p,N}+i\omega\mu_0(s_{p,N-1}-\sigma^-_{N-1})U^-_N\right]+\alpha_0\sqrt{i}\tilde{U}_{p,N} \tag{4.159}$$

where $\kappa_{p,N-1}=\omega\mu_0 s_{p,N-1}$ with

$$s_{p,N-1}=\frac{h_p\sigma_{p,N-1}+h_{p-1}\sigma_{p-1,N-1}}{h^+_p} \tag{4.160}$$

and k_{N-1} as before.

After gathering all coefficients together and simplifying we obtain

$$L_p\tilde{U}_{1,N}+M_p\tilde{U}_{M,N}+N_p\tilde{U}_{p-1,N}+P_p\tilde{U}_{p,N}+Q_p\tilde{U}_{p+1,N}$$
$$+\left(\sum_{m=2}^{p-2}+\sum_{m=p+2}^{M-1}\right)R^m_p\tilde{U}_{m,N}+\frac{\pi}{k_{N-1}}\tilde{U}_{p,N-1}=S_pU^-_N+T_pU^+_N \tag{4.161}$$

where we have defined

$$L_p=-\frac{K^1_0-d_1H^1-d_1K^1_1}{h_1}+\frac{K^2_0-d_2H^2-d_2K^2_1}{h_1}+\frac{K^1_0}{y_p}$$
$$-\frac{\alpha_0\sqrt{i}(y_p-y_1)}{y_p}(H^1+K^1_1)$$
$$-\frac{\alpha_0\sqrt{i}\,\pi y_1}{2y_p}+\frac{\alpha_0\sqrt{i}\,y_1}{y_p}\Theta^1,\quad p\neq 2,\ y_p\neq 0 \tag{4.162}$$

$$M_p=-\frac{K^M_0-d_MH^M-d_MK^M_1}{h_{M-1}}+\frac{K^{M-1}_0-d_{M-1}H^{M-1}-d_{M-1}K^{M-1}_1}{h_{M-1}}-\frac{K^M_0}{y_p}$$
$$+\frac{\alpha_0\sqrt{i}(y_M-y_p)}{y_p}(H^M+K^M_1)$$
$$-\frac{\alpha_0\sqrt{i}\,\pi y_M}{2y_p}+\alpha_0\sqrt{i}\,\Theta^M\frac{y_M}{y_p},\quad p\neq M-1,\ y_p\neq 0 \tag{4.163}$$

$$N_p=\frac{K^{p-2}_0-d_{p-2}H^{p-2}-d_{p-2}K^{p-2}_1}{h_{p-2}}-h^+_{p-1}\frac{K^{p-1}_0-d_{p-1}H^{p-1}-d_{p-1}K^{p-1}_1}{h_{p-2}h_{p-1}}$$
$$+\frac{H^{p+1}+H^{p-1}}{\alpha_0\sqrt{i}\,h_{p-1}h^+_p}+\frac{\pi k_{N-1}}{h_{p-1}h^+_p},\quad p\neq 2 \tag{4.164}$$

$$Q_p = \frac{K_0^{p+2} - d_{p+2}H^{p+2} - d_{p+2}K_1^{p+2}}{h_{p+1}} - h_{p+1}^+ \frac{K_0^{p+1} - d_{p+1}H^{p+1} - d_{p+1}K_1^{p+1}}{h_p h_{p+1}}$$
$$+ \frac{H^{p+1} + H^{p-1}}{\alpha_0\sqrt{i}\, h_p h_p^+} + \frac{\pi k_{N-1}}{h_p h_p^+}, \quad p \neq M-1 \tag{4.165}$$

$$P_p = \frac{K_0^{p-1} - d_{p-1}H^{p-1} - d_{p-1}K_1^{p-1}}{h_{p-1}} + \frac{K_0^{p+1} - d_{p+1}H^{p+1} - d_{p+1}K_1^{p+1}}{h_p}$$
$$- \frac{H^{p+1} + H^{p-1}}{\alpha_0\sqrt{i}\, h_{p-1}h_p} - \frac{\pi}{k_{N-1}} - \frac{\pi k_{N-1}}{2}\left[i\kappa_{p,N-1} + \frac{2}{h_{p-1}h_p}\right] \tag{4.166}$$

$$R_p^m = \frac{K_0^{m-1} - d_{m-1}H^{m-1} - d_{m-1}K_1^{m-1}}{h_{m-1}} + \frac{K_0^{m+1} - d_{m+1}H^{m+1} - d_{m+1}K_1^{m+1}}{h_m}$$
$$- h_m^+ \frac{K_0^m - d_m H^m - d_m K_1^m}{h_{m-1}h_m} \tag{4.167}$$

$$T_p = -\frac{K_0^M}{y_p} + \frac{\alpha_0\sqrt{i}y_M}{y_p}(H^M + K_1^M) - \frac{\alpha_0\sqrt{i}\pi y_M}{2y_p} + \frac{\alpha_0\sqrt{i}y_M}{y_p}\Theta^M$$
$$- \alpha_0\sqrt{i}(H^M + K_1^M) + \frac{\alpha_0\sqrt{i}\,\pi}{2}, \quad y_p \neq 0 \tag{4.168}$$

$$S_p = -T_p + \frac{i\omega\mu_0\pi k_{N-1}}{2}(s_{p,N-1} - \sigma_{N-1}^-). \tag{4.169}$$

If $p = 2$ then N_p and L_p become

$$\mathrm{L}_p = \frac{H^3 + H^1}{\alpha_0\sqrt{i}\, h_1 h_2^+} - \frac{y_1 K_0^1}{h_1 y_2} + \frac{\alpha_0\sqrt{i}y_1}{y_2}(H^1 + K_1^1) - \frac{\alpha_0\sqrt{i}\pi y_1}{2y_2}$$
$$+ \frac{\alpha_0\sqrt{i}\,y_1}{y_2}\Theta^1 + \frac{\pi k_{N-1}}{h_1 h_2^+} \tag{4.170}$$

$$N_p = 0 \tag{4.171}$$

and if $p = M-1$ then Q_p and M_p become

$$M_p = \frac{H^M + H^{M-2}}{\alpha_0\sqrt{i}\, h_{M-1}h_{M-1}^+} - \frac{y_M K_0^M}{h_{M-1}y_{M-1}} + \frac{\alpha_0\sqrt{i}y_M}{y_{M-1}}(H^M + K_1^M) - \frac{\alpha_0\sqrt{i}\pi y_M}{2y_{M-1}}$$
$$+ \frac{\alpha_0\sqrt{i}\,y_M}{y_{M-1}}\Theta^M + \frac{\pi k_{N-1}}{h_{M-1}h_{M-1}^+} \tag{4.172}$$

$$Q_p = 0. \tag{4.173}$$

If $y_p = 0$ L_p, M_p and T_p are replaced by

$$L_p = -\frac{K_0^1 - d_1 H^1 - d_1 K_1^1}{h_1} + \frac{K_0^2 - d_2 H^2 - d_2 K_1^2}{h_1}$$
$$-\alpha_0\sqrt{i}(H^1 + K_1^1) - \frac{K_0^1}{y_1} + 2i\alpha_0^2 y_1 \Upsilon^1 \tag{4.174}$$

$$M_p = -\frac{K_0^M - d_M H^M - d_M K_1^M}{h_{M-1}} + \frac{K_0^{M-1} - d_{M-1} H^{M-1} - d_{M-1} K_1^{M-1}}{h_{M-1}}$$
$$-\alpha_0\sqrt{i}(H^M + K_1^M) + \frac{K_0^M}{y_M} - 2i\alpha_0^2 y_M \Upsilon^M \tag{4.175}$$

$$T_p = \frac{K_0^M}{y_M} - 2i\alpha_0^2 y_M \Upsilon^M - \alpha_0\sqrt{i}(H^M + K_1^M) + \frac{\alpha_0\sqrt{i}\,\pi}{2} \tag{4.176}$$

and S_p will also change due to its dependency on T_p. The equations (4.161)–(4.176) were used in the program to calculate the matrix coefficients associated with the anomalous electric field at the surface of the underlying half-space.

4.10 The Matrix Solution

For the E-polarization case the equations (4.38), (4.68), (4.69), (4.73), (4.74), (4.99) and (4.161) were used to provide the coefficients for the matrix that is solved by the forward modelling program. The equations used in the B-polarization case are (4.52), (4.77), (4.78), (3.13) and (4.134). The resulting matrix is tri-diagonal with fringes (see Press et al. 1992, Fig. 19.0.3) but has denser blocks in the top left (E-polarization only) and bottom right corners of the matrix arising from the top and bottom boundary conditions respectively. The matrix is solved by Gaussian elimination block by block with the resulting coefficients being written

to a file each time so that a large virtual memory is not needed. This method was used in order to facilitate the use of this program on smaller, less powerful computers. During the back substitution the program reads the coefficients from the file as needed. At present the program is limited to 20 periods, 30 specified sites, a numerical grid of 200 by 200 nodes and an input file with information on 5 different models. There is no limit on the number of differently conducting blocks (complexity) the model can have but the limits on the number of grid points in y and z will effectively limit the number of blocks. This limit will depend on the conductivities of the blocks, their arrangement, and the period under investigation. For instance, the COMMEMI model shown at the end of Chapter 5 has a model of 25 separate rectangular blocks and, at a period of 300 s, required a 105 by 36 grid. If the space is available all of these limitations can be changed by simply increasing the sizes of the related arrays in the program.

Chapter 5

AUTOMATIC GRIDDING OF TWO-DIMENSIONAL CONDUCTIVITY MODELS

5.1 Introduction

The solution of 2D inversion problems in electromagnetic induction requires repeated solutions of the corresponding 2D forward problem. The time required for a forward solution is limited by the time it takes the user to design new finite difference grids for the changing model parameters. In order to save time it was common practice to use a uniform grid in which all the cell sizes were equal. Unfortunately, this results in a grid that is not dense enough to maintain accuracy in some areas and is wastefully dense in other areas where it is not required. Practical multigrid methods exist that can be used in combination with numerical solution techniques to find the field (Press et al., 1992). This is done by speeding up the convergence of the traditional relaxation method or by obtaining successively more accurate solutions on finer and finer grids. In general, however, the grid design is done by hand and is therefore not only slow but also user specific. To ensure accuracy the

finite difference solution grids must be set up according to the following guidelines (see e.g. Weaver 1994):

i/ Near boundaries between areas of different conductivity the grid spacings must be no larger than one third the skin depth, and preferably smaller, to at least two to three skin depths away from the boundary after which they can be steadily increased.

ii/ As far as possible the grid spacing must change smoothly. (i.e. there must be no jumps such as from 100 km to 2 km). This criterion is especially important at vertical conductivity boundaries where the cells bordering it should be the same size.

iii/ The edges of the grid should be several skin depths removed from the nearest conductivity boundary.

The "best" grid will fulfill these demands yet minimize the number of nodes to speed the program's execution. Every time another forward solution is needed — due to changes in the model or the period — some of the skin depths and boundaries will change requiring an entirely new grid. This process can be extremely time consuming especially in the case of a very large or complex model. Consequently, in this thesis, an automatic gridding subroutine has been developed which has been incorporated into the forward modelling program (see Appendix B, GRIDYZ.FOR). It this method for automatic gridding that is described in this chapter.

The data required to define the input model are: the period, the polarization

(E-polarization or B-polarization and for B-polarization it must be specified on which side of the node the discontinuous fields are to be calculated), and the model parameters in the following format: (y,z) coordinates of the top left-hand corner of each rectangular block (irregular areas can be split any way), y length and z depth of the block, and resistivity (or conductivity) of the block. The extremities of the grid will be chosen automatically as four skin depths from the nearest boundary or they can be stipulated by the user. Any points in y, such as electrode positions, that must be incorporated into the grid can simply be specified in a separate "sites" file or added interactively. If the model and any sites are symmetric around zero then the grid produced will also be symmetric. If, however, symmetric sites are added interactively the grid may not be symmetric since in this mode the sites are added to the grid one by one in the optimum manner for each site without regard to any that were placed previously or are still to come.

5.2 General Gridding Procedure

The method used to grid a 2D conductivity model starts by compressing it into a single layer of smallest skin depths. For example, when gridding in the y direction, the program will examine each junction (i.e. vertical conductivity boundary) in the entire z range and choose the left-hand and right-hand skin depths which are smallest. Only the skin depths of those conductors that have a boundary at this junction are considered. The skin depths used to calculate the extremes of the grid are the largest skin depths of those layers that extend out to $\pm\infty$ (see

Fig. 5.1) even those that have no vertical boundary somewhere in the 2D model. This is done to avoid problems that can arise when there is a highly resistive surface layer under a highly conductive one. Ranganayaki and Madden (1980) and Weaver and Dawson (1992) have investigated such structures and shown that the anomalous fields persist to larger numbers of skin depths at shorter periods because the resistive layer inhibits vertical current flow into the conductive layers. The larger skin depths of the resistive layers will ensure that the grid extends out far enough to make the 1D approximations at the sides of the grid valid.

Compression in z results in a single layer with y junctions which is the first layer to be passed to the gridding subroutine. Starting from the second junction in the layer, Y_2, the routine grids the leftmost block beginning with cells of 1/4 the smallest skin depth at the junction (i.e. either $\lambda_{R,1}$ or $\lambda_{L,2}$). This is done to insure that the cell sizes will vary smoothly across each junction. If the smallest skin depth is $\lambda_{L,2}$ then the cell sizes double until the spacings are equal to $\lambda_{R,1}/4$. At this point a check is made to determine whether the grid has passed the left-hand extremity for y which is either given by the user or calculated to be $4\lambda^{-}$. If the distance between Y_2 and the user's given endpoint is less than what the program considers necessary, a warning to that effect is printed to the output file. The cell sizes are then increased gradually for a distance of $2\lambda_{R,1}$ with another check for the endpoint after each cell. If the left-hand extremity has still not been reached the cell sizes double until the latest $|y|$ value is greater than or equal to the absolute value of the chosen endpoint. Note that $\lambda_{L,1}$ is not used since the

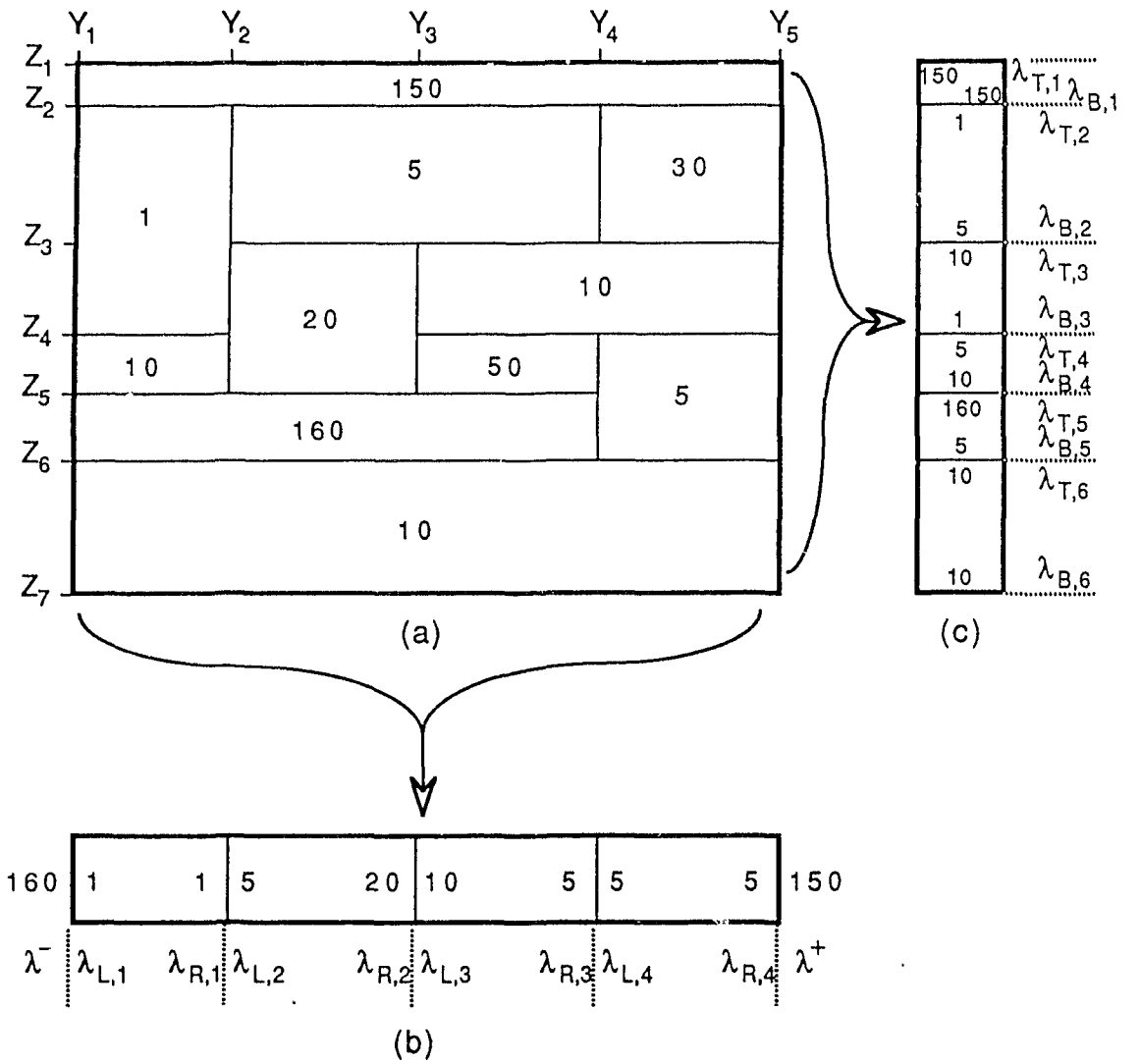

Figure 5.1: The above model illustrates the compression procedure used to generate the single layers for the automatic gridding subroutine. 1(a) is the original model and 1(b) and 1(c) are the single layers resulting from compression in z and y respectively. For each block in y, $Y_{m+1} - Y_m$, there is a smallest left-hand and right-hand skin depth ($\lambda_{L,m}$ and $\lambda_{R,m}$) and for each block in z, $Z_{n+1} - Z_n$, there is a smallest top and bottom skin depth ($\lambda_{T,n}$ and $\lambda_{B,n}$). The largest skin depths at the edges of the y layer, λ^+ and λ^- are used to calculate the left and right-hand extremes of the grid. The numerical values in the diagram are skin depths measured in the same units of length (e.g. km).

junction at Y_1 is not a conductivity boundary but just the edge of the 2D model.

Next all interior blocks of the compressed layer are gridded. A general block in the layer will be gridded using the previously described procedure from both its boundaries across the block until the opposite boundary is reached or overlapped. Thus two separate grids are generated for the same block – one running from Y_m to (or past) Y_{m+1} and the other from Y_{m+1} to (or past) Y_m. After inspecting the last cell in these alternate block grids we drop the larger of the two, thereby decreasing one of the block grids by one grid cell. This process continues with a comparison of the new last cells, i.e. the same one as before in the grid that did not lose a cell, and the last of the ones remaining in the grid that did lose a cell. If the last cells are the same size then a cell is dropped from the block grid that has lost the least number of cells so far or, if this occurs on the very first comparison, an arbitrary choice is made as to which of the last grid cells will be dropped. The two grids are reduced in this manner until eventually they become so short that they no longer overlap and the space between their endpoints is at least twice the smallest terminating cell size. A smooth joining of the two grids is then arranged by filling this space with cells whose size is an average of the last cells in each block grid. As the gridding for each block is completed the new grid points are stored in an array. This array is checked after each block is completed to insure that the total number of grid points for the model has not exceeded its maximum of 200 points in both the y and z directions. A model with many small blocks or small skin depths can cause the number of grid points to exceed 200 resulting in

another array being overwritten and the results being compromised. If this occurs a warning is sent to the output file and the job is terminated. Another check is made to insure that the first cell of the next block will be comparable in size to the last cell of the current block. If the spacing in the previous block is very fine then the size of the gradually increasing cell may not have attained the size allowed by the skin depth of the current block before Y_{m+1} is reached. If this is the case and the grid would not vary smoothly across the junction Y_{m+1} then the $\lambda_{L,m}$ or $\lambda_{T,n}$ is decreased so that the first cell of the next block will be the same size (or for the z grid no more than twice as large) as the last cell of the current block.

The right-hand block of the single layer for y, from Y_{M-1} to Y_M, is treated in an identical manner to the left-hand block except that the gridding proceeds from left to right. Here $\lambda_{R,M}$ is not used. All the same checks are performed to insure that the given or automatic endpoints are reached. It should be noted that since the grid will stop after the endpoint has been reached or passed, the actual extreme values of y, $|y_1|$ and $|y_M|$, will usually be greater than the absolute values of the endpoints.

The procedure used to generate a z grid is virtually identical to that for the y grid. Both the topmost and the bottom most blocks are treated as general interior blocks because integral boundary conditions eliminate the need for extending the grid above the surface of the earth or down into the underlying half space.

The main difference in generating the z grid is that, if the grid extends deeper than 6 skin depths, the cell sizes will be increased more rapidly (i.e. successively

doubled). At this depth a coarser grid will not significantly affect the accuracy of the solution because the field is already extremely small, but will keep the number of nodes to a minimum thereby increasing the speed of the forward solution. After the grids for both y and z have been completed the values obtained for the positions of the nodes are rounded off to make the output files easier to read. In general, if such a value is less than one, it is rounded off to two significant figures and, if greater than one, three significant figures. More significant figures are added if necessary based on the distance between nodes. For instance, if 120.25 and 120.50 are two consecutive nodes in the grid, rounding off to three significant figures would not be enough to differentiate between the nodes.

5.3 Special Cases

There are several special cases that can arise in gridding a model which require treatment that differs from the general procedure.

a/ Small blocks: Blocks with a length, L, less than twice the smallest skin depth, λ_s, at either boundary (eg. $\lambda_{L,m}, \lambda_{R,m-1}, \lambda_{R,m}$ or $\lambda_{L,m+1}$ in y) must be gridded differently.

Case 1/ $0.75 < \lambda_s \leq 2.00$ — The block is filled with uniform cells where cell size is as close to $\lambda_s/4$ as the block size will allow.

Case 2/ $0.50 < \lambda_s \leq 0.75$ — The block is divided into three equal cells.

Case 3/ $0.25 < \lambda_s \leq 0.50$ — The block is divided into two equal cells.

Case 4/ $0.00 < \lambda_s \leq 0.25$ — All the y blocks are divided into two equal cells so that

there is always one grid point contained within each cell. If it is the z grid that is being generated and the top block has already been gridded then the block will consist of only one cell.

b/ Violations of guideline ii/: A problem that can arise while gridding small blocks is that the spacing is often forced to be much smaller than that allowed by the bounding skin depths. This can result in large cells in a previous block occurring next to the much smaller cells of the current block; a situation that would violate guideline ii/ of our rules for creating the grid. To deal with this a check is made on the relative sizes of the last cell of the previous block and the first cell of the current block. If they are not sufficiently close in size then the previous block is regridded so that the cell sizes will vary smoothly across the boundary.

If the model in question is composed of just the right combination of skin depths and small block sizes the program may return to regrid a block over and over, unable to decide on the best of two equally acceptable grids. If this occurs one of the grids is chosen and the program is forced to proceed.

Another place where this violation of guideline ii/ can occur is during the adjustment of the two alternative block grids. If the cell sizes of one of the block grids is consistently larger than the other then, during the procedure described earlier where the last cells in the overlapping grids are dropped until they no longer overlap, this block grid will be reduced to zero (i.e. back to its starting junction) before the other block grid is touched. If this is the case then the second block grid is reduced cell by cell until the space between the last cell of this grid and

the starting junction on the other side of the block is at least twice the smallest terminating cell size or until the other block grid has also been reduced back to its starting junction. The terminating cell size of a block grid that has been reduced back to its starting junction is taken to be 1/4 the smallest skin depth at the junction. The space between the junction and the last cell of the remaining block grid is then filled with cells whose size is an average of the size of the terminating cells flanking the space. If the block grid that began at Y_m is reduced to zero then a check must be made of the relative sizes of the last cell of the previous block and the first cell filling in the space in the current block. If they are not sufficiently close in size then the previous block is regridded so that the cell sizes will vary smoothly across the boundary.

5.4 The Insertion of Sites Into the Grid

An important feature of the automatic gridding program is that it allows the user to insert into the grid any points he choses (such as the locations of data collection sites). This allows the user to immediately compare the results from the program with real data taken at these sites for the purposes of inversion. Before any sites are inserted a check is made to see if the existing grid and the chosen sites listed in a separate site file are symmetric around zero. If this is the case then care must be taken to insure that once the sites have been inserted the grid remains symmetric. Because adding a site will change the grid, symmetry is immediately destroyed once the first site has been inserted. Consequently all sites less than or

equal to zero are inserted and the resulting grid is flipped through the $y = 0$ axis to produce the other half of the desired symmetric grid.

To insert a site, y_s, a search must first be made to locate the two existing grid points on either side of the site, y_m and y_{m+1}. The next step in the procedure depends on the relationship of y_s to y_m and y_{m+1}.

Case 1/ If the site is equal to an existing grid point no change is made in the grid.

Case 2/ If y_m and y_{m+1} are both junctions then y_s is simply inserted between them so that the total number of grid points is increased by one. This can occur since, after insertion in the grid, all sites are treated as junctions so that their positions cannot be changed during the insertion of any other sites. So while the initial gridding in y always inserts a node between any two conductivity boundaries, trying to insert a site between another site and a conductivity boundary would fall into this case.

Case 3/ If y_m is a junction and y_s is close to y_{m+1} (i.e. $(y_s - y_m)/(y_{m+1} - y_m) \geq 0.75$) then it simply replaces y_{m+1} in the grid. Since the first two cells in a block are always 1/4 the skin depth or less this will never violate the condition (i).

Case 4/ If y_m is a junction and the site y_s is not close to y_{m+1} (i.e. $0.4 < (y_s - y_m)/(y_{m+1} - y_m) < 0.75$) then y_{m+1} is replaced by two new points: the site, y_s, and a point, y_{new}, between y_s and y_{m+2} such that

$$\frac{y_{m+2} - y_{\text{new}}}{y_{\text{new}} - y_s} = \frac{y_{m+2} - y_{m+1}}{y_{m+1} - y_m}. \tag{5.1}$$

The total number of grid points is increased by one. If y_s and the junction y_m are very close together so that $(y_s - y_m)/(y_{m+1} - y_m) < 0.4$ the smoothness

criterion (ii) will break down. This is prevented by making a check when the sites are first read in to see if any are closer to a junction than 1/10 of a skin depth. If so, the gridding in this area is forced to be smaller so that $(y_s - y_m)/(y_{m+1} - y_m) < 0.4$ never arises.

Case 5/ If y_{m+1} is a junction and y_s is close to y_m (i.e. $(y_{m+1} - y_s)/(y_{m+1} - y_m) \geq 0.75$) then it simply replaces y_m in the grid.

Case 6/ If y_{m+1} is a junction and y_s is not close to y_m (i.e. $0.4 < (y_{m+1} - y_s)/(y_{m+1} - y_m) < 0.75$) then y_m is replaced by two new points: the site, y_s, and a point, y_{new}, between y_s and y_{m-1} such that

$$\frac{y_{\text{new}} - y_{m-1}}{y_s - y_{\text{new}}} = \frac{y_m - y_{m-1}}{y_{m+1} - y_m}. \tag{5.2}$$

The total number of grid points is increased by one.

Case 7/ If neither y_m nor y_{m+1} is a junction and y_s is close to y_m (i.e. $(y_s - y_{m-1})/(y_m - y_{m-1}) \leq 1.25$) then y_m and y_{m+1} are replaced by two new points: the site, y_s, and a point, y_{new}, between y_s and y_{m+2} such that (5.1) is true.

Case 8/ If neither y_m nor y_{m+1} is a junction and y_s is close to y_{m+1} (i.e. $(y_{m+2} - y_s)/(y_{m+2} - y_{m+1}) \leq 1.25$) then y_m and y_{m+1} are replaced by two new points: the site, y_s, and a point, y_{new}, between y_s and y_{m-1} such that (5.2) is true.

Case 9/ If neither y_m nor y_{m+1} is a junction and y_s is not close to either one (i.e. $(y_s - y_{m-1})/(y_m - y_{m-1}) > 1.25$ and $(y_s - y_{m-1})/(y_m - y_{m-1}) > 1.25$) then y_m and y_{m+1} are replaced by three new points. These points are the site, y_s, a point, y_{new1}, between y_s and y_{m-1} such that (5.2) is true and a point, y_{new2},

between y_s and y_{m+2} such that (5.1) is true. The total number of grid points is increased by one.

The new grid points, y_{new}, are rounded off in the same way as the original grid points were but the site values are, of course, left alone since they are specified by the user. Each cell in the grid is then assigned its correct resistivity value and the solution of the forward problem can begin.

To illustrate the gridding procedure an adaptation of Model 2D-5, the most complex of the COMMEMI project models (Zhdanov 1982), is shown in Fig. 5.2. Fig. 5.3 is the grid produced for this conductivity distribution at a period of 300s by the automatic gridding facility. Note that the grid spacing varies smoothly and that regions of low resistivity are gridded more densely. The autogridding results in 105 y-grid points and 36 z-grid points whereas the original "hand-drawn" grid had 83 and 30 points respectively. The extra grid points arise from the stricter application of guidelines i/ and ii/ and the requirement for small y blocks that there always be at least one point in between two junctions. The savings in gridding time for a model of this complexity is of the order of *several hours* per frequency.

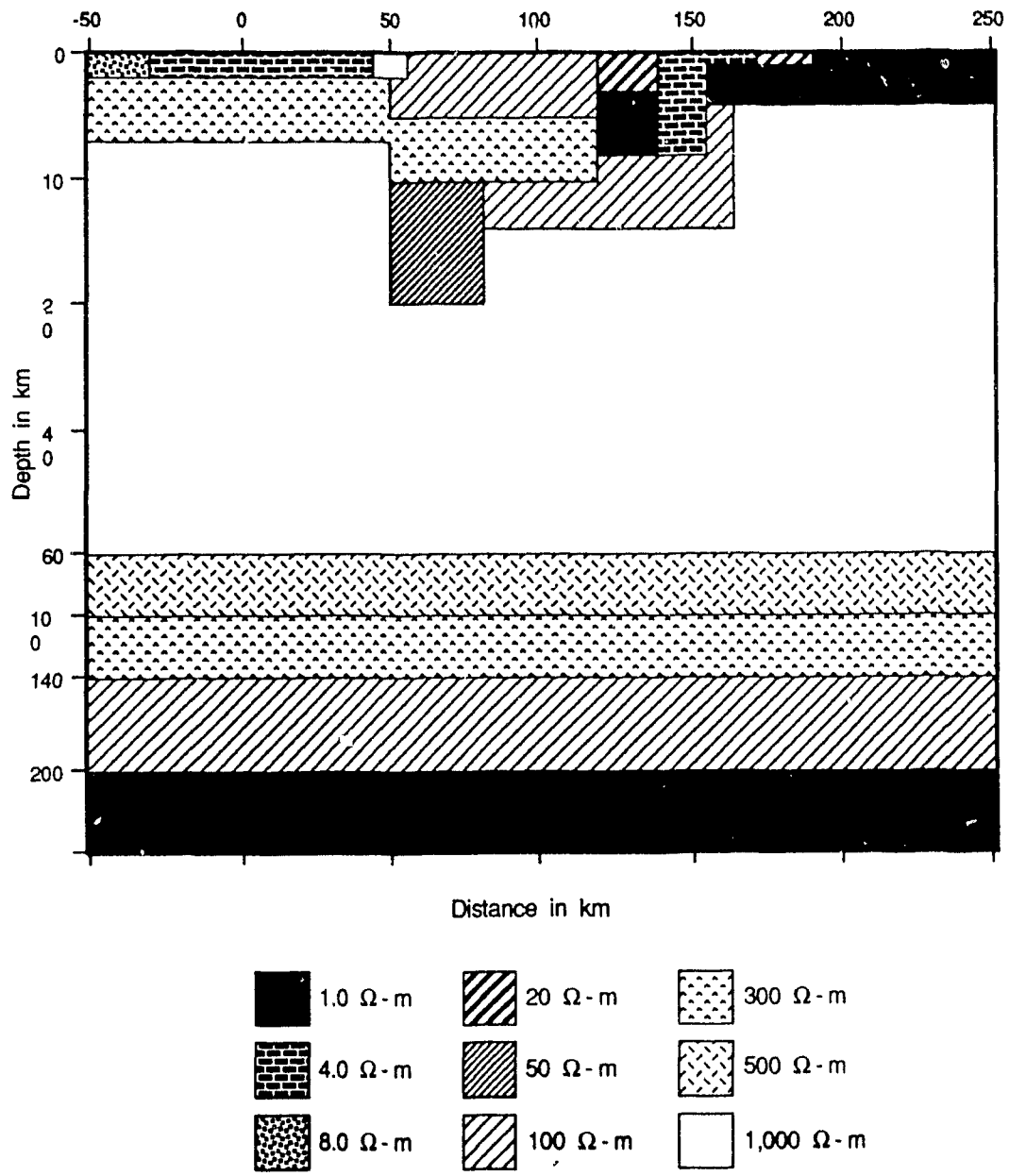

Figure 5.2: The two-dimensional magnetotelluric model shown above is a slightly modified version of Model 2D-5 of the COMMEMI project (Zhdanov 1982). Note that the z-axis is not to scale.

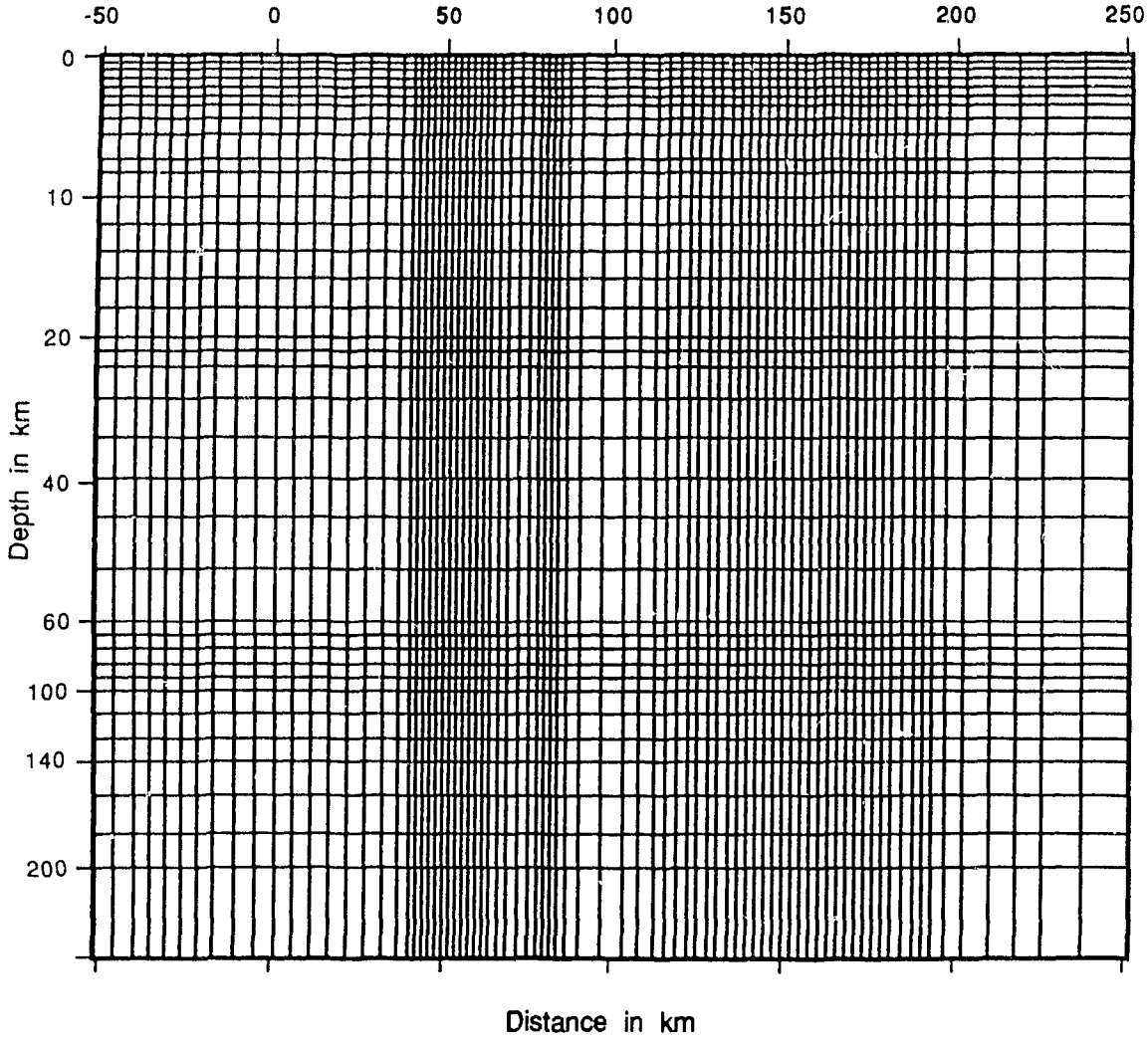

Figure 5.3: The automatically generated grid at a period of 300s for the model in Fig. 5.2. Note that the grid spacing is denser for regions of low resistivity. The z-axis is not to scale so that the area that contains most of the structure can be shown in more detail. This means that the areas of denser spacing of the horizontal lines below 20 km will have more to do with the scale of the axis rather than the relative resistivities of the model. The grid extends out further in the $\pm y$ direction than shown.

Chapter 6

COMPUTATION OF THE REMAINING FIELD COMPONENTS

6.1 Introduction

The remaining field components (the derivative fields) developed in this chapter are essentially those of Brewitt-Taylor and Weaver (1978). The equations for the horizontal electric field at the surface of the earth (6.63–6.71) have been developed here for the program listed in Appendix B. The equations for the derivative fields at the corners of the grid are also original to this thesis.

6.2 The E-polarization Case.

Following the method of Brewitt-Taylor and Weaver (1978) the U derivative fields for the E-polarization problem are calculated using the Taylor expansions around $z = z_n$

$$U_{m,n+1} = U_{m,n} + k_n \left(\frac{\partial U}{\partial z}\right)_{m,n} + \frac{1}{2} k_n^2 \left(\frac{\partial^2 U}{\partial z^2}\right)_{m,n+} \tag{6.1}$$

and

$$U_{m,n-1} = U_{m,n} - k_{n-1}\left(\frac{\partial U}{\partial z}\right)_{m,n} + \frac{1}{2}k_{n-1}^2\left(\frac{\partial^2 U}{\partial z^2}\right)_{m,n-} . \tag{6.2}$$

Using (2.26) to eliminate $(\partial U/\partial z)_{m,n}$ and $(\partial^2 U/\partial z^2)_{m,n}$ in both equations leaves

$$U_{m,n+1} = U_{m,n} - i\omega k_n Y_{m,n} - \frac{i\omega k_n^2}{2}\left(\frac{\partial Y}{\partial z}\right)_{m,n+} \tag{6.3}$$

and

$$U_{m,n-1} = U_{m,n} + i\omega k_{n-1} Y_{m,n} - \frac{i\omega k_{n-1}^2}{2}\left(\frac{\partial Y}{\partial z}\right)_{m,n-} . \tag{6.4}$$

Since $\partial Y/\partial z$ is discontinuous across $z = z_n$ the actual value for $(\partial Y/\partial z)_{m,n}$ will depend on which side of the boundary it is evaluated. Equation (6.3) requires evaluation of the derivative just below the $z = z_n$ boundary and (6.4) just above it. Equation (2.25) is used to obtain a value for the $(\partial Y/\partial z)_{m,n+}$ in (6.3) of

$$\left(\frac{\partial Y}{\partial z}\right)_{m,n+} = -\mu_0 s_{m,n+} U_{m,n} + \left(\frac{\partial Z}{\partial y}\right)_{m,n} \tag{6.5}$$

with

$$s_{m,n+} = \frac{h_m \sigma_{m,n} + h_{m-1}\sigma_{m-1,n}}{h_m^+} . \tag{6.6}$$

The value $s_{m,n+}$ must be used since $\partial Y/\partial z$ is being evaluated just below $z = z_n$ but *at* $y = y_m$ where the conductivity is neither $\sigma_{m,n}$ nor $\sigma_{m-1,n}$ but a weighted average of the two.

Similarly $(\partial Y/\partial z)_{m,n-}$ in (6.4) can be written as

$$\left(\frac{\partial Y}{\partial z}\right)_{m,n-} = -\mu_0 s_{m,n-} U_{m,n} + \left(\frac{\partial Z}{\partial y}\right)_{m,n} \tag{6.7}$$

with

$$s_{m,n-} = \frac{h_m \sigma_{m,n-1} + h_{m-1}\sigma_{m-1,n-1}}{h_m^+}. \tag{6.8}$$

A substitution of (6.5) and (6.7) into (6.3) and (6.4) respectively results in

$$U_{m,n+1} = U_{m,n} - i\omega k_n Y_{m,n} + \frac{i\omega\mu_0 s_{m,n+} k_n^2}{2} U_{m,n} - \frac{i\omega k_n^2}{2}\left(\frac{\partial Z}{\partial y}\right)_{m,n} \tag{6.9}$$

and

$$U_{m,n-1} = U_{m,n} + i\omega k_{n-1} Y_{m,n} + \frac{i\omega\mu_0 s_{m,n-} k_{n-1}^2}{2} U_{m,n} - \frac{i\omega k_{n-1}^2}{2}\left(\frac{\partial Z}{\partial y}\right)_{m,n}. \tag{6.10}$$

Since $(\partial Z/\partial y)$ is continuous across $z = z_n$ these terms can be eliminated from the equations by multiplying (6.9) by k_{n-1}^2 and (6.10) by k_n^2 and subtracting. After some rearrangement the result is

$$\begin{aligned} Y_{m,n} &= \frac{i}{\omega k_n^+}\left(\frac{k_{n-1}}{k_n} U_{m,n+1} - \frac{k_n}{k_{n-1}} U_{m,n-1} - \left[\frac{k_{n-1}}{k_n} - \frac{k_n}{k_{n-1}}\right.\right. \\ &\quad \left.\left. + \frac{i\omega\mu_0 k_n k_{n-1}}{2}(s_{m,n+} - s_{m,n-})\right] U_{m,n}\right). \end{aligned} \tag{6.11}$$

By starting with the Taylor expansions about $y = y_m$ and following a similar procedure to that for the $Y_{m,n}$ calculation is is possible to calculate the Z derivative field for the E-polarization problem

$$\begin{aligned} Z_{m,n} &= -\frac{i}{\omega h_m^+}\left(\frac{h_{m-1}}{h_m} U_{m+1,n} - \frac{h_m}{h_{m-1}} U_{m-1,n} - \left[\frac{h_{m-1}}{h_m} - \frac{h_m}{h_{m-1}}\right.\right. \\ &\quad \left.\left. + \frac{i\omega\mu_0 h_m h_{m-1}}{2}(s_{m+,n} - s_{m-,n})\right] U_{m,n}\right) \end{aligned} \tag{6.12}$$

with

$$s_{m+,n} = \frac{k_n \sigma_{m,n} + k_{n-1}\sigma_{m,n-1}}{k_n^+}, \tag{6.13}$$

$$s_{m-,n} = \frac{k_n \sigma_{m-1,n} + k_{n-1}\sigma_{m-1,n-1}}{k_n^+}. \tag{6.14}$$

At the top of the grid (i.e. where $z = 0$) the formula (6.11) cannot be used because of the dependence on $U_{m,n-1}$ which in this case would be located above the surface of the earth. An alternative expression can be derived for use at $z = z_1 = 0$ by differentiating (2.26) in z, to obtain

$$\left(\frac{\partial Y}{\partial z}\right)_{m,1} = -\frac{1}{i\omega}\left(\frac{\partial^2 U}{\partial z^2}\right)_{m,1} \tag{6.15}$$

and then rewriting it with the aid of (2.32) in the form

$$\left(\frac{\partial Y}{\partial z}\right)_{m,1} = -\frac{1}{i\omega}\left[i\omega\mu_0 s_{m,1+} U_{m,1} - \left(\frac{\partial^2 U}{\partial y^2}\right)_{m,1}\right]. \tag{6.16}$$

Using (4.4) an expression can be found for $(\partial^2 U/\partial y^2)_{m,1}$ which, when substituted into (6.16) and the result into (6.3), yields an alternative equation for $Y_{m,1}$

$$\begin{aligned} Y_{m,1} = \frac{i}{\omega}\Bigg(\frac{U_{m,2}}{k_1} - \left[\frac{1}{k_1} + \frac{k_1}{h_m h_{m-1}} + \frac{i\omega\mu_0 s_{m,1+} k_1}{2}\right] U_{m,1} \\ + \frac{k_1}{h_m h_m^+} U_{m+1,1} + \frac{k_1}{h_{m-1} h_m^+} U_{m-1,1}\Bigg) \end{aligned} \tag{6.17}$$

which can be used at $z = z_1 = 0$.

At the bottom of the grid (i.e. where $z = z_N$) the formula (6.11) cannot be used because of the dependence on $U_{m,n+1}$ which would be located inside the underlying half-space where field values are not available. An alternative expression can be derived for use at $z = z_N$ in the same way as for (6.17) except that $s_{m,N-}$ is used in (6.16) and the starting equation is (6.4) instead of (6.3) so that

$$\begin{aligned} Y_{m,N} = -\frac{i}{\omega}\Bigg(\frac{U_{m,N-1}}{k_{N-1}} - \left[\frac{1}{k_{N-1}} + \frac{k_{N-1}}{h_m h_{m-1}} + \frac{i\omega\mu_0 s_{m,N-} k_{N-1}}{2}\right] U_{m,N} \\ + \frac{k_{N-1}}{h_m h_m^+} U_{m+1,N} + \frac{k_{N-1}}{h_{m-1} h_m^+} U_{m-1,N}\Bigg) \end{aligned} \tag{6.18}$$

which can be used at $z = z_N$. The original expression for $Y_{m,n}$ in (6.11) is more accurate than either (6.17) or (6.18) for all other values of z in the same way that a central difference expression is more accurate than a one-sided difference expression. In fact, in the same way that the addition of one-sided differences yields a central difference, if (6.17) is multiplied by k_{n-1} and (6.18) by k_n with both equations written out for a general interior node (y_m, z_n), the summation of the two yields (6.11).

Equation (6.12) can still be used to calculate $Z_{m,n}$ at $z = 0$ but with $s_{m+,n}$ and $s_{m-,n}$ replaced by $\sigma_{m,n}$ and $\sigma_{m-1,n}$ respectively. Similarly (6.12) can be used to calculate $Z_{m,n}$ at $z = z_N$ but with $s_{m+,n}$ and $s_{m-,n}$ replaced by $\sigma_{m,n-1}$ and $\sigma_{m-1,n-1}$ respectively.

If the underlying half-space is a perfect conductor (i.e. $\sigma_N = \infty$) then $U_{m,N} = 0$ for all m and hence by (2.27) $Z_{m,N} = 0$ for all m. To calculate $Y_{m,N}$ (with $\sigma_N = \infty$) the Taylor expansion

$$U_{m,N-2} = U_{m,N} - (k_{N-1} + k_{N-2}) \left(\frac{\partial U}{\partial z}\right)_{m,N} + \frac{(k_{N-1} + k_{N-2})^2}{2} \left(\frac{\partial^2 U}{\partial z^2}\right)_{m,N-} \quad (6.19)$$

is used together with (6.2). Multiplying (6.2) by $(k_{N-1} + k_{N-2})^2$ and the above equation by k_{N-1}^2 and subtracting eliminates $\left(\frac{\partial^2 U}{\partial z^2}\right)_{m,N-}$. After some rearrangement and using (2.26) the resulting equation is

$$Y_{m,N} = -\frac{i}{\omega k_{N-2}} \left(\frac{k_{N-1}^+}{k_{N-1}} U_{m,N-1} - \frac{k_{N-1}}{k_{N-1}^+} U_{m,N-2} - \left[\frac{k_{N-1}^+}{k_{N-1}} - \frac{k_{N-1}}{k_{N-1}^+} \right] U_{m,N} \right) \quad (6.20)$$

which is used at the surface of a perfect conductor. Of course since $U_{m,N} = 0$ there the corresponding term in the above equation will also be zero.

Equation (6.11) can be used for the values of $Y_{m,n}$ at $m = 1$ or $m = M$ with $s_{m,n+}$ and $s_{m,n-}$ replaced by $\sigma_{m,n}$ and $\sigma_{m,n-1}$ respectively. In order to find an expression for $Z_{m,n}$ at the edges of the grid the side boundary conditions (4.54) and (4.64) are used to obtain values for $\frac{\partial U}{\partial y}$ at the edges. The result is

$$Z_{1,n} = -\frac{i}{\omega}\left(\frac{U_n^- - U_{1,n}}{y_1}\right) \tag{6.21}$$

and

$$Z_{M,n} = -\frac{i}{\omega}\left(\frac{U_n^+ - U_{M,n}}{y_M}\right) \tag{6.22}$$

which are used at the left and right edges respectively.

The corners of the grid also require special treatment and the following equations, which we have derived in a manner similar to that used for (6.20), give the values at these points:

$$Y_{m,1} = \frac{i}{\omega k_2}\left(\frac{k_2^+}{k_1}U_{m,2} - \frac{k_1}{k_2^+}U_{m,3} - \left[\frac{k_2^+}{k_1} - \frac{k_1}{k_2^+}\right]U_{m,1}\right) \tag{6.23}$$

for $m = 1, M$ and $n = 1$ and

$$Y_{m,N} = -\frac{i}{\omega k_{N-2}}\left(\frac{k_{N-1}^+}{k_{N-1}}U_{m,N-1} - \frac{k_{N-1}}{k_{N-1}^+}U_{m,N-2} - \left[\frac{k_{N-1}^+}{k_{N-1}} - \frac{k_{N-1}}{k_{N-1}^+}\right]U_{m,N}\right) \tag{6.24}$$

for $m = 1, M$ and $n = N$. Note that (6.24) and (6.20) are identical. The values for Z at the corners can be obtained from the edge equations (6.21) and (6.22) with $n = 1$ and $n = N$.

6.3 The B-polarization Case

The B-polarization derivatives can be found by beginning with the Taylor expansions

$$X_{m,n+1} = X_{m,n} + k_n \left(\frac{\partial X}{\partial z}\right)_{m,n+} + \frac{k_n^2}{2}\left(\frac{\partial^2 X}{\partial z^2}\right)_{m,n+} \tag{6.25}$$

and

$$X_{m,n-1} = X_{m,n} - k_{n-1} \left(\frac{\partial X}{\partial z}\right)_{m,n-} + \frac{k_{n-1}^2}{2}\left(\frac{\partial^2 X}{\partial z^2}\right)_{m,n-}. \tag{6.26}$$

Using (2.31) expressions can be found for the second derivatives $(\partial^2 X/\partial z^2)_{m,n\pm}$

$$\left(\frac{\partial^2 X}{\partial z^2}\right)_{m,n\pm} = \frac{i\omega\mu_0}{r_{m,n\pm}} X_{m,n} - \left(\frac{1}{\rho}\frac{\partial \rho}{\partial y}\right)_{m,n\pm}\left(\frac{\partial X}{\partial y}\right)_{m,n} - \left(\frac{\partial^2 X}{\partial y^2}\right)_{m,n} \tag{6.27}$$

with

$$r_{m,n+} = \frac{h_m \rho_{m,n} + h_{m-1}\rho_{m-1,n}}{h_m^+}, \tag{6.28}$$

$$r_{m,n-} = \frac{h_m \rho_{m,n-1} + h_{m-1}\rho_{m-1,n-1}}{h_m^+}. \tag{6.29}$$

The term in (2.31) involving $(\partial\rho/\partial z)_{m,n\pm}$ does not appear in (6.27) since $z = z_n$ is considered to be a sharp boundary between two regions whose ρ's vary in y but not in z. When (6.27) is substituted into the expansions (6.25) and (6.26) and both are rearranged somewhat, the results are

$$\begin{aligned} k_n \left(\frac{\partial X}{\partial z}\right)_{m,n+} &= X_{m,n+1} - \left(1 + \frac{i\omega\mu_0 k_n^2}{2r_{m,n+}}\right) X_{m,n} \\ &\quad + \frac{k_n^2}{2}\left(\frac{1}{\rho}\frac{\partial \rho}{\partial y}\right)_{m,n+}\left(\frac{\partial X}{\partial y}\right)_{m,n} + \frac{k_n^2}{2}\left(\frac{\partial^2 X}{\partial y^2}\right)_{m,n} \end{aligned} \tag{6.30}$$

and

$$-k_{n-1}\left(\frac{\partial X}{\partial z}\right)_{m,n-} = X_{m,n-1} - \left(1 + \frac{i\omega\mu_0 k_{n-1}^2}{2r_{m,n-}}\right) X_{m,n} + \frac{k_{n-1}^2}{2}\left(\frac{1}{\rho}\frac{\partial \rho}{\partial y}\right)_{m,n-}\left(\frac{\partial X}{\partial y}\right)_{m,n} + \frac{k_{n-1}^2}{2}\left(\frac{\partial^2 X}{\partial y^2}\right)_{m,n}. \quad (6.31)$$

Multiplying (6.30) by k_{n-1}^2 and (6.31) by k_n^2 and subtracting eliminates the second derivative and leaves

$$\left[k_{n-1}\left(\frac{\partial X}{\partial z}\right)_{m,n+} + k_n\left(\frac{\partial X}{\partial z}\right)_{m,n-}\right] k_n k_{n-1} = k_{n-1}^2 X_{m,n+1} - k_n^2 X_{m,n-1} - \left[k_{n-1}^2 - k_n^2 + \frac{i\omega\mu_0 k_n^2 k_{n-1}^2}{2}\left(\frac{1}{r_{m,n+}} - \frac{1}{r_{m,n-}}\right)\right] X_{m,n} + \frac{k_n^2 k_{n-1}^2}{2}\left[\left(\frac{1}{\rho}\frac{\partial \rho}{\partial y}\right)_{m,n+} - \left(\frac{1}{\rho}\frac{\partial \rho}{\partial y}\right)_{m,n-}\right]\left(\frac{\partial X}{\partial y}\right)_{m,n}. \quad (6.32)$$

The term in the second pair of square brackets can be written as

$$\left(\frac{1}{\rho}\frac{\partial \rho}{\partial y}\right)_{m,n+} - \left(\frac{1}{\rho}\frac{\partial \rho}{\partial y}\right)_{m,n-} = \frac{1}{r_{m,n+}}\frac{\rho_{m,n} - \rho_{m-1,n}}{\frac{1}{2}h_m^+} - \frac{1}{r_{m,n-}}\frac{\rho_{m,n-1} - \rho_{m-1,n-1}}{\frac{1}{2}h_m^+} \quad (6.33)$$

and $(\partial X/\partial y)_{m,n}$, in finite difference form, as

$$\left(\frac{\partial X}{\partial y}\right)_{m,n} = \frac{1}{h_m h_{m-1} h_m^+}\left(h_{m-1}^2 X_{m+1,n} - h_m^2 X_{m-1,n} - \left(h_{m-1}^2 - h_m^2\right) X_{m,n}\right). \quad (6.34)$$

After substitution of (6.33) and (6.34) into (6.32) and some rearrangement we have

$$k_{n-1}\left(\frac{\partial X}{\partial z}\right)_{m,n+} + k_n\left(\frac{\partial X}{\partial z}\right)_{m,n-} = \frac{k_{n-1}}{k_n} X_{m,n+1} - \frac{k_n}{k_{n-1}} X_{m,n-1} - \left[\frac{k_{n-1}}{k_n} - \frac{k_n}{k_{n-1}} + \frac{i\omega\mu_0 k_n k_{n-1}}{2}\left(\frac{1}{r_{m,n+}} - \frac{1}{r_{m,n-}}\right) - C_{m,n}\left(\frac{h_{m-1}}{h_m} - \frac{h_m}{h_{m-1}}\right)\right] X_{m,n} - C_{m,n}\frac{h_{m-1}}{h_m} X_{m+1,n} + C_{m,n}\frac{h_m}{h_{m-1}} X_{m-1,n} \quad (6.35)$$

where

$$C_{m,n} = \frac{k_n k_{n-1}}{(h_m^+)^2}\left[\frac{\rho_{m,n-1} - \rho_{m-1,n-1}}{r_{m,n-}} - \frac{\rho_{m,n} - \rho_{m-1,n}}{r_{m,n+}}\right]. \tag{6.36}$$

Now using the definition of the current density $\mathbf{J} = \mathbf{E}/\rho$ and (2.23), $(\partial X/\partial z)_{m,n\pm}$ can be written

$$\left(\frac{\partial X}{\partial z}\right)_{m,n\pm} = \mu_0 (j_y)_{m,n\pm}. \tag{6.37}$$

Also, since $V = \rho j_y$ is continuous across $z = z_n$, it is possible to construct a definition of $(j_y)_{m,n}$ by the formula

$$r_{m,n+}(j_y)_{m,n+} = r_{m,n-}(j_y)_{m,n-} = \frac{k_n r_{m,n+} + k_{n-1} r_{m,n-}}{k_n^+}(j_y)_{m,n}. \tag{6.38}$$

Substituting (6.37) into (6.35) and using (6.38) to convert $(j_y)_{m,n\pm}$ to $(j_y)_{m,n}$ leads to

$$\begin{aligned}(j_y)_{m,n} = \frac{k_n^+ r_{m,n-} r_{m,n+}}{\mu_0 (k_{n-1} r_{m,n-} + k_n r_{m,n+})^2}\Bigg[&\frac{k_{n-1}}{k_n} X_{m,n+1} - \frac{k_n}{k_{n-1}} X_{m,n-1} - \left[\frac{k_{n-1}}{k_n} - \frac{k_n}{k_{n-1}}\right.\\ &+ \frac{i\omega\mu_0 k_n k_{n-1}}{2}\left(\frac{1}{r_{m,n+}} - \frac{1}{r_{m,n-}}\right) - C_{m,n}\left(\frac{h_{m-1}}{h_m} - \frac{h_m}{h_{m-1}}\right)\Bigg] X_{m,n}\\ &- C_{m,n}\frac{h_{m-1}}{h_m} X_{m+1,n} + C_{m,n}\frac{h_m}{h_{m-1}} X_{m-1,n}\Bigg].\end{aligned} \tag{6.39}$$

Now the following can be defined

$$V_{m-,n} = r_{m-,n}(j_y)_{m,n} \tag{6.40}$$

and

$$V_{m+,n} = r_{m+,n}(j_y)_{m,n} \tag{6.41}$$

with

$$r_{m-,n} = \frac{k_n \rho_{m-1,n} + k_{n-1} \rho_{m-1,n-1}}{k_n^+} \tag{6.42}$$

and

$$r_{m+,n} = \frac{k_n \rho_{m,n} + k_{n-1} \rho_{m,n-1}}{k_n^+} \tag{6.43}$$

except for the special case of a "vertical fault" at the horizontal boundaries of the model (see Fig. 6.1). This is due to the fact that it is not possible to obtain a valid finite difference representation for the electromagnetic field at a node where both $y = y_m$ and $z = z_n$ represent sharp boundaries between areas of different conductivity. For a more detailed discussion of this see Brewitt-Taylor and Weaver (1976). Inside the grid this problem can be overcome by regarding each node of the grid as being inside a region whose conductivity is an average of that of the four surrounding regions. At the top and bottom of the grid however, $z = 0$ and $z = z_N$ *must* be regarded as sharp boundaries. A vertical fault at the nodes $(m, 1)$ (point A in the vertical fault shown in Fig. 6.1) or (m, n) must therefore be dealt with by assuming that the conductivity just inside the grid edges varies smoothly in the horizontal direction so that when $\rho_{m-1,n-1} = \rho_{m,n-1}$ and $\rho_{m,n-1} \neq \rho_{m,n} \neq \rho_{m-1,n}$ then

$$V_{m-,n} = \rho_{m-1,n} (j_y)_{m,n+} \tag{6.44}$$

$$V_{m+,n} = \rho_{m,n} (j_y)_{m,n+} \tag{6.45}$$

and when $\rho_{m-1,n} = \rho_{m,n}$ and $\rho_{m,n} \neq \rho_{m-1,n-1} \neq \rho_{m,n-1}$

$$V_{m-,n} = \rho_{m-1,n-1} (j_y)_{m,n-} \tag{6.46}$$

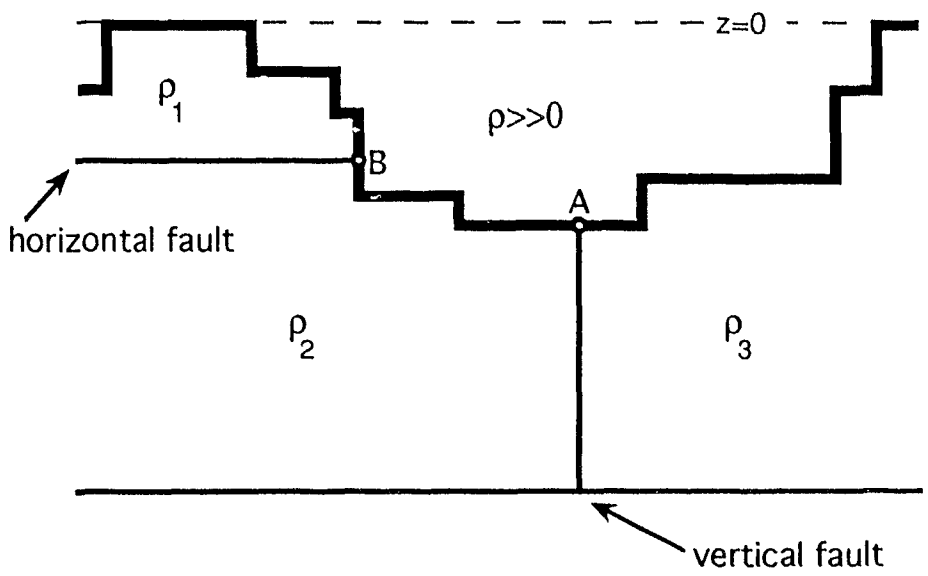

Figure 6.1: The figure above illustrates the fault cases that could arise while modelling topography. The thick line represents the surface of the earth while the thinner ones are boundaries between regions of different resistivity. The special case formulas for V and W are required to handle the situations at A and B respectively.

$$V_{m+,n} = \rho_{m,n-1}(j_y)_{m,n-}. \tag{6.47}$$

The values for $(j_y)_{m,n\pm}$ can be easily obtained from $(j_y)_{m,n}$ with the aid of (6.38). These "vertical fault" situations can arise inside the grid when modelling topographic features of the earth in which $z = 0$ is defined as the point of highest altitude in the model and the air space between $z = 0$ and lower ground levels is treated as an area of very high resistivity (see Fig. 6.1).

To calculate the W derivative field Taylor expansions are used around $y = y_m$ and a similar procedure to that of the $(j_y)_{m,n}$ calculation is followed so that eventually we obtain

$$\begin{aligned}(j_z)_{m,n} = \frac{h_m^+ r_{m+,n} r_{m-,n}}{\mu_0(h_{m-1}r_{m-,n} + h_m r_{m+,n})^2}\Bigg[&\frac{h_m}{h_{m-1}}X_{m-1,n} - \frac{h_{m-1}}{h_m}X_{m+1,n} + \Bigg[\frac{h_{m-1}}{h_m} - \frac{h_m}{h_{m-1}} \\ &+ \frac{i\omega\mu_0 h_m h_{m-1}}{2}\left(\frac{1}{r_{m+,n}} - \frac{1}{r_{m-,n}}\right) - D_{m,n}\left(\frac{k_{n-1}}{k_n} - \frac{k_n}{k_{n-1}}\right)\Bigg]X_{m,n} \\ &+ D_{m,n}\frac{k_{n-1}}{k_n}X_{m,n+1} - D_{m,n}\frac{k_n}{k_{n-1}}X_{m,n-1}\Bigg]\end{aligned} \tag{6.48}$$

with

$$D_{m,n} = \frac{h_m h_{m-1}}{(k_n^+)^2}\left[\frac{\rho_{m-1,n} - \rho_{m-1,n-1}}{r_{m-,n}} - \frac{\rho_{m,n} - \rho_{m,n-1}}{r_{m+,n}}\right]. \tag{6.49}$$

Now

$$W_{m,n-} = r_{m,n-}(j_z)_{m,n} \tag{6.50}$$

and

$$W_{m,n+} = r_{m,n+}(j_z)_{m,n} \tag{6.51}$$

except for the case of the "horizontal fault" exposed by a vertical dip in the earths topography (in the manner shown at point B, Fig. 6.1) which needs special

treatment for reasons analogous to those given for the vertical fault. So when $\rho_{m-1,n-1} = \rho_{m-1,n}$ and $\rho_{m,n-1} \neq \rho_{m,n} \neq \rho_{m-1,n}$ then

$$W_{m,n-} = \rho_{m,n-1}(j_z)_{m+,n} \tag{6.52}$$

$$W_{m,n+} = \rho_{m,n}(j_z)_{m+,n} \tag{6.53}$$

and when $\rho_{m,n-1} = \rho_{m,n}$ and $\rho_{m-1,n-1} \neq \rho_{m-1,n} \neq \rho_{m,n}$ (which is the case for point B in Fig. 6.1) then

$$W_{m,n-} = \rho_{m-1,n-1}(j_z)_{m-,n} \tag{6.54}$$

$$W_{m,n+} = \rho_{m-1,n}(j_z)_{m-,n}. \tag{6.55}$$

The values for $(j_z)_{m\pm,n}$ can be easily obtained from $(j_z)_{m,n}$ by using the equation analogous to (6.38)

$$r_{m-,n}(j_z)_{m-,n} = r_{m+,n}(j_z)_{m+,n} = \frac{h_m r_{m+,n} + h_{m-1} r_{m-,n}}{h_m^+}(j_z)_{m,n}. \tag{6.56}$$

The above equations for all the special cases in finding the B-polarization derivatives are used in the program.

At the top of the grid where $z = 0$ the expressions derived for $V_{m\pm,n}$ could be used since, from (2.32), the value of X on or above the surface of the earth is a real constant X_0 so that

$$X_{m+1,1} = X_{m-1,1} = X_{m,1} = X_{m,0} = X_0. \tag{6.57}$$

In this case the equations (6.44) and (6.45) must be used and if we recall that in $z < 0$, $1/\rho \to 0$ then they simplify to

$$V_{m-,1} = \frac{\rho_{m-1,1}}{\mu_0}\left[\frac{X_{m,2} - X_0}{k_1} - \frac{i\omega\mu_0 k_1 X_0}{2r_{m,1+}}\right] \tag{6.58}$$

$$V_{m+,1} = \frac{\rho_{m,1}}{\mu_0}\left[\frac{X_{m,2} - X_0}{k_1} - \frac{i\omega\mu_0 k_1 X_0}{2r_{m,1+}}\right]. \tag{6.59}$$

The problem with these formulae becomes apparent when the phase is calculated. The phase is

$$\phi = \arg\left(\frac{-V}{X_0}\right) = \tan^{-1}\left(\frac{\Im V}{\Re V}\right) \tag{6.60}$$

and therefore, using (6.58) and (6.59)

$$\phi_{m-,1} = \phi_{m+,1} = \tan^{-1}\left(\frac{\Im X_{m,2} - \frac{\omega\mu_0 k_1^2 X_0}{2r_{m,1+}}}{\Re X_{m,2} - X_0}\right) \tag{6.61}$$

where $y = y_m$ is a boundary between two conducting media with resistivities $\rho_{m-1,1}$ and $\rho_{m,1}$ (see Fig. 6.2). If $y = y_{m-1}$ is not another such boundary (i.e. $\rho_{m-2,1} = \rho_{m-1,1}$) then

$$\phi_{m-1,1} = \tan^{-1}\left(\frac{\Im X_{m-1,2} - \frac{\omega\mu_0 k_1^2 X_0}{2\rho_{m-1,1}}}{\Re X_{m-1,2} - X_0}\right). \tag{6.62}$$

If we let $h_{m-1} \to 0$ then $X_{m-1,2} \to X_{m,2}$ but $r_{m,1+} \to \rho_{m,1}$ rather than $\rho_{m-1,1}$, so the phases calculated this way will not match well at $y = y_m$.

Because of this problem we have developed an alternative approach to finding the horizontal electric field at the surface which can be used in the program. It involves fitting three adjacent points in the z-direction with a parabola. In order to do this the first two layers of grid cells must have identical conductivity values since if $\rho_{m,2} \neq \rho_{m,1}$ then $\partial X/\partial z = \mu_0 V/\rho$ would not be continuous across $z = z_2$ and any parabola fitted through $X_{m,1}$, $X_{m,2}$ and $X_{m,3}$ would be meaningless. The grid generation program takes this into account and if the top two layers are not

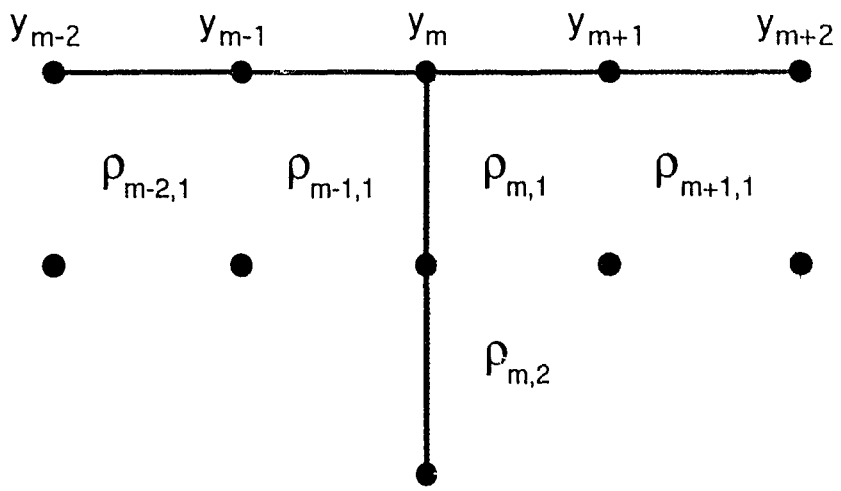

Figure 6.2: A boundary between two conducting media with resistivities $\rho_{m-1,1}$ and $\rho_{m,1}$ and with $\rho_{m-2,1} = \rho_{m-1,1}$ and $\rho_{m+1,1} = \rho_{m,1} = \rho_{m,2}$.

already identical it splits the top row into two narrower ones. In this case we can write

$$X(y_m,z) = X_0 + z\frac{X_{m,2}-X_0}{k_1} + z(z-k_1)\frac{k_1X_{m,3}-(k_1+k_2)X_{m,2}+k_2X_0}{k_1k_2(k_1+k_2)} \quad (6.63)$$

which is the formula for a parabola satisfying $X(y_m,0) = X_{m,1} = X_0$, $X(y_m,k_1) = X_{m,2}$ and $X(y_m,k_1+k_2) = X_{m,3}$. Now since $V_{m\pm,1} = \rho_{m\pm,1}X'(y_m,0)/\mu_0$ we have

$$V_{m-,1} = \frac{\rho_{m-1,1}}{\mu_0}\left[\frac{k_2^+}{k_1k_2}X_{m,2} - \frac{k_2+2k_1}{k_1k_2^+}X_0 - \frac{k_1}{k_2k_2^+}X_{m,3}\right] \quad (6.64)$$

and

$$V_{m+,1} = \frac{\rho_{m,1}}{\mu_0}\left[\frac{k_2^+}{k_1k_2}X_{m,2} - \frac{k_2+2k_1}{k_1k_2^+}X_0 - \frac{k_1}{k_2k_2^+}X_{m,3}\right]. \quad (6.65)$$

At the surface of the earth $W_{m,n\pm}$ is set equal to zero. This equation was used in the program to find the horizontal electric field at the surface of the earth.

At the bottom of the grid $(j_y)_{m,N}$ is dependent on $X_{m,N+1}$ for which there is no value so (6.26) is combined with (6.27), (6.33), (4.3) and (4.4) to find the expression:

$$\begin{aligned}(j_y)_{m,N-} = \frac{1}{\mu_0}\Bigg[&-\frac{1}{k_{N-1}}X_{m,N-1} + \left[\frac{1}{k_{N-1}} + \frac{k_{N-1}}{h_mh_{m-1}} + \frac{i\omega\mu_0k_{N-1}}{2r_{m,N-}}\right.\\ &\left.+C_{m,N}\left(\frac{h_{m-1}}{h_m} - \frac{h_m}{h_{m-1}}\right)\right]X_{m,N} - \left(C_{m,N}\frac{h_{m-1}}{h_m} + \frac{k_{N-1}}{h_mh_m^+}\right)X_{m+1,N}\\ &+\left(C_{m,N}\frac{h_m}{h_{m-1}} - \frac{k_{N-1}}{h_{m-1}h_m^+}\right)X_{m-1,N}\Bigg]\end{aligned} \quad (6.66)$$

with

$$C_{m,N} = \frac{k_{N-1}}{(h_m^+)^2}\frac{\rho_{m,N-1}-\rho_{m-1,N-1}}{r_{m,N-}}. \quad (6.67)$$

Hence, at $z = z_N$ we have

$$V_{m-,N} = \rho_{m-1,N-1}(j_y)_{m,N-} \tag{6.68}$$

$$V_{m+,N} = \rho_{m,N-1}(j_y)_{m,N-}. \tag{6.69}$$

Equations (6.68) and (6.69) are programmed with the help of (6.66) and (6.67).

For $W_{m,N\pm}$ we use one-sided finite difference formulas for the z derivative substitutions in $(j_z)_{m,n}$ so that it becomes

$$\begin{aligned}(j_z)_{m,N} = \frac{h_m^+ r_{m+,N} r_{m-,N}}{\mu_0(h_{m-1}r_{m-,N} + h_m r_{m+,N})^2}\Bigg[&\frac{h_m}{h_{m-1}}X_{m-1,N} - \frac{h_{m-1}}{h_m}X_{m+1,N} \\ &+\left[\frac{h_{m-1}}{h_m} - \frac{h_m}{h_{m-1}} + \frac{i\omega\mu_0 h_m h_{m-1}}{2}\left(\frac{1}{r_{m+,N}} - \frac{1}{r_{m-,N}}\right)\right. \\ &\left.-D_{m,N}\left(\frac{k_{N-1}^+}{k_{N-1}k_{N-2}} - \frac{k_{N-1}}{k_{N-1}^+ k_{N-2}}\right)\right]X_{m,N} \\ &+D_{m,N}\frac{k_{N-1}}{k_{N-1}^+ k_{N-2}}X_{m,N-2} - D_{m,N}\frac{k_{N-1}^+}{k_{N-1}k_{N-2}}X_{m,N-1}\Bigg]\end{aligned} \tag{6.70}$$

with

$$D_{m,N} = \frac{h_m h_{m-1}}{2k_{N-1}}\left[\frac{\rho_{m-1,N} - \rho_{m-1,N-1}}{r_{m-,N}} - \frac{\rho_{m,N} - \rho_{m,N-1}}{r_{m+,N}}\right]. \tag{6.71}$$

Using the above value for $(j_z)_{m,N}$, we can use (6.50) and (6.51) to calculate $W_{m,N\pm}$ in the program.

If $z = z_N$ is the surface of a perfect conductor then $V_{m\pm,N} = 0$ which can be seen from the fact that $X' = \mu_0\sigma V$ and the bottom boundary condition is $X' = 0$. Since $r_{m,N+} = 0$ equation (6.51) requires $W_{m,N+} = 0$. The only non-zero derivative is

$$W_{m,N-} = r_{m,N-}(j_z)_{m,N} \tag{6.72}$$

where the $r_{m\pm,N}$ in $(j_z)_{m,N}$ are replaced by $\rho_{\binom{m}{m-1},N-1}$ and $D_{m,N}=0$.

At the edges, which are sufficiently far removed from all anomalies that $X_{1,n}=X_n^-$ and $X_{M,n}=X_n^+$, the model is essentially a 1D conductivity profile where the only differences in ρ are in the z-direction. Hence $C_{1,n}=0$ and (6.40) and (6.41) are replaced by

$$V_{1,n}=\frac{\rho_{1,n-1}\rho_{1,n}}{\mu_0 k_n^+ r_{1+,n}}\left[\frac{k_{n-1}}{k_n}X_{1,n+1}-\frac{k_n}{k_{n-1}}X_{1,n-1}\right.$$
$$\left.-\left[\frac{k_{n-1}}{k_n}-\frac{k_n}{k_{n-1}}+\frac{i\omega\mu_0 k_n k_{n-1}}{2}\left(\frac{1}{\rho_{1,n}}-\frac{1}{\rho_{1,n-1}}\right)\right]X_{1,n}\right] \tag{6.73}$$

for $m=1$ and

$$V_{M,n}=\frac{\rho_{M-1,n-1}\rho_{M-1,n}}{\mu_0 k_n^+ r_{M-,n}}\left[\frac{k_{n-1}}{k_n}X_{M,n+1}-\frac{k_n}{k_{n-1}}X_{M,n-1}\right.$$
$$\left.-\left[\frac{k_{n-1}}{k_n}-\frac{k_n}{k_{n-1}}+\frac{i\omega\mu_0 k_n k_{n-1}}{2}\left(\frac{1}{\rho_{M-1,n}}-\frac{1}{\rho_{M-1,n-1}}\right)\right]X_{M,n}\right] \tag{6.74}$$

for $m=M$. The equations for $W_{m,n\pm}$ at $m=1$ and $m=M$ are straightforward since $W=-\frac{1}{\mu_0\sigma}\left(\frac{\partial X}{\partial y}\right)$ and, as stated above, the only differences in X at the edges are in the z-direction so that $W_{1,n\pm}=0$ and $W_{M,n\pm}=0$.

At the top corners we can use (6.65) for $V_{1,1}$, and (6.64) for $V_{M,1}$, while $W_{1,1}$ and $W_{M,1}$ will both be zero. At the bottom corners $W_{1,N}$ and $W_{M,N}$ will be zero as well, but (6.66) must be calculated using one-sided derivatives to give

$$V_{1\pm,N}=\frac{\rho_{1,N-1}}{\mu_0}\left[-\frac{1}{k_{N-1}}X_{1,N-1}+\left[\frac{1}{k_{N-1}}-\left(\frac{k_{N-1}}{h_1 h_2}-\frac{k_{N-1}}{h_2 h_2^+}\right)\right.\right.$$
$$\left.\left.+\frac{i\omega\mu_0 k_{N-1}}{2\rho_{1,N-1}}\right]X_{1,N}+\frac{k_{N-1}}{h_1 h_2}X_{2,N}-\frac{k_{N-1}}{h_2 h_2^+}X_{3,N}\right] \tag{6.75}$$

and

$$V_{M\pm,N}=\frac{\rho_{M-1,N-1}}{\mu_0}\left[-\frac{1}{k_{N-1}}X_{M,N-1}+\left[\frac{1}{k_{N-1}}-\left(\frac{k_{N-1}}{h_{M-1}h_{M-2}}-\frac{k_{N-1}}{h_{M-2}h_{M-1}^+}\right)\right.\right.$$

$$+\frac{i\omega\mu_0 k_{N-1}}{2\rho_{M-1,N-1}}\Bigg] X_{M,N} + \frac{k_{N-1}}{h_{M-1}h_{M-2}} X_{M-1,N} - \frac{k_{N-1}}{h_{M-2}h^{+}_{M-1}} X_{M-2,N}\Bigg]. \quad (6.76)$$

Chapter 7

TWO-DIMENSIONAL INVERSION OF SARDINIAN MAGNETOTELLURIC DATA

7.1 Introduction

To illustrate the use of the forward modelling program, we have used it, together with a simple trial and error inversion, to perform a two-dimensional inversion on magnetotelluric (MT) data from a profile in Sardinia. It is obvious from Fig. 7.1 that the overall prevailing strike for the island is north-south (NS). The east side of the island is mainly Paleozoic granites or metamorphic rocks which are generally found to have high resistivities of about 10^4 ohm-m. Faults are a basic element of this structure, cutting it deeply into horsts and grabens. The western surface formations are primarily a mixture of volcanics and lacustrine and marine depositional rocks with low resistivities of about 10 ohm-m. There is one major fault, the Campidano, with a strike approximately NW-SE. The local strike is, however, generally oriented in an east-west (EW) direction creating, in effect, a three dimensional problem.

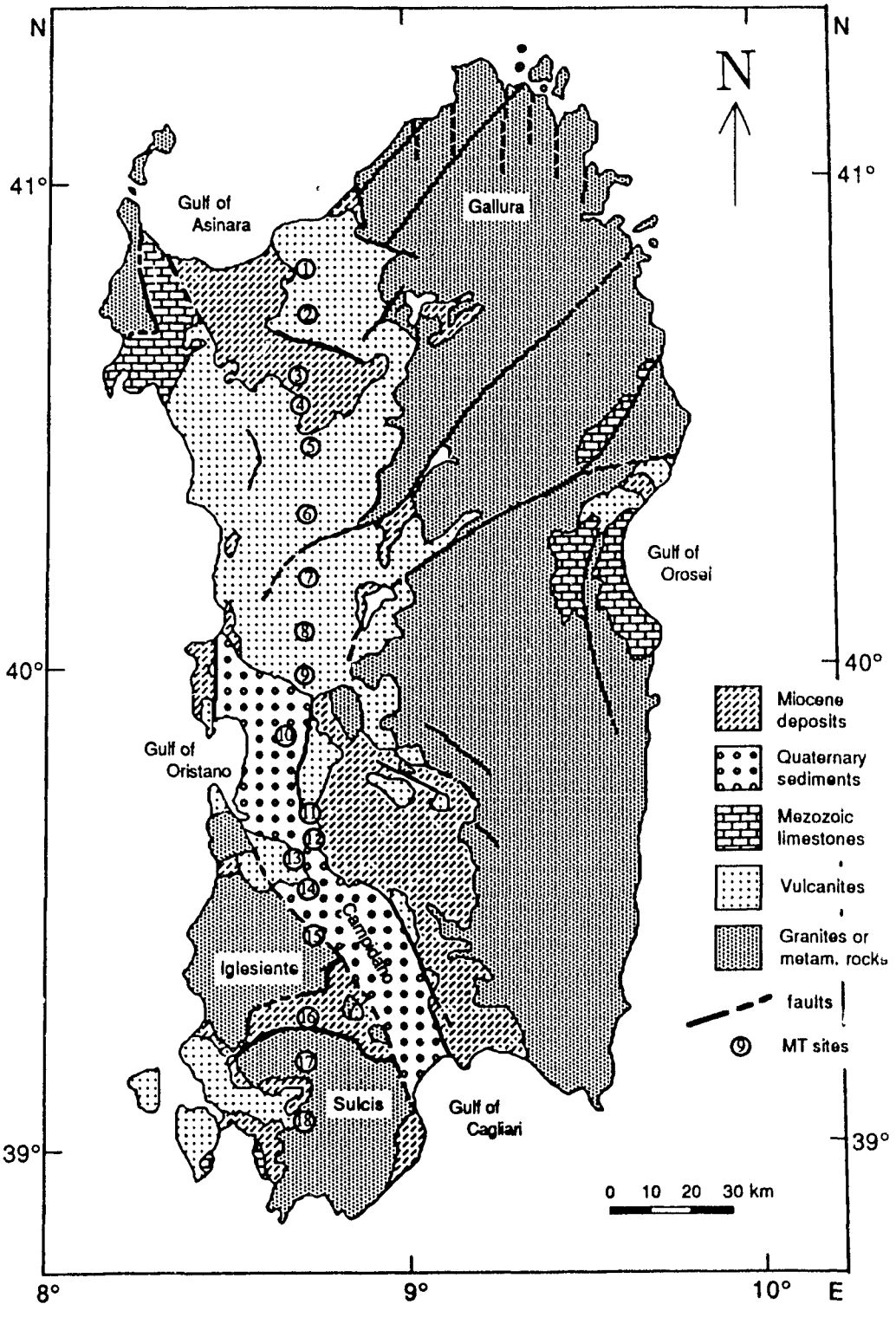

Figure 7.1: Tectonic map of Sardinia and location of the magnetotelluric sounding sites based on a map from Peruzza et al. (1990).

The data from the NS profile (sites 1–18) shown in Fig. 7.1 were collected by Fischer et al. (1990) in 1987 and have been analysed by them in terms of one and two-dimensional models (Peruzza et al., 1990). The original data are E- and B-polarization apparent resistivities and phases derived from an MT time series. The phase data were considered to be too scattered to be useful and were occasionally even outside the accepted range of $0 - 90^{o}$. For the period range under investigation ($10^{-3} - 250$ s.) Perruzza et al. found that the sea was too far removed (10–30 km) to produce a coast effect at any of the sites. Most of their sites were also far enough away from the eastern granites not to be affected by their high resistivities — with the exception of sites 9 and 10. The effect of the neighbouring resistors on these sites was to depress the long period apparent resistivities for the polarization with the electric field pointing EW. By ignoring the long period data for this polarization at sites 9 and 10 as well as at sites 12–14, which are similarly affected by the highly resistive Iglesiente metamorphic formations to the west of them, Peruzza et al. (1990) were able to interpret the remaining data on a purely 2D basis. The result of this investigation is the 2D magnetotelluric model of the NS profile shown in Fig. 7.2.

In this chapter we are concerned with sites 9 and 10 which cannot be considered to be solely 2D in the NS direction. As a first look at the underlying geology that may be causing the long period anisotropy of these data sets we have performed 2D inversions on them to obtain models for the EW direction. For an EW conductivity variation the B-polarization apparent resistivity curves will be affected

(i.e.: depressed) as can be seen in Fig. 7.3 and 7.4 which show the data sets for sites 9 and 10. To reduce the computing time only ten periods were selected from the total period range available. First the entire data set, minus a few outliers, was fitted with a low order polynomial and then the values of this curve at the desired periods were calculated. These data, tabulated in Table 7.1, were provided by Gaston Fischer (private communication).

7.2 The Two-dimensional Inversion

The 2D inversion program uses the auto-gridding forward program, together with a 2D adaptation of the optimization subroutine MINDEF used by Fischer and Le Quang (1981), to search for a minimum of the standard deviation ϵ in the space of the model parameters. The minimum obtained is usually not the global minimum but some local minimum determined by the choice of the initial model. In general the program inverts the complex surface impedance $Z(T)$ given in terms of apparent resistivity $\rho_a(T)$ and phase $\phi(T)$ versus period T

$$Z(T) = \sqrt{\omega \mu_0 \rho_a(T)}\, e^{i\phi(T)}. \tag{7.1}$$

Since the natural scales of both the period and the apparent resistivity are logarithmic we take the log of (7.1), i.e.

$$\ln Z(T) = \ln \sqrt{\omega \mu_0} + \frac{1}{2} \ln \rho_a(T) + i\phi(T) \tag{7.2}$$

and actually fit $\frac{1}{2} \ln \rho_a(T)$ and $\phi(T)$, since the first term is constant for a given period T. The standard deviation ϵ between the measured field data (indicated

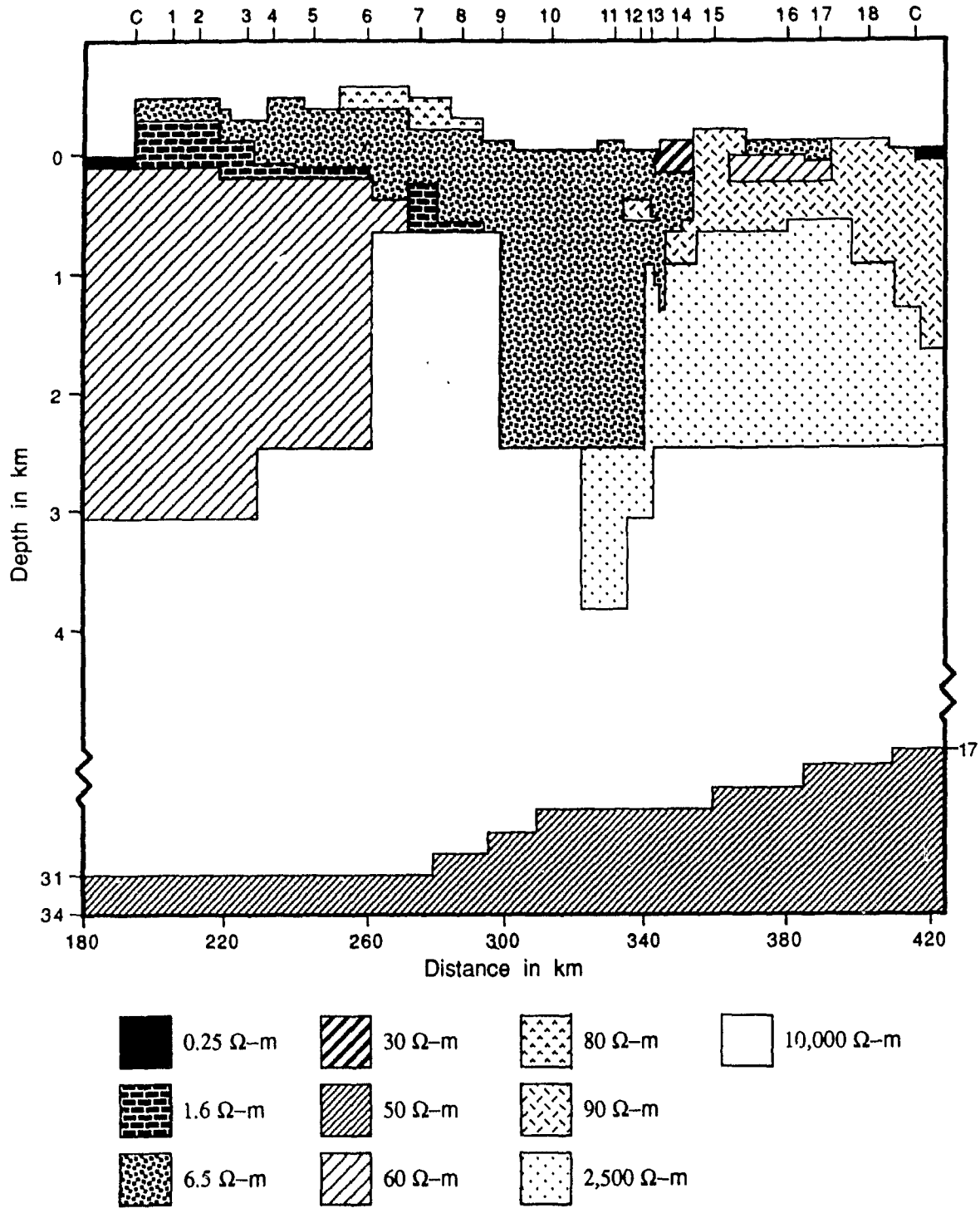

Figure 7.2: The two-dimensional magnetotelluric model of Peruzza et al. (1990) for the NS Sardinian profile shown in Fig. 7.1. The black areas are seawater and the symbols C indicate the locations of the coastline.

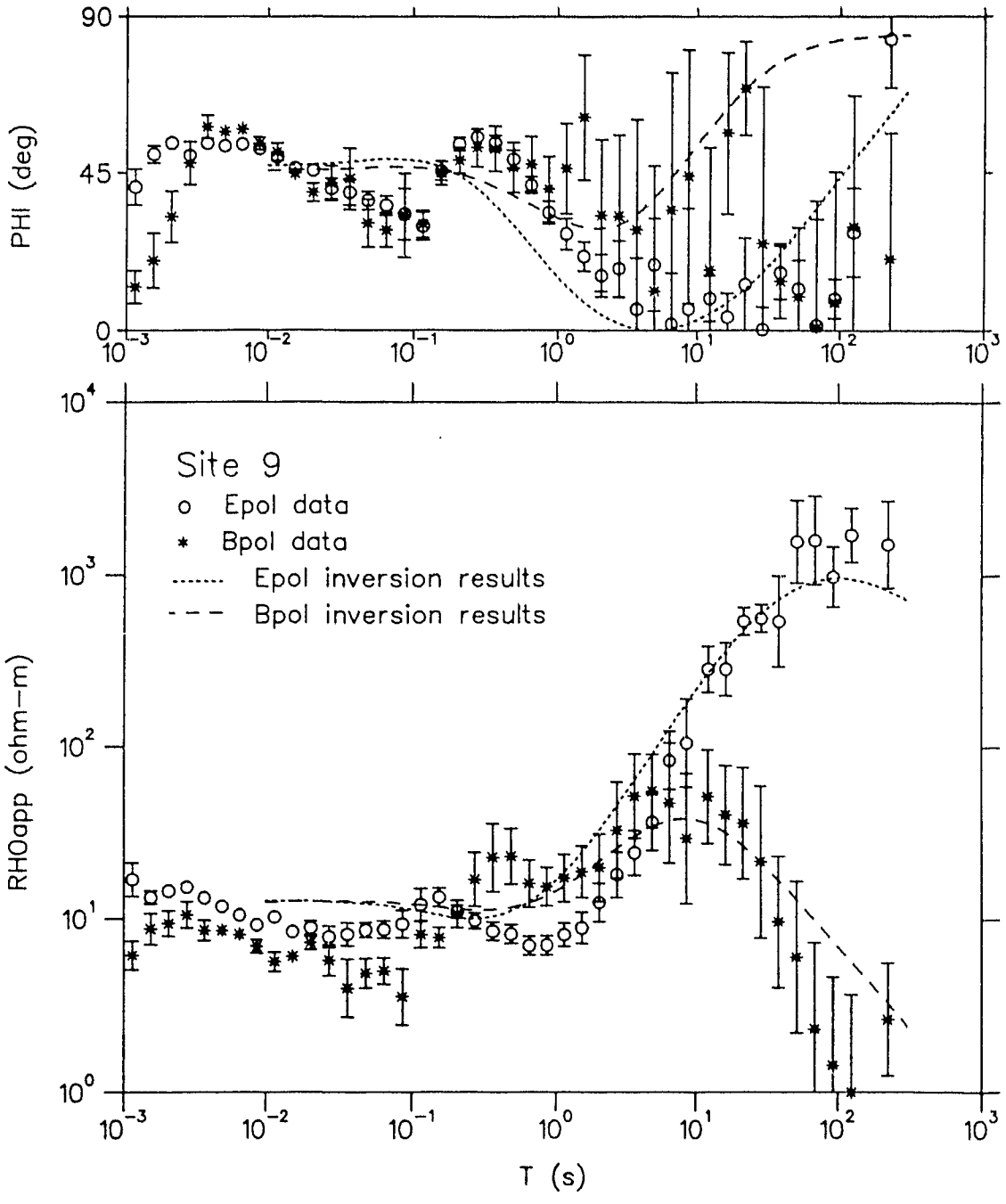

Figure 7.3: The magnetotelluric Sardinian data collected by Fischer et al. (1990) along with the ρ_{app} and ϕ data from the 2D model generated by the inversion for site 9. The E-pol data are represented by open cicles and the B-pol data by asterisks. The dashed lines are polynomial fits to the inversion results for the two polarizations. The ε value is 0.0441. Although phase data were not used for the inversion the trend of the phases is reproduced quite well by the inversion curves.

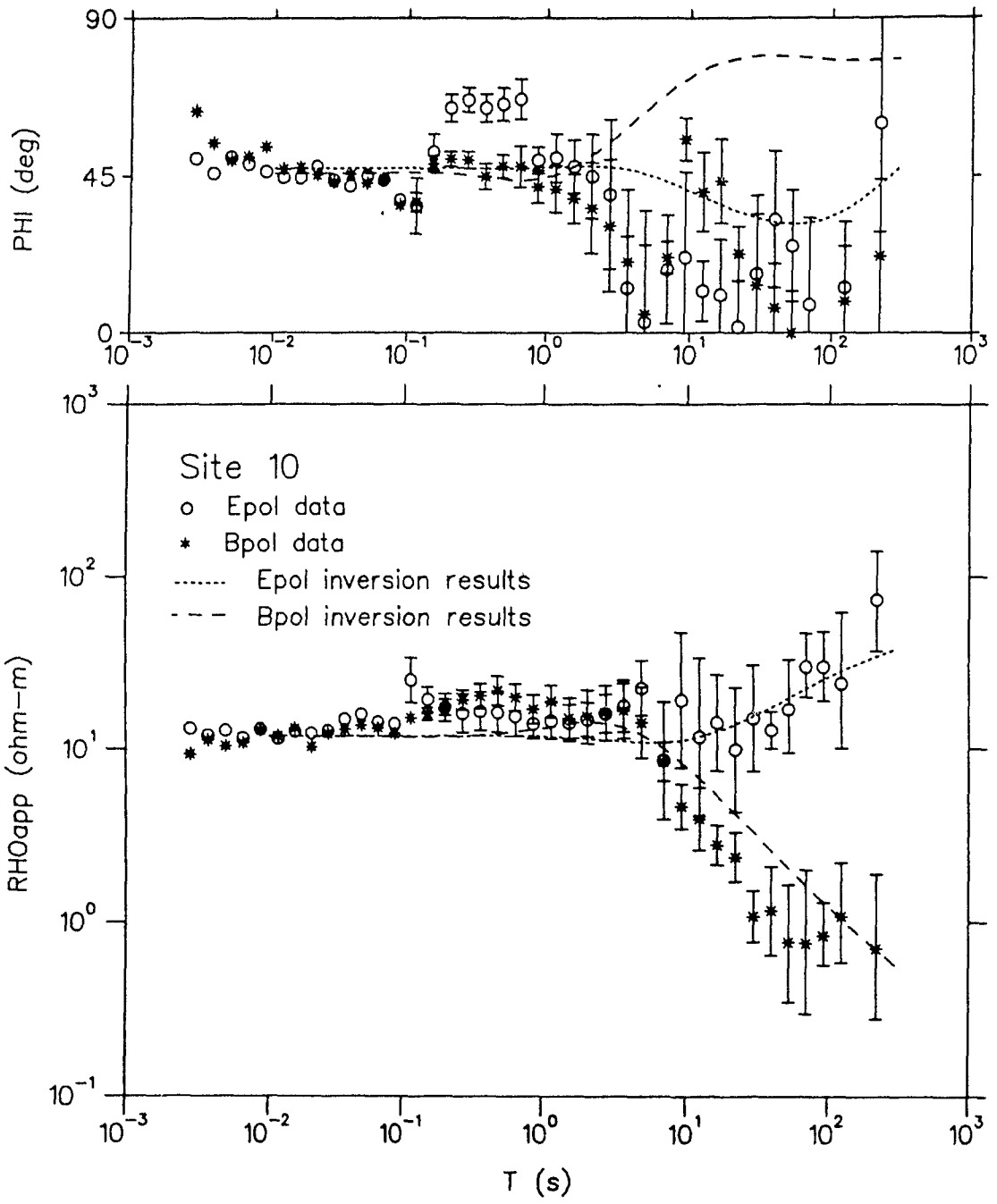

Figure 7.4: The magnetotelluric Sardinian data collected by Fischer et al. (1990) along with the ρ_{app} and ϕ data from the 2D model generated by the inversion for site 10. The E-pol data are represented by open cicles and the B-pol data by asterisks. The dashed lines are polynomial fits to the inversion results for the two polarizations. The ε value is 0.0224. The trend of the long period phase data is not reproduced very well by the inversion curves.

Period (s)	Apparent Resistivity (ohm-m)			
	Site 9		Site 10	
	E-pol	B-pol	E-pol	B-pol
0.01	10.0	10.0	12.4	12.4
0.03	10.2	10.2	12.9	12.9
0.1	10.8	10.8	13.4	13.4
0.3	11.9	11.9	14.4	14.4
1.0	17.6	17.6	15.9	15.9
3.0	36.1	36.0	16.1	13.5
10.0	128.	50.3	13.8	6.04
30.0	631.	20.0	14.5	1.72
100.0	1470.	2.95	25.1	0.81
300.0	1800.	1.38	63.1	0.64

Table 7.1: Selected data collected by Fischer et al. (1990) at sites 9 and 10 of their NS profile in Sardinia.

below by the subscript m) and the calculated data (subscript c) at each site is

$$\epsilon = \frac{1}{\sqrt{2}} \left[\frac{1}{4N} \sum_{i=1}^{N} w_{\rho i} \left\{ \ln \frac{\rho_{ac}(T_i)}{\rho_{am}(T_i)} \right\}^2 + \frac{1}{N} \sum_{i=1}^{N} w_{\phi i} \{ \phi_c(T_i) - \phi_m(T_i) \}^2 \right]^{1/2} \tag{7.3}$$

where the phases are in radians and N is the total number of periods T_i $(i = 1, \ldots, N)$ at which data were collected. The weights are normalized so that

$$\sum_{i=1}^{N} w_{\rho i} = \sum_{i=1}^{N} w_{\phi i} = N. \tag{7.4}$$

For sites 9 and 10 we were inverting only apparent resistivity data and all the values were given equal weight, so that the standard deviation became

$$\epsilon_\rho = \left[\frac{1}{4N} \sum_{i=1}^{N} \left\{ \ln \frac{\rho_a(T_i)}{\rho_{am}(T_i)} \right\}^2 \right]^{1/2}. \tag{7.5}$$

For two polarizations and only one site we have

$$\epsilon = \frac{1}{\sqrt{2}} [\epsilon^2_{\rho,Epol} + \epsilon^2_{\rho,Bpol}]^{1/2}. \tag{7.6}$$

The step sizes in parameter space are controlled by the size of the parameters themselves so that small parameters change by small steps and large parameters by large steps. The resistivities were restricted to remain within the range of 10^{-1} to 10^6 ohm-m. The program stores the smallest value of ϵ found and, using a technique similar to a 'ravine search' (Bevington 1969, pg 207), searches for a model that will have an even smaller ϵ. When such a model is found the new model parameters and their corresponding ϵ are stored and the program begins a new search. A solution is reached when ϵ falls below a desired value, when a given number of iterations have been performed or when no appreciable decrease in ϵ has occurred for a given number of iterations.

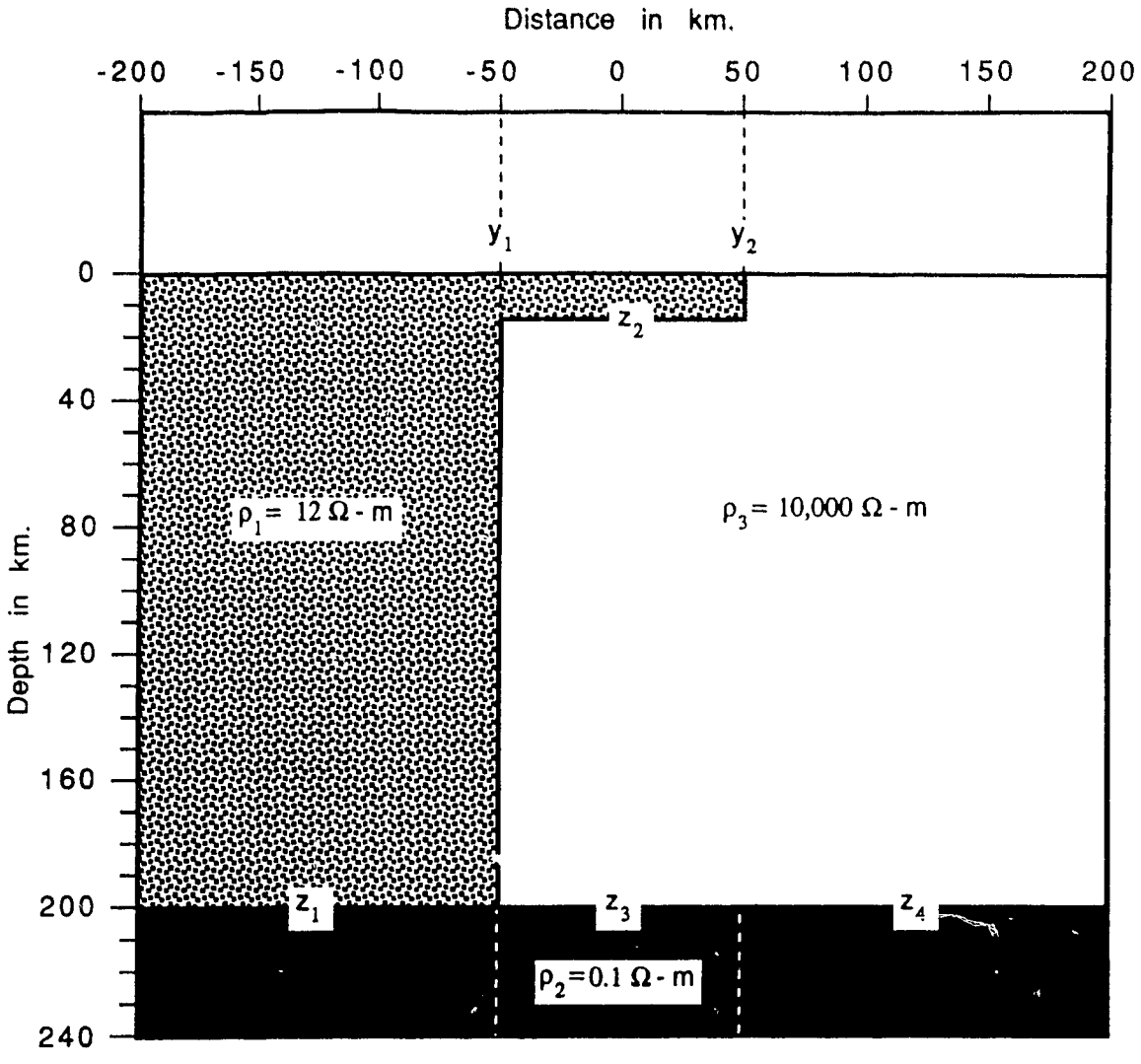

Figure 7.5: The first of the two 2D starting models for use at sites 9 and 10 in the inversion of magnetotelluric Sardinian data collected by Fischer et al. (1990). The underlying half-space has a resistivity of 0.1 ohm-m. The dashed lines are the boundaries between the vertical strips required by the inversion program. The model is an EW profile.

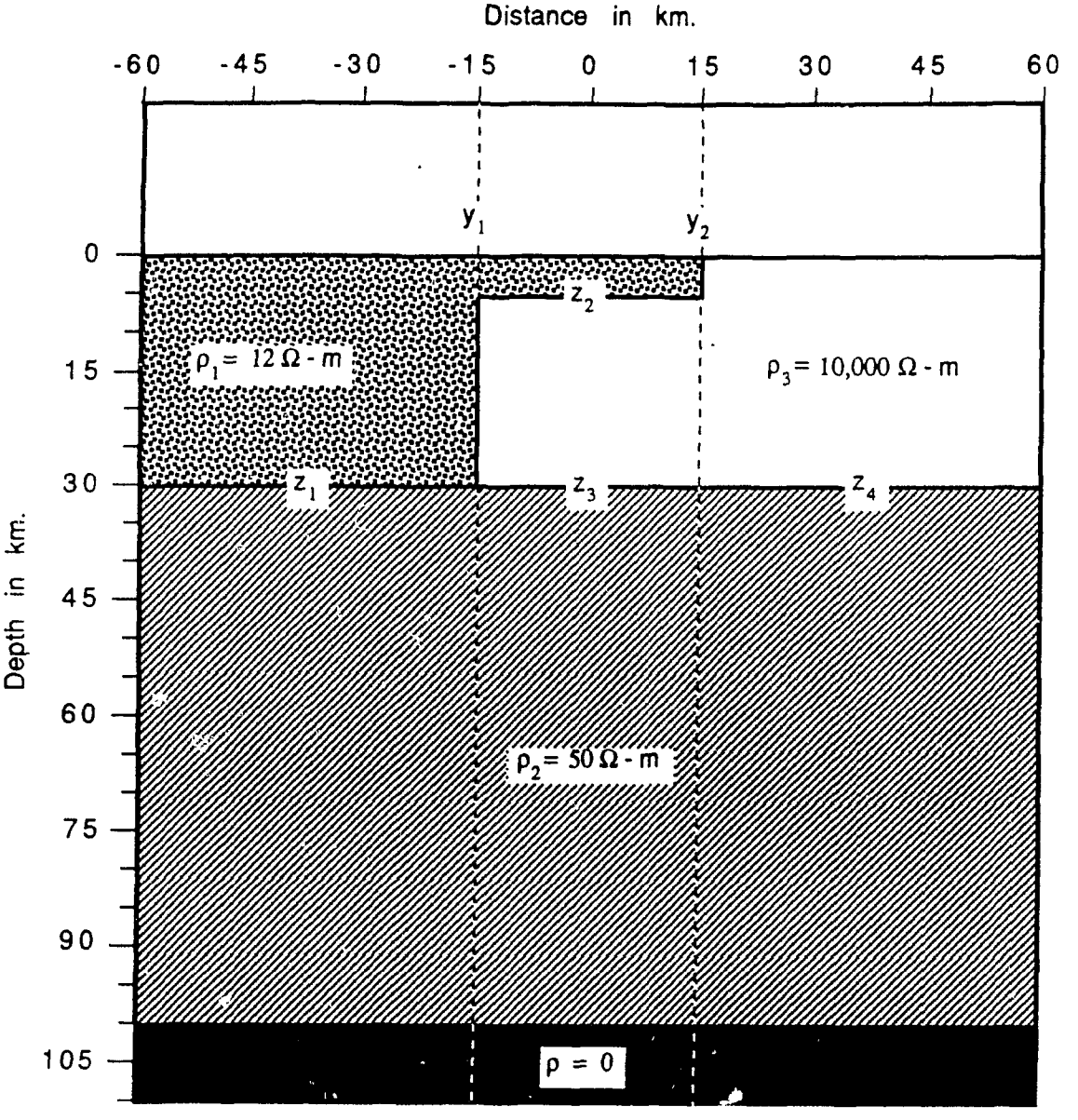

Figure 7.6: The second of the two 2D starting models for use at sites 9 and 10 in the inversion of magnetotelluric Sardinian data collected by Fischer et al. (1990). The dashed lines are the boundaries between the vertical strips required by the inversion program. Note that the vertical scale is different than that for Fig. 7.5. The model is an EW profile.

Two starting models were used for both sites 9 and 10 (Fig. 7.5 and 7.6). The inversion program requires that these models be split up into three vertical strips resulting in nine parameters each. Three of the parameters are the resistivities initialized to the ρ_1, ρ_2, and ρ_3 values shown in the diagrams. Two more parameters are for the initial y values of ± 50 km for Fig. 7.5 and ± 15 km for Fig. 7.6 while the remaining parameters represent the z values which start at 200, 15, 200 and 200 km for Fig. 7.5 and 30, 5, 30 and 30 km for Fig. 7.6. The maximum depth any z value can attain in the two models is 209 and 99 km respectively. Both models have underlying half spaces; the first with a resistivity of 0.1 ohm-m commencing at a depth of 210 km and the second perfectly conducting at a depth of 100 km. The first model was suggested by Fischer (private communication) whereas the second was based on the 2D model obtained by Peruzza et al. (1990) and shown in Fig. 7.2.

7.3 Discussion of Results

Both starting models were used to try and fit the data at both sites. For site 9 the first starting model gave the best fit to the data and for site 10 the second model performed best.

The results for site 9 are shown in Fig. 7.7, Fig. 7.8 and Fig. 7.3. The ϵ value decreased from 1.525 to 0.0441 after 485 iterations. For two polarizations and 10 periods this translates into 9700 forward problems! Obviously a powerful computer is necessary for this kind of trial and error inversion. The results for site 9 were

generated on a RISC 6000 computer which completed the job in approximately 48 hours of real time (ie: $\approx$ 500 forward problems an hour).

Both polarizations exhibit a good fit to the data at long periods as can be seen in Fig. 7.3. Only at a few of the longest periods in B-polarization does the curve ever leave the bounds of the error bars on the observed data. Since the values of apparent resistivity used to calculate the best fit in the inversion were derived from the smooth curve through the data which removed most of the short period fluctuations, the best we can expect from our results is that they mimic this smooth curve as well (Fig. 7.8). The match for both polarizations is quite good at short periods with the ρ_{ap} responses from the models generated by the 2D inversion only rising above the polynomial fitted to the observed data for periods of $T < 0.3$ seconds.

The results for site 10 are presented in Fig. 7.9 and 7.10 as well as Fig. 7.4. Here the ϵ value decreased from 0.0428 to 0.0244 in 98 iterations. The E-polarization curve is within the error bounds of the data for almost all periods greater than about 0.3 seconds (Fig. 7.4) and below this it is an excellent match to the smooth curve on which the inversion data were based (Fig. 7.10). The short period fit for the B-polarization case is also better than that for the previous site, which is not unexpected considering the lack of short period fluctuations for this site. A data set such as this implies a fairly simple shallow structure which our simple 2D models have a better chance of fitting well than they do with the more complicated possibilities implied by the fluctuations at site 9. The longer period B-polarization

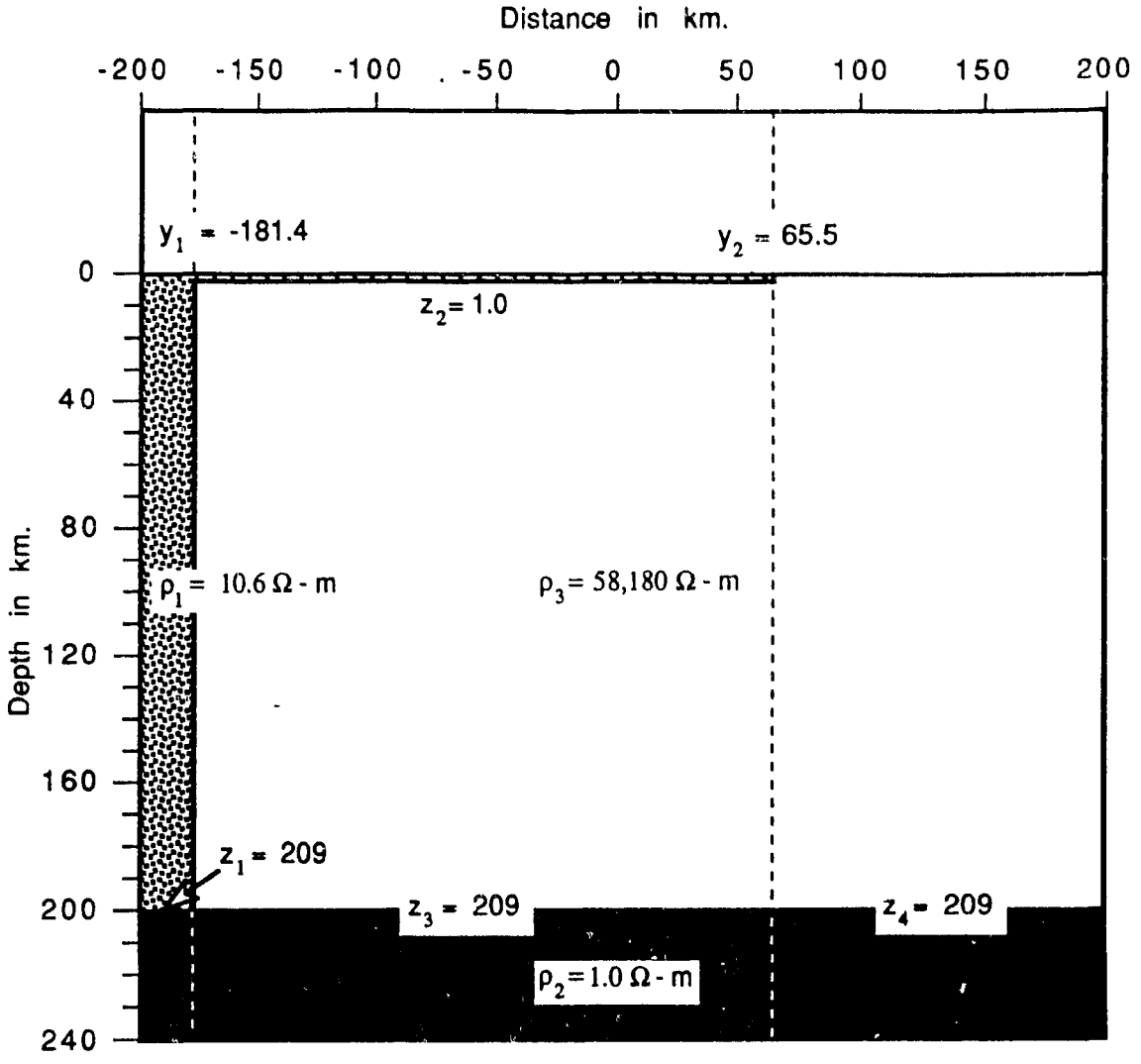

Figure 7.7: The 2D model obtained from the inversion of magnetotelluric data at site 9 using the first starting model (Fig. 7.5). The inversion required 485 iterations and the final value of ε was 0.044[1]. The model is an EW profile.

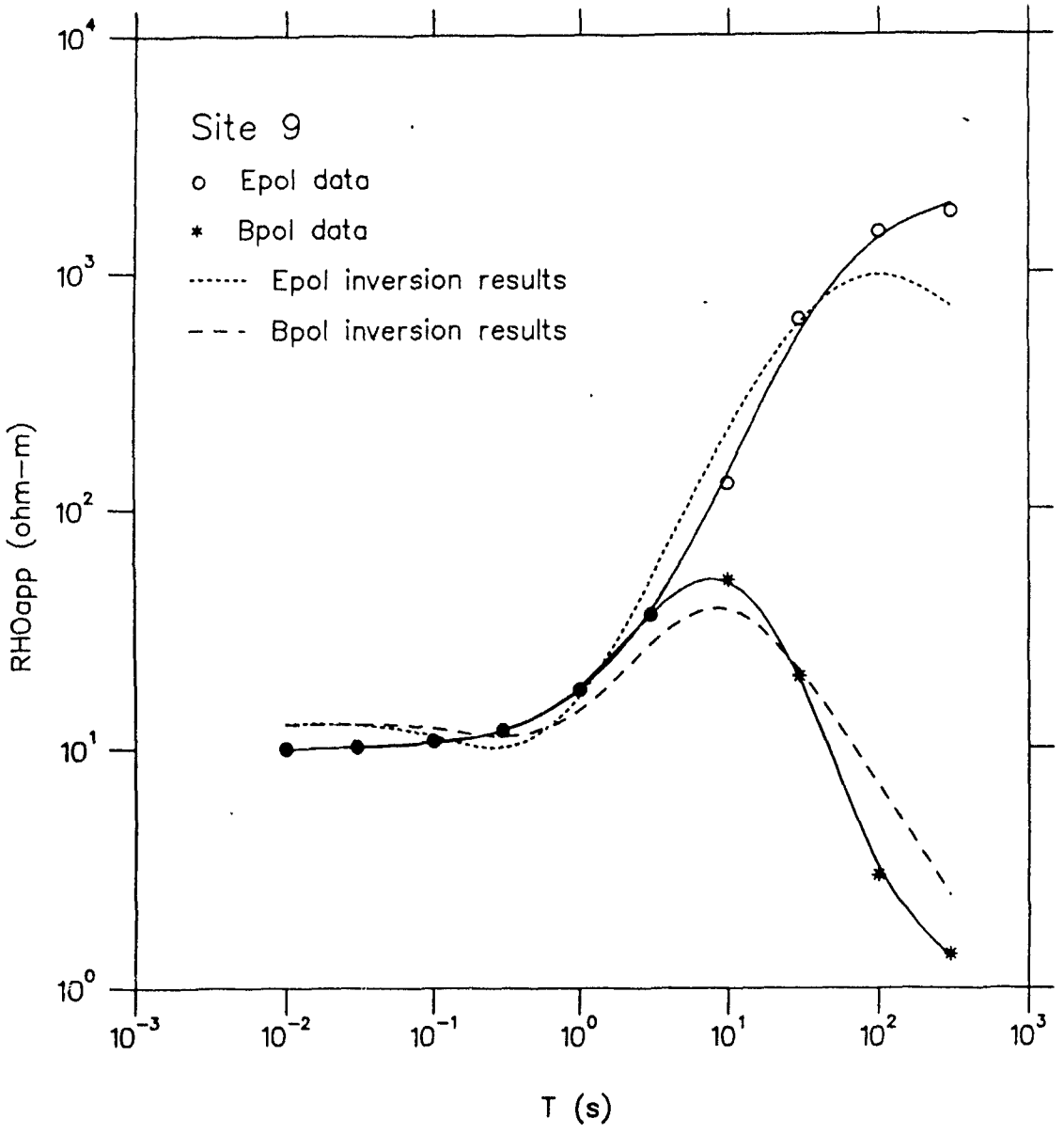

Figure 7.8: The ρ_{ap} response from the 2D model generated by the inversion of magnetotelluric data at site 9. The solid lines are the polynomials fitted to the observed data in Fig. 7.3 from which the values for the inversion were obtained. These values are represented by open circles, for the E-pol data, and by asterisks, for the B-pol data. The dashed lines are polynomial fits to the inversion results for the two polarizations. The ε value is 0.0441.

response is not as good. It follows the trend for the data but displays apparent resistivities consistently higher than those required. This may be due to the fact that the large resistive block in the best-fitting 2D model stretching from 17.6 km to 100 km under site 10 is of higher resistivity than postulated by Perruza et al. (1990) (see Fig. 7.2).

The phase data obtained from the 2D models generated for both sites are, in general, not in good agreement with the data (see Fig. 7.3 and 7.4). In both cases the E-polarization curve is the best fit although the B-polarization curve for site 9 is a reasonable fit at all but the highest periods. Since phase data were not used in the inversion this behavior is not surprising and is no doubt due in part to the scatter in the data mentioned by Peruzza et al. (1990).

Although both the 2D models that were obtained (Fig. 7.7 and 7.9) are the result of data taken at only one site and are subject to the nonuniqueness common to all inversions they can still provide some useful insights into the geology of the area.

The model that was generated by the 2D inversion for site 9, shown in Fig. 7.7, is essentially 1D. Although the misfit of the model resulting from the inversion using the second starting model has a much larger ϵ value, it also exhibits a 1D structure almost identical to that seen in Fig. 7.7 (from the first starting model) except for a shallower underlying conductive half-space imposed by the maximum allowable depth of this model.

By inspection of the model in Fig. 7.2 we can see that site 9 is directly over a

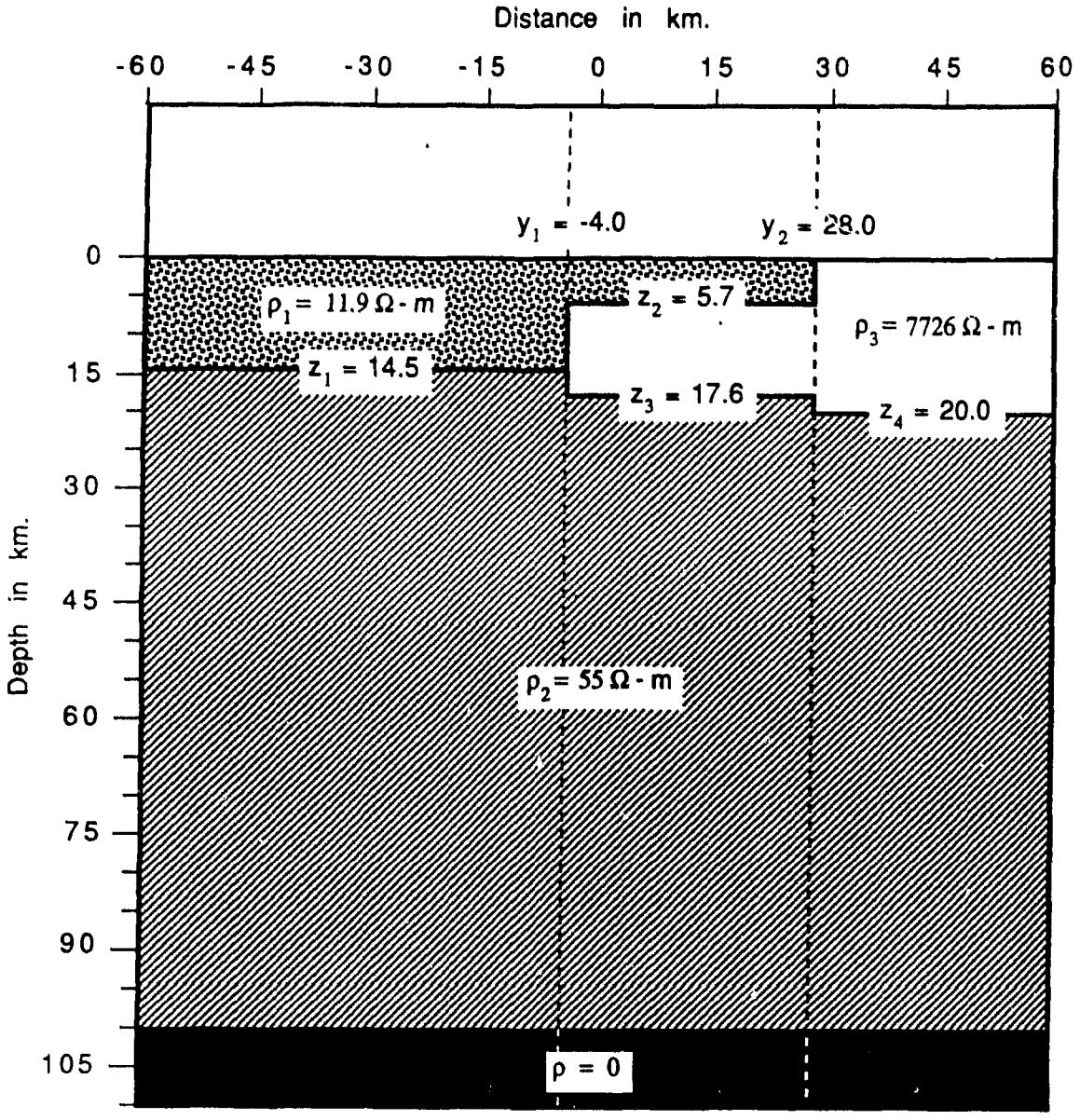

Figure 7.9: The 2D model obtained from the inversion of magnetotelluric data at site 10 using the second starting model (Fig. 7.6). The inversion required 98 iterations and the final value of ε was 0.0244. The model is an EW profile.

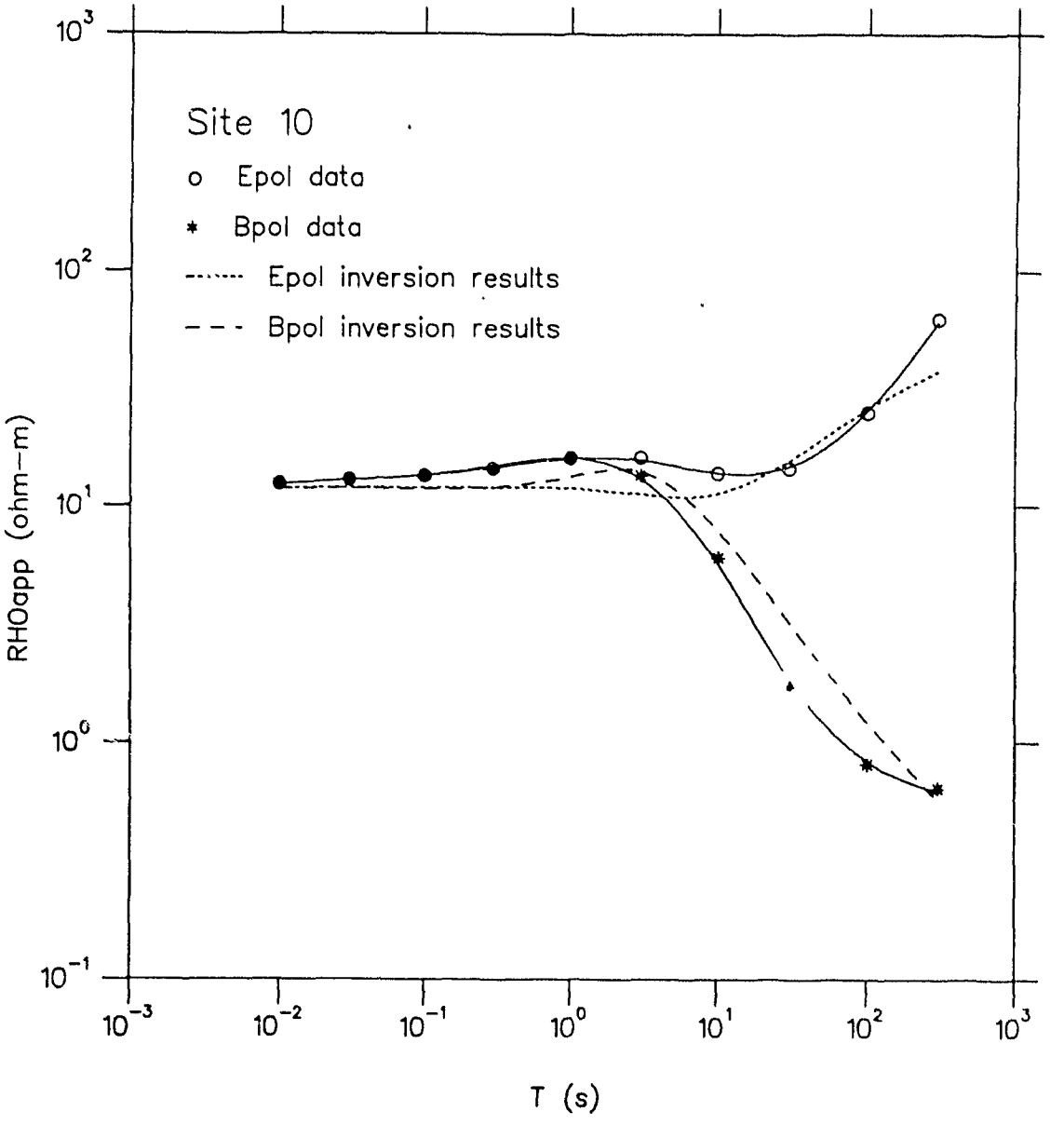

Figure 7.10: The ρ_{ap} response from the 2D model generated by the inversion of magnetotelluric data at site 10. The solid lines are the polynomials fitted to the observed data in Fig. 7.4 from which the values for the inversion were obtained. These values are represented by open circles, for the E-pol data, and by asterisks, for the B-pol data. The dashed lines are polynomial fits to the inversion results for the two polarizations. The ϵ value is 0.0244.

vertical boundary between a resistive region of 10^4 ohm-m and a more conductive one of 6.5 ohm-m. This vertical boundary starts at a depth of ≈800 m and continues down to a depth of ≈2600 m. If we assume that site 9 is actually located over the upwelling of the resistive region our 1D structure directly under the site compares well with that from Fig. 7.2. The absence of the underlying 50 ohm-m layer present in Fig. 7.2 may account for some of the longer period misfit at site 9 as well as for the depth, z_3, to which our resistive layer extends.

Site 10 exhibits a thicker low resistive layer at the surface below the site than does site 9. This also agrees with the model of Peruzza et al. (1990) shown in Fig. 7.2 although our thickness for the surface layer is about twice the size of theirs whereas our thickness for the high resistive layer underneath is less than theirs. By comparison with the geological map in Fig. 7.1 we can see that the distance to the surface outcrop of the resistive granites given by the model as 28 km is very close to that actual value of 27 km obtained by measuring the distance on the map. Our model also indicates that the underlying granites are cut off at or just before the coast of the Gulf of Oristano. The low resistive surface formation becomes thicker here and the underlying 55 ohm-m layer becomes shallower.

As was mentioned earlier, inversion techniques such as this require the solutions to many forward problems. More complex models with more parameters will result in more and larger forward problems. Consequently a fast and efficient forward modelling scheme with automatic gridding is imperative for this kind of inversion. work.

Chapter 8

INDUCTION ARROWS OVER A BURIED CONDUCTIVITY CONTRAST

8.1 Introduction

In this chapter we have applied our forward modelling program to the problem of the behaviour of 2D induction arrows over a buried conductivity contrast. Induction arrows are actually more properly called induction vectors since they have the properties of and conform to the definition of a vector. In this chapter we have, however, refered to them in the traditional way as arrows. Many studies have been performed on the direction of these arrows and the model-dependent periods at which they reverse direction. Quadrature arrow reversals near a conductive-resistive interface have been observed in sea-floor field data (DeLaurier et al., 1983), in laboratory analogue model studies (Hebert et al., 1983; Nienaber at al., 1983; Hu et al., 1989), and in numerical model studies (Chen and Fung, 1985, 1987; Agarwal and Dosso, 1990). It has been noted that, although the general trend of in-phase arrows is to point towards the regions of high electrical conduc-

tivity, some investigators have found small amplitude in-phase arrows that point away from these same regions. This behaviour has been reported for both a conductive prism in a resistive host (Jones, 1986) and a resistive cylindrical seamount in a conductive ocean (Hu et al., 1989).

The effects of mutual coupling between conductive bodies at the surface have been examined by Weaver and Agarwal (1991). Dosso and Meng (1992) have studied a 2D model of an ocean underlain by a conductive substratum for an upwelling and also for a depression in the substratum at depth. The mutual coupling depends on the geometry of both the conductors and on their orientation with respect to one another. As the conductor separation increases the mutual coupling decreases since the magnetic flux linking them decreases. The model under investigation in this chapter was designed to explore the effect of mutual coupling in connection with the in-phase arrows and their reversals.

8.2 Numerical Models and Calculations

The base model (MOD1) consists of two semi-infinite conducting plates; the first at the surface of depth $d_1 = 4$ km and conductivity $\sigma_1 = 4.0$ S/m and the second buried 20 km underground with a depth of $d_2 = 20$ km and a conductivity $\sigma_3 = 1.0$ S/m. These plates are imbedded in a resistive host of $\sigma_2 = 0.01$ S/m underlain by a more conductive ($\sigma_4 = 0.1$ S/m) half-space at a depth of 40 km. The surface conducting plate extends from $y = -\infty$ to $y = 0$ while the buried conducting plate extends through the range $-20 < y < \infty$. This model was intended to simulate a

continental conductive sill at crustal depths buried near the straight coastline of a uniform depth ocean. The underlying half-space of $\sigma_4 = 0.1$ S/m can be regarded as a conductive layer in the upper asthenosphere. Various starting positions were considered for the conductive sill (parameter y_1) but $y_1 = -20$ km was chosen for the base model since it is known that the effects of mutual coupling are more pronounced when the two conductors overlap (Wolf, 1983). All the parameters were varied one by one keeping the others set to the base model values in order to observe the effects on the induction arrows. The ocean conductivity (σ_1) was kept constant at the value 4.0 S/m. The base model and the parameter values are shown in Fig. 8.1. The period range studied was $T = 0.1$–500 s.

Each model was solved for the E-polarization case to obtain values for the horizontal electric field U and the magnetic field components Y and Z at the surface of the earth ($z = 0$). In the horizontal plane an induction vector is defined by the ordered pair of transfer functions (A, B) given by the linear relation

$$Z = AX + BY \tag{8.1}$$

between the vertical magnetic field Z at some particular location and the components of the horizontal magnetic field $\mathbf{B} = (X, Y)$ at the same location. For this 2D E-polarization case, the magnetic field component in the x-direction (X) is zero so that equation (8.1) becomes $Z = BY$. It is obvious that the real ($\Re$) and imaginary ($\Im$) parts of the transfer function B will be

$$\Re B = \Re(Z/Y) \tag{8.2}$$

and

$$\Im B = \Im(Z/Y) \tag{8.3}$$

and in the absence of A the real part of B is the in-phase induction arrow and the imaginary part is the quadrature induction arrow. The signs of both the arrows were reversed so that they would agree with the convention that requires them to point towards areas of electric current concentration. Hence, in the graphs of the responses $\Re B$ and $\Im B$ versus y shown, all the positive values indicate arrows pointing in the direction of positive y while negative values indicate arrows pointing in the direction of negative y.

In order to examine the effects of mutual coupling in the various models, 'difference vectors' can be calculated by subtracting the induction arrows due to models containing only a single conducting plate from the arrows due to models containing a combination of the two plates. If the two plates are far apart then the vector sum of the arrows from each single plate model ($\mathbf{P}_1$ for the ocean and $\mathbf{P}_2$ for the buried conductor) will equal the vector representing the arrow produced by the double plate model ($\mathbf{P}_{12}$). If the 'coupling vector' $\mathbf{\Delta} \equiv \mathbf{P}_{12} - \mathbf{P}_1 - \mathbf{P}_2$ is non-vanishing, then $\mathbf{\Delta}$ reveals a mutual inductance between the two conductors. In order to calculate these differences for each $\mathbf{P}_{12}$ based on MOD1 we must generate results for the corresponding $\mathbf{P}_1$ and $\mathbf{P}_2$ as well.

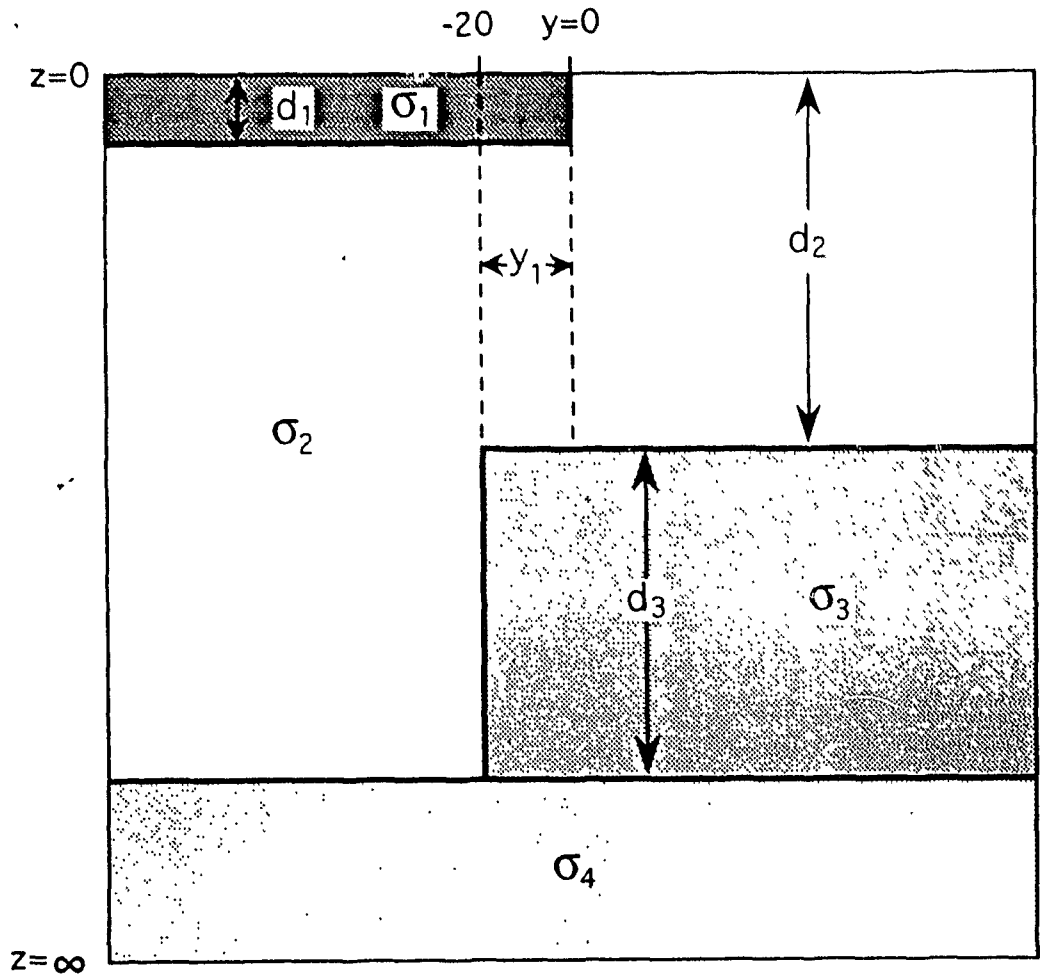

BASE MODEL: (MOD1)

d_1 =4.0 km	σ_1 =4.0 S/m	σ_4 =0.1 S/m
d_2 =20.0 km	σ_2 =0.01 S/m	y_1 =-20 km
d_3 =20.0 km	σ_3 =1.0 S/m	

PARAMETERS:	MODEL CODES:
d_1 = 0.0, 0.1, 0.35, 1.0 km	D1a, D1b, D1c, D1d
d_2 = 10 km	D2a
d_3 = 10, 25 km	D3a, D3b
σ_2 = 0.001, 0.0001 S/m	S2a, S2b
σ_3 = 4.0, 10.0 S/m	S3a, S3b
σ_4 = 0.01 S/m	S4a
y_1 = -30, 0, 10, 20, 30 km	Y1a, Y1b, Y1c, Y1d, Y1e

Figure 8.1: The model, base model values, and parameters for the induction arrow study. Parameters are varied one at a time with all the others held constant at the base model values. The period range studied was $T = 0.1$–500s.

8.3 The Buried Plate Model

The response of the buried plate alone exhibits reversals in the in-phase arrows for all parameter variations studied here. Fig. 8.2 shows the response $\Re B$ produced by the base model with no surface conductor (SILL-0, $d_1 = 0$ km) and one of its parameter variations (SILL-S2a, $\sigma_2 = 0.001$ S/m). There can be no mutual coupling in this case since there is only one conducting body per model. The overall trend of the in-phase arrows for SILL-0 is for them to increase in length with increasing period for $T = 0$–20 s, then to decrease and, after reversing direction at $T \approx 28$ s, to increase in length once again. Although not shown, the in-phase arrows continue to become larger at higher periods to a maximum located somewhere between 20,000 and 50,000 s, after which they diminish with increasing period. For periods shorter than 28 s, the arrows are very small and point away from the conductor. As $T \rightarrow 28$ s the in-phase arrows decrease in length much faster directly over the $y = -20$ discontinuity than they do in the regions farther removed from the conductor boundary. Thus the arrows around $y = -20$ will change direction first resulting in two reversals of arrow direction for $28 \text{ s} < T < 45$ s. The first reversal occurs over the resistor at a point on the left of $y \doteq -20$ and all arrows to the left of this point are directed away from the conductor. The second reversal occurs over the conductor at a point on the right of $y = -20$ and all arrows further to the right also point away from the conductor although they are much smaller than those to the left of $y = -20$ having decreased in length much

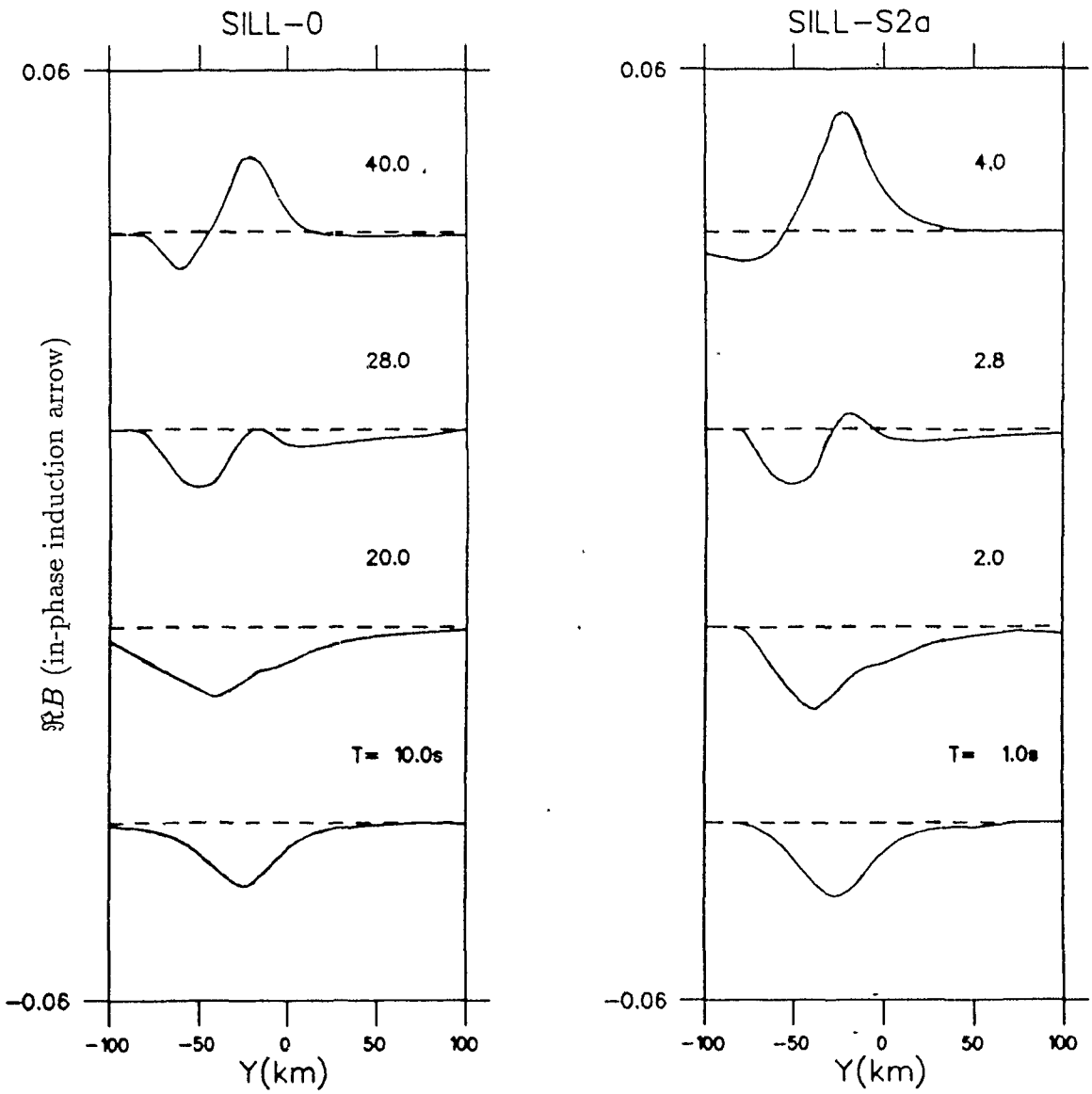

Figure 8.2: Response $\Re B$ (in-phase arrow) for the buried plate models SILL-0 (base model with no surface conductor) and SILL-S2a (SILL-0 with $\sigma_2 = 0.001$ S/m). The dashed lines are the zero lines for each curve. The scale is the same for each curve and has the limiting values (-0.06 and 0.06) shown at the top and bottom of the y-axis on the graph composed of the four separate curves.

more quickly. In between these two points the arrows point towards the conductor. The range of y over which the in-phase arrows point toward the conductor increases as T increases, spreading gradually outward from $y = -20$ in both directions. The negative $\Re B$ responses gradually decrease in amplitude and are positioned farther and farther away from $y = -20$ until they disappear altogether at $T \approx 100$ s (not shown). Above this period all the arrows follow the accepted trend of pointing towards zones of high conductivity. The imaginary (quadrature) arrows are not under investigation in this chapter and so are not shown, but for SILL-0 and all its parameter variations, the quadrature arrows increase in length with increasing period then decrease to a minimum at a period between 20,000 and 50,000 s after which they reverse direction and their length increases again.

Fig. 8.2 also shows the response $\Re B$ for the model with σ_2 =0.001 S/m (SILL-S2a). The most obvious effect of changing σ_2 is to decrease the value of the period at which the reversal occurs from $T \approx 28$ s to $T \approx 2.8$ s and to increase the amplitude of the response. For a single buried prism in a homogeneous host Jones (1986) reported the period of reversal as

$$T_r = 4\pi^2 \times 10^{-7} \sigma_h d_b^2 \tag{8.4}$$

which is simply the skin depth relationship (1.4) with σ_h representing the conductivity of the homogeneous host and d_b the depth of burial. The period of reversal (T_r) is the period at which the induction arrows appear to change direction and point towards regions of high conductivity instead of away from them.

The unconventional orientation of the in-phase arrows at periods less than T_r

is due to the fact that the anomaly is buried at a depth greater than one host skin depth and hence the response of the model at these smaller periods will be out of phase with its response at periods larger than T_τ. The controlling factor is the sign of $\Re(Z)$ which changes at T_τ.

Also SILL-0 and SILL-S2a contain semi-infinite plates in a *layered* host so that the left-hand side of (8.4) is not equal to but rather nearly proportional to the right-hand side. The value that replaces σ_h in the case of a layered host should be close to the σ_2 for our model. Thus decreasing σ_2 from 0.01 S/m to 0.001 S/m should reduce T_τ by a factor of approximately 10. This continues to hold true when σ_2 =0.0001 S/m resulting in a T_τ of about 0.28 s. The new T_τ are not *exactly* 2.8 and 0.28 s, since σ_2 is only an approximation for σ_h in the homogeneous host equation (8.4). Another reason that our T_τ's are only proportional to the right-hand side of (8.4) is the geometry of the conductor (i.e. the sill) which affects the apparent resistivity of the host medium. Jones obtained his results with a block imbedded in a homogeneous medium and the edges of the block produced $\Re B$ curves for $T < T_\tau$ that exhibited a zero node at $y = 0$. For this case when the conventional $\Re B$ response occurs for the first time at T_τ it quickly results in a change of sign of the very small positive and negative response values near $y = 0$ seen at smaller periods. Because our model uses a semi-infinite sill we have no such $y = 0$ node but a negative response which decreases gradually to zero as we move further away from the edge of the sill at $y = -20$ km. Consequently the induction arrows at $y = -20$ start to decrease in length at $T \approx 14$s but do not

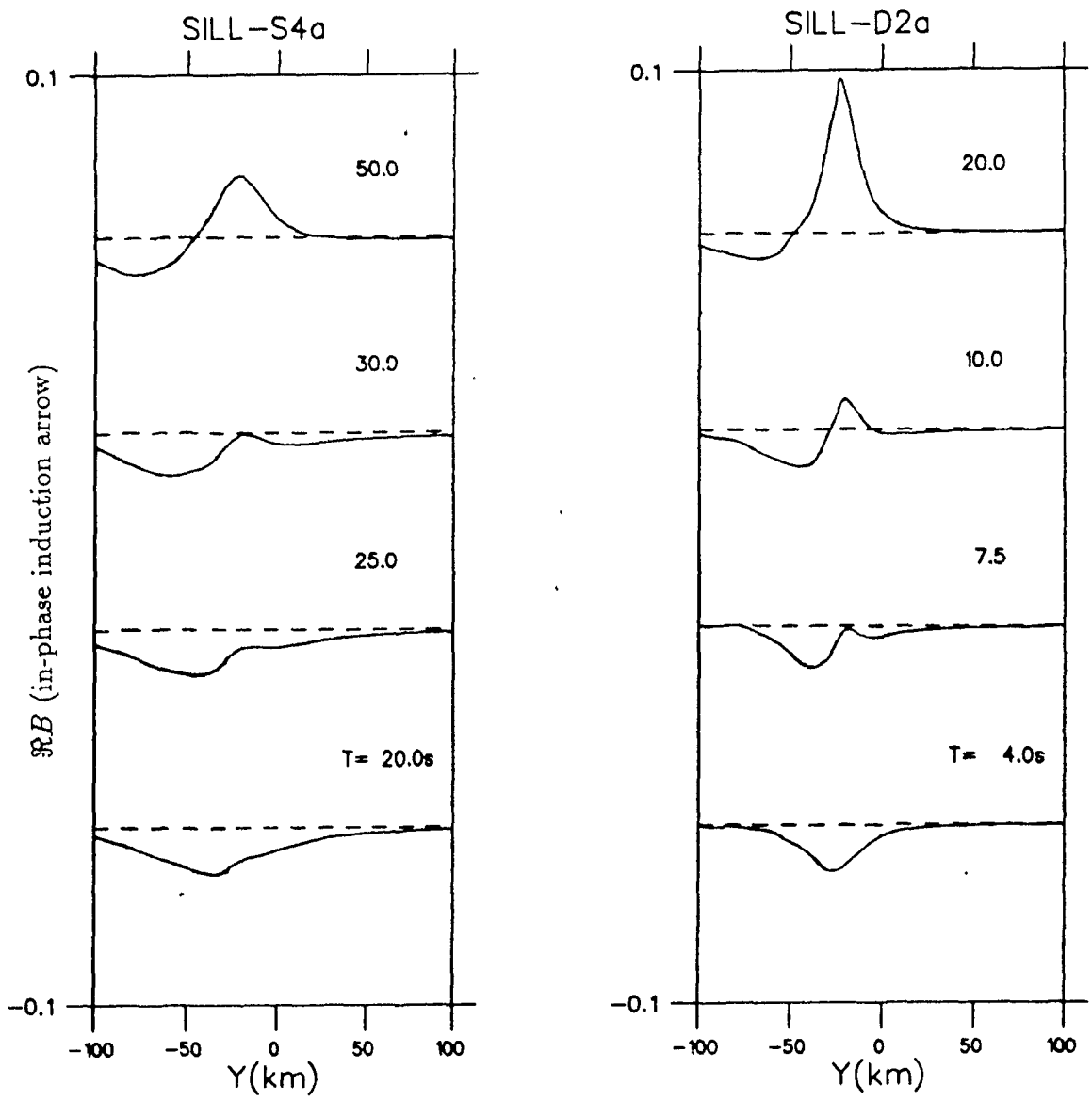

Figure 8.3: Response $\Re B$ (in-phase induction arrow) for the buried plate models SILL-S4a ($\sigma_4 = 0.01$ S/m) and SILL-D2a ($d_2 = 10$ km).

reverse direction until some later $T \approx 28$s when the conventional $\Re B$ response becomes large enough to take the curve through the zero line. Changing σ_3 (not shown) has no effect on the location of the reversal, which is expected, since it does not appear in (8.4) but, as expected, it does increase the amplitude of the response.

Reducing the depth of burial to $d_2 = 10$ km also yields the expected results by decreasing T_r to approximately 7.5 s and increasing the amplitude of the $\Re B$ response (see Fig. 8.3). Changing the parameter d_3 to 10 km has no perceivable effect for the periods around T_r. When d_3 is increased to 25 km it not only increases the size of the conductor but also requires the underlying half-space to start 5 km lower at $z = 45$ km. The combined effect of these two changes is to slightly increase the amplitude of the response for higher periods. Only at $T > 100$ s do the amplitudes for SILL-D3a start to decrease and those for SILL-D3b start to increase with respect to the SILL-0 values.

It can be seen from Fig. 8.3 that decreasing σ_4 to 0.01 S/m (SILL-S4a) has the curious effect of raising T_r to about 30 s. Intuitively one would expect a decrease in the conductivity of a host layer to decrease the layer equivalent of σ_h and therefore T_r as well. By examining the apparent resistivity (ρ_a) for each value of σ_4 (not shown) it was found that a decrease in the latter resulted in a decrease of the former in the region $z < 20$ km, especially in the area of the host medium just to the left of the anomaly boundary at $y = -20$ km. This behaviour seems to indicate that for a layered host the proper replacement value for σ_h in equation

(8.4) is some function of the apparent resistivity of the layered host medium which is affected by all the parameters in the model. If this is so, then the increase in T_r follows from the fact that a smaller ρ_a means a larger σ_h which, from (8.4), results in a rise in reversal period. This idea can also be used to explain why the T_r for SILL-D2a is slightly higher than 7.0 s. The apparent resistivies for the $d_2 = 10$ km model are slightly smaller than those for model SILL-0 in the region $z < 20$ km which should require a higher T_r. At the same time, however, the d_b has changed from 20 km to 10 km requiring T_r be reduced by a factor of 4. The combination of these two effects could result in the T_r of 7.5 s shown in Fig. 8.3.

8.4 The Surface Plate Model

The $\Re B$ responses for a model containing only the surface conductor (ocean) are shown by the widely spaced dashed line in Fig 8.4. For all applicable parameter variations and the entire range of periods it was found that the in-phase arrows always point towards the ocean-coast boundary for $y > 0$ and taper off to zero almost immediately for $y < 0$ (i.e. over the ocean). The amplitude of the ocean responses increases when d_1 decreases or σ_2 decreases. The range of values in y for which there is a response also increases for both these cases (i.e. the curve becomes broader). Decreases in d_1 extend the range towards the left and decreases in σ_2 extend it to the right: compare, for instance, the ocean responses OCEAN-0 at 28 s and OCEAN-S2a at 10 s shown by the widely spaced dashed lines in Fig. 8.4. The 10 s response for OCEAN-S2a is already much broader and larger in amplitude

than the higher period OCEAN-0 response. Although not shown, changing σ_4 to 0.01 S/m creates only a slight increase in the amplitudes of $\Re B$ responses for $T > 100$ s and changing the depth to the half-space of conductivity σ_4 produces no visible change at all for the study range of $T < 500$ s.

8.5 The Two Plate Models

It can easily be seen in Fig. 8.4 that the $\Re B$ responses for the SILL models are completely overwhelmed by the much larger responses from the OCEAN models. This results in responses for a combined model (MOD1) with characteristics similar to that of the OCEAN models. Only for the larger periods (far from T_r) does the increasing SILL response start to make itself felt in MOD1. This implies that deep buried conductors in the presence of highly conductive (non-infinite) surface layers may remain unidentified if in-phase arrows are not obtained for a large enough period range. Evidence of a buried conductor can be seen, however, in the 'coupling vector' ($\mathbf{\Delta}$) that arises due to mutual coupling.

The introduction of an ocean into the SILL model, even an ocean as shallow as 0.1 km, causes mutual coupling, evidence of which can be seen in the 'coupling vector'. In other words, the currents induced in the conducting ocean act as a secondary source field inducing currents in the buried conductor and therefore generating a response on the surface that was not present in the original SILL models. The reverse also occurs so that a response is generated in the ocean by the secondary source field induced in the buried conductor. This, in fact, is the

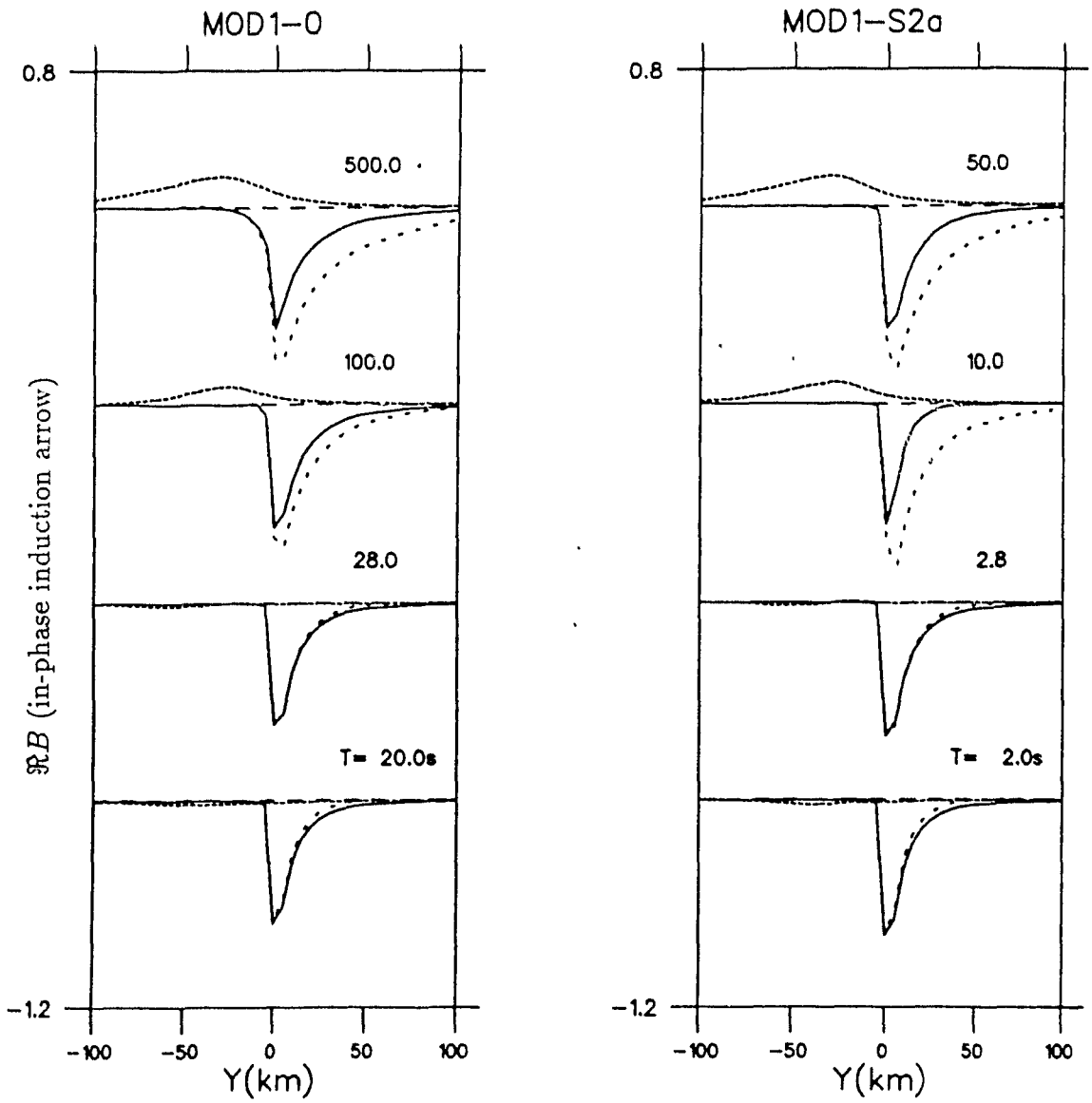

Figure 8.4: The response $\Re B$ (in-phase induction arrow) for SILL-0, OCEAN-0, and the combined two plate model MOD1-0 as well as for SILL-S2a, OCEAN-S2a and MOD1-S2a. The ocean response is represented by the widely spaced dashed line and the sill response by the closely spaced dashed line. The solid line represents the MOD1 response. Note the different periods in the two models.

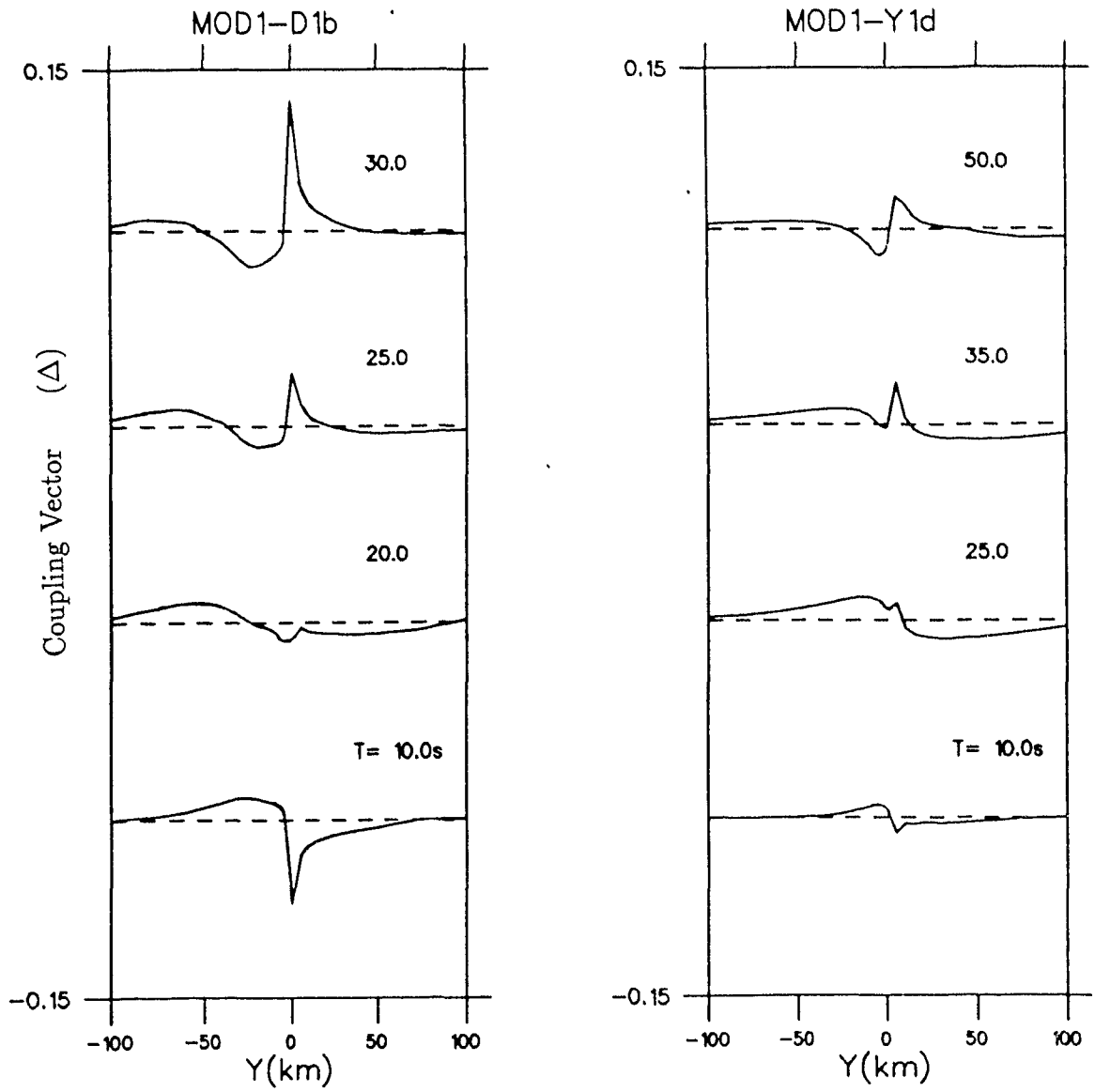

Figure 8.5: The 'coupling vector' ($\mathbf{\Delta}$) for MOD1-D1b and MOD1-Y1d. Note that different periods are shown for the two different models.

dominant response since the ocean is a good conductor close to the surface of the earth.

At long periods the currents flowing in the sill will be strongly in phase with the currents flowing in the ocean. The induction arrows for the sill alone should therefore be not only smaller than for the ocean alone (because the sill is at depth) but also oppositely directed, as observed in Fig. 8.4 where the response to the sill alone is positive compared with a larger negative response for the ocean alone. At much shorter periods, which put the sill at a depth of one skin depth, the currents in the sill alone will be out-of-phase (i.e. in the opposite direction) with those that flow in the ocean alone, and at the same time very much attenuated. This accounts for the small negative response for the sill at short periods (see Fig 8.2–8.4). In the long period combined response, where mutual induction occurs, the secondary field, whose source is the current flow in the sill, induces secondary currents in the ocean whose vertical magnetic field opposes that of the primary field. A similar mutual induction occurs in the sill of course, but being at depth, it exerts less influence on the surface response. The response of the combined model is therefore more dramatically affected by the secondary currents induced in the ocean and the vertical magnetic fields resulting from them. This can be seen in Fig. 8.6 where the 'coupling vector' in $y > 0$, due to secondary currents in the ocean, is larger in size than the 'coupling vector' in $y < 0$, due to the buried sill. The mutual coupling contribution from the sill (Fig. 8.5 and 8.6, $y < 0$) seems to cancel out any contribution from the sill alone in the combined model. Notice

that the combined model response in Fig. 8.4 shows no evidence of a sill in $y < 0$.

Looking at Fig. 8.5 it is obvious not only that significant mutual induction occurs, but also that the reversals seen in the SILL models cause similar reversals in the 'coupling vector' for the combined model (MOD1). The reversal periods for the 'coupling vector' (T_τ') are all lower than those exhibited by the $\Re B$ responses for the buried plate alone. For the base model MOD1-0, for instance, Fig. 8.6 shows that the reversal occurs about 3 s earlier. This is probably due to a change in ρ_{ap} of the layered host caused by the interaction of the two conductors. As expected the mutual coupling will increase (i.e.: the 'coupling vector' amplitudes will increase) when either of the conducting plates becomes larger (d_1 or d_3 increases), when the conductors move closer together (d_2 or y_1 decreases) or when either of the two becomes relatively more conductive (σ_2 or σ_4 decreases or σ_3 increases). This is dramatically illustrated by Fig. 8.6 where the larger amplitude of the 'coupling vector' on the right reveals as much or more mutual coupling than the higher period results for the base model on the left. Notice that the T_τ' for these models maintain the same relationship that exists in the corresponding SILL models. Increasing the depth of the ocean shifts T_τ' upward from about 20 s at $d_1 = 0.1$ km to 28 s at $d_1 = 4$ km. Changing d_2 and d_3 create similar changes to the location of T_τ' as for the SILL models. Notice also that as the starting position of the buried plate is changed from $y_1 = 20$ km to $y_1 = -20$ km not only does the amplitude of the 'coupling vector' increase with the mutual coupling but the value of T_τ' changes slightly as well (compare MOD1-Y1d in Fig. 8.5 with MOD1-0 in Fig. 8.6). The

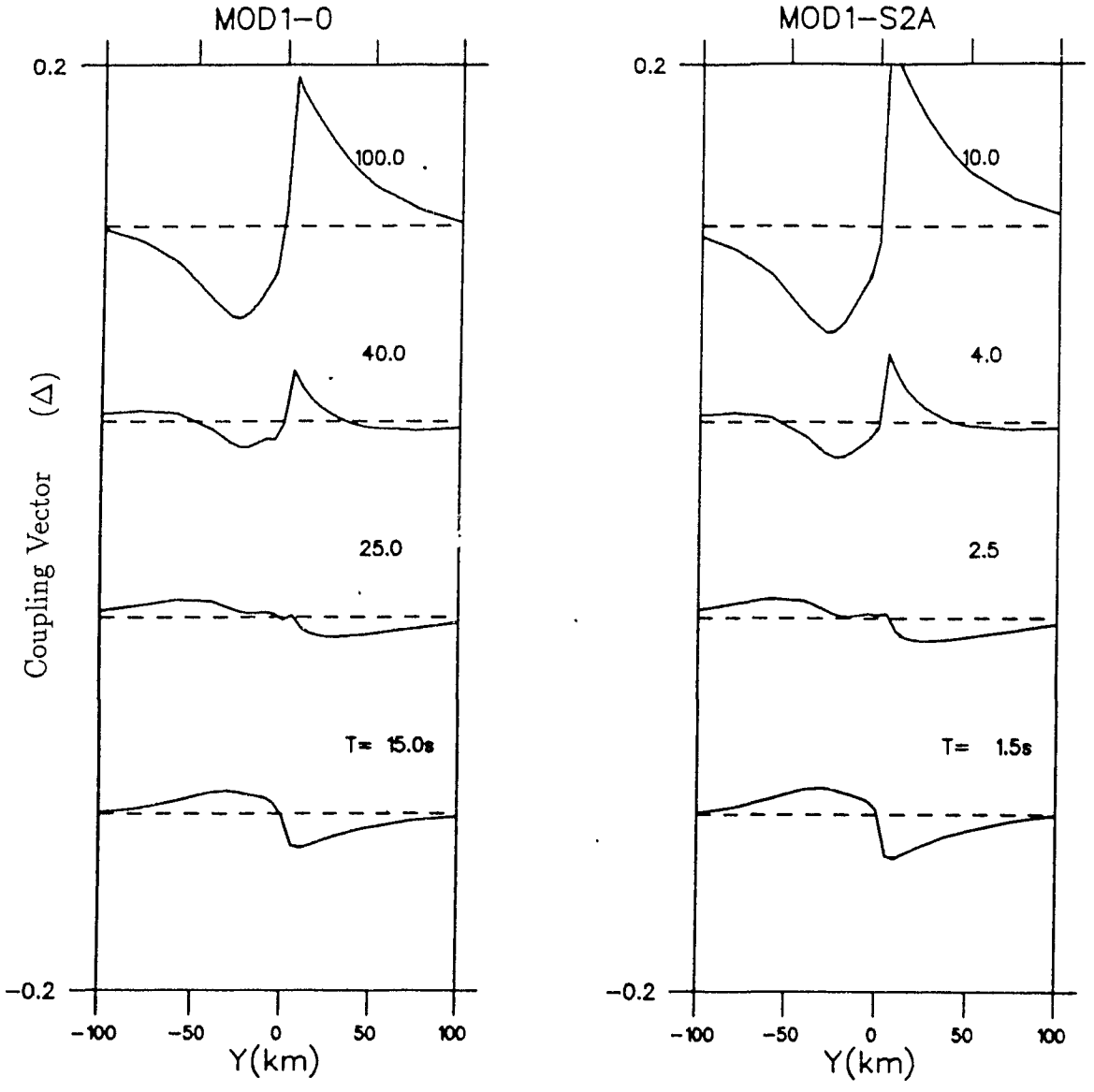

Figure 8.6: The 'coupling vector' ($\mathbf{\Delta}$) for MOD1-0 and MOD1-S2a. Note that different periods are shown for the two different models.

single buried plate model (SILL-0) will have the same response, and therefore the same T_r, for all values of y_1 since shifting y_1 simply shifts the coordinate axis without changing the model. So any change in the value of T_r' is due solely to the introduction of an ocean and the mutual coupling effects.

Now if we look at the response for $\sigma_2 = 0.001$ S/m (MOD1-S2a) in Fig. 8.6 it is obvious that the mutual coupling (reflected in the amplitude of the 'coupling vector') is larger for $T = 1.5$ s than for $T = 2.5$ s especially near the plate boundaries. For a smaller period the distances are increased in terms of skin depths so that mutual coupling *should* always decrease with period. This anomalous behaviour was noticed by Weaver and Agarwal (1991) in their investigation of thin sheet surface anomalies near coastlines. For our model it appears that the reversals exhibited by SILL models carry over into the 'coupling vectors' as well so that at each T_r', the 'coupling vector' will change direction (which occurs first at $y = 0$ km) and eventually exhibit normal mutual coupling behaviour where the 'coupling vector' ($\mathbf{\Delta}$) increases with T. Note that for $T = 2.5$ s and $T = 1.5$ s where the unconventional mutual coupling behaviour exists in our model the 'coupling vectors' are still pointing in the opposite direction to the those at higher periods whereas this does not seem to be the case for the Weaver and Agarwal model. It is not known whether there is a reversal in the 'coupling vector' for the model used by Weaver and Agarwal since only a few periods were calculated. The periods they used were, however, comparitively large (20 min–1 hour) and all our studies have shown that the reversals tend to be confined to shorter periods. Their study was also different

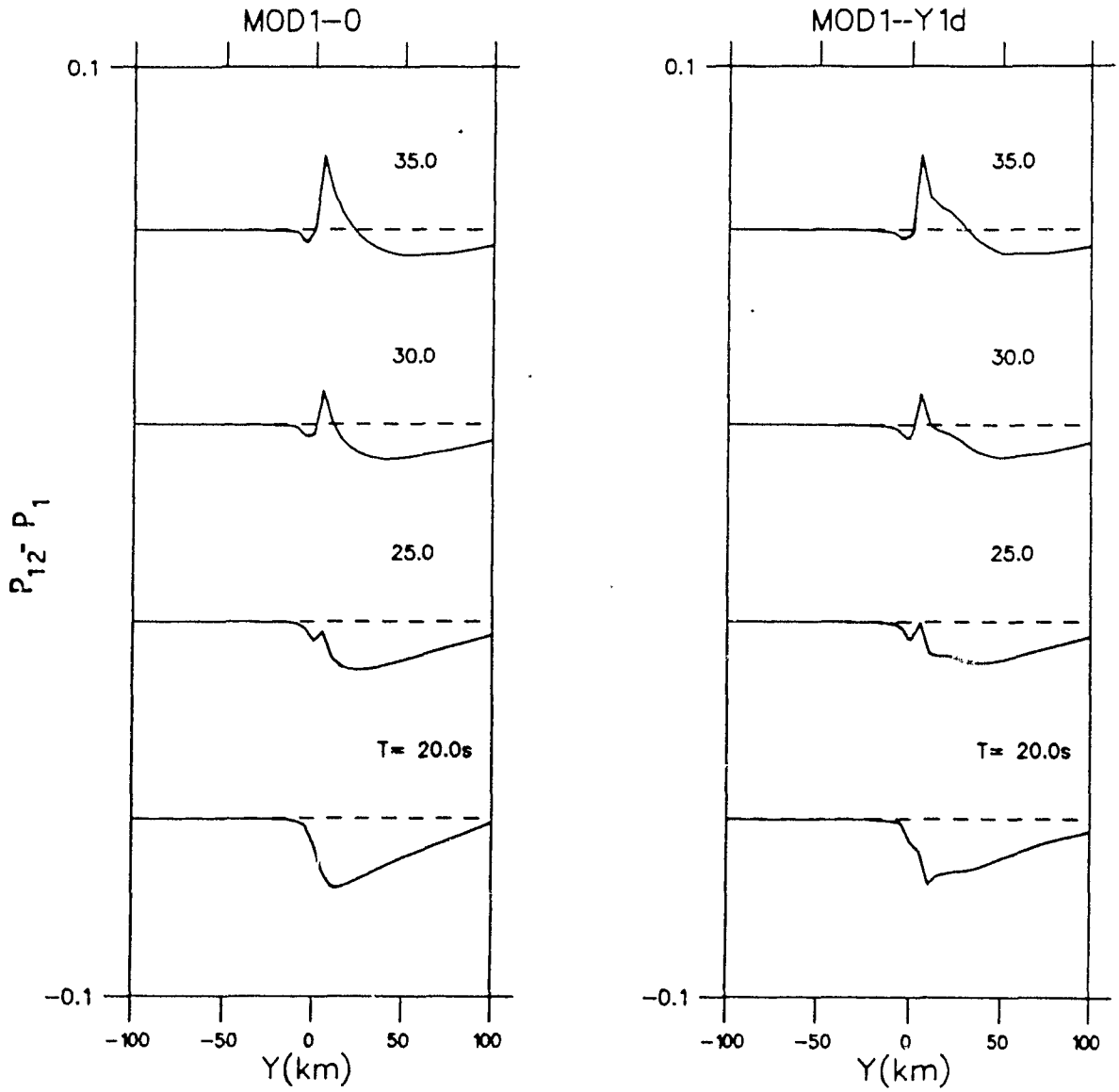

Figure 8.7: Difference arrows $\mathbf{P}_{12} - \mathbf{P}_1$ for MOD1-0 and MOD1-Y1d (i.e. the coast effect has been removed).

in that the mutual coupling was between an island and a coastline in a thin sheet model and the host material is conductive rather than resistive.

The possiblity of having greater mutual coupling effects at small periods combined with reversals can cause problems in the interpretation of in-phase induction arrows. In recent years the difference arrows have been used by some authors (e.g. Hubert et al. 1983; Meng and Dosso, 1990; Chen et al. 1993; Kang et al. 1993) in the investigation of geoelectric structures of the earth. The validity of the difference arrow method has been studied by Wolf (1983), Weaver and Agarwal (1990) and Dosso and Meng (1992). These difference arrows should point towards any conducting anomaly in the area. From Fig. 8.7 we can see that this is not always the case. For MOD1-0 and MOD1-Y1d all the difference vectors for $T \lesssim 30$ s seem to indicate an anomaly lying to the left of $y = 0$ km even though the buried plate in MOD1-Y1d does not even extend under the ocean. This may be interpreted erroneously as a shallow anomaly to the left of $y = 0$ km with a deeper anomaly buried to the right of $y = 0$ km.

Obviously great care must be taken in interpreting in-phase induction arrows and difference arrows for both single conductor and multiple conductor models. Although most of our examples were confined to lower periods with a deeper burial depth and a highly resistive host, in-phase induction arrow (as well as difference arrow and 'coupling vector') reversals can show up at much longer periods and over a larger period range. More work needs to be done on both two and three-dimensional models before this behaviour can be properly understood.

Chapter 9

AUTOMATED TWO-DIMENSIONAL INVERSION OF MAGNETOTELLURIC DATA

9.1 Introduction

This chapter presents the results of a study that was performed using a 2D inversion program that incorporates the automatic forward modelling program developed in this thesis. The inversion section of the program was written by A.K. Agarwal in conjunction with J.T. Weaver and Helena E. Poll. The actual inversions were performed by A.K. Agarwal.

Two-dimensional inversion schemes are crucial to the interpretation of magnetotelluric data. Although a three-dimensional inversion method would, of course, be preferable there is still a lack of practical inversion methods that can deal with a general three-dimensional anomaly. The two-dimensional approach described here requires the construction of a starting model with variable parameters which is used together with an optimization routine to reduce the misfit between MT data

and a model response. The search for an optimum model requires hundreds of 2D forward calculations even for a relatively simple structure. A fast 2D forward program with automatic gridding is indispensible for this type of inversion.

A common method for acquiring a starting model for a 2D inversion is to string together the results from a series of 1D inversions along the 2D profile. This method has the advantage of providing a model which is almost certainly closer to the true 2D structure than a general half-space or other arbitrarily selected starting model and therefore much more likely to yield a sensible 2D inversion result with a minimum number of iterations. The 1D profiles are sensitive to the data used to obtain them so that using different responses (such as the TM or TE data) to calculate the misfit in the 1D inversions can result in startlingly different 2D starting models. One type of response that can be used to calculate these starting models is the rotationally invariant impedance. The "effective impedances" (Berdichevsky and Dmitriev, 1976; Ranganayaki, 1984) are

$$Z_{\text{ave}} = \frac{1}{2}(Z_{xy} - Z_{yx}), \quad Z_{\text{eff}} = \sqrt{Z_{xx}Z_{yy} - Z_{xy}Z_{yx}}. \tag{9.1}$$

where Z_{xy} etc. are components of the impedance tensor. If the axes are rotated so that x is parallel to the strike of the 2D structure the impedances can be written as

$$Z_{xy} = Z_{TE}, \quad Z_{yx} = -Z_{TM} \tag{9.2}$$

and the invarient impedances become

$$Z_{\text{ave}} = \frac{1}{2}(Z_{TE} + Z_{TM}), \quad Z_{\text{eff}} = \sqrt{Z_{TE}Z_{TM}}. \tag{9.3}$$

The apparent resistivities and phases are

$$\rho_a(T) = |Z|^2 T/2\pi\mu_0, \quad \phi(T) = \arg Z \tag{9.4}$$

which are dependent on the impedances from which they are derived.

9.2 1D Inversions

This chapter summarizes work done in collaboration with A.K. Agarwal and J.T. Weaver. The aim of the study was to employ a variety of 2D synthetic models to investigate the relative merits of using the impedances Z_{TE}, Z_{TM}, Z_{ave} and Z_{eff} to calculate 'least layered' 1D results that can be combined into a 2D pseudosection for a model (see Fig 9.1). The pseudosection can then be used as a starting model in performing 2D inversions. The results of this study are given in more detail in the paper written by Agarwal et al. (1993).

'Least layered' 1D profiles are obtained from the 1D program AUTOMOD (Weaver and Agarwal, 1993) which starts with 2, 3, 4... layer models based on approximate Niblett-Bostick inversions and adjusts their layer thicknesses and resistivities until the smallest misfit is found. When an increase in layers no longer results in a significant decrease in misfit the 'least layered' model has been found. The 2D starting model is composed of the least layered models at a number of sites taken across the model. The misfit s was defined as

$$s^2 = (\epsilon_{TE}^2 + \epsilon_{TM}^2 + \eta_{TE}^2 + \eta_{TM}^2)/v. \tag{9.5}$$

where $v = 4KN - p$ is the number of degrees of freedom, p is the number of adjustable model parameters and

$$\epsilon^2 = \frac{1}{4}\sum_{k=1}^{K}\sum_{n=1}^{N} W_{k,n}[\log\left(\rho_a(T_n)/\rho_a^{(c)}(T_n)\right)]^2_{y=y_k}, \tag{9.6}$$

$$\eta^2 = \sum_{k=1}^{K}\sum_{n=1}^{N} w_{k,n}[\phi(T_n) - \phi^{(c)}(T_n)]^2_{y=y_k}. \tag{9.7}$$

$$W_{k,n} = \left(\frac{\bar{\sigma}^{(\rho)}}{\sigma_{k,n}^{(\rho)}}\right)^2, \quad w_{k,n} = \left(\frac{\bar{\sigma}^{(\phi)}}{\sigma_{k,n}^{(\phi)}}\right)^2 \tag{9.8}$$

with

$$(\bar{\sigma}^{(\rho)})^2 = \frac{1}{(1/KN)\sum_{k=1}^{K}\sum_{n=1}^{N}[1/(\sigma_{k,n}^{(\rho)})^2]}, \tag{9.9}$$

$$(\bar{\sigma}^{(\phi)})^2 = \frac{1}{(1/KN)\sum_{k=1}^{K}\sum_{n=1}^{N}[1/(\sigma_{k,n}^{(\phi)})^2]}. \tag{9.10}$$

N is the number of periods $T_n (n = 1, 2, ..., N)$, K is the number of sites $y_k (k = 1, 2, ..., K)$ and W and w are the normalized weighting functions. The variables $\rho_a^{(c)}$ and $\phi_a^{(c)}$ refer to the calculated responses of the model as opposed to field data. The variances of the data

$$\sigma_{k,n}^{(\rho)} = \frac{1}{2}\lambda \ln(\rho_a^{max}/\rho_a^{min}), \quad \sigma_{k,n}^{(\phi)}\lambda(\phi^{max}/\phi^{min}) \tag{9.11}$$

contain the factor λ which has been introduced to take into account how the error bars are defined (Weaver and Agarwal, 1993).

It was found that Z_{TE} (see Fig. 9.1(b)) was good at revealing conductive anomalies and the layering beneath them. Non-existent conductive layers that dip down and away from the anomalies at their edges were generated by Z_{TE} but were found

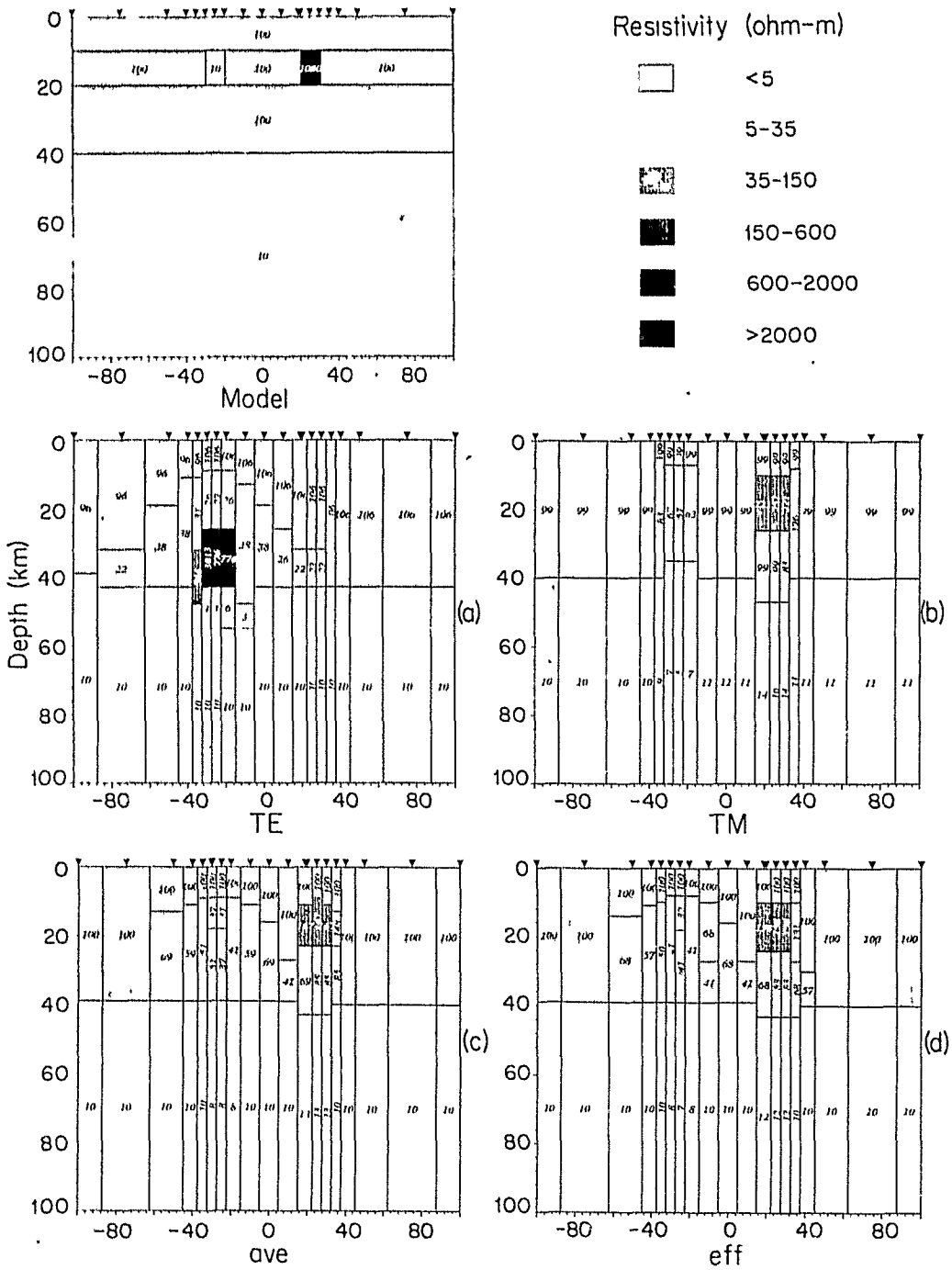

Figure 9.1: A model with both a resistive and conductive block shown with four pseudosections obtained by inverting apparent resistivities and phases associated with the impedances Z_{TE}, Z_{TM}, Z_{ave} and Z_{eff}. The distances marked on the horizontal axis are in kilometers and the positions of the sites at the 1D inversions were done are indicated by the inverted black triangles. The figure is taken from Agarwal et al. (1993).

to disappear during the subsequent 2D inversion. These non-existent layers have been reported previously by Berdichevsky and Dmitriev (1976) and others and explained by Jiracek (1990). Although thin resistive layers underneath a conductor were not seen, the other impedances also failed to resolve this structure. The best estimate of the vertical boundaries of small anomalous resistors was provided by the Z_{TM} impedance (Fig. 9.1(c)) but the resulting starting model was, in general, inferior. The pseudosections that were generated by the rotationally invariant impedances Z_{ave} and Z_{eff} (Fig. 9.1(d) and (e)) exhibited characteristics of both Z_{TE} and Z_{TM} but failed to expose the structure beneath a conductive layer. It was concluded that Z_{TE} is the impedance of choice for generating 2D start models but that it is prudent to use a Z_{ave} or Z_{eff} pseudosection to check that no possible resistors have been overlooked.

9.3 2D Inversion of COPROD2 Data

Next a 2D inversion of real data was performed which combined the minimization routine MINDEF, used in the 1D inversion program AUTOMOD, with the 2D forward program discussed earlier in this thesis. The 2D inversion begins with a series of starting models composed of 3,4,5... columns where each column is the 'least layered' result of a 1D inversion. Each of these starting models is optimized by MINDEF with adjustments to its vertical and horizontal boundaries and resistivities until a change in successive misfits for the model is less than 0.01% or 2400 iterations have been performed. Then, analogous to the way in which the

least layered 1D profiles are found, the optimized model misfits are compared in order (the model with n columns always being compared to the model with $n+1$ columns) until a case is found where the starting model with more columns does not result in a significant decrease in the misfit. Whether or not an improvement in the fit of the magnetotelluric responses to the real data is significant is determined by the application of a statistical F-test:

$$F = \frac{\Delta\chi^2/(v_1 - v_2)}{\chi^2_{v_2}} \tag{9.12}$$

where v_2 is the smaller number of degrees of freedom of the model with more columns. The value $\Delta\chi^2$ is the difference of the χ^2 distributions of the two models where

$$\chi^2 = \left(\epsilon_{TE}/\bar{\sigma}^{(\rho)}_{TE}\right)^2 + \left(\epsilon_{TM}/\bar{\sigma}^{(\rho)}_{TM}\right)^2 + \left(\eta_{TE}/\bar{\sigma}^{(\phi)}_{TE}\right)^2 + \left(\eta_{TM})/\bar{\sigma}^{(\phi)}_{TM}\right)^2 \tag{9.13}$$

and $\chi^2_v = \chi^2/v$. We are essentially testing to see whether the value we obtain for F could have arisen by chance. If the probability of occurance of our value of F (where F has a well-known probability distribution that can be calculated using available library subroutines) is less than 5%, then it is assumed, with a 95% confidence level, that the additional column led to significant improvement in the fit. A negative value for F would indicate an increase (worsening) in misfit for the model with more columns. The model with the least structure (number of columns) and lowest significant misfit, found by application of the above method, is called the 'least blocked' model.

The MT data under study were recorded by an array laid out across the Phanerozoic Williston Basin in South Saskatchewan Canada. This data set is the subject of COPROD2 — an international comparison project on 2D inversion techniques. The data have been corrected for static shift (Jones, 1988) and incorporate the TM and TE responses of 35 sites spread out over 407 km for the period range $2.6 \times 10^{-3} - 1.82 \times 10^{3}$s. Previous studies (Jones and Savage, 1986) have shown that for smaller periods up to 4 s the two polarizations produce similar responses which supports the presence of a uniform layer of Palacozoic sediments across the entire profile. Although two distinct anomalies have been identified in the basin (the North American Central Plains (NACP) anomaly and the Thompson Belt (TOBE) anomaly) only the NACP anomaly will be discussed here due to the unmanageably large width required for a model that combines the two. Since evidence (Jones and Craven, 1990) suggests that the two anomalies are separated by more than 100 km such an approach will certainly be valid.

The NACP anomaly has its centre in the array and extends downwards from approximately 10 km to perhaps as deep as the base of the crust. Of the 35 sites in the data set twenty in the region of the NACP anomaly were chosen for the 2D inversion. Their positions are −113.5, −100.9, −93.0, −84.6, −74.4, −64.9, −55.7, −45.8, −35.0, −25.9, −14.6, −5.9, 4.9, 22.8, 41.8, 54.5, 64.2, 79.5, 96.2, 117.3 km with Macoun, Saskatchewan at the origin. Seven periods (10.7, 21.3, 42.7, 85.3, 170.7, 341.3, 682.7 s) were used together with the maximum and minimum of ρ_a and ϕ provided with the COPROD2 data. The maximum and minimum values of

ρ_a and ϕ made up the error bars for the data, whose lengths were equal to two standard deviations; for error bars such as these $\lambda = 0.74$ in (9.11).

Three starting models of 3, 4 and 5 columns are shown in Fig. 9.2. The three column start model was generated by Z_{TE} 1D inversions at the sites -100.9 km, -5.9km and 117.3km. The boundaries between the columns were located midway between the sites. The side columns extended out to infinity and below 60 km was a uniform half space whose resistivity was set equal to the resistivity of the deepest layer in the left most column. The misfit between this model and the observed TE and TM apparent resistivities and phases was calculated for all 20 sites and 7 periods. In all there were 18 adjustable parameters (10 resistivities for the 9 blocks and the underlying half-space and the positions of two vertical and 6 horizontal boundaries) which were allowed free movement during the optimization which required hundreds of calls to MINDEF. For each call, 14 solutions of the forward problem were required: one for each of the 7 periods for both polarizations. The 18 adjustable parameters in this model continued to change until the difference between successive misfits (s^2) was less than 0.01% or when the number of calls to MINDEF reached 2400. Repeating this procedure for 4 and 5 column models showed that while the 4 column model misfit was 24% smaller than the 3 column misfit, the 5 column misfit was slightly worse (2% larger) than the 4 column misfit. Since there was no significant improvement with the addition of an extra column the result was a 'least blocked' model of 4 columns shown in Fig. 9.3(b) along with the optimized results for the 3 and 5 column models (Fig. 9.3 (a) and (c)).

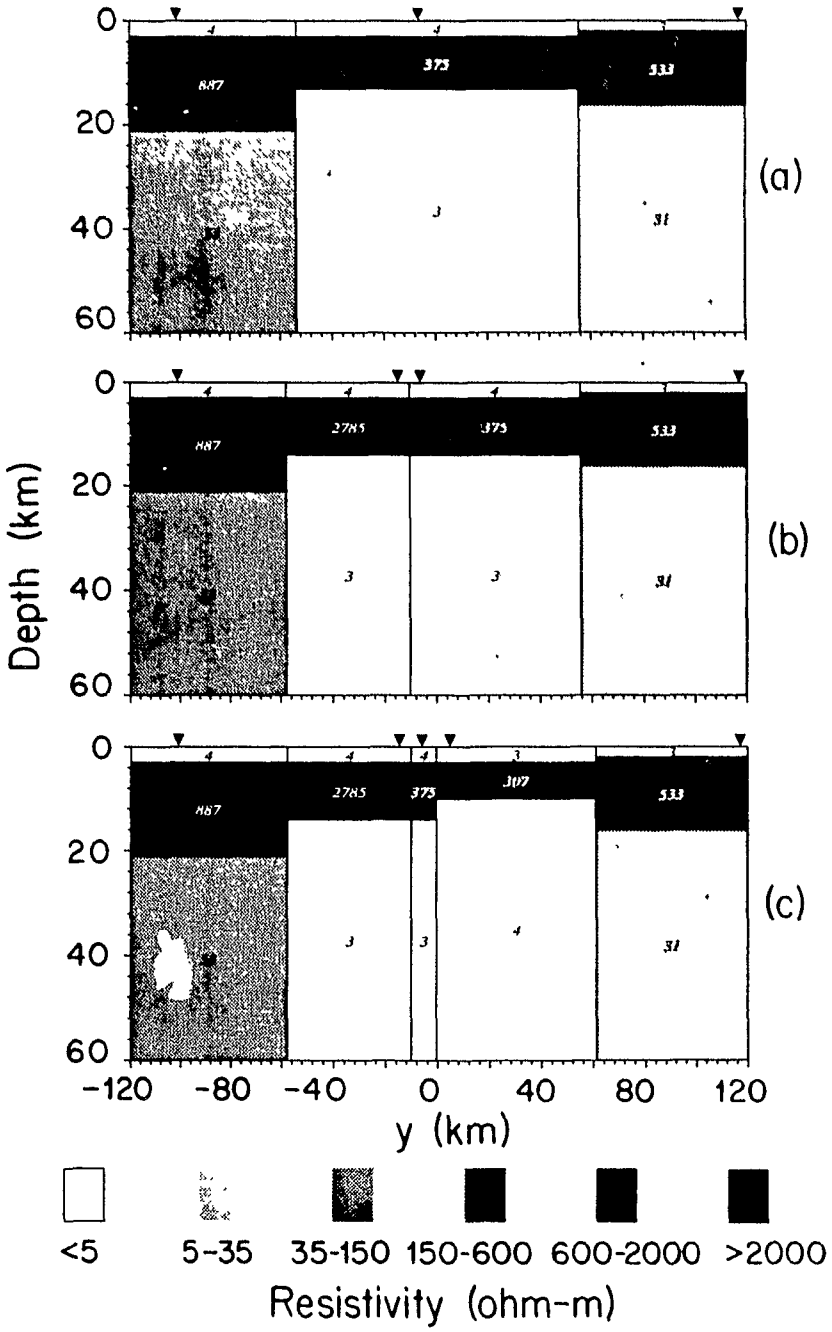

Figure 9.2: The 2D starting models with three, four and five columns used in the optimization of the NACP anomaly (shown above in (a), (b) and (c) respectively. The positions of the sites at which the 1D inversions were made are indicated by the inverted black triangles. The figure is taken from Agarwal et al. (1993).

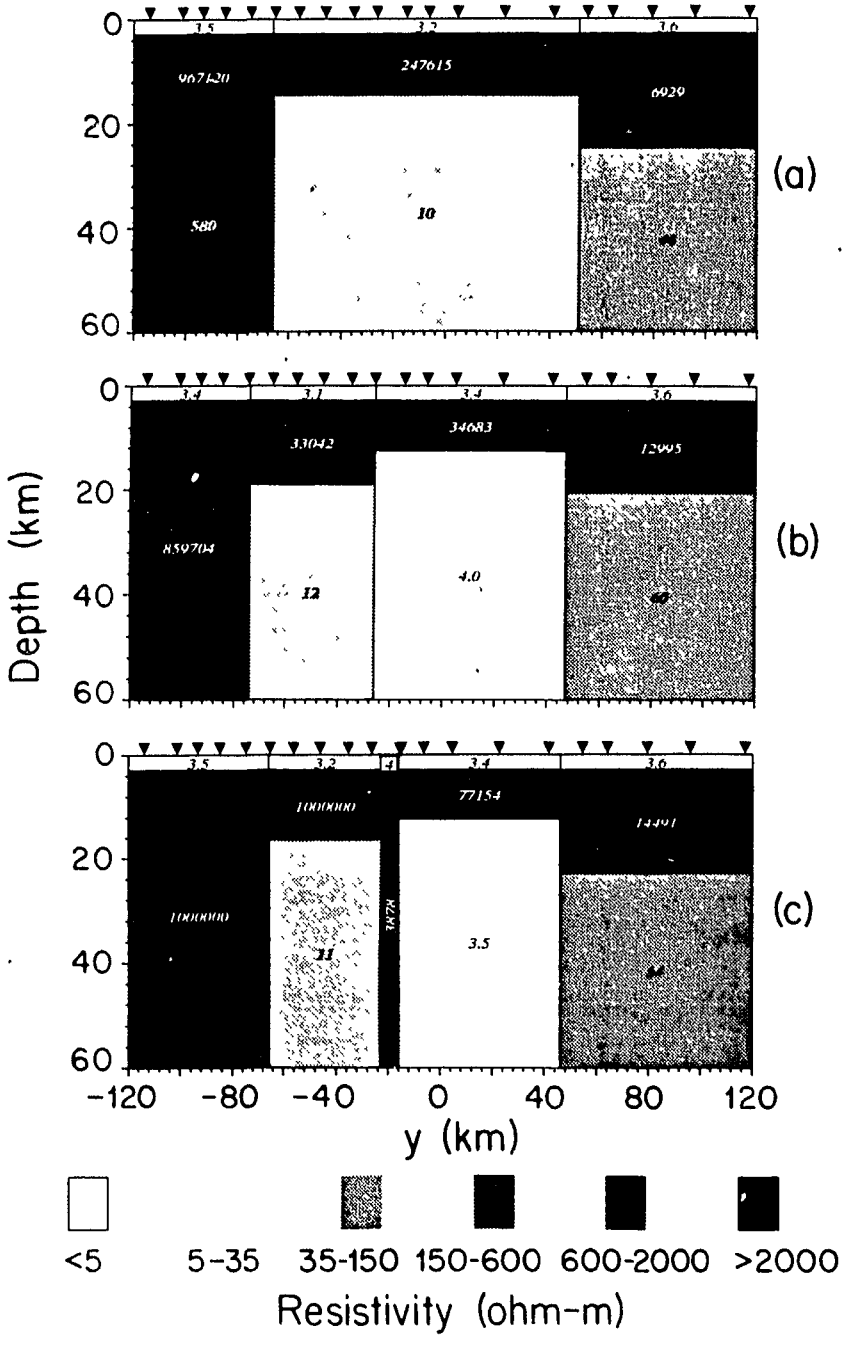

Figure 9.3: The above models are the optimized three, four and five-column models of the NACP anomaly shown in (a), (b) and (c) respectively. The best-fitting 'least-blocked' model is the four-column model in (b). The data sites are shown by the inverted black triangles. The figure is taken from Agarwal et al. (1993).

The surface sedimentary layer is readily apparent as are the two vertical blocks extending from −74 km to 47 km that make up the NACP anomaly. Because the 1D inversions over the NACP anomaly only generated 3 layers the vertical blocks must extend down to 60 km and no underlying structure that may exist can be resolved. The crust surrounding the anomaly is extremely resistive except east of the anomaly where the resistivity is only 60 Ωm. These high resistivities must be viewed as merely qualitative since the response of the model becomes insensitive to changes in the host resistivity above about 2000 Ωm. In Fig. 9.3(c) the left most host resistivity has, in fact, reached the program's upper limit of 10^6Ωm.

Agarwal et al. (1993) also compared the resistivity and phase curves (not shown here) from 20 sites for the real data and model responses concluding that the agreement was good except for an under-estimate of the long period TE response at 64.2 km and an over-estimate at −5.9 and 117.3 km. They point out that the discrepancy in the 117.3 km response may be due to its proximity to the TOBE anomaly.

Although the NACP anomaly revealed by the optimization process dips down and to the west it does not agree with the results of Jones and Craven (1990) who found a sharp dipping angle of 60°. To check this point an extra column was added to the 'least blocked' model by dividing the third column in two at y = 10 km. The 6 extra adjustable parameters should have allowed the generation of a steeper dipping staircase anomaly upon further optimization of the model if the data required it. The final result, shown in Fig. 9.4(a), had a misfit only

1% smaller than previously and is not markedly different from the original 'least blocked' model. Since the starting model did not preclude the emergence of a steeply dipping anomaly it was felt that an oversimplification of the model was not responsible for its absence.

In addition the Jones and Craven anomaly (arrived at by trial and error forward modelling) is vertically thin which they claim is borne, out by the insensitivity of the TM response to the NACP anomaly. Agarwal et al. find, however, that their TM responses are also insensitive to the anomaly unless the host resistivity is significantly less than 2000 Ωm. In addition there is no indication of such thin conducting layers in the 1D inversion of either Agarwal et al. or Jones and Craven, although the Z_{TE} response was certainly capable of resolving them. But since our starting models had only three layers above the basement they could not have resolved such a thin structure. In order to check that oversimplification of the starting model was not the cause for the lack of a thin anomaly, extra layers were added to the two anomalous blocks in Fig. 9.3(b). Further optimization of this model resulted in the model shown in Fig. 9.4(b) whose misfit is only 1% smaller than the original 'least blocked' model. Once again the new structure is not significantly different from the original.

Of course, since there is no unique solution, the model shown in Fig. 9.3(b) is merely one possible configuration of many, each of which may fit the data equally well. In all, this approach to the 'least blocked' model required 7067 calls to MINDEF which spawned a total of 98,966 forward calculations. The difficulties

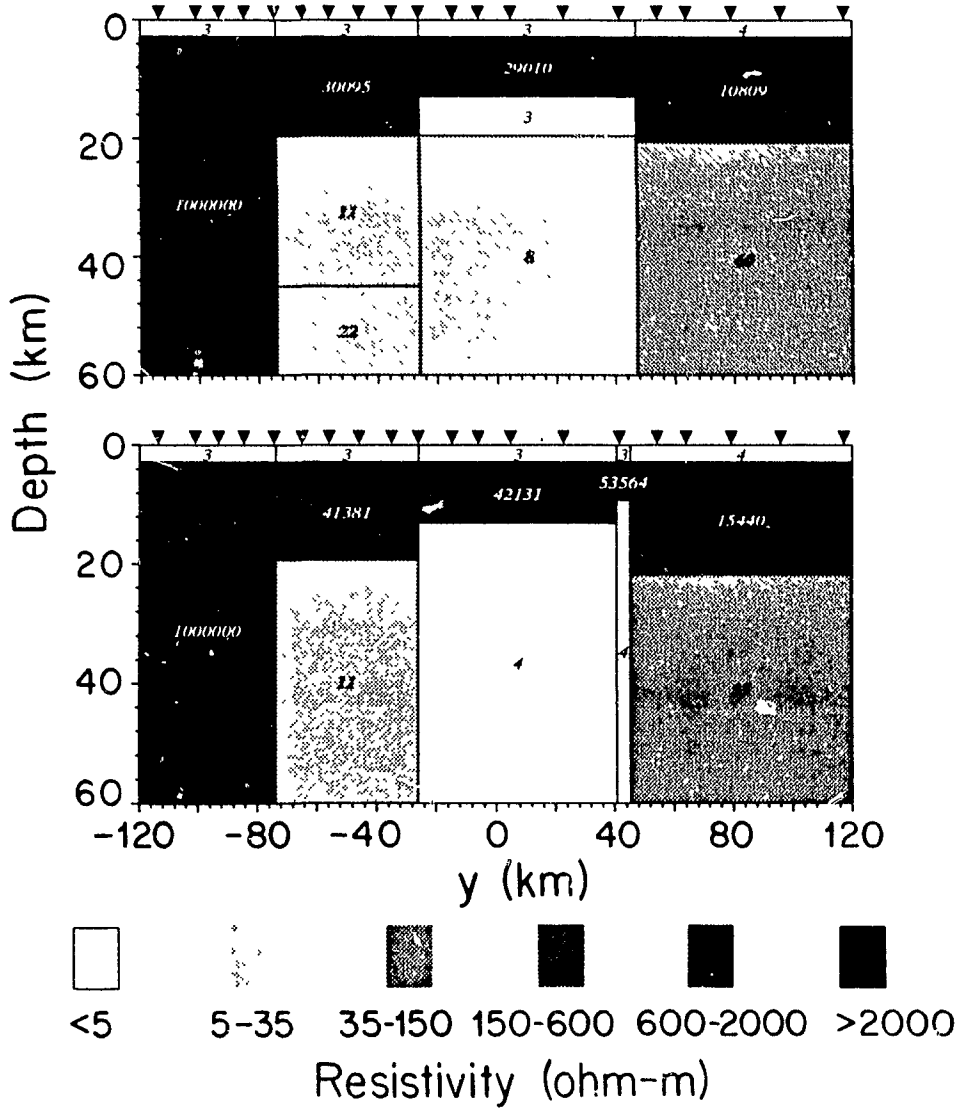

Figure 9.4: Best-fitting models obtained by further optimization from the 'least-blocked' model in Figure 9.3 (b) after increasing the number of parameters by adding (a) one extra layer in each of the two central columns and (b) one extra column. The figure is taken from Agarwal et al. (1993).

of undertaking such a massive task without automatic gridding, an efficient 2D modelling program and sufficient computer power are obvious.

Chapter 10

CONCLUSIONS AND SUGGESTIONS FOR FURTHER WORK

10.1 The Automatic Forward Modelling Program

In chapters 2–6 of this thesis a finite difference algorithm for solving the forward modelling problem of geoelectromagnetic induction in two-dimensional structures was developed. The governing equations were modified to solve for the anomalous field by separating out the 'host' field which is assumed to be the field generated by the 1D conductivity distribution on the left hand side of the model. This was done to prevent the 'swamping out' or masking of the small anomalous fields by the much larger host field which can occur as a result of the finite length of the computer word.

The most important feature of this program is an automatic gridding subroutine which greatly reduces the amount of time required to design a suitable grid for a model and removes the human element from such grid design. Subsequent investigations in chapters 7–9 demonstrate that the savings in time due to this

feature are enormous. For instance in chapter 7 the calculation of the best-fitting 2D models at sites 9 and 10 required 485 iterations. For two polarizations and 10 periods this translates into 9700 forward problems. Each time a period or any of the model parameters changes a new grid must be designed. If we assume that this grid design can be done by hand in an average time of only 10 minutes per period (which is still very fast work) it would take 800 hours just to design the grids. Using the automatic gridding program and submitting only the parameters for the starting models our final best fit models were obtained, without further human interaction, in only 48 hours of real time. The 2D inversion of the COPROD data in chapter 9 spawned a total of 98,966 forward calculations in its quest for the 'least-blocked' model. The savings in time due to the automatic gridding were obviously crucial in performing this task. A logical next step in the automatic gridding process would be to develop a gridding routine that could handle triangular elements instead of only rectangular ones. This would allow greater flexibility in handling sloping boundaries and could be linked with finite element routines to enable them to run with greater speed and no user specific elements. Other future work could include an adaptation of the multigrid method (Press et al. 1992) to be used with the finite difference forward modelling program. Also, instead of adding specific sites to the grid, it is possible to obtain the field at a required location by interpolating between the fields at the grid points on either side of it. If many, or closely spaced, sites were involved this could make the final grid smaller. This, of course, would lead to a savings in computation time.

10.2 Two-Dimensional Inversion of Sardinian Data

The program was used to perform a two-dimensional (2D) inversion on magnetotelluric data from a profile in Sardinia. Two sites along this profile could not be considered to be solely 2D in the direction of the profile. Two-dimensional inversions were performed on the data from these two sites to obtain models for the 2D structure perpendicular to the profile. The apparent resistivity curves from the models fit the data fairly well at both sites especially at short periods. The phase results for both sites were, in general, not in good agreement with the data. Since phase data were not used in the inversion this behaviour was not surprising and was no doubt due in part to the scatter in the data mentioned by Peruzza et al. (1990). Although both the 2D models obtained (Fig. 7.7 and 7.9) were the result of data taken at only one site and were subject to the nonuniqueness common to all inversions thay still provided some useful insights into the geology of the area. The two-dimensional magnetotelluric model of Peruzza et al. (1990) for the NS Sardianian profile (Fig. 7.2) indicated that site 9 is directly over a vertical boundary between a resistive region of 10^4 ohm-m and a more conductive one of 6.5 ohm m. The inversion results place site 9 firmly over the upwelling of the resistive region. The absence of the underlying 50 ohm-m layer present in Fig. 7.2 may account for some of the longer period misfit at site 9. The results for site 10 agree in general with the model in Fig. 7.2 although our thickness for the surface layer directly under the site is about twice that found in the model of

Peruzza et al. (1990). Our results also indicated that the granites underlying site 10 are cut off at, or just before, the coast of the Gulf of Oristano.

10.3 Induction Arrows Over a Buried Conductivity Contrast

A study was made of the behaviour of 2D induction arrows over a buried conductivity contrast. It was noted that, although the general trend of in-phase arrows is to point towards the regions of high electrical conductivity, some investigators have found small amplitude in-phase arrows that point away from these same regions. Reversals such as these, which do not behave according to the general trend, can cause confusion and erroneous interpretation of the in-phase induction arrows. This is especially true when two or more conductors are present and mutual coupling between them affects the induction arrows. Using a model with two semi-infinite conducting plates, one at the surface and one buried at a depth d in a layered half space, it was found that the period at which a reversal in the in-phase induction arrow direction occurred was a function of the apparent resistivity of the layered host. This reversal was seen at small periods and for models which contained only the buried conducting plate. For the model containing both this and the surface ocean conductor the in-phase arrow reversals are masked by the strong response of the ocean. The reversal caused by the buried plate spawned a similar reversal in the mutual coupling in our models. The mutual coupling, reflected in the difference response (see Fig. 8.5 and 8.5), was larger for very small periods than for slightly larger ones. For a smaller period the distances between

the two conductors are increased in terms of skin depths so that mutual coupling *should* always decrease with period. This anomalous behaviour can cause problems in the interpretation of induction arrows obtained by the subtraction of the total model arrows from ocean arrows (removal of the 'coast effect'). It had been supposed that these arrows would always point towards a conducting anomaly in the area but at short periods it was seen that they can point away from them instead. It is important that those who use the in-phase arrows to locate and characterize conductivity anomalies be aware of this phenomenon. More work needs to be done on both two and three dimensional models before this behaviour can be properly understood. The examination of a finite conducting block in different layered hosts may lead to an empirical formula for T_r as a function of ρ_a.

10.4 Automated Two-Dimensional Inversion

A two-dimensional inversion scheme which incorporates the 2D forward modelling program and a minimization routine MINDEF has been described. An investigation was made into the relative merits of using the impedances Z_{TE}, Z_{TM}, Z_{ave} and Z_{eff} to calculate the one-dimensional inversions that are combined to form starting models for the 2D inversions. It was found that Z_{TE} is the impedance of choice for generating 2D start models but that it is prudent to use a Z_{ave} or Z_{eff} pseudosection to check that no possible resistors have been overlooked.

A two-dimensional inversion of the North American Central Plains (NACP) anomaly resulted in a best fit model whose responses showed good agreement to

the apparent resistivity and phase field data from 20 sites. The surface sedimentary layer was well resolved and the anomaly was made up of two vertical blocks (of 12 and 4.0 ohm-m) that spanned a distance of 121 km and extended down to 60 km. Although this model of the NACP anomaly did dip down to the west it did not exhibit a sharp dipping angle of 60° found by other investigators. Giving the model additional freedom to move in this direction resulted in a final model that had changed little from its predecessor. A similar experiment, performed to see if the anomaly might be vertically thin, as found by some other authors, resulted in another model that exhibited no significant change from its simpler counterpart. It was concluded that the model did not require either of these two features to produce a good fit to the data.

The amalgamation of a fast automatic forward modelling routine with a quick and efficient inversion process is an extremely useful geophysical tool. Improved minimization routines could lead to acceptable results requiring fewer forward modelling solutions. The inversion scheme could be improved further by allowing the incorporation of data from other experiments (not necessarily electromagnetic) since this information could be crucial in the search for geologically plausible earth models.

REFERENCES

Agarwal, A.K. and Dosso, H.W. (1990). On the behaviour of the induction arrows over a buried conductive plate – a numerical study. Phys. Earth Planet. Inter., **60**, 265–277.

Agarwal, A.K. and Weaver, J.T. (1989). Regional electromagnetic induction around the Indian Peninsula and Sri Lanka: a three-dimensional numerical model study using the thin sheet approximation. Phys. Earth Planet. Inter., **54**, 320–331.

Agarwal, A.K., Poll, H.E. and Weaver, J.T. (1993). One- and two-dimensional inversion of magnetotelluric data in continental regions. Phys. Earth Planet. Inter., **81**, 155–176.

Ashour, A.A. (1971). Electromagnetic induction in thin finite sheets having conductivity decreasing to zero at the edge, with geomagnetic applications.–I. Geophys. J. R. astr. Soc., **8**, 375–388.

Berdichevsky, M.N. and Dmitriev, V.I. (1976). Basic principles of interpretation of magnetotelluric sounding curves. In: A. Ádám (ed.), Geoelectric and Geothermal Studies. KAPG Geophysical Monograph, Akademiai Kiado., pp. 165–221.

Best, M.E., Duncan, P., Jacobs, F.J., and Scheen, W.L. (1985). Numerical modelling of the electromagnetic response of three-dimensional conductors in a layered earth. Geophysics, **50**, 665-676.

Bevington, P.R. (1969) *Data Reduction and Error Analysis for the Physical Sciences.* McGraw-Hill Inc., New York.

Brewitt-Taylor, C.R. and Weaver, J.T. (1976). On the finite difference solution of two-dimensional induction problems. Geophys. J. R. astr. Soc., **47**, 375–396.

Cagniard, L. (1953). Basic theory of the magneto-telluric method of geophysical prospecting. Geophysics, **18**, 605–635.

Chan, G.H., Dosso, H.W. and Law, L.K. (1981). An analogue model study of electromagnetic induction for cape and bay coastlines. Phys. Earth Planet. Inter., **25**, 167–176.

Charters, R.A., Dosso, H.W., Best, M.E. and Nienaber, W. (1989). Induction coupling for a conductive dike in a resistive earth. Phys. Earth Planet. Inter., **54**, 140–148.

Chave, A.D. and Booker, J.R. (1987). Electromagnetic Induction studies. Rev. Geophys., **25**, 989–1003.

Chen, P.F. and Fung, P.C.W. (1985). On the finite difference method of three-dimensional electromagnetic induction problems. Acta Geophysica Sinica. vol. **28**, No. 3.

Chen, P.F. and Fung, P.C.W. (1987). On the behaviour of the imaginary Parkinson arrows near the anomalous conductor-host medium interface. Phys. Earth Planet. Inter., **50**, 195–198.

Chen, J., Dosso, H.W., and Nienaber, W. (1989). Laboratory electromagnetic model results for the EMSLAB region. J. Geophys. Res., **84**, 14167–14172.

Chen, J., Dosso, H.W., and Ingham, M. (1990). Electromagnetic induction in New Zealand: Analogue model and field results. Phys., Earth Planet., Inter., **62**, 257–270.

Chen, J., Dosso, H.W., and Ingham, M. (1993). Electromagnetic induction in the New Zealand South Island. Phys. Earth Planet. Inter., **81**, 253–260.

Coggon, J.H. (1971). Electromagnetic and electrical modeling by the finite-element method. Geophysics, **36**, 132–155.

Dawson, T.W. (1983). E-polarization induction in two thin half-sheets. Geophys. J. R. astr. Soc., **73**, 83-107.

Dawson, T.W. and Weaver, J.T. (1979). H-polarization induction in two thin half-sheets. Geophys. J. R. astr. Soc., **56**, 419–438.

Dawson, T.W., Weaver, J.T. and Raval, U. (1982). B-polarization induction in two generalized thin sheets at the surface of a conducting half-space. Geophys. J. R. astr. Soc., **69**, 209–234.

DeLaurier, J.M., Auld, D.R. and Law, L.K., (1983). The geomagnetic response across the continental margin off Vancouver Island: comparison of results from numerical modelling and field data. J. Geomagn. Geoelectr., **35**, 517–528

Dey, G. and Morrisson, H.F. (1979). Resistivity modelling for arbitrary two-dimensional structures. Geophys. Prosp., **27**, 106–136.

Dosso, H.W. (1973). A review of analogue model studies of the coast effect. Phys. Earth and Planet. Inter., **7**, 294–302.

Dosso, H.W., Nienaber, W., and Parkinson, W.D. (1985). An analogue model study of electromagnetic induction in the Tasmania region. Phys., Earth Planet., Inter., **39**, 118–133.

Dosso, H.W., Chan, G.H. and Nienaber, W. (1986). An analogue model study of electromagnetic induction for an island near bay and cape coastlines. Phys. Earth Planet. Inter., **42**, 178–183.

Dosso, H.W., Nienaber, W. and Chen, J. (1989). Laboratory electromagnetic modelling of the subducting Juan de Fuca plate. Phys. Earth Planet. Inter., **53**, 221–227.

Dosso, H.W., Chen, J. and Nienaber, W. (1990). Comparison of analogue model and field station EM responses on Southern Vancouver Island. Phys. Earth Planet. Inter., **60**, 18–24.

Dosso, H.W. and Meng, Z.W. (1992). The coast effect response in geomagnetic field measurements. Phys. Earth Planet. Inter., **70**, 39–56.

d'Erceville, I. and Kunetz, G. (1962). The effect of a fault on the earth's natural electromagnetic field. Geophysics, **27**, 651–665.

Erdélyi, A. (ed.) (1954). *Tables of Integral Transforms* Vols. I and II. McGraw-Hill, New York.

Filloux, J.H. (1979). Magnetotelluric and related electromagnetic investigations in geophysics. Rev. Geophys., **17** 282–294.

Fischer, G. and Le Quang, B.V. (1981). Topography and minimization of the standard deviation in one-dimensional magnetotelluric modelling. Geophys. J. R. astr. Soc., **67**, 279–292.

Fischer, G., Schnegg, P.A. and Ranieri, G. (1990). Magnetotellurics over the Sardinian Segment, Proc. Sixth Workshop of the EGT (Data Compilation and Synoptic Interpretation, held in Einsiedeln, Switzerland, 29.11–05.12, 1989), pp.333–339.

Geyer, R.G. (1972). The effect of dipping contact on the behavior of the electromagnetic field. Geophysics, **37**, 337–350.

Green, R. (1978). The Two-Dimensional Theory of Electromagnetic Induction in Thin Sheets with Applications to the Earth. M.Sc. Thesis, University of Victoria, Victoria, B.C.

Green, V.R. and Weaver, J.T. (1978). Two-dimensional induction in a thin sheet of variable integrated conductivity at the surface of a uniformly conducting earth. Geophys. J. R. astr. Soc., **55**, 721–736.

Gregori, G.P. and Lanzerotti, L.J. (1980). Geomagnetic Depth Sounding by induction arrow representation: a review. Rev. Geophys. Space Phys., **18**, 203–209.

Gregori, G.P. and Lanzerotti, L.J. and Meloni, A. (1982). Reply. Rev. Geophys. Space Phys., **20**, 523–528.

Gupta, P.K., Bennett, L.A., and Raiche, A.P. (1987). Hybrid calculations of the three-dimensional electromagnetic response of buried conductors. Geophysics, **51**, 1450–1461.

Gupta, P.K., Raiche, A.P. and Sugeng, F. (1989). Three-dimensional time-domain electromagnetic modelling using a compact finite-element frequency-stepping method. Geophysical J., **96**, 457–468.

Hebert, D., Dosso, H.W., Nienaber, W. and Wright, J.A., (1983). Analogue model study of electromagnetic induction in the Newfoundland region. Phys. Earth Panet. Inter., **32**, 65–84

Hermance, J.F. (1983). Electromagnetic induction studies. Rev. Geophys. **21**, 652–664,

Hohmann, G.W. (1975). Three-dimensional induced polarization and eletromagnetic modelling. Geophysics, **40**, 309–324.

Hohmann, G.W. (1983). Three-dimensional EM modelling. Geophysical Surveys, **6**, 27–53.

Hohmann, G.W. and Raiche, A.P. (1988). Inversion of controlled source electromagnetic data. *Electromagnetic methods in applied Geophysics*, Vol 1, Theory. edited by M.N. Nabighian. Soc. Expl. Geophys.

Hu, W.B., Dosso, H.W. and Nienaber, W. (1984). Analogue model magnetic field responses of an ocean channel, an island, and a seamount in the Hainan Island region. J. Geohys., **55**, 222–227.

Hu, W.B., Dosso, H.W. and Nienaber, W. (1986). Model magnetic field responses of an ocean channel, an island, and a seamount for two polarizations. Annales Geophysicae **4**, 165–172.

Hu, W.B., Nienaber, W. and Dosso, H.W. (1989). Vertical magnetic field response of a seamount. Phys. Earth Planet. Inter., **54**, 135–139.

Jackson, J.D. (1975). *Classical Electrodynamics*, 2nd ed. John Wiley and Sons Inc., New York.

Jiracek, G.R. (1990). Near-surface and topographic distortions in electromagnetic induction. Geophys. Surv., **11**, 163–203.

Jones, A.G. (1981). Comment on "Geomagnetic depth sounding by induction arrow representation: A review" by G.P. Gregori and L.J. Lanzerotti. Rev. Geophys. Space Phys., **19**, 687–688.

Jones, A.G. (1986). Parkinson's pointers' potential perfidity. Geophys. J. R. astr. Soc., **87**, 1215–1224.

Jones, A.G. (1988). Static-shift of magnetotelluric data and its removal in a sedimentary basin environment. Geophysics, **53**, 967–978.

Jones, A.G. and Craven, J.A. (1990). The North American Central Plains conductivity anomaly and its correlation with gravity, magnetic, seismic, and heat flow data in Saskatchewan, Canada. Phys. Earth Planet. Inter., **63**, 169–194.

Jones, A.G. and Savage, P.J. (1986). North American Central Plains conductivity anomaly goes east. Geophys. Res. Lett., **13**, 685–688.

Jones, D.S. (1964). *The Theory of Electromagnetism.* Permagon Press, Oxford.

Jones, F.W. and Vozoff, K. (1978). The calculation of magnetotelluric quantities for three-dimensional conductivity inhomogeneities. Geophysics, **43**, 1167–1175.

Jupp, D.L.B. and Vozoff, K. (1977). Two-dimensional magnetotelluric inversion. Geophys. J. R. Astr. Soc. **50**, 333–352.

Kaikkonen, P. (1977). A finite element program package for electromagnetic modeling. J. Geophys, **43**, 179–192.

Kaikkonen, P. (1980). Numerical Finite Element Modeling in Geophysical Applications of Electromagnetic Fields. Ph.D. Thesis, Acta Univ. Oul. A 93, 1980. Phys. 18, 135 pp.

Kaikkonen, P. (1986). Numerical electromagnetic modeling including studies of characteristic dimensions: A review. Surveys in Geophysics, **8**, 301–337.

Kang, S., Dosso, H.W. and Ogunade, S.O. (1993). Electromagnetic induction in South-West Nigeria: analogue model and field results. J. Geomagn. Geoelectr., **45**, 805–816

Kaufman, A.A. and Keller, G.V. (1981). *The Magnetotelluric Sounding Method.* Elsevier Scientific Pub. Co., New York.

Kertz, W. (1954). Modelle für erdmagnetisch induzierte elektrische Ströme im Untergrund. Nachr. Akad. Wiss. Göttingen, Math.-Phys. Kl. Abt. IIa, 101–110.

Lee, K.H., Pridmore, D.F. and Morisson, H.P. (1981). A hybrid 3D EM modelling scheme. Geophysics, **51**, 1819–1829.

Lilley, F.E.M. and Arora, B.R. (1982). The sign convention for quadrature Parkinson arrows in geomagnetic induction studies. Rev. Geophys. Space Phys., **20**, 513–518.

Lines, L.R. and Jones, F.W. (1973). The perturbation of alternating Geomagnetic fields by 3D island structures. Geophys. J. R. **32**, 133–154.

McKirdy, D.McA. and Weaver, J.T. (1984). Induction in a thin sheet of variable conductance at the surface of a stratified earth — I: Two-dimensional theory. Geophys. J. R. astr. Soc., **78**, 93–103.

McKirdy, D.McA., Weaver, J.T. and Dawson, T.W. (1985). Induction in a thin sheet of variable conductance at the surface of a stratified earth — II: Three-dimensional theory. Geophys. J. R. astr. Soc., **80**, 177–194.

Meng, Z. and Dosso, H.W. (1990). An analogue model study of EM induction in the Japan-Korea-China region. Phys. Earth Planet. Inter., **62** 246–256.

Neves, A.S. (1957). The Magneto-Telluric Method in Two-Dimensional Structures. Ph.D. Thesis, Dept of Geology and Geophysics, MIT.

Nicoll, M.A. and Weaver, J.T. (1977). H-polarization induction over an ocean edge coupled to the mantle by a conducting crust. Geophys. J. R. astr. Soc., **49**, 427–442.

Nienaber, W., Dosso, H.W., Law, L.K., Jones, F.W. and Ramaswamy, V. (1976). An analogue model study of electromagnetic induction for island-continent ocean channels. Phys. Earth Planet. Inter., **13** 169–183.

Nienaber, W., Dosso, H.W., Law, L.K., Jones, F.W. and Ramaswamy, V. (1977). Studies of electromagnetic induction for island-continent ocean channels with applications to Vancouver Island. Acta. Geodaet., Geophys. et Montanist. Acad. Sci. Hung. **12**, 187–190.

Nienaber, W., Herbert, D. and Dosso, H.W. (1983). Induction arrows for a buried conducting plate. Phys. Earth Planet. Inter. **32**, 306–311.

Oldenburg, D. (1990). Inversion of electromagnetic data: An Overview of new techniques. Surveys in Geophysics **11**, 231–270.

Park, S.K. (1985). Distortion of magnetotelluric sounding curves by three-dimensional structures. Geophysics, **50**, 785–797.

Parker, R.L. (1983). The magnetotelluric inverse problem. Geophys. Surv., **6**, 5–25.

Parkinson, W.D. (1959). Directions of rapid geomagnetic fluctuations. Geophys. J. R. astr. Soc. **2**, 1–14.

Parkinson, W.D. (1962). The influence of continents and oceans on geomagnetic variations. Geophys. J. R. astr. Soc. **6**, 441–449.

Peruzza, L., Fischer, G., Schnegg, P.A. and Ranieri, G. (1990). Analysis of Sardinian NS Magnetotelluric Profile, The European Geotraverse: Integrative Studies (Results from the Fifth Study Centre) ed. R. Freeman, P. Giese and St. Mueller. pp. 329–346.

Press, W.H., Teukolsky, S.A., Vetterling, W.T. and Flannery, B.P. (1992). *Numerical Recipes in FORTRAN* Second Edition, Cambridge University Press, New York.

Price, A.T. (1949). The induction of electric currents in non-uniform thin sheets and shells. Quart. J. Mech. Appl. Math., **2**, 283–310.

Price, A.T. (1950). Electromagnetic induction in a semi-infinite conductor with a plane boundary. Quart. J. Mech. Appl. Math., **3**, 385–410.

Pridmore, D.F., Hohmann, G.W., Ward, S.H. and Sill, W.R. (1981) An investigation of finite element modeling for electrical and electromagnetic data in three dimensions. Geophysics, **46**, 1009–1024.

Raiche, A.P. (1974). An integral equation approach to three-dimensional modelling. Geophys. J. R. astr. Soc., **36**, 363–376.

Ramaswamy, V. and Dosso, H.W. (1973). Locating a horizontal magnetic dipole buried in a 2-layer earth. Electronics Letters. Vol. 9, No. 4.

Ramaswamy, V., Nienaber, W., Dosso, H.W., Jones, F.W. and Law, L.K. (1975). Numerical and analogue model results for electromagnetic induction for an island situated near a coastline. Phys. Earth Planet. Inter., **11**, 81–90.

Ranganayaki, R.P. (1984). An interpretive analysis of magnetotelluric data. Geophysics **49**, 1730–1748.

Ranganayaki, R.P. and Madden, T.R. (1980). Generalized thin sheet analysis in magnetotellurics: and extension of Price's analysis. Geophys. J. R. astr. Soc., **60**, 445–457.

Rankin, D. (1962). The magnetotelluric effect of a dike. Geophysics, **27**, 666–676.

Raval, U., Weaver, J.T. and Dawson, T.W. (1981) The ocean-coast effect reexamined. Geophys. J. R. astr. Soc., **67**, 115–123.

Reddy, I.K. and Rankin, D. (1973). Magnetotelluric response of a two-dimensional sloping contact by the finite element method. Pure and Appl. Geophys., **105**, 847–857.

Reddy, I.K., Rankin, D. and Phillips, R.J. (1977). Three-dimensional modeling in magnetotelluric and magnetic variational sounding. Geophys. J. R. astr. Soc., **51**, 313–326.

Rikitake, T. (1966). *Electromagnetism and the Earth's Interior.* Elsevier Publishing Co., Amsterdam.

Rikitake, T. (1973). Global electrical conductivity of the earth, Phys. Earth Planet. Inter., **7**, 245–250.

Roberts, R.G. (1986). Global electromagnetic induction. Survey in Geophysics., **8**, 339–374.

Roden, R.B. (1964). The effect of an ocean on magnetic diurnal variations. Geophys. J. R. astr. Soc., **8**, 375–388.

Rodi, W.L. (1976). A technique for improving the accuracy of finite element solutions for magnetotelluric data. Geophys. J. R. astr. Soc., **44**, 483–506.

Rokityansky, I.I. (1982). *Geoelectromagnetic Investigation of the Earth's Crust and Mantle.* Springer-Verlag, Berlin, 287 pp.

Schmucker, U. (1970). Anomalies of geomagnetic variations in the southwestern United States. Bull. Scripps Inst. Oceanog., **13**, Univ. Calif. Press.

Schmucker, U. (1971). Interpretation of induction anomalies above non-uniform surface layers. Geophysics, **36**, 156–165.

Siebert, M. (1962). Die Zerlegung eines zweidimensionalen Magnetfeldes in äusseren und inneren Anteil mit Hilfe der Cauchyschen Integralformel. Z. Geophys., **28**, 33–38.

Siebert, M. and Kertz, W. (1957). Zur Zerlegung eines lokalen erdmagnetischen Feldes in äusseren und inneren Anteil. Nachr. Akad. Wiss. Göttingen, Math.-Phys. Kl. Abt. IIa, 87–112.

Summers, D.M. and Weaver, J.T. (1973). Electromagnetic induction in a stratified conducting half space by an arbitrary periodic source. Can. J. Phys., **51**, 1064–1074.

Tikhonov, A.N. (1950). On the determination of electric characteristics of deep layers of the earth's crust. Dokl. Akad. Nauk. S.S.S.R. **73**, 295–297.

Uyeda, S. and Rikitake, T. (1970). Electrical conductivity anomaly and terristrial heat flow. J. Geomag. Geoelectr. **22**, 75–90.

Vasseur, G. and Weidelt, P. (1977). Bimodal electromagnetic induction in non-uniform thin sheets with an application to the Northern Pyrenian induction anomaly. Geophys. J. R. astr. Soc., **51**, 668–690.

Wait, J.R. (1953). Propagation of radio waves over a stratified ground. Geophysics, **18**, 416–422.

Wait, J.R. (1954). On the relation between telluric currents and the earth's magnetic field. Geophysics, **19**, 281–289.

Wait, J.R. (1962). Theory of magnetotelluric fields. J. Res. Natl. Bur. Std., D. **66**, 509–541.

Wait, J.R. (1982). *Geo-electromagnetism.* pp. 197–201. Academic Press, New York.

Wait, J.R. and Spies, K.P. (1974). Magneto-telluric fields for a segmented overburden. J. Geomag. Geoelec., **26**, 449–458.

Wannamaker, P.E., Hohmann, G.W. and SanFilipo, W.A. (1984) Electromagnetic modeling of three-dimensional bodies in layered earths using integral equation. Geophysics, **49** , 60–74.

Wannamaker, P.E. (1985). PW2D—finite element program for solution of magnetotelluric responses of two-dimensional earth resistivity structure. Program Documentation. University of Utah Research Institute Report ESL-158

Wannamaker, P.E., Stodt, J.A. and Rijo, L. (1987). A stable finite element solution for two-dimensional magnetotelluric modeling. Geophys. J. R. astr. Soc., **88**, 277–296.

Ward, S.H., Peeples, W.J. and Ryu, U. (1973). Analysis of geomagnetic data. Methods in computational physics, **13**, 163–238, ed. Bruce A. Bolt, Academic Press, New York.

Weaver, J.T. (1963). The electromagnetic field within a discontinuous conductor with reference to geomagnetic micropulsations near a coastline. Can. J. Phys., **41**, 484–495.

Weaver, J.T. (1964). On the separation of local geomagnetic fields into external and internal parts. Z. Geophys. **30**, 29–36.

Weaver, J.T. (1971). The general theory of electromagnetic induction in a conducting half-space. Geophys. J. R. astr. Soc., **22**, 83–100.

Weaver, J.T. (1973). Induction in a layered plane earth by uniform and non-uniform source fields. Phys. Earth Planet. Inter., **7**, 266–281.

Weaver, J.T. (1982). Regional induction in Scotland: an example of three-dimensional numerical modelling using the thin sheet approximation. Phys., Earth Planet. Inter., **28.**, 161–180.

Weaver, J.T. (1987). The Mathematical Solution of the Geomagnetic Coast Effect. Proceedings of the Conference on Applied Mathematics (in honour of Prof. A.A. Ashour), Cairo University (Egypt), Cairo, pp. 1-34.

Weaver, J.T. (1994). *Mathematical Methods for Geo-electromagnetic Induction*, Research Studies Press Ltd., Taunton, Somerset, England.

Weaver, J.T. and Agarwal, A.K. (1991). Is addition of induction vectors meaningful? Phys. Earth Planet. Inter., **65**, 267–275.

Weaver, J.T. and Agarwal, A.K. (1993). Automatic one-dimensional inversion of magnetotelluric data by the method of modelling. Geophys. J. Int., **112**, 115–123.

Weaver, J.T. and Brewitt-Taylor, C.R. (1978). Improved boundary conditions for the numerical solution of E-polarization problems in geomagnetic induction. Geophys. J. R. astr. Soc., **54**, 309–317.

Weaver, J.T. and Dawson, T.W. (1992). Adjustment distance in TM mode electromagnetic induction. Geophys. J. R. astr. Soc., **108**, 293–300.

Weaver, J.T., Le Quang, B.V. and Fischer, G. (1985). A comparison of analytical and numerical results for a two-dimensional control model in electromagnetic induction–I. B-polarization calculations. Geophys. J. R. astr. Soc., **82**, 263–278.

Weaver, J.T., Le Quang, B.V. and Fischer, G. (1986). A comparison of analytical and numerical results for a 2-D control model in electromagnetic induction–II. E-polarization calculations. Geophys. J. R. astr. Soc., **87**, 917–948.

Weidelt, P. (1971). The electromagnetic induction in two thin half-sheets. Z. Geophys., **37**, 649–665.

Weidelt, P. (1975). Electromagnetic induction in three-dimensional structures. J. Geophys., **41**, 85–109.

Wolf, D. (1982). Comment on "Geomagnetic depth sounding by induction arrow representation: a review" by G.P. Gregori and L.J. Lanzerotti. Rev. Geophys. Space Phys., **20**, 519–521.

Wolf, D. (1983). Inductive coupling between idealized conductors and its significance for the geomagnetic coast effect. J. Geophys., **52**, 22–23.

Zhdanov, M.S. (1982). Comparison of Modelling Methods in Electromagnetic Induction (COMMEMI Project). IZMIRAN, Troitsk, Moscow Region, USSR.

Zhdanov, M.S., Golubev, N.G., Spichak, V.V. and Varentsov, Iv.M. (1982). The Construction of Effective Methods for Electromagnetic Modeling. Geophys. J. R. astr. Soc., **68**, 589–607.

APPENDIX A

A.1 Comparison to an Analytic Solution

Because of the mathematical difficulties encountered, analytic solutions of two-dimensional conductivity models are only practical for problems of simple geometry. Yet, although analytic solutions are limited to a few simple models, they are extremely useful as accuracy checks on the various numerical techniques in use. Figure A.1 shows a control model for which there exists an analytic solution (Weaver et al., 1985,1986). The control model consists of a conducting plate in $0 < z < d$ divided into three regions $y < -a$, $|y| < a$ and $y > a$. These regions have conductivities of σ_1, σ_2 and $\sigma 3$ respectively. The entire plate is underlain by a perfect conductor.

Figures A.2 and A.3 compare this analytical solution with the numerical solution for this model obtained by the forward modelling program develloped in this thesis. The numerical solutions show excellent agreement with the analytic solutions for both the E-polarization and the B-polarization cases. This would seem to indicate that our forward modelling program is accurate, at least for this simple model.

Analytic Control Model

a=10 km
d=50 km
$\sigma_1 = 0.1$ S/m
$\sigma_2 = 1.0$ S/m
$\sigma_3 = 0.5$ S/m

T=394.784 (E-pol)
T=300.000 (B-pol)

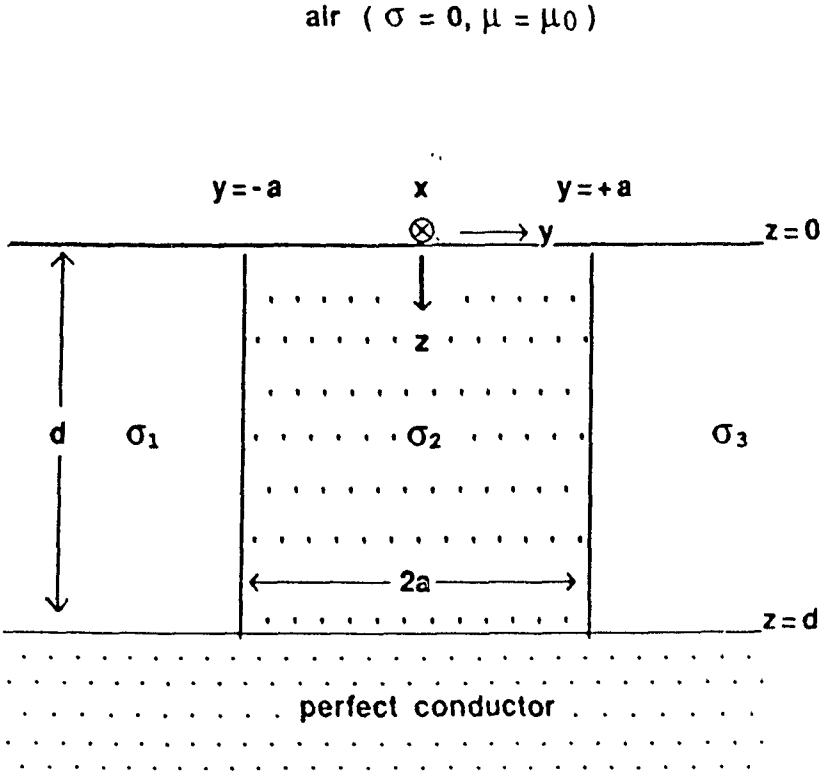

Figure A.1: The three segment analytic control model used in the check the accuracy of the forward modelling program.

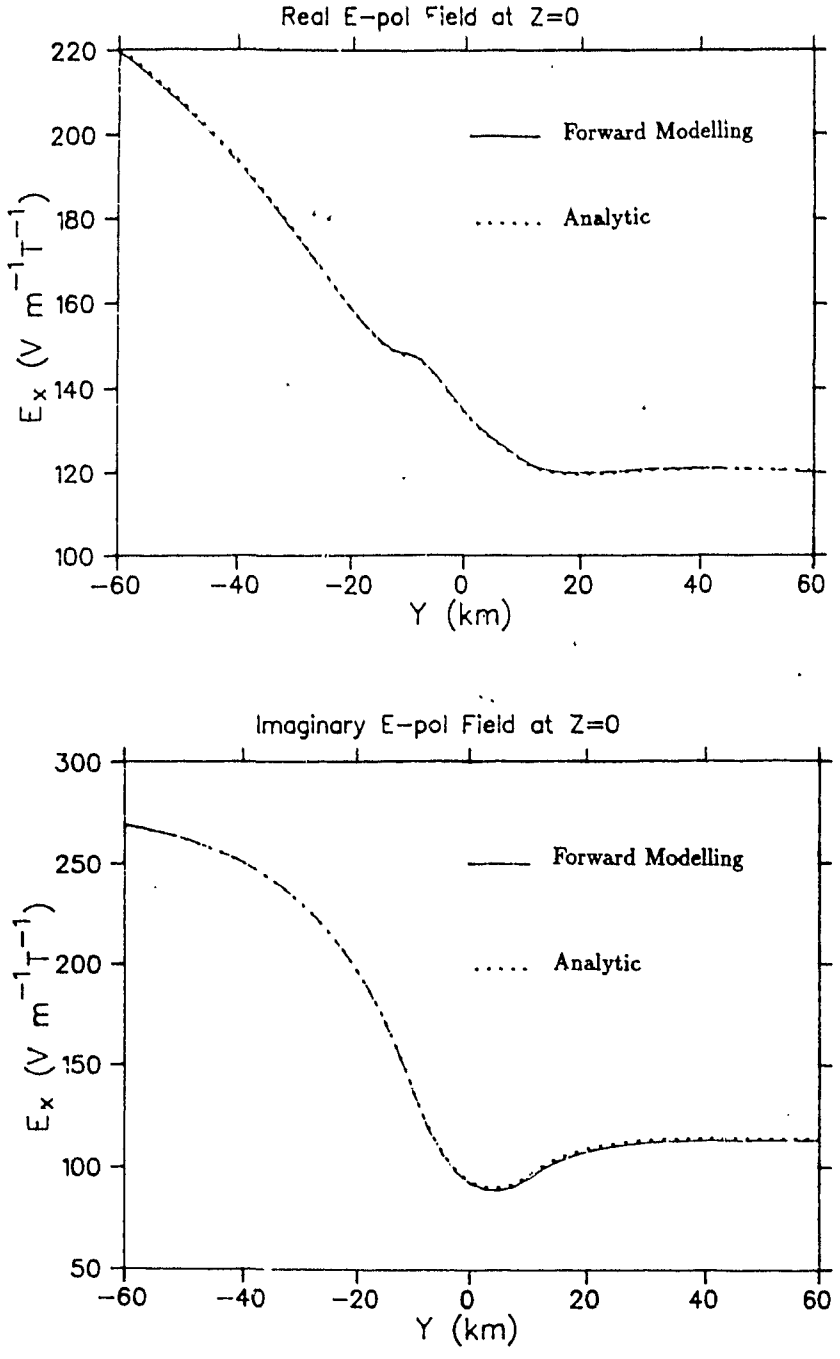

Figure A.2: The real and imaginary E-polarization horizontal electric field $E_x = U$ for the analytic control model and the forward modelling program.

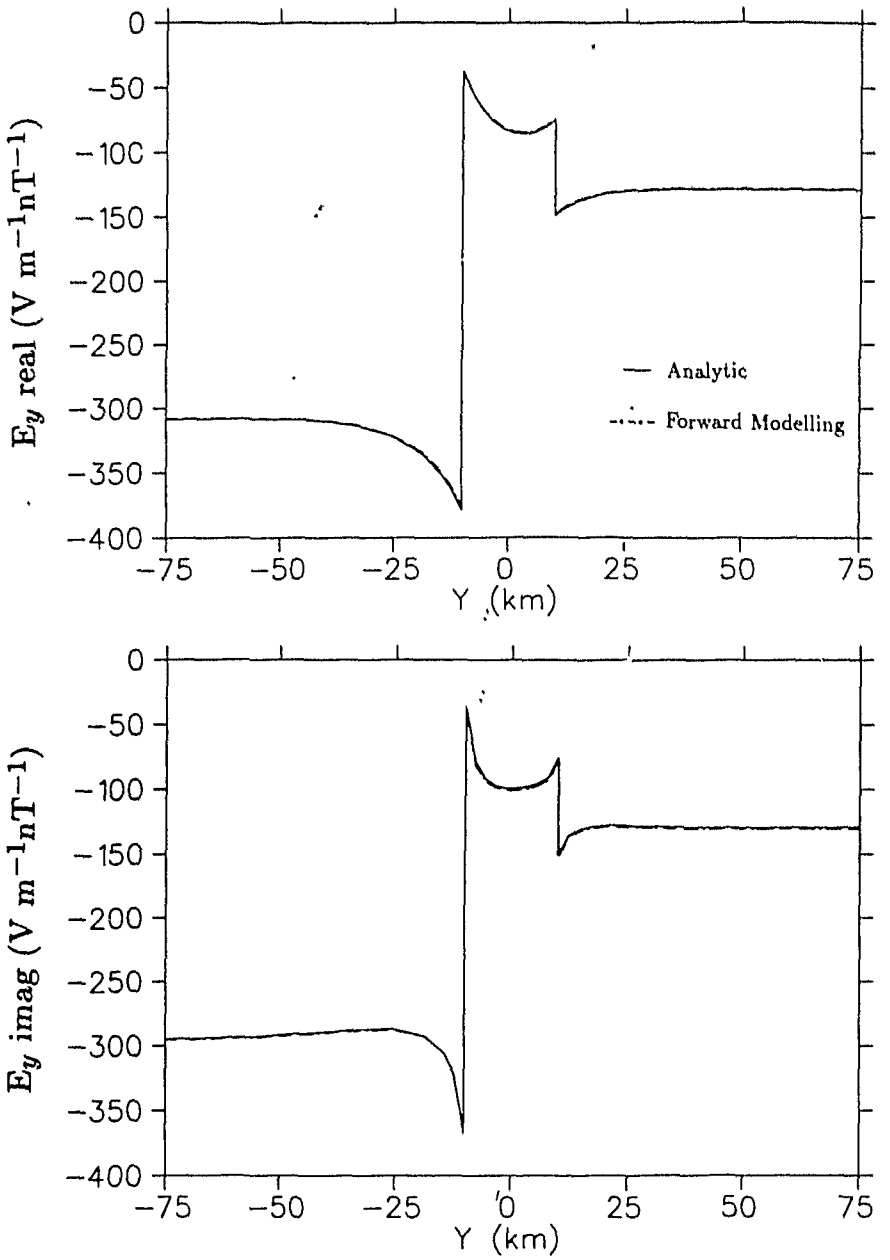

Figure A.3: The real and imaginary B-polarization horizontal electric field $E_y = V$ for the analytic control model and the forward modelling program.

APPENDIX B

The Program Listing

This appendix contains a sample input file (for the COMMEMI model discussed in Chapter 5) and the program listing for the forward modelling program. All the programs are written in FORTRAN and the main program is FR2D. The subroutines appear in the following order:

FR2D, GRIDYZ, RNDOFF, SITEMRG, ONED, MATRIX, CPNTA, SURF, COEFF2, MODBES, BESCOF, INTK0, GAUSSJF, GAUSSJB, BACKSUB, WRITE, BDERIV, EDERIV, APRES2.

```
2       !number of models
1       !number of periods
300     !period (in seconds)
BPOL    !polarization (note next line is for BPOL only)
0       !Ey field calculated on the left (0) or right (1) of the boundary
RES     !RESistivity or CONductivity
 -60    0  30  2    8      ! blocks: upper left hand corner (y,z)
 -60    2 110  5  300      ! y    z   dy   dz   resistivity
 -60    7 110 13 1000      ! all distances in km
 -60   20 360 40 1000
 -60   60 360 40  500
 -60  100 360 40  300
 -60  140 360 60  100
 -60  200 360 100  50
 -30    0  75  2    4
  45    0  10  2 1000
  50    2   5  3  100
  55    0  65  5  100
  50    5  70  5  300
  50   10  30 10    1
 120    0  20  3   20
 120    3  20  5   50
  80   10  40  4  100
  80   14  85  6 1000
 120    8  45  6  100
 140    0  15  8    4
 155    0  15  1    4
 155    1  35  3   50
 155    4  10  4  100
 165    4  90 16 1000
 170    0  20  1   20
 190    0  65  4   50
 255    0  45 20 1000
 5555   0   0  0    0 !indicates the end of the list of model blocks
SET                   !AUTOgrid endpoints or SET endpoints
 -1000 1000           !SET endpoints...ignored if AUTO
PRINT ABBREV          !PRINT command (FULL,ABBREV,SHORT,NONE)
NOGRAPH               !GRAPH or NOGRAPH options
NOINTERACT            !INTERACTion options..add points, restrict printing
2           !number of periods
20 300      !period (in seconds)
EPOL        !polarization
RES         !RESistivity or CONductivity
 -60    0  30  2    8      ! blocks: upper left hand corner (y,z)
 -60    2 110  5  300      ! y    z   dy   dz   resistivity
 -60    7 110 13 1000      ! all distances in km
 -60   20 360 40 1000
 -60   60 360 40  500
 -60  100 360 40  300
 -60  140 360 60  100
 -60  200 360 100  50
 -30    0  75  2    4
  45    0  10  2 1000
  50    2   5  3  100
  55    0  65  5  100
  50    5  70  5  300
  50   10  30 10    1
 120    0  20  3   20
 120    3  20  5   50
  80   10  40  4  100
  80   14  85  6 1000
 120    8  45  6  100
 140    0  15  8    4
 155    0  15  1    4
 155    1  35  3   50
 155    4  10  4  100
```

```
 165   4  90 16 1000
 170   0  20  1   20
 190   0  65  4   50
 255   0  45 20 1000
 5555  0   0  0    0 !indicates the end of the list of model blocks
SET                  !AUTOgrid endpoints or SET endpoints
 -1000 1000          !SET endpoints...ignored if AUTO
PRINT FULL           !PRINT command (FULL,ABBREV,SHORT,NONE)
NOGRAPH              !GRAPH or NOGRAPH options
NOINTERACT           !INTERACTion options..add points, restrict printing
```

```
C**** PROGRAM FR2D    --does automatic gridding for a 2-D        ****
C**** electromagnetic induction problem. Data is read in by      ****
C**** rectangles....(CY,CZ) is the coordinate of the top left    ****
C**** hand corner of the rectangle, DY and DZ are the Y and Z    ****
C**** dimensions of the rectangle and COND is the conductivity of****
C**** the block. The last data set should consist of 5555,0,0,0,0****
C**** to indicate the end of the data file                       ****
C
      PARAMETER (M1=100,MD=200,MDZ=200)
      REAL CY(M1),CZ(M1),DY(M1),DZ(M1)
     *,CY2(M1),CZ2(M1),YJUNC(M1),JUNC(M1),YPTS(MD),ZJUNC(M1)
     *,ZPTS(MD),TMOD(20),T,JUNK(M1),TSKD,SDBND,SDPT
      REAL*8 RES(M1),WRES(M1),SKIND(M1),SKTINY(M1),SMT(M1),
     *SMB(M1),SML(M1),SMR(M1),LGT(M1),LGB(M1),
     *RESGR(MD,MDZ),ZSKTINY(M1)
     *,SKINL,SKINR,SKINT,SKINB,YGRID(MD),ZGRID(MDZ),PRCOND,PRINSUL
     *,VYMIN,VYMAX,VZMAX,PI,EXST(30),STS(30),YHLF,YJ10,YJN0
      INTEGER NSTY(M1),NSTZ(M1),IOPS,YMAX,YMIN,ZMAX,NSTS,NSTMAX
     *,STNUM(30),MINCHG,MAXCHG
      CHARACTER*6 CONRES,EXTR,GRAP,INTER,PCOMD
      CHARACTER*10 MODNAM
      CHARACTER*4 CPOL,CMOD
      CHARACTER*1 SP,INCOM,PLOTCH(MD,MDZ),CHAR(20)
      COMPLEX*16 FIELD(MD,MDZ)
      COMMON /LIMITS/NY,NZ
      COMMON /PER/T
      COMMON /GROPT/NUN,YMIN,YMAX,ZMAX,GRAP
      COMMON /YJNUM/NJCY
      COMMON /INCREASED/SDBND,SDPT
      EQUIVALENCE (SML(1),SMT(1))
      EQUIVALENCE (SMR(1),SMB(1))
      EQUIVALENCE (YPTS(1),ZPTS(1))
      EQUIVALENCE (SKTINY(1),ZSKTINY(1))
      DATA NSTMAX,NPERMAX/30,20/
      DATA (CHAR(i),i=1,20)/'1','o','@','!','$','%','&','*'
     1,'^','<','>','?','-','a','b','c','d','e','f','g'/
      PI=3.14159265358979D0
      NPOL=0
      NUN=15
      PRCOND=1.1D-20
      PRINSUL=0.9D+20
C      READ(9,1010) SP
      READ(9,*) NMOD
      IF(NMOD.GT.5) THEN
        PRINT *,'NUMBER OF MODELS EXCEEDS 5...ONLY DOING 5'
        NMOD=5
      END IF
      CMOD='MOD1'
      DO 2222 JMOD=1,NMOD
      SP='Y'
      NPC=0
      READ(9,*) NPER
      NPERORG=NPER
      IF(NPER.GT.20) THEN
        PRINT *,'NUMBER OF PERIODS EXCEEDS 20...ONLY READING 20'
        NPER=20
      END IF
      READ(9,*) (TMOD(I),I=1,NPER)
      IF(NPERORG.GT.20) READ(9,*) (JUNK(I),I=NPER+1,NPERORG)
      READ(9,1010) CPOL
*** READING IN PERIOD AND E- OR B-POL OPTION *****
      IF(CPOL.GT.'CPOL') NPOL=1  !EPOL
      IF(CPOL.LT.'CPOL') NPOL=0  !BPOL
*** A '1' IS E-POL AND A '0' IS B-POL      *****
      IF(NPOL.EQ.0) READ(9,*) IOPS
      READ(9,1010) CONRES
```

```
      M1D=0

      DO 10 I=1,M1
         READ(9,*) CY(I),CZ(I),DY(I),DZ(I),RES(I)
C
C**** '5555' indicates end of data file      ****
C
         IF (CY(I).EQ.5555) GOTO 15
         IF(CONRES.LT.'QRES') THEN
           IF(RES(I).EQ.0.00) THEN
             RES(I)=1D+20
           ELSE
            IF(RES(I).EQ.1D+20) then
              RES(I)=0.00D0
            ELSE
              RES(I)=1/RES(I)
            END IF
           END IF
         END IF
c
c**** error check ****
c
         IF (DY(I).EQ.0.OR.DZ(I).EQ.0) WRITE(14,1001) I
         CY2(I)=CY(I)+DY(I)
         CZ2(I)=CZ(I)+DZ(I)

   10 CONTINUE
c
c**** JJJ=total number of blocks ****
c
   15 JJJ=I-1

C*** Looping for periods for same model ****

      DO 1111 NTT=1,NPER
      T=TMOD(NTT)


c
c**** calculating skind depths (SD's) ****
c
      DO 22,I=1,JJJ

c
c**** setting NPC (perfect conductor indicator) ****
c
      IF (RES(I).EQ.0.d0) then
       NPC=1
       SKIND(I)=5555.d0
       GOTO 22
      END IF

      SKIND(I)=DSQRT(DBLE(T)*10*RES(I))/(2*PI)
   22 CONTINUE

c
C**** specifying gridding out to right and left autogrid ****
c**** extremes or to set extremes from data file         ****
c
   23 IF(NTT.EQ.1) THEN
       READ(9,1010) EXTR
       YLEND=0
       YREND=0
       IF(EXTR.GT.'BAUTO') THEN
           READ(9,*) YLEND,YREND
       ELSE
```

```
            READ(9,*) YLEND,YREND
            YLEND=0
            YREND=0
          END IF
        END IF

C****    Reading print options                                          ****

C
      IF(NTT.EQ.1) READ(9,1020) PCOMD  !only read if 1st period for this model

C**** Site values for which the data is desired are read    ****
C**** from a file  'filename'.STS                           ****
C**** Reading in sites and checking if any are very close   ****
C**** to a junction.                                        ****
C
      IF(NTT.EQ.1) READ(9,1010) GRAP
      IF(GRAP.LT.'NOGRAP') THEN
        IF(NTT.EQ.1) THEN
          READ(10,*) NSTS
          IF(NSTS.GT.30) PRINT *,'Number of sites must not
     * exceed 30...only reading 30'
          NSTS=MIN(NSTS,NSTMAX)
          DO 130 I=1,NSTS
  130     READ(10,*) STS(I)
        end if
        do i=1,nsts
          do j=2,jjj
            if(abs(cy(j)-sts(i)).lt.skind(i)/10.and.
     1        cy(j)-sts(i).gt.0.d0) skind(i)=4*abs(cy(j)-sts(i))
          end do
        end do
      end if
C
C****    Sorting corner designators in order of increasing Y     ****
C
      CALL SORT(CY,SKIND,CZ,DY,DZ,CY2,CZ2,RES,JJJ,M1)
C
C**** Find largest skin depth's on edges so that grid will be    ****
C**** extended out far enough on both sides. Also...eliminate    ****
C**** all complete horizontal layers from junction calculations  ****
C**** because, even with small skin depths, since they don't     ****
C**** have vertical conductivity boundaries they do not need to  ****
C**** be considered.                                             ****
C
      ICHKL=0
      ICHKR=0
C**** dtot=y length of model from start of first to end ****
c**** of last block                                    ****
c
      DTOT=CY2(JJJ)-CY(1)
c**** inititalize largest left-hand SD ****
      SKINL=SKIND(1)
      ICHKL=1
   39 continue

      DO 30 NL=1,JJJ
C**** assigning largest left-hand SD  ****
C
        IF(SKIND(NL).NE.5555D0.AND.SKIND(NL).GT.SKINL) THEN
        DIFF=CY2(NL)-10*SKIND(NL)
        if(cy2(nl).eq.cy2(jjj)) diff=cy2(ichkl)-10*skind(nl)
        DIFF2=CY2(ICHKL)-10*SKINL
          IF(DIFF-DIFF2.le.0.0001) THEN
            SKINL=SKIND(NL)
            ICHKL=NL
```

```
            END IF
          END IF
   30 CONTINUE
C**** initialize largest right-hand SD ****
      SKINR=SKIND(JJJ)
      ICHKR=JJJ

      DO 50 NR=JJJ,1,-1
C**** assigning largest right-hand SD ****
C
            IF(SKIND(NR).NE.5555.D0.AND.SKIND(NR).GT.SKINR) THEN
            DIFF=CY(NR)+10*SKIND(NR)
            if(cy(nr).eq.cy(1)) diff=cy(ichkr)+10*skind(nr)
            DIFF2=CY(ICHKR)+10*SKINR
              IF(DIFF-DIFF2.GE.-0.0001) THEN
                SKINR=SKIND(NR)
                ICHKR=NR
              END IF
            END IF
          END IF
   50 CONTINUE
C
C**** Compress model to single layer of smallest skin depths.     ****
C**** IE: find all junctions and smallest skin depths to the      ****
C**** right and left of them.                                     ****
C
      SML(1)=SKINL
      N=1
      YJUNC(1)=CY(N)
   60 IF(ABS(DY(N)-DTOT).GT.0.0001) THEN
         SMR(1)=SKIND(N)
      ELSE
         N=N+1
         IF(ABS(CY(N)-CY(N-1)).GT.0.0001) THEN
            IF(CY(N).NE.5555) GOTO 1002
            M1D=1  !One dimensional model
            NNNY=2
            NJCY=2
            YGRID(1)=CY(1)*1000
            YJUNC(1)=CY(1)
            JUNC(1)=YGRID(1)
            YGRID(2)=(CY(1)+DY(1))*1000
            YJUNC(2)=CY(1)+DY(1)
            JUNC(2)=YGRID(2)
            WRITE(14,61)
   61       FORMAT ('THIS IS A ONE-DIMENSIONAL MODEL!')
            GOTO 8888
         END IF
         GOTO 60
      END IF
      SKTINY(1)=DMIN1(SML(1),SMR(1))
      IB=1
      DO 70 IC=1,JJJ
         IF(abs(YJUNC(IB)-CY(JJJ)).le.0.0001) GOTO 80
         IF(CY(IC).GT.YJUNC(IB)) THEN
            IB=IB+1
            YJUNC(IB)=CY(IC)
            SMR(IB)=SKIND(IC)
            SML(IB)=2000.D0
            DO 71 ID=1,JJJ
               IF(abs(DY(IC)-DTOT).le.0.0001) GOTO 72
               IF(CY(IC).EQ.0.D0) THEN
                IF(CY2(ID).EQ.0.D0) THEN
                  CTES=1.00
                ELSE
                  CTES=0.00
```

```
                END IF
               ELSE
                CTES=CY2(ID)/CY(IC)
               END IF
               IF(CTES.LT.1.0001.AND.CTES.GT.0.9999)
     1                          SML(IB)=DMIN1(SKIND(ID),SML(IB))
    71       CONTINUE
    72     CONTINUE
           END IF
        SKTINY(IB)=DMIN1(SML(IB),SMR(IB))
    70 CONTINUE
    80 NJCY=IB+1
       YJUNC(NJCY)=CY2(JJJ)
       SML(NJCY)=SMR(IB)
       SMR(NJCY)=SKINR
       SKTINY(NJCY)=DMIN1(SML(NJCY),SMR(NJCY))
       NNNY=0
       CALL GRIDYZ(YJUNC,SML,SMR,NJCY,YPTS,SKTINY,NNNY,SKINL,SKINR,
      1YLEND,YREND,NSTY,SP,M1,MD)

C**** rounding off y grid points to 2 or 3 significant figures ***
       CALL RNDOFF(YPTS,YJUNC,NNNY,NJCY,MD,M1)
       YJ10=YJUNC(1)
       YJN0=YJUNC(NJCY)
       YJUNC(1)=YPTS(1)/1000.0
       YJUNC(NJCY)=YPTS(NNNY)/1000.0
       DO 90 N=1,NJCY
    90 JUNC(N)=YJUNC(N)*1000.0
       DO 95 N=1,NNNY
    95 YGRID(N)=DBLE(YPTS(N))

C
C****    Sorting corner designators in order of increasing Z      ****
C
8888   CALL SORT(CZ,SKIND,CY,DZ,DY,CZ2,CY2,RES,JJJ,M1)
C
C
       ICHKB=0
       ZTOT=CZ2(JJJ)
       SKINT=SKIND(1)
       SKINB=SKIND(JJJ)
       DO 100 N1=JJJ-1,1,-1
          IF(abs(CZ2(JJJ)-CZ2(N1)).le.0.0001) THEN
             IF(SKIND(N1).GT.SKINB.AND.DZ(N1).NE.ZTOT) THEN
                SKINB=SKIND(N1)
                ICHKB=N1
             END IF
          END IF
   100 CONTINUE
C
C**** Compress model to single layer of smallest skin depths.      ****
C**** IE: find all junctions and smallest skin depths to the       ****
C**** top and bottom of them.                                      ****
C
       SMT(1)=SKINT
       N=1
       ZJUNC(1)=CZ(N)
   110 IF(DZ(N).NE.ZTOT) THEN
          SMB(1)=SKIND(N)
       ELSE
          N=N+1
          IF(ABS(CZ(N)-CZ(N-1)).GT.0.0001) GOTO 1006
          GOTO 110
       END IF
       IB=1
       DO 111 IC=1,JJJ
```

```
            IF(abs(ZJUNC(IB)-CZ(JJJ)).le.0.0001) GOTO 113
            IF(CZ(IC).GT.ZJUNC(IB)) THEN
               IB=IB+1
               ZJUNC(IB)=CZ(IC)
               SMB(IB)=SKIND(IC)
               SMT(IB)=2000
               DO 114 ID=1,JJJ
                  IF(abs(DZ(IC)-ZTOT).le.0.0001) GOTO 112
                  IF(CZ(IC).EQ.0.D0) THEN
                   IF(CZ2(ID).EQ.0.D0) THEN
                     CTES=1.00
                   ELSE
                     CTES=0.00
                   END IF
                  ELSE
                   CTES=CZ2(ID)/CZ(IC)
                  END IF
                  IF(CTES.LT.1.0001.AND.CTES.GT.0.9999)
     1                              SMT(IB)=DMIN1(SKIND(ID),SMT(IB))
  114          CONTINUE
  112       CONTINUE
            END IF
         ZSKTINY(IB)=DMIN1(SMT(IB),SMB(IB))
  111    CONTINUE
  113    NJCZ=IB+1
         ZJUNC(NJCZ)=CZ2(JJJ)
         SMT(NJCZ)=SMB(IB)
         SMB(NJCZ)=SKINB
         zSKTINY(NJCZ)=DMIN1(SMT(NJCZ),SMB(NJCZ))
         IF(NPC.EQ.1) ZSKTINY(NJCZ-1)=SMT(NJCZ-1)
         IF(ICHKB.NE.0.AND.NPC.NE.1) THEN
            DIFF=ZJUNC(ICHKB)+10*SKIND(ICHKB)
            DIFF2=ZJUNC(NJCZ-1)+10*SMB(NJCZ-1)
            IF(DIFF2-DIFF.GE.-0.0001) SKINB=SMB(NJCZ-1)
         END IF

C**** Compressing the model to a single layer of largest skin
c**** depths to check extent of model and see grid size can be
c**** reduced at depth (ie greater than 6 skin depths)

         N=1
         LGT(1)=SKIND(N)
         ZJUNC(1)=CZ(N)
         IF(ABS(DZ(N)-ZTOT).GT.0.0001) THEN
            LGB(1)=SKIND(N)
            DO 120 IE=1,JJJ
              IF(abs(CZ(IE)-ZJUNC(1)).le.0.0001)
     1           LGB(1)=DMAX1(SKIND(IE),LGB(1))
  120       CONTINUE
         ELSE
            N=N+1
            IF(ABS(CZ(N)-CZ(N-1)).GT.0.0001) GOTO 1006
            GOTO 110
         END IF
         IB=1
         DO 121 IC=1,JJJ
            IF(abs(ZJUNC(IB)-CZ(JJJ)).le.0.0001) GOTO 123
            IF(CZ(IC).GT.ZJUNC(IB)) THEN
               IB=IB+1
               ZJUNC(IB)=CZ(IC)
               LGB(IB)=SKIND(IC)
               LGT(IB)=0.0D0
               DO 124 ID=1,JJJ
                 IF(abs(DZ(IC)-ZTOT).le.0.0001) GOTO 121
                 IF(CZ(ID).LT.CZ(IC).AND.CZ2(ID)-CZ(IC).ge.-0.0001)
     1                              LGT(IB)=DMAX1(SKIND(ID),LGT(IB))
```

```
  124       CONTINUE
            DO 122 IE=1,JJJ
              IF(abs(DZ(IC)-ZTOT).le.0.0001) GOTO 121
              IF(CZ(IE)-ZJUNC(IB).le.0.0001.AND.CZ2(IE).GT.ZJUNC(IB))
     1                          LGB(IB)=DMAX1(SKIND(IE),LGB(IB))
  122       CONTINUE
          END IF
  121 CONTINUE
  123 NJCZ=IB+1
      ZJUNC (NJCZ)=CZ2(JJJ)
      LGT(NJCZ)=LGB(IB)

c**** checking to see if model extends deep enough to warrent large
C     increases in grid size at depth

      TSKD=0.0
      DO 125 I=2,NJCZ
      TSKD=TSKD+(ZJUNC(I)-ZJUNC(I-1))/MIN(LGB(I-1),LGT(I))
      IF(TSKD-6.0.GE.-0.0001) GOTO 126
  125 CONTINUE
      I=NJCZ
  126 SDBND=ZJUNC(I)
      SDPT=SDBND-(TSKD-6)*MIN(LGB(I-1),LGT(I))
      NNNZ=12
      CALL GRIDYZ(ZJUNC,SMT,SMB,NJCZ,ZPTS,ZSKTINY,NNNZ,SKINT,SKINB,
     1YLEND,YREND,NSTZ,SP,M1,MD)
      IF(NPC.EQ.1) SMB(NJCZ-1)=0
C**** rounding off z grid points to 2 or 3 significant figures ***
      CALL RNDOFF(ZPTS,ZJUNC,NNNZ,NJCZ,MD,M1)
      DO 129 N=1,NNNZ
  129 ZGRID(N)=DBLE(ZPTS(N))

C**** assigning print options for LIS file. All values of Y will ****
c**** be printed and all (FULL), 5 (ABBREV) or 1 (SHORT) values  ****
C**** of Z. If only graphics are desired and no field values or  ****
c**** ap.res. and phase values are needed in the LIS file use    ****
c**** the NONE option. (used only in conjunction with GRAPH)     ****

      IF(PCOMD.LT.'NONE') THEN
         IF(PCOMD.LT.'FULL') THEN
            ZMAX=MIN(NNNZ-1,5)
         ELSE
            ZMAX=NNNZ-1
         END IF
      ELSE
         IF(PCOMD.LT.'SHORT') THEN
            ZMAX=0
         ELSE
            ZMAX=1
         END IF
      END IF
      IF(ZMAX.NE.0) THEN
        IF(NPOL.EQ.0) WRITE(14,20) CPOL,IOPS,T   !Bpol
        IF(NPOL.EQ.1) WRITE(14,21) CPOL,T        !Epol
   20   FORMAT('1'///,2X,A4,' solution (flag=',I1,')...T=',G13.5,'s'//)
   21   FORMAT('1'///,2X,A4,' solution...T=',G13.5,'s'//)
      END IF
C
C**** Graph output option. If GRAPH then app.res. and phase ****
C**** values for each specified period and polarization are ****
C**** printed out in files for later concantation and       ****
C**** graphing. Site values are inserted into text         ****
C
      IF(GRAP.LT.'NOGRAP') THEN
        IF(NTT.EQ.1) THEN
          IF(CPOL.LT.'EPOL') THEN
```

```
              IF(IOPS.EQ.0) THEN
                MODNAM = CMOD//'B0.RES'
              ELSE
                MODNAM=CMOD//'B1.RES'
              END IF
            ELSE
              MODNAM=CMOD//'E.RES'
            END IF
            OPEN(UNIT=NUN,FILE=MODNAM,ACCESS='SEQUENTIAL',STATUS='NEW')
          END IF
          NJ=NJCY
C**** checking for symmetry ****
          NSYM=0
          NORG=NNNY
          NHLF=NINT(NNNY/2.0)
          DO 134 IY=1,NHLF
          IF(ABS(ABS(YGRID(IY))-YGRID(NNNY-IY+1)).GT.0.00001) THEN
             NSYM=0
             GOTO 135
          ELSE
             NSYM=1
          END IF
 134      CONTINUE
 135      NSYMST=0
          DO 137 I=1,NINT(NSTS/2.0)
            IF(ABS(ABS(STS(I))-STS(NSTS-I+1)).GT.0.00001) THEN
               NSYMST=0
               GOTO 138
            ELSE
               NSYMST=1
            END IF
 137      CONTINUE
 138      NSTS1=NSTS
          YHLF=YGRID(1)+(YGRID(NNNY)-YGRID(1))/2
          IF(NSYMST.EQ.1.AND.NSYM.EQ.1) NSTS1=NINT(NSTS/2.0)
          DO 133 I=1,NSTS1
          EXST(1)=STS(I)*1000
          CALL SITEMRG(YGRID,NNNY,EXST,1,NSTY,STNUM,JUNC,NJ,M1,MD)
          IF (I.EQ.1) NSTNUM=STNUM(I)
          STNUM(I)=STNUM(1)
          STNUM(1)=NSTNUM
          JUNC(NJCY+I)=STS(I)*1000
 133      NJ=NJCY+I

          IF(NSYMST.EQ.1.AND.NSYM.EQ.1) THEN
            DO 136 IY=1,NNNY
              IF(YGRID(IY).GT.YHLF) GOTO 141
 136        CONTINUE
 141        NHALF=IY-1
            IF(INT(NSTS/2.).NE.NINT(NSTS/2.0)) NTOT=2*NHALF-1
            IF(INT(NSTS/2.).EQ.NINT(NSTS/2.0)) NTOT=2*NHALF
            DO 139 IY=1,NHALF
              YGRID(NTOT-IY+1)=-YGRID(IY)
 139        CONTINUE
            DO 140 IY=1,NINT(NJCY/2.0)
              NNEW=NTOT-NSTY(IY)+1
              NSTY(NJCY-IY+1)=NNEW
              YJUNC(NJCY-IY+1)=YGRID(NNEW)/1000
 140        CONTINUE
            DO 167 I=1,NSTS1
              STNUM(NSTS-I+1)=NTOT-STNUM(I)+1
 167        CONTINUE
            NNNY=NTOT
          END IF
        END IF
```

```
C
C**** Doing INTERACTION option...adding points interactively****
C**** or changing the print options                            ****
C
      YMIN=1
      YMAX=NNNY
      IF(NTT.EQ.1) READ(9,1010) INTER !read option only once for each model
      IF(INTER.LT.'NOINTE') THEN
        NEXST=0
  142   PRINT *,'Points in Y in metres'
        DO 143 I=1,NNNY
  143   PRINT *,YGRID(I)
        PRINT *,'Do you wish to add a point? ([Y]es,[N]o,[S]ee again)'
        READ(6,1010) INCOM
        IF(INCOM.EQ.'Y'.OR.INCOM.EQ.'y') THEN
          PRINT *,'Input Y value in metres'
          READ(6,*) EXST(1)
          NJ=NJ+NEXST
          NCHECK=NNNY
          CALL SITEMRG(YGRID,NNNY,EXST,1,NSTY,STNUM,JUNC,NJ,M1,MD)
          NSTCHECK=STNUM(1)
          STNUM(1)=NSTNUM
          IF(NCHECK.NE.NNNY) THEN
            NDIF=NNNY-NCHECK
            DO 166 J=1,NSTS
  166       IF(STNUM(J).GE.NSTCHECK) STNUM(J)=STNUM(J)+NDIF
          END IF
          NEXST=NEXST+1
          JUNC(NJ+NEXST)=EXST(1)
          GOTO 142
        END IF
        IF(INCOM.EQ.'S'.OR.INCOM.EQ.'s') GOTO 142
        PRINT *,'Do you wish to restrict Y output? (Y,N)'
        READ(6,1010) INCOM
        IF(INCOM.EQ.'Y'.OR.INCOM.EQ.'y') THEN
  145     PRINT *,'Input YMIN and YMAX ...these must be existing Y
     * values in metres.'
          MINCHG=0
          MAXCHG=0
          READ(6,*) VYMIN,VYMAX
          DO 144 I=1,NNNY
            IF(ABS(YGRID(I)-VYMIN).LT.0.000001) THEN
             YMIN=I
             MINCHG=1
            END IF
            IF(ABS(YGRID(I)-VYMAX).LT.0.000001) THEN
             YMAX=I
             MAXCHG=1
            END IF
  144     CONTINUE
          IF(MINCHG.EQ.0.OR.MAXCHG.EQ.0) THEN
            PRINT *,'Your YMIN or YMAX is not a site value.'
            PRINT *,'Points in Y in metres.'
            DO 146 I=1,NNNY
  146       PRINT *,YGRID(I)
            GOTO 145
          END IF
        END IF

        PRINT *,'Do you wish to restrict Z output? (Y,N)'
        READ(6,1010) INCOM
        IF(INCOM.EQ.'Y'.OR.INCOM.EQ.'y') THEN
          ZMAX=0
  147     PRINT *,'Points in Z in metres.'
          DO 148 I=1,NNNZ-1
  148     PRINT *,ZGRID(I)
```

```
            PRINT *,'Input ZMAX ...this must be an existing Z
          * value in metres.'
            MAXCHG=0
            READ(6,*) VZMAX
            DO 149 I=1,NNNZ-1
              IF(ABS(ZGRID(I)-VZMAX).LT.0.000001) then
               ZMAX=I
               MAXCHG=1
              ENDIF
  149       CONTINUE
            IF(MAXCHG.EQ.0) THEN
              PRINT *,'Your ZMAX is not a site value.'
              GOTO 147
            END IF
          END IF
        END IF
C**** oned merging -- assigning res values to grid cells *****
        YJUNC(1)=YJ10
        YJUNC(NJCY)=YJN0
        DO 150 K=1,JJJ
        IF(M1D.NE.1) THEN
           DO 152 K2=1,NJCY
              IF(CY(K).EQ.0.00) THEN
                IF(ABS(YJUNC(K2)-CY(K)).LT.0.0001) THEN
                  YTES1=1.000
                ELSE
                  YTES1=0.000
                END IF
              ELSE
                YTES1=YJUNC(K2)/CY(K)
              END IF
              IF(CY2(K).EQ.0.00) THEN
                IF(ABS(YJUNC(K2)-CY2(K)).LT.0.0001) THEN
                  YTES2=1.000
                ELSE
                  YTES2=0.000
                END IF
              ELSE
                YTES2=YJUNC(K2)/CY2(K)
              END IF
              IF(YTES1.LT.1.0001.AND.YTES1.GT.0.9999) MI=NSTY(K2)
              IF(YTES2.LT.1.0001.AND.YTES2.GT.0.9999) MF=NSTY(K2)
  152      CONTINUE
        ELSE
           MI=1
           MF=2
        END IF
           DO 153 K3=1,NJCZ
              IF(CZ(K).EQ.0.00) THEN
                IF(ABS(ZJUNC(K3)-CZ(K)).LT.0.0001) THEN
                  ZTES1=1.000
                ELSE
                  ZTES1=0.000
                END IF
              ELSE
                ZTES1=ZJUNC(K3)/CZ(K)
              END IF
              IF(CZ2(K).EQ.0.00) THEN
                IF(ABS(ZJUNC(K3)-CZ2(K)).LT.0.0001) THEN
                  ZTES2=1.000
                ELSE
                  ZTES2=0.000
                END IF
              ELSE
                ZTES2=ZJUNC(K3)/CZ2(K)
              END IF
```

```
            IF(ZTES1.LT.1.0001.AND.ZTES1.GT.0.9999) NI=NSTZ(K3)
            IF(ZTES2.LT.1.0001.AND.ZTES2.GT.0.9999) NF=NSTZ(K3)
  153     CONTINUE
          DO 154 K4=MI,MF-1
            DO 155 K5=NI,NF-1
              RESGR(K4,K5)=RES(K)
  155       CONTINUE
  154     CONTINUE
  150 CONTINUE

C**** PRINT OUT FOR LINE PLOTTER *****

      LCNT=1
      NZ=NNNZ-1
      NY=NNNY-1

      IF(ZMAX.NE.0) THEN
c**** eliminating redundent resistivities ***
      DO 161 L=1,JJJ
        DO 162 LL=1,L
          IF(L.NE.LL.AND.RES(L).EQ.RES(LL)) GOTO 161
          IF(L.EQ.LL) THEN
            WRES(LCNT)=RES(L)
            LCNT=LCNT+1
          END IF
  162   CONTINUE
  161 CONTINUE
c*** sorting resistivities from small to large for legend ***
      DO 163 I=1,LCNT-2
        J=LCNT-1-I
        MARK=0
        DO 164 K=1,J
          KP1=K+1
          IF(WRES(K).LE.WRES(KP1)) GOTO 164
          B=WRES(KP1)
          WRES(KP1)=WRES(K)
          WRES(K)=B
          MARK=1
  164   CONTINUE
        IF(MARK.EQ.0) GOTO 170
  163 CONTINUE
C
c*** printing plot legend *****
c
  170 WRITE(14,172)
  172 FORMAT(/2X,'SYMBOL        RES          COND     SKIN DEPTH'/)

      DO 173 I=1,LCNT-1
        WSKIN=SQRT(T*10*WRES(I))/(2*PI)
        IF(WRES(I).EQ.0.0) THEN
         WCON=1.0E+20
         WRITE(14,175) CHAR(I),WRES(I),WCON,WSKIN
        ELSE
         WCON=1/WRES(I)
         WRITE(14,174) CHAR(I),WRES(I),WCON,WSKIN
        END IF
  174   FORMAT(4X,A1,5X,3G12.5)
  175   FORMAT(4X,A1,5X,G12.5,G12.5,g12.5)
  173 CONTINUE
C
c**** assigning symbols and printing plot ****
c
      DO 180 L1=1,NZ
        DO 181 L2=1,NY
          PLOTCH(L2,L1)=' '
          DO 182 LQ=1,LCNT-1
```

```
                IF(RESGR(L2,L1).EQ.WRES(LQ)) PLOTCH(L2,L1)=CHAR(LQ)
  182       CONTINUE
  181     CONTINUE
  180   CONTINUE

        NYF=NY
        IF(NY.GT.130) NYF=130
        WRITE(14,185) (PLOTCH(N,1),N=1,NYF)
  185   FORMAT (/2X,130A1)
        DO 190 L1=2,NZ
           WRITE(14,191) (PLOTCH(N,L1),N=1,NYF)
  191      FORMAT (2X,130A1)
  190   CONTINUE
        IF(NY.GT.130) THEN
           DO 192 L1=1,NZ
              WRITE(14,193) (PLOTCH(N,L1),N=131,NY)
  193         FORMAT (/,2X,130A1)
  192      CONTINUE
        END IF
        END IF
c
c**** calling one-dimensional solution****
c

        NY=NNNY
        PRINT *,'PERIOD = ',T,' s'
        PRINT *,'NY,NZ',NY,NZ
        DO 200 I=1,NZ
  200   RESGR (NY,I)=RESGR(NY-1,I)
        IQ=9999
        DO 201 I=1,NY
        WRITE(14,*) SNGL(YGRID(I)/1000)
  201   CONTINUE
        WRITE(14,*) IQ
        DO 202 J=1,NZ
        WRITE(14,*) SNGL(ZGRID(J)/1000)
  202   CONTINUE
        WRITE(14,*) IQ

        CALL ONED(ZGRID,RESGR,T,FIELD,NPOL,MD,MDZ,M1D)
        IF(M1D.EQ.1)THEN
           GOTO 1111
        END IF
c
c**** calling field solution ****
c
        CALL MATRIX(YGRID,ZGRID,RESGR,FIELD,NPOL,MD,MDZ)
C
C**** calling derivative field solution ****
c
        IF(NPOL.EQ.1) THEN
           CALL EDERIV(FIELD,YGRID,ZGRID,RESGR,T,STNUM,NSTS,STS,MD,MDZ)
        ELSE
           CALL BDERIV(FIELD,YGRID,ZGRID,RESGR,T,STNUM,NSTS,STS,MD,MDZ
       1,IOPS)
        END IF
C
C**** DATA files for graphing program        ***
C**** (app.res., phase and deriv) are        ***
c**** written out in the E/Bderiv subroutine ***
C
 1111 CONTINUE
        NUN=NUN+1
        IF(JMOD.EQ.1) CMOD='MOD2'
        IF(JMOD.EQ.2) CMOD='MOD3'
        IF(JMOD.EQ.3) CMOD='MOD4'
```

```
      IF(JMOD.EQ.4) CMOD='MOD5'
 2222 CONTINUE
      STOP

 1001 FORMAT (5X,'*** warning *** rectangle ',I3,' has zero length
     1 or width')
 1002 WRITE(14,1003) N
 1003 FORMAT (5X,'***.ERROR *** CHECK STARTING CORNERS OF ALL LEFT-MOST
     1RECTANGLES ARE THE SAME IN Y...',I4)
 1004 FORMAT (2X,I4,' JUNCTIONS IN Y DIRECTION   period=',F10.4,/,3X,
     *' yjunc(n)    sml(n)   sml(n)/4   smr(n)   smr(n)/4'/)
 1005 FORMAT (2X,5(F10.4))
 1006 WRITE(14,1007) N
 1007 FORMAT (5X,'*** ERROR *** CHECK STARTING CORNERS OF ALL TOP-MOST
     1RECTANGLES ARE THE SAME IN Z...',I4)
 1008 FORMAT (2X,I4,' JUNCTIONS IN Z DIRECTION'/,2X,'   zjunc(n)
     *   smt(n)   smt(n)/4   smb(n)   smb(n)/4'/)
 1009 FORMAT (2X,5(F10.4))
 1010 FORMAT (A)
 1020 FORMAT (6X,A)
      END
C-----------------------------------------------------------------------
C
      SUBROUTINE SORT(A,B,C,D,E,F,G,H,JJJ,M1)
C
C****                    SORTING SUBROUTINE                          ****
C**** SORT is called from FR2D.    The sort used is a "tree          ****
C**** sort"  or  "monkey  puzzle  sort".  See  for  example          ****
C**** "Fortran Techniques" by A.Colin Day. UVIC call number          ****
C**** QA76.73 F25D39 (double precision)                              ****
C
      PARAMETER (M2=100)
      INTEGER ILB(M2),IRB(M2)
      REAL A(M1),C(M1),D(M1),E(M1),F(M1),G(M1)
     1,TEMP1(M2),TEMP2(M2),TEMP3(M2),TEMP4(M2),TEMP5(M2)
     2,TEMP6(M2),TEMP7(M2),TEMP8(M2)
      REAL*8 B(M1),H(M1)
C
C**** Assigning left, right and back pointers to all "A's"  ****
C
      ILB(1)=0
      IRB(1)=0
      DO 100 I=2,JJJ
      ILB(I)=0
      IRB(I)=0
    1 J=1
    2 IF(A(I).GT.A(J)) GOTO 5
      IF(A(I).EQ.A(J).AND.B(I).GT.B(J)) GOTO 5
    3 IF(ILB(J).EQ.0) GOTO 4
      J=ILB(J)
      GOTO 2
    4 IRB(I)=-J
      ILB(J)=I
      GOTO 100
    5 IF(IRB(J).LE.0) GOTO 6
      J=IRB(J)
      GOTO 2
    6 IRB(I)=IRB(J)
      IRB(J)=I
  100 CONTINUE
C
C****  Extracting sorted array by following pointers      ****
C
      K=1
    7 J=1
      GOTO 8
```

```
110 J=ILB(J)
  8 IF(ILB(J).GT.0) GOTO 110
  9 TEMP1(K)=A(J)
    TEMP2(K)=B(J)
    TEMP3(K)=C(J)
    TEMP4(K)=D(J)
    TEMP5(K)=E(J)
    TEMP6(K)=F(J)
    TEMP7(K)=G(J)
    TEMP8(K)=H(J)
    K=K+1
 10 IF(IRB(J)) 12,200,120
120 J=IRB(J)
    GOTO 8
 12 J=-IRB(J)
    GOTO 9
200 CONTINUE
    DO 300 K=1,JJJ
       A(K)=TEMP1(K)
       B(K)=TEMP2(K)
       C(K)=TEMP3(K)
       D(K)=TEMP4(K)
       E(K)=TEMP5(K)
       F(K)=TEMP6(K)
       G(K)=TEMP7(K)
       H(K)=TEMP8(K)
300 CONTINUE
    RETURN
    END
```

```
      SUBROUTINE GRIDYZ(JUNC,SML,SMR,NJC,YPTS,SKTINY,NNN,SKINL,
     1SKINR,YLEND,YREND,NST,SP,M1,MD)

C **** This subroutine automatically creates a grid based on  ****
C **** block sizes, conductivities, density requirements and  ****
C **** symmetry considerations in both the Y and Z directions.****
C **** Called by FR2D.. (double precision)                    ****

      PARAMETER (NM=200)
      CHARACTER*1 SP
      LOGICAL INCREASE,SDPST
      COMMON /INCREASED/SDBND,SDPT
      REAL JUNC(M1),YPTS(MD),ARR(NM),BARR(NM)
     *,HDIST,HFRAC,SDBND,SDPT,DIFFGR,DIFFGRCHK
      REAL*8 SML(M1),SMR(M1),SKTINY(M1),SKINL,SKINR,ECON
      INTEGER NST(NJC),NENTER,STARTPT(NM),LOOP(NM)

C **** if doing Z points go directly to middle block type     ****
C
      HFRAC=0
      IFLAG=0
      IKEEP=0
      SDPST=.FALSE.
      INCREASE=.FALSE.
      IDQ=0
      DO I=1,NM
       LOOP(I)=0
      END DO
   10 IF(NNN.EQ.12) THEN
         IJK=1
         N1=1
         QSMALL=SDPT/3
         YPTS(1)=JUNC(1)
         SKTINY(NJC-1)=SKTINY(NJC-2)
         IF(SKINR.EQ.5555) NPC=1
         GOTO 100
      END IF
      N=1
      STARTPT(1)=1
      NST(1)=1
C
C **** Start by gridding the extreme left hand block.        *****
C
      BARR(1)=JUNC(2)
      IF(SKTINY(2).NE.SML(2)) THEN
         BARR(2)=BARR(1)-SKTINY(2)/4
         BARR(3)=BARR(2)-SKTINY(2)/4
C*** keeping grid symmetrical by gradually increasing from the ****
c*** smallest SD at the junction to the SD for the left-hand block*
         X=DLOG(SML(2)/SKTINY(2))/DLOG(2.D0)
         INCR=INT(ABS(X))
         DO 20 IS=4,3+INCR
            BARR(IS)=BARR(IS-1)-(SKTINY(2)/4)*2**(IS-3)
   20    CONTINUE
         IS=4+INCR
      ELSE
         IS=2
      END IF

c**** finding the extreme and gridding out to it ****

c****    first: check for and grid left edge     ****
c****  check if extremes were set in data file   ****
      BEGIN=JUNC(2)-4*SKINL
      IF(YLEND.NE.0) THEN
```

```
            IF(BARR(IS-1).LE.BEGIN) BEGIN=BARR(IS-1)
            IF(BEGIN.LT.YLEND) THEN
               WRITE(14,35) BEGIN
   35          FORMAT (2X,'YOUR LEFT-HAND EXTREME FOR Y SHOULD BE
     1 LESS THAN OR EQUAL TO ',F10.4)
            END IF
            BEGIN=YLEND
            if(barr(is-1).le.begin) then
               nl=is-1
               goto 40
            end if
          END IF
          if(barr(is-1).lt.junc(2)-3*sml(2))then
            nl=is-1
            goto 40
          end if
          DO 31 I1=IS,IS+3
             BARR(I1)=BARR(I1-1)-SML(2)/4
             IF(BARR(I1).LE.BEGIN.or.barr(i1).lt.junc(2)-3*sml(2)) THEN
                N1=I1
                GOTO 40
             ENDIF
   31    CONTINUE
          DO 32 I2=I1,I1+2  ! changed from i1+5
             BARR(I2)=BARR(I2-1)-SML(2)/3
             IF(BARR(I2).LE.BEGIN.or.barr(i2).lt.junc(2)-3*sml(2)) THEN
                N1=I2
                GOTO 40
             ENDIF
   32    CONTINUE
          N1=I1+2

   40    IF(BARR(N1).LE.BEGIN) THEN
             N2=1
             DO 50 NZ=N1,1,-1
                YPTS(N2)=BARR(Nz)
                N2=N2+1
   50        CONTINUE
             STARTPT(2)=N2
             GOTO 70
          ELSE
             DIFF=BARR(N1-1)-BARR(N1)
             N2=N1+1
             DO 60 N1=N2,N2+200
                BARR(N1)=BARR(N1-1)-2*DIFF
                IF(BARR(N1).LE.BEGIN) GOTO 40
                DIFF=2*DIFF
   60         CONTINUE
          END IF
   70    CONTINUE
          IJK=2
C
C**** FOR GENERAL MIDDLE BLOCK  ***********
C
          QSMALL=SDPT/3
  100     DO 1000 NQ=IJK,NJC-2
             N=NQ
  105        KKK=0
             LLL=0
             ARR(1)=JUNC(N)
             SKMINI=DMIN1(SKTINY(N),SKTINY(N+1))
             DIST=JUNC(N+1)-JUNC(N)
             IF(INCREASE) GOTO 600
             IF(JUNC(N).GE.SDBND.AND.NNN.EQ.12) THEN
               INCREASE=.TRUE.
               NENTER=N
```

```
            GOTO 600
          END IF
          QSKD=DIST/SKMINI
          NADD=0
c          IF(SKMINI.EQ.4*HFRAC) QSKD=QSKD*4

C**** gridding for very small blocks (less than or equal to ****
c**** smallest SD at either boundary)                        ****
          ILE2=0
          IF(QSKD.LE.2) THEN
             ILE2=1
             IF(QSKD.LE.0.75.AND.QSKD.GT.0.5) INCR=3
             IF(QSKD.LE.0.5.AND.QSKD.GT.0.25) INCR=2
             IF(QSKD.LE.0.25) THEN
                if(nnn.eq.12.and.n.gt.3) then
                  INCR=1
                ELSE
                  INCR=2
                END IF
             END IF
             IF(QSKD.LE.2.AND.QSKD.GT.0.75) THEN
                INCR=NINT(4*DIST/SKMINI)
             END IF
             HFRAC=DIST/INCR
             IF(NNN.EQ.12.AND.N.EQ.1) GOTO 107
             IF(N.NE.NQ.AND.abs(HFRAC-DIFFGRCHK).le.0.00001)
     1                        HFRAC=DIST/(INCR+1)
             NUE=N1-1
             IF(N.NE.NQ) NUE=STARTPT(N)-2
             DIFFGR=JUNC(N)-YPTS(NUE)
             if(nnn.eq.12) then
               if(diffgr/hfrac.le.2.00001.and.
     1           diffgr/hfrac.ge.0.499999) goto 107
             end if
             IF(DIFFGR-HFRAC.GT.0.00001) THEN
c             IF(DIFFGR-1.1*HFRAC.GT.0.00001) THEN
               LOOP(N)=LOOP(N)+1
               IF(LOOP(N).GT.40) IFLAG=1
               IF(IFLAG.NE.1) THEN
c                SKTINY(N)=HFRAC*4*1.1
                 SKTINY(N)=HFRAC*4
                 IF(NNN.NE.12.AND.N.EQ.2) THEN
                   GOTO 10
                 ELSE
                   N=N-1
                   DIFFGRCHK=DIFFGR
                   GOTO 105
                 END IF
               END IF
               IFLAG=0
             END IF
  107        CONTINUE

             IF(QSKD.LE.0.75) THEN
                IF(QSKD.LE.0.25) THEN
                  IF(NNN.EQ.12.AND.JUNC(N).GT.QSMALL) THEN
                   ARR(2)=ARR(1)+HFRAC
                   I=3
                  ELSE
                   ARR(2)=ARR(1)+HFRAC
                   IF(nnn.eq.12.and.n.gt.3) then
                     I=3
                   ELSE
                     ARR(3)=ARR(2)+HFRAC
                      I=4
                   END IF
```

```
                  END IF
                  GOTO 130
                END IF
                if(qskd.le.0.5) then
                 DO 111 I=2,3
                   ARR(I)=ARR(I-1)+HFRAC
  111            CONTINUE
                goto 130
                end if
                DO 110 I=2,4
                  ARR(I)=ARR(I-1)+HFRAC
  110           CONTINUE
              ELSE
                DO 120 I=2,INCR+1
                  ARR(I)=ARR(I-1)+HFRAC
  120           CONTINUE
              END IF
  130         if(nnn.eq.12) then
                SKTINY(N+1)=DMIN1(DBLE(8*HFRAC),SKTINY(N+1))
              else
                SKTINY(N+1)=DMIN1(DBLE(4*HFRAC),SKTINY(N+1))
              end if
              GOTO 950
            ELSE
            DIFFGRCHK=0.0
c****       for larger blocks (greater than smallest SD)  ****
              IF(abs(SKTINY(N+1)-SKMINI).le.0.0001) THEN
  200           IF(LLL.EQ.1) IA=I
                IF(KKK.EQ.1) GOTO 400
                KKK=1
c*** if the gridding to the left(up) goes past (or equals) the starting value
c*** for the block gridding will stop...checking for equality with reals is
c*** difficult so a small value has been added (subtracted for gridding to
c*** the right (down)) so only LT (or GT) commands are needed.
                HDIST=JUNC(N)+0.000001
                BARR(1)=JUNC(N+1)
                BARR(2)=BARR(1)-SKTINY(N+1)/4
                BARR(3)=BARR(2)-SKTINY(N+1)/4
                X=DLOG(SML(N+1)/SKTINY(N+1))/DLOG(2.D0)
                INCR=INT(ABS(X))

C
C***  IF SKMINI=SML(N+1) THEN FRAC=0 AND LOOP 210 YIELDS FOUR* ****
C***  SMR/4 OR ONE SKIN DEPTH                                  ****
C
                DO 210 JJ=1,INCR
                   I=JJ+3
                   BARR(I)=BARR(I-1)-(SKTINY(N+1)/4)*2**JJ
                   IF(BARR(I).LT.HDIST) GOTO 300
  210           CONTINUE
                JJ=INCR+4
                if(barr(incr+3).lt.junc(n+1)-3*sml(n+1)) goto 241
                BARR(JJ)=BARR(JJ-1)-SML(N+1)/4
                I=JJ
                IF(BARP(I).LT.HDIST) GOTO 300
                JJ=JJ+1
                if(barr(jj-1).lt.junc(n+1)-3*sml(n+1)) goto 241
                DO 220 I=JJ,JJ+2 ! from jj+6
                   BARR(I)=BARR(I-1)-SML(N+1)/3
                   IF(BARR(I).LT.HDIST) GOTO 300
                if(barr(i).lt.junc(n+1)-3*sml(n+1)) then
                 jj=i+1
                 go to 241
                end if
  220           CONTINUE
                DO 230 I=JJ+3,JJ+4 ! from +7 and +8
```

```
                  BARR(I)=BARR(I-1)-SML(N+1)/2
                  IF(BARR(I).LT.HDIST) GOTO 300
               if(barr(i).lt.junc(n+1)-3*sml(n+1)) then
                jj=i+1
                go to 241
               end if
230            CONTINUE
               FACTOR=1
               jj=jj+5
241            DO 250 I=JJ,JJ+200 !from jj+11
                  BARR(I)=BARR(I-1)-SML(N+1)*2**FACTOR
                  IF(BARR(I).LT.HDIST) GOTO 300
                  FACTOR=FACTOR+1
250            CONTINUE
               WRITE(14,251) I,BARR(I)
251 FORMAT(2X,'YARRAY in GRIDYZ went past continue I=',
   +       I4,'BARR(I)=',F10.4)
            ELSE
300            IF(KKK.EQ.1) IB=I
               IF(LLL.EQ.1) GOTO 400
               LLL=1
               HDIST=JUNC(N+1)-0.000001
               ARR(1)=JUNC(N)
               ARR(2)=ARR(1)+SKTINY(N)/4
               ARR(3)=ARR(2)+SKTINY(N)/4

               X=DLOG(SMR(N)/SKTINY(N))/DLOG(2.D0)
               INCR=INT(ABS(X))
               DO 310 JJ=1,INCR
                  I=JJ+3
                  ARR(I)=ARR(I-1)+(SKTINY(N)/4)*2**JJ
                  IF(ARR(I).GT.HDIST) GOTO 200
310            CONTINUE
               JJ=INCR+4
               if(arr(incr+3).gt.junc(n)+3*smr(n)) goto 341
               ARR(JJ)=ARR(JJ-1)+SMR(N)/4
               I=JJ
               IF(ARR(I).GT.HDIST) GOTO 200
               JJ=JJ+1
               if(arr(jj-1).gt.junc(n)+3*smr(n)) goto 341
               DO 320 I=JJ,JJ+2 ! from 6
                  ARR(I)=ARR(I-1)+SMR(N)/3
                  IF(ARR(I).GT.HDIST) GOTO 200
               if(arr(i).gt.junc(n)+3*smr(n)) then
                 jj=i+1
                 goto 341
               end if
320            CONTINUE
               DO 330 I=JJ+3,JJ+4 ! from 7,8
                  ARR(I)=ARR(I-1)+SMR(N)/2
                  IF(ARR(I).GT.HDIST) GOTO 200
               if(arr(i).gt.junc(n)+3*smr(n)) then
                 jj=i+1
                 goto 341
               end if
330            CONTINUE
               FACTOR=1
               jj=jj+5
341            DO 350 I=JJ,JJ+200 !from jj+11,
                  ARR(I)=ARR(I-1)+SMR(N)*2**FACTOR
                  IF(ARR(I).GT.HDIST) GOTO 200
                  FACTOR=FACTOR+1
350            CONTINUE
            END IF

400         ILRG=IA+IB+1
```

```
              LLA=IA
              LLB=IB
              ICA=0
              ICB=0

             DO 405 I=1,ILRG
                  BDIF=BARR(LLB-1)-BARR(LLB)
                  ADIF=ARR(LLA)-ARR(LLA-1)
                  IF(INCREASE) THEN
                    IF(LLB.EQ.1) BDIF=DIFF2
                    IF(LLA.EQ.1) ADIF=DIFF1
                  ELSE
                    IF(LLB.EQ.1) BDIF=SKTINY(N+1)/4
                    IF(SDPST.and.llb.eq.1) BDIF=DIFF2
                    IF(LLA.EQ.1) ADIF=SKTINY(N)/4
                  END IF
                  SMALL=AMIN1(BDIF,ADIF)
                  IF (BARR(LLB).GT.ARR(LLA).AND.
     *                BARR(LLB)-ARR(LLA).GT.2*SMALL-.00001) THEN
                      IF(ICA.NE.0.AND.ICB.NE.0) GOTO 500
                  END IF
                  IF(LLA.EQ.1.AND.LLB.EQ.1) GOTO 500
                  IF(LLB.EQ.1) BDIF=0.0
                  IF(LLA.EQ.1) ADIF=0.0
                  SMALL=AMIN1(BDIF,ADIF)
                  IF(abs(ADIF-bdif).LE.0.0001) THEN
                    IF(ICA.LE.ICB) THEN
                      LLA=LLA-1
                      ICA=ICA+1
                      GOTO 406
                    ELSE
                      LLB=LLB-1
                      ICB=ICB+1
                      GOTO 406
                    END IF
                  END IF
                  IF(abs(SMALL-ADIF).le.0.0001) THEN
                    LLB=LLB-1
                    ICB=ICB+1
                  ELSE
                    LLA=LLA-1
                    ICA=ICA+1
                  END IF
406             CONTINUE
405          CONTINUE
             WRITE(14,411) BARR(LLB),ARR(LLA),N,SKTINY(N),SKTINY(N+1)
411          FORMAT(5X,'GRIDYZ 400 BLOCK FAILED! BARR(LLB),ARR(LLA)
       *,N,SKTINY(N),SKTINY(N+1)'/2X,2(F10.4),I5,2(F15.8))
             RETURN


500          IF(ICA+1.EQ.ICB.AND.LLA.NE.1) THEN
                IF(abs(ABS(ARR(LLA-1))-BARR(LLB)).le.0.0001)
       1                              LLA=LLA-1
             END IF
             IF(ICB+1.EQ.ICA.AND.LLB.NE.1) THEN
                IF(abs(BARR(LLB-1)-ABS(ARR(LLA))).le.0.0001)
       1                               LLB=LLB-1
             END IF
             BDIF=BARR(LLB-1)-BARR(LLB)
             ADIF=ARR(LLA)-ARR(LLA-1)
             IF(INCREASE) THEN
               IF(LLB.EQ.1) BDIF=DIFF2
               IF(LLA.EQ.1) ADIF=DIFF1
             ELSE
                IF(LLB.EQ.1) BDIF=SKTINY(N+1)/4
```

```
                IF(SDPST.and.llb.eq.1) BDIF=DIFF2
                IF(LLA.EQ.1) ADIF=SKTINY(N)/4
              END IF
              SMALL=AMIN1(ADIF,BDIF)
              SPACE=BARR(LLB)-ARR(LLA)
              EXTR=(ABS(ADIF-BDIF))/2
              IF(LLA.EQ.1.AND.abs(SMALL-BDIF).le.0.0001) EXTR=0.0
              IF(LLB.EQ.1.AND.abs(SMALL-ADIF).le.0.0001) EXTR=0.0
              AVG=SMALL+EXTR
              NDIF=NINT(SPACE/AVG)
              IF(NDIF.EQ.0) THEN
                BDIFCHK=SPACE
              ELSE
                BDIFCHK=SPACE/NDIF
              END IF
              IF(INCREASE.AND.N.EQ.NENTER) THEN
                IF(LLA.EQ.1.AND.BDIFCHK.LT.DIFF1/2) THEN
                  IDQ=1
                  N=N-1
                  GOTO 105
                END IF
              END IF
              IF(LLA.EQ.1.AND.BDIFCHK-SKTINY(N)/4.lt.-0.00001) THEN
              SKTINY(N)=4*BDIFCHK
                 IF(N.EQ.2.AND.NNN.NE.12) THEN
                    GOTO 10
                 ELSE
                    SDPST=.FALSE.
                    IF(NNN.EQ.12.AND.N.EQ.1) GOTO 105
                    N=N-1
                    GOTO 105
                 END IF
              END IF
              DO 505 I=1,NDIF
                ARR(LLA+I)=ARR(LLA)+I*BDIFCHK
  505         CONTINUE
              ICONT=LLA+NDIF
              DO 510 I=1,LLB-1
                ARR(ICONT+I)=BARR(LLB-I)
  510         CONTINUE
            I=ICONT+LLB
            GO TO 950
            END IF

C*** Increasing grid separation size if the model extends down
c     far enough to warrent it.
  600     IF(.NOT.INCREASE) GOTO 950
            NUE=N1-1
            IF(N.NE.NQ) NUE=STARTPT(N)-2
            DIFF1=JUNC(N)-YPTS(NUE)
            IF(N.EQ.NENTER.AND.DIST/DIFF1.LT.0.40) THEN
              INCREASE=.FALSE.
              SDPST=.FALSE.
              SKTINY(N)=DIST*6
              IF(N.EQ.2) THEN
                GOTO 10
              ELSE
                N=N-1
                GOTO 105
              END IF
            END IF
            IF(DIST/DIFF1.GT.0.40.AND.DIST/DIFF1.LT.2.0) THEN
              ARR(2)=JUNC(N+1)
              I=2
              GOTO 950
            END IF
```

```
            IF(N+2.NE.NJC) THEN
              DIFF2=JUNC(N+2)-JUNC(N+1)
            ELSE
              DIFF2=500
            END IF
            IF(IDQ.NE.0) DIFF2=BDIFCHK/2
            IDQ=0
            NIT=1
            ARR(1)=JUNC(N)
  605       BARR(1)=JUNC(N+1)
            II=NIT+1
            DO 610 I=2,200
              ARR(II)=ARR(II-1)+DIFF1*2**(I-1)
              IF(ARR(II).GT.JUNC(N+1)) GOTO 620
              II=II+1
  610       CONTINUE
  620       IA=II
            DO 650 I=2,200
              BARR(I)=BARR(I-1)-DIFF2*2**(I-1)
              IF(BARR(I).LT.JUNC(N)) GOTO 660
  650       CONTINUE
  660       IB=I
            GOTO 400
c*** adding the new points for block 'n' to the already ***
c*** determined points: YPTS(n2)                        ***
  950       IF (.NOT.SDPST.AND.NNN.EQ.12) THEN
              DO 953 NIT=2,I-1
                IF(ARR(NIT).GT.SDPT) THEN
                  DIFF1=ARR(NIT)-ARR(NIT-1)
                  IF(N+2.NE.NJC) THEN
                    DIFF2=JUNC(N+2)-JUNC(N+1)
                  ELSE
                    DIFF2=500
                  END IF
                  SDPST=.TRUE.
                  GOTO 605
                END IF
  953         CONTINUE
            END IF
c*** checking that the first grid distance of the next block ***
c*** will be comparable in size to the last grid distance of ***
c*** this block                                              ***
            DIFFGR=(JUNC(N+1)-ARR(I-2))*4
            IF(INCREASE.OR.SDPST) GOTO 954
            IF(DIFFGR-SNGL(SKTINY(N+1)).lt.-0.000009
           1   .AND.ILE2.EQ.0) THEN
              SKTINY(N+1)=DIFFGR
              IF(N.EQ.1.AND.NNN.NE.12) THEN
                GOTO 10
              ELSE
                SDPST=.FALSE.
                GOTO 105
              END IF
            END IF


  954       N2=N1+1
            IF(N.NE.NQ) N2=STARTPT(N)
            STARTPT(N)=N2
            NST(N)=N2-1
            DO 951 NZ=2,I-1
              YPTS(N2)=ARR(NZ)
              N2=N2+1
  951       CONTINUE
            IF(I.EQ.2) NZ=N2+1 !loop 951 skipped so must do this
            YPTS(N2-1)=JUNC(N+1)
```

```
c*** checking that the gridpoints don't overflow the arrays***
          IF(N2.GT.MD) THEN
c*** only want to write warning once ***
             IKEEP=IKEEP+1
             IF (IKEEP.EQ.1) WRITE(14,952) MD
             IF (IKEEP.EQ.1) WRITE(6,952) MD
  952     FORMAT(2X,'Your grid has exceeded the allowed ',I5,
     &' mesh points in the Y or Z direction.'/2X,'To up your
     &limit change the parameter "MD" in AUTOGRID.FOR. You
     &can also run the model in two sections. The rest of
     &'/2X,'this grid is now overwriting the "SMR" array and
     &has become suspect...')
          END IF

          STARTPT(N+1)=N2
          N1=N2-1
          IF(INCREASE.OR.SDPST) GOTO 1000
          IF(N.NE.NQ) THEN
              N=N+1
              GOTO 105
          END IF
 1000 CONTINUE
**** now do the extreme right hand/bottom block ****
       NST(NJC-1)=N1
       ARR(1)=JUNC(NJC-1)
       IF(NNN.EQ.12) THEN
          YPTS(N2)=YPTS(N2-1)+SKTINY(NJC-1)/4
          IF(INCREASE.OR.SDPST) YPTS(N2)=YPTS(N2-1)+DIFFGR/4
          NNN=N2
          NST(NJC)=N2
          RETURN
       END IF
       IF(SKTINY(NJC-1).NE.SMR(NJC-1)) THEN
          ARR(2)=ARR(1)+SKTINY(NJC-1)/4.
          ARR(3)=ARR(2)+SKTINY(NJC-1)/4
          X=DLOG(SMR(NJC-1)/SKTINY(NJC-1))/DLOG(2.D0)
          INCR=INT(ABS(X))
          DO 720 I=4,3+INCR
             ARR(I)=ARR(I-1)+(SKTINY(NJC-1)/4)*2**(I-3)
  720     CONTINUE
          I=4+INCR
       ELSE
          I=2
       END IF


       REND=JUNC(NJC-1)+4*SKINR
       IF(YREND.NE.0) THEN
          IF(ARR(I-1).GE.REND) REND=ARR(I-1)
          IF(REND.GT.YREND) THEN
             WRITE(14,735) REND
  735        FORMAT(2X,'YOUR RIGHT-HAND EXTREME FOR Y SHOULD BE
     1 GREATER THAN OR EQUAL TO ',F10.4)
          END IF
          REND=YREND
          if(arr(i-1).ge.rend) then
            iex=i-1
            goto 750
          end if
       END IF
       if(arr(i-1).gt.junc(njc-1)+3*smr(njc-1)) THEN
         iex=i-1
         goto 750
       end if
       DO 731 I1=I,I+3
```

```
          ARR(I1)=ARR(I1-1)+SMR(NJC-1)/4
          IF(ARR(I1).GE.REND.or.arr(i1)
     1              .gt.junc(njc-1)+3*smr(njc-1)) THEN
            IEX=I1
            GOTO 750
          ENDIF
  731 CONTINUE
      DO 732 I2=I1,I1+2 !from 5
          ARR(I2)=ARR(I2-1)+SMR(NJC-1)/3
          IF(ARR(I2).GE.REND.or.arr(i1)
     1              .gt.junc(njc-1)+3*smr(njc-1)) THEN
            IEX=I2
            GOTO 750
          ENDIF
  732 CONTINUE
      IEX=I1+2

  750 IF(ARR(IEX).GE.REND) THEN
          N2=N1+1
          DO 751 NZ=2,IEX
             YPTS(N2)=ARR(NZ)
             N2=N2+1
  751     CONTINUE
c*** checking that the gridpoints don't overflow the arrays***
          IF(N2.GT.MD) THEN
c*** only want to write warning once ***
            IKEEP=IKEEP+1
            IF (IKEEP.EQ.1) WRITE(14,952) MD
          END IF
          N1=N2-1
          NNN=N1
          GOTO 760
      ELSE
          DIFF=ARR(IEX)-ARR(IEX-1)
          I=IEX+1
          DO 740 IEX=I,I+200
              ARR(IEX)=ARR(IEX-1)+2*DIFF
              IF(ARR(IEX).GE.REND) GOTO 750
              DIFF=2*DIFF
  740     CONTINUE
      END IF
  760 CONTINUE
      NST(NJC)=N1
      RETURN
      END
```

```
      SUBROUTINE RNDOFF(PTS,JUNC,NNN,NJC,MD,M1)
C
C****                  ROUNDING OFF SUBROUTINE                  ****
C**** This routine is called from  FR2D  and rounds off the ****
C**** grid points to 2 significant figures (if the point is ****
C**** less than zero) or 3 significant figures (if the point****
C**** is greater than zero)  H.POLL 1988                       ****
C
      REAL PTS(MD),JUNC(M1)
      REAL*8 PT,PTNXT,PTLOG,FACT,HUNPT,NEWPT,DiLOG
     1,DIFF,REX
      INTEGER FLAG

      DO 9 N=1,NNN
    9 PTS(N)=1000.0*PTS(N)

      DO 10 N=1,NNN-1
         FLAG=0
         DO 30 I=1,NJC
           IF(MD.EQ.5) THEN
            IF(PTS(N).EQ.JUNC(I)) FLAG=1 !for sitemrg rounding
           ELSE
            IF(PTS(N).EQ.1000.0*JUNC(I)) FLAG=1 !for Y/Zgrid rounding
           END IF
   30    CONTINUE
         IF(FLAG.EQ.1) GO TO 10
         PT=DABS(DBLE(PTS(N)))
         PTNXT=DABS(DBLE(PTS(N+1)))
         IF(PTS(N).LT.0) MUL=-1
         IF(PTS(N).GT.0) MUL=1
         IF(PTS(N).EQ.0) GOTO10
         PTLOG=DLOG10(PT)
         IF(PTLOG.LT.0) THEN
           FACT=10.**(INT(DABS(PTLOG)))
           HUNPT=100*PT*FACT
           NEWPT=NINT(HUNPT)
           PTS(N)=MUL*NEWPT/(100*FACT)
           IF(ABS(PTS(N)-PTS(N-1)).LE.0.00001) THEN
             FACT=FACT*10
             PTS(N)=MUL*NINT(100*PT*FACT)/(100*FACT)
           END IF
         ELSE
           Q=ABS(PTS(N+1)-PTS(N))
           DILOG=DLOG10(DBLE(Q))
           DIFF=DABS(DILOG-PTLOG)
           IF(DIFF.GE.2)  THEN
              REX=10**(1+INT(DIFF))
           ELSE
              REX=10**2
           END IF
           FACT=10.**(INT(PTLOG))
           PTS(N)=MUL*FACT*(NINT(REX*(PT/FACT)))/REX
           IF(ABS(PTS(N)-PTS(N-1)).LE.0.00001) THEN
             REX=REX*10
             PTS(N)=MUL*FACT*(NINT(REX*(PT/FACT)))/REX
           END IF
         END IF
   10 CONTINUE
C*** LAST POINT ***
      FLAG=0
         DO 40 I=1,NJC
           IF(MD.EQ.5) THEN
            IF(PTS(N).EQ.JUNC(I)) FLAG=1 !for sitemrg rounding
           ELSE
            IF(PTS(N).EQ.1000.0*JUNC(I)) FLAG=1 !for Y/Zgrid rounding
           END IF
```

```
 40    CONTINUE
       IF(FLAG.EQ.1) GOTO 100
       IF(MD.EQ.5) GOTO 100
       IF(PTS(N).LT.0) MUL=-1
       IF(PTS(N).GT.0) MUL=1
       IF(PTS(N).EQ.0) RETURN
       PT=PTNXT
       PTLOG=DLOG10(PT)
       IF(PTLOG.LT.0) THEN
          FACT=10.**(INT(DABS(PTLOG)))
          HUNPT=100*PT*FACT
          NEWPT=NINT(HUNPT)
          PTS(N)=MUL*NEWPT/(100*FACT)
          IF(ABS(PTS(N)-PTS(N-1)).LE.0.00001) THEN
            FACT=FACT*10
            PTS(N)=MUL*NINT(100*PT*FACT)/(100*FACT)
          END IF
       ELSE
          FACT=10.**(INT(PTLOG))
          PTS(N)=MUL*FACT*(NINT(REX*(PT/FACT)))/REX
          IF(ABS(PTS(N)-PTS(N-1)).LE.0.00001) THEN
            REX=REX*10
            PTS(N)=MUL*FACT*(NINT(REX*(PT/FACT)))/REX
          END IF
       END IF
100    RETURN
       END
```

```
      SUBROUTINE SITEMRG(YGRID,NY,STS,NST,NSTY,STNUM,JUNC,NJC,M1,MD)
C*** This subroutine merges the chosen site points (or extra mesh ***
C*** points chosen interactively) into the already existing grid. ***
C*** Junction (ie: block boundary) points can't be shifted but    ***
C*** other points are rearranged around the new grid points to    ***
C*** maintain symmetry and correct grid spacing for that area.    ***
C*** Called from FR2D.                                            ***

      REAL*8 YGRID(MD),STS(30)
      REAL RAT1,RAT2,ERAT,P(5),JUNC(M1)
      INTEGER NY,NST,NJC,NYN,STNUM(30),NSTY(M1)
      COMMON /YJNUM/NJCY

      NYN=NY
      DO 100 I=1,NST
       DO 200 J=1,NY-1
        IF(STS(I).GE.YGRID(J).AND.STS(I).LE.YGRID(J+1)) THEN
          IF(DABS(STS(I)-YGRID(J)).LE.0.00001) THEN
            STNUM(I)=J
            GOTO 900
          END IF
          IF(DABS(STS(I)-YGRID(J+1)).LE.0.00001) THEN
            STNUM(I)=J+1
            GOTO 900
          END IF
          DO 250 L=1,NJC
           IF(ABS(YGRID(J)-DBLE(JUNC(L))).LT.0.0001) THEN
            DO 220 MK=1,NJC
             IF(DABS(YGRID(J+1)-DBLE(JUNC(MK))).LT.0.0001) THEN
                NYN=NY+1
                DO 225 K=NYN,J+2,-1
225             YGRID(K)=YGRID(K-1)
                YGRID(J+1)=STS(I)
                STNUM(I)=J+1
                GOTO 900
             END IF
220         CONTINUE
            RAT1=(STS(I)-YGRID(J))/(YGRID(J+1)-YGRID(J))
            IF(RAT1.GE.0.75) THEN
              YGRID(J+1)=STS(I)
              STNUM(I)=J+1
            ELSE
              NYN=NY+1
              DO 260 K=NYN,J+3,-1
260           YGRID(K)=YGRID(K-1)
              ERAT=(YGRID(J+1)-YGRID(J))/(YGRID(J+2)-YGRID(J))
              YGRID(J+1)=STS(I)
              STNUM(I)=J+1
              P(1)=STS(I)/1000.0
              P(2)=(STS(I)+ERAT*(YGRID(J+2)-STS(I)))/1000.0
              P(3)=YGRID(J+3)/1000.0  !include p(3) for rndoff purposes
              CALL RNDOFF(P,JUNC,3,NJC,5,M1)
              YGRID(J+2)=P(2)
            END IF
            GOTO 900
           END IF
           IF(DABS(YGRID(J+1)-DBLE(JUNC(L))).LT.0.0001) THEN
            DO 270 MK=1,NJC
              IF(DABS(YGRID(J)-DBLE(JUNC(MK))).LT.0.0001) THEN
                NYN=NY+1
                DO 275 K=NYN,J+2,-1
275             YGRID(K)=YGRID(K-1)
                YGRID(J+1)=STS(I)
                STNUM(I)=J+1
                GOTO 900
              END IF
```

```
270        CONTINUE
           RAT1=(YGRID(J+1)-STS(I))/(YGRID(J+1)-YGRID(J))
           IF(RAT1.GE.0.75) THEN
             YGRID(J)=STS(I)
             STNUM(I)=J
           ELSE
             NYN=NY+1
             DO 280 K=NYN,J+2,-1
280          YGRID(K)=YGRID(K-1)
             ERAT=(YGRID(J+1)-YGRID(J))/(YGRID(J+1)-YGRID(J-1))
             YGRID(J+1)=STS(I)
             STNUM(I)=J+1
             P(1)=YGRID(J-1)/1000.0
             P(3)=STS(I)/1000.0
             P(2)=(STS(I)-ERAT*(STS(I)-YGRID(J-1)))/1000.0
             P(4)=YGRID(J+2)/1000.0
             CALL RNDOFF(P,JUNC,4,NJC,5,M1)
             YGRID(J)=P(2)
           END IF
           GOTO 900
         END IF
250      CONTINUE
         RAT1=(STS(I)-YGRID(J-1))/(YGRID(J)-YGRID(J-1))
         RAT2=(YGRID(J+2)-STS(I))/(YGRID(J+2)-YGRID(J+1))
         IF(RAT1.LE.1.25) THEN
           ERAT=(YGRID(J+1)-YGRID(J))/(YGRID(J+2)-YGRID(J))
           YGRID(J)=STS(I)
           STNUM(I)=J
           P(1)=STS(I)/1000.0
           P(2)=(STS(I)+ERAT*(YGRID(J+2)-STS(I)))/1000.0
           P(3)=YGRID(J+2)/1000.0
           CALL RNDOFF(P,JUNC,3,NJC,5,M1)
           YGRID(J+1)=P(2)
         ELSE
           IF(RAT2.LE.1.25) THEN
             ERAT=(YGRID(J+1)-YGRID(J))/(YGRID(J+1)-YGRID(J-1))
             YGRID(J+1)=STS(I)
             STNUM(I)=J+1
             P(1)=YGRID(J-1)/1000.0  !include for rndoff purposes
             P(3)=STS(I)/1000.0
             P(2)=(STS(I)-ERAT*(STS(I)-YGRID(J-1)))/1000.0
             P(4)=YGRID(J+2)/1000.0
             CALL RNDOFF(P,JUNC,4,NJC,5,M1)
             YGRID(J)=P(2)
           ELSE
             NYN=NY+1
             DO 300 K=NYN,J+3,-1
300          YGRID(K)=YGRID(K-1)
             ERAT=(YGRID(J+3)-YGRID(J+1))/(YGRID(J+3)-YGRID(J))
             P(4)=(YGRID(J+3)-ERAT*(YGRID(J+3)-STS(I)))/1000.0
             ERAT=(YGRID(J)-YGRID(J-1))/(YGRID(J+1)-YGRID(J-1))
             P(2)=(YGRID(J-1)+ERAT*(STS(I)-YGRID(J-1)))/1000.0
             YGRID(J+1)=STS(I)
             STNUM(I)=J+1
             P(1)=YGRID(J-1)/1000.0
             P(3)=STS(I)/1000.0
             P(5)=YGRID(J+3)/1000.0
             CALL RNDOFF(P,JUNC,5,NJC,5,M1)
             YGRID(J+2)=P(4)
             YGRID(J)=P(2)
           END IF
         END IF
         GOTO 900
       END IF
200    CONTINUE
900    DO 920 K=1,NJCY
```

```
      IF(DBLE(JUNC(K)).GT.STS(I)) THEN
        IF(NYN.GT.NY) THEN
          DO 930 IGG=K,NJCY
930       NSTY(IGG)=NSTY(IGG)+1
        END IF
        GOTO 940
      END IF
920  CONTINUE
940  NY=NYN
100 CONTINUE
    RETURN
    END
```

```
C  This is the version with the improved recursion relation
      SUBROUTINE ONED(ZGRID,RES,T,FIELD,NPOL,MD,MDZ,M1D)
C ****Subroutine to calculate the one dimensional solution***
C     called by FR2D
      IMPLICIT REAL*8 (A-H,O-Z),INTEGER(I-N)
      PARAMETER (MD2=200)
      REAL T
      COMMON /LIMITS/NY,NZ
      COMMON /CONST/PI,OMEGA,RMU,PRCOND,PRINSUL
      COMMON /CPLX/CI,RTI,RTIN,ARTI
      COMMON /GROPT/NUN,YMIN,YMAX,ZMAX,GRAP
      CHARACTER*6 GRAP
      INTEGER YMIN,YMAX,ZMAX,NUN
      REAL*8  RES(MD,MDZ),RMU,PI,FACT,ALPHA,RHOA,PHI,DN,ZN
     1,OMEGA,ZGRID(MDZ),PRINSUL,PRCOND,ZF,DD(MD2)
      COMPLEX*16 FIELD(MD,MDZ),GAM,GAMMA(MD2),CN0,CN1,GC
     1,GPRIME(200,MD2),CNN(MD2),RN,CI,RTI,RTIN,ARTI,TPFLD
     2,THET,CNI,EN,FAC,FAC1,CN,FACTOR

C**defining values in COMMON blocks CONST and CPLX ***

      PI=3.141592653589793D0
      OMEGA=2.0D0*PI/DBLE(T)
      RMU=PI*4.0D-7
      PRCOND=1.1D-20
      PRINSUL=0.9D+20
      CI=DCMPLX(0.0D0,1.0D0)
      RTI=(1.0D0+CI)/DSQRT(2.D0)
      RTIN=(1.0D0-CI)/DSQRT(2.D0)
      J=1
      FACT=OMEGA*RMU

   10 ZF=ZGRID(NZ)
      IF(RES(J,NZ).LE.PRCOND.OR.RES(J,NZ).EQ.0.0) THEN
         CNN(1)=DCMPLX(0.0D0,0.d0)
         MARK=1
         GOTO 20
      ENDIF
      ALPHA=DSQRT(FACT/RES(J,NZ))
      GAMMA(NZ)=RTI*ALPHA

C*** C(NZ-1) ***
      CNN(1)=1.D0/GAMMA(NZ)
      MARK=1
C
C***** Recursion relation for C(v,w)

   20 DO 100 I=NZ-1,1,-1
      if(res(j,i).eq.0.d0) then
        print *,'!!!!Divide by zero in subroutine ONED...Most likely
     1  cause is some error in the model data. Check all blocks
     1  of the model design to make sure edges match etc. !!!!'
      end if
      ALPHA=dSQRT(FACT/RES(J,I))
      GAMMA(I)=RTI*ALPHA

      IF(RES(J,I).NE.RES(J,I-1).OR.I.EQ.1) THEN
        MARK=MARK+1
        DD(MARK)=ZF-ZGRID(I)
        GC=GAMMA(I)*CNN(MARK-1)
        THET=CDEXP(-2.D0*GAMMA(I)*DD(MARK))
        CNN(MARK)=(1.D0+GC-(1.D0-GC)*THET)/(GAMMA(I)
     &                    *(1.D0+GC+(1.D0-GC)*THET))
        ZF=ZGRID(I)
```

```
      END IF
  100 CONTINUE
      CN=CNN(MARK)
C*****Calculation of field (G)
      FIELD(J,1)=DCMPLX(1.0D0,0.0D0)
      GPRIME(J,1)=-FIELD(J,1)/CNN(MARK)
      CN0=CN
      CN1=CNN(MARK-1)
      GAM=GAMMA(1)
      RN=(1.D0-CN1*GAM)/(1.D0+CN1*GAM)
      EN=FIELD(J,1)
      DN=DD(MARK)
      ZN=0.D0
C***Recursion
      DO 200 I=2,NZ
       FAC=1.D0+CN0*GAM
       IF (RES(J,I).NE.RES(J,I-1)) THEN
        FACTOR=EN*CDEXP(-GAM*DN)/(CN0*(1.D0+CN1*GAM))
        FIELD(J,I)=CN1*FACTOR*FAC
        GPRIME(J,I)=-FACTOR*FAC
        MARK=MARK-1
        CN0=CN1
        CN1=CNN(MARK-1)
        GAM=GAMMA(I)
        RN=(1.D0-CN1*GAM)/(1.D0+CN1*GAM)
        EN=FIELD(J,I)
        ZN=ZN+DN
        DN=DD(MARK)
       ELSE
        FAC1=GAM*(ZGRID(I)-ZN)
        FIELD(J,I)=FAC*EN*(CDEXP(-FAC1)-RN*CDEXP(FAC1-2.D0*GAM*DN))/
     1             (CN0*GAM*2.D0)
        GPRIME(J,I)=-FAC*EN*(CDEXP(-FAC1)+RN*CDEXP(FAC1-2.D0*GAM*DN))/
     1             (CN0*2.D0)
       END IF
  200 CONTINUE

      IF (NPOL.EQ.1) THEN
C***E-pol soln ****
         DO 300 I=1,NZ
            FIELD(J,I)=CI*OMEGA*(1.0D0,0.0D0)*CN*FIELD(J,I)
  300    CONTINUE
      IF(RES(J,NZ).LE.PRCOND) FIELD(J,NZ)=DCMPLX(0.D0,0.D0)
      ELSE
C***B-pol solution***
         TPFLD=-(1.0D0,0.0D0)*CN*GPRIME(J,1)
         DO 400 I=1,NZ
            FIELD(J,I)=-(1.0D0,0.0D0)*CN*GPRIME(J,I)/TPFLD
  400    CONTINUE
      END IF

C*** If the model is only 1-D compute the rho and phi now and stop
      IF(M1D.EQ.1.AND.J.EQ.1) THEN
       RHOA=OMEGA*RMU*CN*DCONJG(CN)
       PHI=DATAN2(DIMAG(CI*CN),DREAL(CI*CN))*180.0D0/PI
       NSTN=1
       SNST=0.00
       IF(GRAP.LT.'NOGRAP') THEN
       WRITE(NUN,500) T
  500  FORMAT(' Resistivities and Phases for period = ',f10.3)
       IF(NPOL.EQ.1) WRITE(NUN,501)
       IF(NPOL.EQ.0) WRITE(NUN,502)
  501  FORMAT('  No       Y          Res          Phase      EPOL')
  502  FORMAT('  No       Y          Res          Phase      BPOL')
       WRITE(NUN,505) NSTN,SNST,RHOA,PHI
  505  FORMAT(I4,F12.4,1X,F13.6,1X,F8.3)
```

```
      END IF

      DO 430 I=1,NZ
430   WRITE(80,426) I,ZGRID(I)/1000,DREAL(FIELD(J,I)),DIMAG(FIELD(J,I))
426   FORMAT(2X,I3,2X,F10.4,2X,2(G13.6,2X))
      RETURN
     END IF

     IF(J.EQ.1) THEN
        J=NY
        GOTO 10
     END IF
     RETURN
     END
```

```
      SUBROUTINE MATRIX(YGRID,ZGRID,RESGR,FIELD,NPOL,MD,MDZ)
c**** this subroutine, called by FR2D, directs the matrix  ***
c**** elimination procedure and prints out the fields.POLL'88***
      IMPLICIT REAL*8 (A-H,K,O-Z)
      PARAMETER (MD1=200,MD2=200)
      COMMON /LIMITS/NY,NZ
      REAL*8 YGRID(MD),ZGRID(MDZ),RESGR(MD,MDZ)
      INTEGER NPOL,NSM,LENR
      INTEGER KSTART,KFLAG,KEND,KFIRST
      COMPLEX*16 TA(MD1,MD2),B(MD1),TC(MD1,MD2),A(MD1),RHS
     +  ,C(MD1),DIYM1,FIELD(MD,MDZ),RSLOPE,FONE(2,MD2)
      COMMON /BAND/NSM,KSTART,KFLAG,KEND,KFIRST
      COMMON /CONST/pi,OMEGA,rmu,PRCOND,PRINSUL,RSLOPE
      COMMON /SV1/NQ

      RSLOPE=(0.0D0,0.0D0)
      RSLOPE=(FIELD(NY,NZ)-FIELD(1,NZ))/(YGRID(NY)-YGRID(1))
      KFIRST=1
      KEND=0
      KFLAG=0
      KSTART=1
      NSM=NY
      NQ=0
C
C*** RECORD LENGTH IN LONGWORDS: nsm*16 bytes for 1 row of
c     matrix C(i,j) and 1*16 bytes for 1 row of matrix B(i).
c     Each longword is 4 bytes ... so divide the total number of
c     bytes by 4.  The records are written in GAUSSJ.FOR,

      LENR=4*NSM+4
      OPEN(UNIT=13,FILE='SCRATCH.DAT',ACCESS='DIRECT',
     &     RECL=LENR,STATUS='NEW')

C*** FIELDS AT INFINITY (IMPORTANT FOR EPOL) ***
      DO 8 IZ=1,NZ
        FONE(1,IZ)=FIELD(1,IZ)
        FONE(2,IZ)=FIELD(NY,IZ)
    8 CONTINUE

C*** TOP BC FIRST ***
      IZ=1
      DO 10 IY=1,NY
        CALL CPNTA(YGRID,ZGRID,RESGR,FONE,A,RHS,C,DIYM1,FIELD
     +    ,NPOL,IZ,IY,MD,MDZ,MD1,MD2)
        IF (NPOL.EQ.0) GOTO 50
        CALL GAUSSJF(A,RHS,C,DIYM1,IZ,IY,TA,TC,B,MD1,MD2,npol)
   10 CONTINUE
      CALL GAUSSJB(TA,B,TC,IZ,MD1,MD2)
      PRINT *,IZ,' COMPLETE'

C*** GENERAL BLOCK ***
   50 DO 100 IZ=2,NZ-1
        DO 110 IY=1,NY
          CALL CPNTA(YGRID,ZGRID,RESGR,FONE,A,RHS,C,DIYM1
     +      ,FIELD,NPOL,IZ,IY,MD,MDZ,MD1,MD2)
        CALL GAUSSJF(A,RHS,C,DIYM1,IZ,IY,TA,TC,B,MD1,MD2,npol)
  110   CONTINUE
        CALL GAUSSJB(TA,B,TC,IZ,MD1,MD2)
        PRINT *,IZ,' COMPLETE'
  100 CONTINUE

C*** BOTTOM BLOCK ***
      KEND=1
      IZ=NZ
      PRINT *,IZ,'START BOTTOM BLOCK'
      DO 210 IY=1,NY
```

```
            CALL CPNTA(YGRID,ZGRID,RESGR,FONE,A,RHS,C,DIYM1,FIELD
           +    ,NPOL,IZ,IY,MD,MDZ,MD1,MD2)
            CALL GAUSSJF(A,RHS,C,DIYM1,IZ,IY,TA,TC,B,MD1,MD2,npol)
  210 CONTINUE
      CALL GAUSSJB(TA,B,TC,IZ,MD1,MD2)
      CALL BACKSUB(TA,B,FIELD,NPOL,MD,MDZ,MD1,MD2)
      PRINT *,IZ,'COMPLETE....END'

C*** PRINT FIELD ***
      CLOSE(UNIT=13,STATUS='DELETE')
      CALL WRITE(YGRID,ZGRID,FIELD,MD,MDZ,NPOL)
      RETURN
      END
```

```
C     ------------------------------------------------------
      SUBROUTINE CPNTA(YGRID,ZGRID,RESGR,FONE,A,RHS,C,DIYM1,FIELD
     &,NPOL,IZ,IY,MD,MDz,md1,md2)
C     ------------------------------------------------------
C     SET UP EQUATION FOR POINTS WITH SPECIAL BOUNDARY CONDITION.
C     PLACE COEEFS IN BAND STORAGE MATRIX ABD IN POSTIONS TO BE SOLVED.
C     MODIFIED FOR INTEGRAL BOUNDARY CONDITIONS.... called by MATRIX
C ** VARIABLE: VECTOR A -  COEFFS IN DIAGONAL BLOCK
C **           VALUE RHS -  RIGHT HAND SIDE OF EQUATIONS
C              VECTOR C -  COEFFS IN RIGHT HAND OFF DIAGONAL
C              DIYM1 - COEFFS IN LEFT HAND OFF DIAGONAL
      COMMON /LIMITS/NY,NZ
      PARAMETER (MD3=200)
      REAL*8 COF(5),K1,KN0,PI,OMEGA,RMU,PRINSUL,PRCOND
     1,YGRID(MD),ZGRID(MDz),RESGR(MD,MDz),SIGFACT(2),splus,rminus
      COMMON/BAND/NSM,KSTART,KFLAG,KEND,KFIRST
      COMPLEX*16 A(MD1),RHS,C(MD1),EP,EM
     1,E(MD3),FIELD(MD,MDz),DIYM1,FONE(2,MD2)
      COMPLEX*16 CI,RTI,RTIN,ARTI,RSLOPE
      COMMON /CONST/PI,OMEGA,RMU,PRCOND,PRINSUL,RSLOPE
      INTEGER NC,NY,NZ,IFLAG,IZ,IY
      integer  NSM,KFLAG,KSTART,KEND,KFIRST
      COMMON/CPLX/CI,RTI,RTIN,ARTI

C**************************************
C     WRITE (6,*) '*** START CPNTA...'
C**************************************
C

      IF (KSTART.eq.1) THEN
C ZERO COEFFICIENTS...ON FIRST PASS ONLY
        CI=(0.D0,1.D0)
        RTI=(1.D0,1.D0)/DSQRT(2.D0)
        RTIN=(1.D0,-1.D0)/DSQRT(2.D0)
        KSTART=0
      END IF
      DO 10 IE=1,NSM
         A(IE) = (0.D0,0.D0)
         C(IE) = (0.D0,0.D0)
10    CONTINUE
      RHS = (0.D0,0.D0)
      EP = (0.D0,0.D0)
      EM = (0.D0,0.D0)
      DIYM1=(0.D0,0.D0)

      DO 20 IE=1,NY
20    E(IE) = (0.D0,0.D0)
      IF(IZ.NE.1) GOTO 1000

      IF(NPOL.EQ.1) THEN
C  AT TOP SURFACE: HILBERT TRANSFORM INTEGRAL TO BE SOLVED
        CALL SURF(IY,IZ,IFLAG,SPLUS,RMINUS,E,EP,EM,K1,YGRID,ZGRID
     +           ,RESGR,NPOL,MD,mdz,MD3)
        RHS = EP * FONE(2,IZ) + EM * FONE(1,IZ)
        DO 31 K=1,NY
31      A(K)=E(K)
        C(IY)=DCMPLX(PI/K1,0.D0)

      ELSE
        DO 35 I=1,NY
35      FIELD(I,1)=(0.0D0,0.0D0)
      END IF
      RETURN

1000  IF(IZ.NE.NZ) GOTO 2000
      IF(RESGR(1,NZ).GE.PRINSUL) GOTO 2000
```

```
      IF(kFLAG.eq.1) GOTO 2000
C  FOR B AND E-POL BOTTOM INTEGRAL CONDITION****
C AT BOTTOM SURFACE. INTEGRAL BOUNDARY CONDITION SOLVED
        CALL SURF(IY,IZ,IFLAG,SPLUS,RMINUS,E,EP,EM,KN0,YGRID,ZGRID,
     +              RESGR,NPOL,MD,mdz,MD3)
C  FLAG 0 INDICATES ZERO CONDUCTIVITY FOR LOWER LAYER
        IF (IFLAG.EQ.0)THEN
           KFLAG = 1
           GO TO 2000
        END IF

        RHS = EP*FIELD(NY,IZ)+EM*FIELD(1,IZ)
        IF(NPOL.EQ.0) THEN
          RHS=RHS +(SPLUS*PI*RMINUS-RESGR(1,NZ-1)*
     1      PI/RESGR(1,NZ))*((FIELD(1,NZ)-FIELD(1,NZ-1))
     1      /KN0+KN0*0.5D0*CI*OMEGA*RMU*FIELD(1,NZ)
     1      /RESGR(1,NZ-1) )
          KN0=KN0/(SPLUS*RMINUS)
        END IF
        DIYM1=DCMPLX(PI/KN0,0.D0)
        DO 41 K=1,NY
41      A(K)=E(K)
      RETURN

C***  GENERAL MIDDLE BLOCKS ****

2000  IZ1=IZ-1
C CHECK FOR EDGE CONDITON
C NORMAL PROCESSING AT NON-BOUNDARY.

      IF(IY.EQ.1.OR.IY.EQ.NY) then
      if(NPOL.EQ.1)  THEN
C *** SPECIAL ACTION AT  SIDE EDGES. ***
        IF(IY.EQ.NY.or.iy.eq.1) THEN
          IF(IY.NE.1) GOTO 109
          DIYM1 = FONE(1,IZ)
          A(IY)=-FONE(1,IZ1)
          IF(DIYM1.EQ.0.D0.AND.A(IY).EQ.0.D0) THEN
             DIYM1=(1.0D0,0.D0)
             A(IY)=(1.0D0,0.0D0)
          END IF
          GOTO 113
109       DIYM1 = FONE(2,IZ)
          A(IY)=-FONE(2,IZ1)
          RHS=-FONE(2,IZ)*FONE(1,IZ1)+
     &       FONE(1,IZ)*FONE(2,IZ1)
          IF(DIYM1.EQ.0.D0.AND.A(IY).EQ.0.D0) THEN
             DIYM1=(1.0D0,0.D0)
             A(IY)=(1.0D0,0.0D0)
          END IF
          GOTO 113
        END IF
      END IF
      END IF

      CALL COEFF2(IY,IZ,5,NC,IFLAG,COF,YGRID,
     +      ZGRID,RESGR,SIGFACT,NPOL,MD,mdz)

c *** right hand side of matrix equation  *****

      IF(IZ.EQ.NZ) THEN
        RHS = -COF(1)*FONE(1,IZ1)-COF(3)*FONE(1,IZ)
     &  -(COF(2)+COF(4))*FONE(1,IZ)+(COF(5)+CI)*FONE(1,IZ)
      ELSE
        RHS = -COF(1)*FONE(1,IZ1)-COF(3)*FONE(1,IZ+1)
     &  -(COF(2)+COF(4))*FONE(1,IZ)+(COF(5)+CI)*FONE(1,IZ)
```

```
      END IF

C *** COEFF FOR E[IY,IZ-1] ***
      DIYM1=DCMPLX(COF(1),0.D0)
C      IF(NPOL.EQ.0.AND.IZ.EQ.2) DIYM1=(0.D0,0.D0)

C *** COEFF FOR E[IY,IZ]    ***
      A(IY)=DCMPLX(-COF(5), -1.D0)

C *** COEFF FOR E[IY+1,IZ] ***
      IF(NPOL.EQ.0.AND.IY.NE.NY-1) GOTO 110
      RHS=RHS-COF(2)*(FONE(2,IZ)-FONE(1,IZ))
      GOTO 111
110   A(IY+1) = DCMPLX(COF(2),0.D0)

C *** COEFF FOR E[IY,IZ+1] ***
111   IF(IZ.NE.NZ) GOTO 115
      RHS=RHS-COF(3)*RSLOPE*(YGRID(IY)-YGRID(1))
      goto 114
115   C(IY) = DCMPLX(COF(3),0.D0)

C *** COEFF FOR E[IY-1,IZ] ***
114   IF(NPOL.EQ.0.AND.IY.EQ.2) GOTO 113
      A(IY-1) = DCMPLX(COF(4),0.D0)

113   CONTINUE
      RETURN
      END
```

```
C     ------------------------------------------------------
      SUBROUTINE SURF(IY,IZ,IFLAG,SPLUS,RMINUS,CO,COP,COM,KSURF
     &      ,YGRID,ZGRID,RESGR,NPOL,MD,mdz,MD3)
C     -------------- calculates equation coeffs for one point at the
C surface of the earth (lower and  upper) using the integral B.C.
C version for two-dimensional electric and magnetic polarisation by
C called by CPNTA
      IMPLICIT REAL*8 (A-H,K,O-Z)
      COMPLEX*16  CI,RTI,ARTI,RTIN,a1,a2
      COMMON /LIMITS/NY,NZ
      PARAMETER (MD4=200)
      COMPLEX*16 CO(MD3),COP,COM,K0(200),K1(200),HI(200)
      COMPLEX*16 LP,MP,NP,PP,QP,SP,TP,F1,THE1,THEM,UPS1,UPSM
      REAL*8 DENOM,HSUM,HM(200),SPLUS,KSURF,RMINUS,APP,DI(200)
     +,      RESGR(MD,MDz)
     +,      YGRID(MD)
     +,      ZGRID(MDz)
     +,      R(4)
     +,      RDIV
      INTEGER  IFLAG
      INTEGER NSM,KSTART,KFLAG,KEND,KFIRST
      COMMON /GRID/Y1,Y2,YM,YM0,HM
      COMMON /CONST/
     +       PI
     +,      OMEGA
     +,      RMU
     +,      PRCOND
     +,      PRINSUL
      COMMON/ALPHA/ALPHA
      COMMON/CPLX/CI,RTI,RTIN,ARTI
      COMMON/BAND/NSM,KSTART,KFLAG,KEND,KFIRST
C*************************************
C     WRITE (6,*) '*** START SURF  ...'
C*************************************
C
c method identification message on first entry.
      IF(KFIRST.EQ.0) GO TO 10
      KFIRST = 0.0
c define edge grid pts,y1,ym,y2,ym-1
c and other 'grid' common values
      YM=YGRID(NY)
      YM0=YGRID(NY-1)
      Y1=YGRID(1)
      Y2=YGRID(2)

C find grid spacings.
      DO 5  I=1,NY-1
         HM(I) = YGRID(I+1) - YGRID(I)
5     CONTINUE

C Normal calculation within model.
10    IFLAG  = 1

C Define position of pt on surface,Y
      Y=YGRID(IY)
      HSUM=HM(IY)+HM(IY-1)
      HP0=HM(IY-1)
      IF(IY.GT.2) HP0SUM=HM(IY-1)+HM(IY-2)
      HP=HM(IY)
      HPSUM=HSUM
      IF(IY.LT.NY-1) THEN
       HP1=HM(IY+1)
       HP1SUM=HM(IY+1)+HM(IY)
      END IF

C Setup initial coeffs ( see documentation )
```

```
      DENOM=  1.0E0/(HM(IY-1)*HM(IY)* HSUM )
      PY    =  2.0E0*DENOM*HM(IY)
      QY    =  -2.0E0*DENOM*HSUM
      RY    =  2.0E0*DENOM*HM(IY-1)
      AY    =  -DENOM*HM(IY)**2
      BY    =  DENOM*(HM(IY)**2-HM(IY-1)**2)
      CY    =  DENOM*HM(IY-1)**2

C Find resistivities of regions.
C  Check if upper surface
      IF(IZ.EQ.1) GO TO 12
      R00   = RESGR(IY-1,IZ-1)
      R20   = RESGR(IY  ,IZ-1)
12    R02   = RESGR(IY-1,IZ  )
      R22   = RESGR(IY  ,IZ  )

C Check for zero resitivity
      IF(R02 .LT. PRCOND) GO TO 60

      IF(IZ.EQ.1) GOTO 16
C  for sigma+ (z=Zn)
      KAPPA  = OMEGA * RMU *
     +      (HM(IY-1)/R00+HM(IY)/R20)/ HSUM
C  for sigma- (z=0)
16    ALPHA  =DSQRT( OMEGA * RMU *
     +      (HM(IY-1)/R02+HM(IY)/R22)/ HSUM )
      ARTI=RTI*ALPHA

C Check whether lower or upper. Calcualte  integral coefficients
      IF(IZ.EQ.1) THEN
C************ Epol top boundary condition **********************
         KAPPA= ALPHA**2
         KSURF = ZGRID(IZ+1)- ZGRID(IZ)
         IF (ABS(Y).LE.PRCOND) THEN
           TP=-0.5D0/YM
           SP=0.5D0/YM+PI*0.5D0*KSURF*CI*
     1          (KAPPA-OMEGA*RMU/RESGR(1,IZ))
           IF(IY.NE.2) LP=DLOG(ABS(Y1/Y2))/HM(1)+0.5D0/Y1
           IF(IY.NE.NY-1) MP=DLOG(ABS(YM/YM0))/HM(NY-1)-0.5D0/YM
         ELSE
           TP=1.0D0/Y-DLOG(ABS(YM/(Ym-Y)))*YM/Y**2
           SP=-TP+PI*0.5D0*KSURF*CI*
     1          (KAPPA-OMEGA*RMU/RESGR(1,IZ))
           IF(IY.NE.2) LP=DLOG((Y-Y1)/(Y-Y2))/HM(1)
     1          +DLOG(ABS(Y1)/(Y-Y1))*Y1/Y**2-1.0D0/Y
           IF(IY.NE.NY-1) MP=DLOG((YM-Y)/(YM0-Y))/HM(NY-1)
     1          -DLOG(ABS(YM)/(YM-Y))*YM/Y**2+1.0D0/Y
         END IF

         PP=DLOG(HP/HP0)*(HP-HP0)/(HP*HP0)-2.D0*HPSUM/(HP*HP0)
     1          -PI/KSURF-PI*KSURF*(0.5D0*CI*KAPPA+1.D0/(HP*HP0))
         IF(IY.EQ.2) THEN
           IF(ABS(Y).LE.PRCOND) THEN
             LP=2.D0/HP0+DLOG(HP0/HP)*HP/(HP0*HPSUM)
     1          +PI*KSURF/(HP0*HPSUM)-0.5D0/Y1
           ELSE
             LP=DLOG(ABS(Y1)/HP0)*Y1/Y2**2+DLOG(HP0/HP)
     1          *HP/(HP0*HPSUM)+(Y1+Y2)/(Y2*HP0)+PI*KSURF/(HP0*HPSUM)
           END IF
           NP=(0.D0,0.D0)
         ELSE
           NP=DLOG(HP0/HP0SUM)/HM(IY-2)+2.D0/HP0+DLOG(HP0/HP)*HP
     1          /(HP0*HPSUM)+PI*KSURF/(HP0*HPSUM)
         END IF
         IF(IY.EQ.NY-1) THEN
           IF(ABS(Y).LE.PRCOND) THEN
```

```
                MP=2.D0/HP+DLOG(HP/HP0)*HP0/(HP*HPSUM)
     1            +PI*KSURF/(HP*HPSUM)-0.5D0/YM
              ELSE
                MP=-DLOG(ABS(YM)/HP)*YM/YM0**2+DLOG(HP/HP0)
     1            *HP0/(HP*HPSUM)+(YM+YM0)/(YM0*HP)+PI*KSURF/(HP*HPSUM)
              END IF
              QP=(0.D0,0.D0)
            ELSE
              QP=DLOG(HP/HP1SUM)/HP1+2.D0/HP+DLOG(HP/HP0)*HP0/(HP*HPSUM)
     1            +PI*KSURF/(HP*HPSUM)
            END IF

            CO(IY)=PP
            CO(IY-1)=NP
            CO(IY+1)=QP
            IF(IY.GE.4) THEN
              DO I=2,IY-2
c*** these are the first summation values for rp(i)
                CO(I)=DLOG(ABS((Y-YGRID(I))/(Y-YGRID(I-1))))/HM(I-1)
     1            -DLOG(ABS( (Y-YGRID(I+1)) / (Y-YGRID(I)) ))/HM(I)
              END DO
            END IF
            IF(IY.LE.NY-3) THEN
              DO I=IY+2,NY-1
c*** these are the second summation values for rp(i)
                CO(I)=DLOG(ABS((Y-YGRID(I))/(Y-YGRID(I-1))))/HM(I-1)
     1            -DLOG(ABS( (Y-YGRID(I+1)) / (Y-YGRID(I)) ))/HM(I)
              END DO
            END IF


            CO(1)=LP
            CO(NY)=MP
            COM=SP
            COP=TP
          ELSE
            ALPHA  = DSQRT( OMEGA * RMU *
     +        (HM(IY-1)/R02+HM(IY)/R22)/ HSUM )
            CALL BESCOF(K0,K1,HI,DI,THE1,THEM,UPS1,UPSM,YGRID,IY,MD,mdz)
          ENDIF
          IF(NPOL.EQ.1.AND.IZ.EQ.1) goto 999

C NORMAL CACLULATION AWAY FROM PERFECT CONDUCTORS
          IF(NPOL.EQ.0) THEN
C ************** Bpol bottom boundary condition ***************
            KSURF = ZGRID(IZ) - ZGRID(IZ-1)
            RMINUS=(HM(IY-1)*R00+HM(IY)*R20)/(HSUM)
            SPLUS=(HM(IY-1)/R02+HM(IY)/R22)/(HSUM)
            KAPPA=RMU*OMEGA/RMINUS
            RDIV=2.D0*(R20-R00)/(HSUM*RMINUS)

            PP=(K0(IY-1)-DI(IY-1)*HI(IY-1)-DI(IY-1)*K1(IY-1))/HP0
     1        +(K0(IY+1)-DI(IY+1)*HI(IY+1)-DI(IY+1)*K1(IY+1))/HP
     1        -(HI(IY+1)+HI(IY-1))/(ARTI*HP*HP0)-PI*SPLUS*RMINUS/KSURF
     1        -PI*0.5D0*SPLUS*RMINUS*KSURF*(CI*KAPPA-BY*RDIV-QY)

            IF(IY.EQ.2) THEN
              NP=(0.D0,0.D0)
            ELSE
              NP=(K0(IY-2)-DI(IY-2)*HI(IY-2)-DI(IY-2)*K1(IY-2))/HM(IY-2)
     1          -HP0SUM*(K0(IY-1)-DI(IY-1)*HI(IY-1)-DI(IY-1)*K1(IY-1))
     1          /(HM(IY-2)*HP0)+(HI(IY+1)+HI(IY-1))/(ARTI*HP0*HPSUM)
     1          +PI*0.5D0*KSURF*SPLUS*RMINUS*(AY*RDIV+PY)
            END IF

            IF(IY.EQ.NY-1) THEN
```

```
            QP=(0.D0,0.D0)
            TP=ARTI*PI*0.5D0+(K0(NY)-DI(NY)*HI(NY)
     1        -DI(NY)*K1(NY))/HM(NY-1)
     1        -(HI(NY)+HI(NY-2))/(ARTI*HP*HPSUM)
     1        -PI*0.5D0*KSURF*SPLUS*RMINUS*(CY*RDIV+RY)
          ELSE
            QP=(K0(IY+2)-DI(IY+2)*HI(IY+2)-DI(IY+2)*K1(IY+2))/HP1
     1        -HP1SUM*(K0(IY+1)-DI(IY+1)*HI(IY+1)-DI(IY+1)*K1(IY+1))
     1        /(HP*HP1)+(HI(IY+1)+HI(IY-1))/(ARTI*HP*HPSUM)
     1        +PI*0.5D0*KSURF*SPLUS*RMINUS*(CY*RDIV+RY)
            TP=(K0(NY)-DI(NY)*HI(NY)-DI(NY)*K1(NY))/HM(NY-1)
     1         -(K0(NY-1)-DI(NY-1)*HI(NY-1)-DI(NY-1)*K1(NY-1))/HM(NY-1)
     1         +ARTI*PI*0.5D0
          END IF
          SP=-TP+PI*0.5D0*SPLUS*RMINUS*KSURF*CI*(KAPPA
     1         -OMEGA*RMU/RESGR(1,IZ-1))

          CO(IY)=PP
          CO(IY-1)=NP
          CO(IY+1)=QP
          COM=SP
          COP=TP
          IF(IY.GE.4) THEN
            DO I=2,IY-2
c*** these are the first summation values for rp(i)
              CO(I)=(K0(I-1)-DI(I-1)*HI(I-1)-DI(I-1)*K1(I-1))/HM(I-1)
     1       +(K0(I+1)-DI(I+1)*HI(I+1)-DI(I+1)*K1(I+1))/HM(I)
     1       -(HM(I)+HM(I-1))*(K0(I)-DI(I)*HI(I)-DI(I)*K1(I))
     1       /(HM(I)*HM(I-1))
            END DO
          END IF
          IF(IY.LE.NY-3) THEN
            DO I=IY+2,NY-1
c*** these are the second summation values for rp(i)
              CO(I)=(K0(I-1)-DI(I-1)*HI(I-1)-DI(I-1)*K1(I-1))/HM(I-1)
     1       +(K0(I+1)-DI(I+1)*HI(I+1)-DI(I+1)*K1(I+1))/HM(I)
     1       -(HM(I)+HM(I-1))*(K0(I)-DI(I)*HI(I)-DI(I)*K1(I))
     1       /(HM(I)*HM(I-1))
            END DO
          END IF
        ELSE
c ************* Epol bottom boundary condition ******************
          KSURF = ZGRID(IZ) - ZGRID(IZ-1)
          KAPPA  = OMEGA * RMU *
     +       (HM(IY-1)/R00+HM(IY)/R20)/ HSUM
          IF (ABS(Y).LE.PRCOND) THEN
            TP=(K0(NY)/YM-2.D0*ARTI**2*YM*UPSM)
     1        -ARTI*(HI(NY)+K1(NY))+ARTI*PI*0.5D0
            SP=-TP+PI*KSURF*0.5D0*CI*(KAPPA-RMU*OMEGA/RESGR(1,NZ-1))
            IF(IY.NE.2) LP=-(K0(1)-DI(1)*HI(1)-DI(1)*K1(1))/HM(1)
     1        +(K0(2)-DI(2)*HI(2)-DI(2)*K1(2))/HM(1)-ARTI*(HI(1)+K1(1))
     1        -K0(1)/Y1+2.0D0*ARTI**2*UPS1*Y1
            IF(IY.NE.NY-1) MP=-(K0(NY)-DI(NY)*HI(NY)-DI(NY)
     1        *K1(NY))/HM(NY-1)
     1        +(K0(NY-1)-DI(NY-1)*HI(NY-1)-DI(NY-1)*K1(NY-1))/HM(NY-1)
     1        -ARTI*(HI(NY)+K1(NY))+K0(NY)/YM-2.0D0*ARTI**2*UPSM*YM
          ELSE
            TP=(-K0(NY)/Y +ARTI*YM*(HI(NY)+K1(NY))/Y-ARTI*PI*0.5D0*YM/Y
     1        +ARTI*YM*THEM/Y)-ARTI*(HI(NY)+K1(NY))+ARTI*PI*0.5D0
            SP=-TP+PI*KSURF*0.5D0*CI*(KAPPA-RMU*OMEGA/RESGR(1,NZ-1))
            IF(IY.NE.2)  LP=(HM(1)-Y)*(K0(1)-DI(1)*HI(1)
     1        -DI(1)*K1(1))/(HM(1)*Y)
     1        +(K0(2)-DI(2)*HI(2)-DI(2)*K1(2))/HM(1)-ARTI*PI*Y1*0.5D0/Y
     1        +ARTI*THE1*Y1/Y
            IF(IY.NE.NY-1) MP=-(HM(NY-1)+Y)*(K0(NY)-DI(NY)*HI(NY)
     1        -DI(NY)*K1(NY))/(HM(NY-1)*Y)
```

```
     1       +(K0(NY-1)-DI(NY-1)*HI(NY-1)-DI(NY-1)*K1(NY-1))/HM(NY-1)
     1       -ARTI*PI*0.5D0*YM/Y+ARTI*THEM*YM/Y
           END IF

           PP=(K0(IY-1)-DI(IY-1)*HI(IY-1)-DI(IY-1)*K1(IY-1))/HP0
     1       +(K0(IY+1)-DI(IY+1)*HI(IY+1)-DI(IY+1)*K1(IY+1))/HP
     1       -(HI(IY+1)+HI(IY-1))/(ARTI*HP*HP0)-PI/KSURF
     1       -PI*0.5D0*KSURF*(CI*KAPPA-QY)

           IF(IY.EQ.2) THEN
             IF(ABS(Y).LE.PRCOND) THEN
               LP=(HI(3)+HI(1))/(ARTI*HP0*HPSUM)-Y*K0(1)/(Y1*HP0)
     1           +2.0D0*ARTI**2*UPS1*Y1+PI*KSURF/(HP0*HPSUM)
             ELSE
               LP=(HI(3)+HI(1))/(ARTI*HP0*HPSUM)
     1           -Y1*K0(1)/(Y*HP0)
     1           +Y1*ARTI*(HI(1)+K1(1))/Y-ARTI*Y1*0.5D0*PI/Y
     1           +ARTI*THE1*Y1/Y+PI*KSURF/(HP0*HPSUM)
             END IF
             NP=(0.D0,0.D0)
           ELSE
             NP=(K0(IY-2)-DI(IY-2)*HI(IY-2)-DI(IY-2)*K1(IY-2))/HM(IY-2)
     1       -HP0SUM*(K0(IY-1)-DI(IY-1)*HI(IY-1)-DI(IY-1)*K1(IY-1))
     1       /(HM(IY-2)*HP0)+(HI(IY+1)+HI(IY-1))/(ARTI*HP0*HPSUM)
     1       +PI*0.5D0*KSURF*PY
           END IF

           IF(IY.EQ.NY-1) THEN
             IF(ABS(Y).LE.PRCOND) THEN
               MP=(HI(NY)+HI(NY-2))/(ARTI*HP*HPSUM)-YM0*K0(NY)/(YM*HP)
     1           -2.0D0*ARTI**2*UPSM*YM+PI*0.5D0*KSURF*RY
             ELSE
               MP=(HI(NY)+HI(NY-2))/(ARTI*HP*HPSUM)-YM*K0(NY)/(YM0*HP)
     1           +ARTI*YM*(HI(NY)+K1(NY))/YM0-ARTI*PI*0.5D0*YM/YM0
     1           +PI*0.5D0*KSURF*RY+ARTI*THEM*YM/YM0
             END IF
             QP=(0.D0,0.D0)
           ELSE
             QP=(K0(IY+2)-DI(IY+2)*HI(IY+2)-DI(IY+2)*K1(IY+2))/HP1
     1       -HP1SUM*(K0(IY+1)-DI(IY+1)*HI(IY+1)-DI(IY+1)*K1(IY+1))
     1       /(HP*HP1)+(HI(IY+1)+HI(IY-1))/(ARTI*HP*HPSUM)
     1       +PI*0.5D0*KSURF*RY
           END IF

           CO(IY)=PP
           CO(IY-1)=NP
           CO(IY+1)=QP

           IF(IY.GE.4) THEN
             DO I=2,IY-2
c*** these are the first summation values for rp(i)
               CO(I)=(K0(I-1)-DI(I-1)*HI(I-1)-DI(I-1)*K1(I-1))/HM(I-1)
     1       +(K0(I+1)-DI(I+1)*HI(I+1)-DI(I+1)*K1(I+1))/HM(I)
     1       -(HM(I)+HM(I-1))*(K0(I)-DI(I)*HI(I)-DI(I)*K1(I))
     1       /(HM(I)*HM(I-1))

             END DO
           END IF
           IF(IY.LE.NY-3) THEN
             DO I=IY+2,NY-1
c*** these are the second summation values for rp(i)
               CO(I)=(K0(I-1)-DI(I-1)*HI(I-1)-DI(I-1)*K1(I-1))/HM(I-1)
     1       +(K0(I+1)-DI(I+1)*HI(I+1)-DI(I+1)*K1(I+1))/HM(I)
     1       -(HM(I)+HM(I-1))*(K0(I)-DI(I)*HI(I)-DI(I)*K1(I))
     1       /(HM(I)*HM(I-1))
```

```
            END DO
          END IF

          COM=SP
          COP=TP
          CO(1)=LP
          CO(NY)=MP

        END IF
        GO TO 999
C Perfect conductor, field must be zero
60      DO 65 I = 1, NY
65      CO(I)   =(0.D0,0.0D0)
        IFLAG=0
C
C*********************************
C       WRITE (6,*) '*** END SURF  '
C*********************************
999     RETURN
        END
```

```
      SUBROUTINE COEFF2(IY,IZ,NC0,NC,IFLAG,COF,YGRID,ZGRID,
     &       RESGR,SIGFACT,NPOL,MD,MDZ)
C     ------------------ CALCULATES EQUATION COEFFS FOR ONE POINT.
C VERSION FOR TWO-DIMENSIONAL ELECTRIC AND MAGNETIC POLARISATION
C BY BREWITT-TAYLOR INTEGRATED METHOD...called by CPNTA
      IMPLICIT REAL*8 (A-H,K,O-Z)
      COMMON /LIMITS/NY,NZ
      REAL*8    COF(nc0)
     1,       RESGR(MD,MDZ)
     1,       YGRID(MD)
     1,       ZGRID(MDZ)
     1,       R(8)
     1,       SIGFACT(2)
      REAL*8 PI,OMEGA,RMU,PRCOND,PRINSUL,R00,R02,R20,R22
     1,       H2,H0,K2,K0,C5IM
      INTEGER   NC
     1,       IFLAG
      COMMON /CONST/PI,OMEGA,RMU,PRCOND,PRINSUL

10    IF(IY.LE.1 .OR. IY.GE.NY) GO TO 50
C NORMAL CALCULATION WITHIN MODEL.
      NC     = 5
      IFLAG  = 1
C FIND GRID SPACINGS.
      H2     = YGRID(IY+1) - YGRID(IY)
      H0     = YGRID(IY) - YGRID(IY-1)
      K2     = ZGRID(IZ+1) - ZGRID(IZ)
      K0     = ZGRID(IZ) - ZGRID(IZ-1)
C FIND RESISTIVITIES OF REGIONS.
      R02    = RESGR(IY-1,IZ  )
      R22    = RESGR(IY  ,IZ  )
      R20    = RESGR(IY  ,IZ-1)
      R00    = RESGR(IY-1,IZ-1)
C CALCULATE COEFFICIENTS.
      IF(NPOL.NE.1) GOTO 900
C E-POL CALCULATIONS
      IF(R02.LT.PRCOND.OR.R22.LT.PRCOND) GO TO 30
      IF(R20.LT.PRCOND.OR.R00.LT.PRCOND) GO TO 30
C NORMAL CACLULATION AWAY FROM PERFECT CONDUCTORS
      C5IM   = 0.5D0 * OMEGA * RMU *
     &       ( H0 * K0 / R00
     &       + H0 * K2 / R02
     &       + H2 * K0 / R20
     &       + H2 * K2 / R22 )
      COF(1)   = (H0 + H2) / (C5IM * K0)
      COF(3)   = (H0 + H2) / (C5IM * K2)
      COF(2)   = (K0 + K2) / (C5IM * H2)
      COF(4)   = (K0 + K2) / (C5IM * H0)
      COF(5)   = COF(1) + COF(2) + COF(3) + COF(4)
      SIGFACT(1)=1.D0-(0.5D0*OMEGA*RMU*(H0+H2)*(K0*(1/RESGR(1,IZ-1))
     &          +K2*(1/RESGR(1,IZ)))/C5IM)
      GO TO 999

C*** B-POL SOLUTION
900   IF(R02 .LT. PRCOND .OR. R22 .LT. PRCOND) THEN
        KPLUS = K0
        K2=K0
      ELSE
        KPLUS = K0+K2
      END IF
      C5IM   = 0.5D0 * RMU * OMEGA * (H0+H2) * KPLUS
      COF(1)   = (H0*R00 + H2*R20) / (K0*C5IM)
      COF(2)   = (K0*R20 + K2*R22) / (H2*C5IM)
      COF(3)   = (H2*R22 + H0*R02) / (K2*C5IM)
      COF(4)   = (K2*R02 + K0*R00) / (H0*C5IM)
      COF(5)   = COF(1) + COF(2) + COF(3) + COF(4)
```

```
C EXTRA STUFF DUE TO SOLVING FOR ANOMALOUS FIELDS
      SIGFACT(1)=(H2*(RESGR(1,IZ-1)-R20)
     &           +H0*(RESGR(1,IZ-1)-R00))/(K0*C5IM)
      SIGFACT(2)=(H2*(RESGR(1,IZ)-R22)
     &           +H0*(RESGR(1,IZ)-R02))/(K2*C5IM)
      GC TO 999

C PERFECT CONDUCTOR, FIELD MUST BE ZERO
30    DO 35 I = 1, 5
35    COF(I)   = 0.D0
      GO TO 999
C
C AT EDGES OF MODEL. NO COEFFICIENTS
50    NC     = 0
      IFLAG  = 0
999   RETURN
      END
```

```
C     ---------------------------------------
      SUBROUTINE MODBES(KK0,KK1,X)
C     ---------------------------------------
C     SUBROUTINE TO DETERMINE THE ZEROTH AND FIRST ORDER MODIFIED
C     BESSEL FUNCIONS OF THE SECOND KIND, K0 AND K1..called by BESCOF
C     AMS 55 - REFERS TO TEXT:  HANDBOOK OF MATHEMATICAL FUNCTIONS
C          BY ABRAMOWITZ AND STEGUN,1964.

      IMPLICIT COMPLEX*16(E,F,I,X,Z),REAL*8(A-D,K,O-W)
      COMPLEX*16 CDEXP,KK0,KK1,RTI,RTIN,ARTI,CI,THETA,PHI
      COMMON/CPLX/CI,RTI,RTIN,ARTI
      REAL*8   X,X8,X8DX
      COMMON/PI/PI,PID2,PID4,D2


C
C  AMS 55 - 9.11.1
      BER(U,V,W) =1.0D0 + V*( 113.77777778D0 + V*( 2.64191484D0 +
     +    V  * ( .00122678D0)))
     +   -W*(64.D0+V*(32.36345681D0+V*(.08349755D0+V*.00000948D0)))
C
C  AMS 55 - 9.11.2
      BEI(U,V,W) = (16.D0+V*(72.81777778D0+V*(.52185972D0+V*.00011615D0
     +   ))-W*(113.77777778D0+V*(10.56765936D0+V*.01104100D0)))*U*U*D2
C
C  AMS 55 - 9.11.5
      DBER(U,V,W) = (W*(14.22222222D0+V*(.66047849D0+V*.00045957D0))
     +   -(4.D0+V*(6.0681481D0+V*(.02609253D0+V*.00000394D0))))*U*U*U*D2
C
C  AMS 55 - 9.11.6
      DBEI(U,V,W)=(.5D0+V*(11.37777772D0+V*(.14677204D0+V*.00004609D0))
     +      -W*(10.66666666D0+V*(2.31167514D0+V*.00379386D0)))*U
C
C  AMS 55 - 9.11.11
      THETA(U)= -.3926991D0*CI+U*(.0110486D0-.0110485D0*CI+U*(
     +   -.0009765D0*CI+U*(-.0000906D0-.0000901D0*CI+U*(-.0000252D0+U*
     +   ( -.0000034D0+.0000051D0*CI+U*(.0000006D0+.0000019D0*CI))))))
C
C  AMS 55 - 9.11.9
      FF(U,V) = DSQRT(PID2/U)*CDEXP(-U*RTI+THETA(-V))
C
C  AMS 55 - 9.11.14
      PHI(U)=RTI+U*(-.0625001D0-.0000001D0*CI+U*(-.0013813D0+.0013811D0
     +   *CI+U*(.0000005D0+.0002452D0*CI+U*(.0000346D0+.0000338D0*CI +
     +   U*(.0000117D0-.0000024D0*CI+U*(.0000016D0-.0000032D0*CI))))))
C ---------------------------------------------------------------------
C ---------------------------------------------------------------------

      KK0=(0.D0,0.D0)
      KK1=(0.D0,0.D0)
C
C     constants for common block PI
C
      PI=3.14159265358979D0
      PID2=.5D0*PI
      PID4=.25D0*PI
      D2=1.0D0/(8.D0**2)

      X8 = (0.125*X)**8
      SQX8 = DSQRT(X8)
      IF(X.GT.8.D0) GOTO 20
      BERX  =  BER(X,X8,SQX8)
      BEIX  =  BEI(X,X8,SQX8)
      DBERX = DBER(X,X8,SQX8)
      DBEIX = DBEI(X,X8,SQX8)
C
```

```
C  AMS 55 - 9.11.3
      KER =-DLOG(X/2)*BERX+PID4*BEIX-.5772156649D0-SQX8*(59.05819744D0+
     +       X8*(60.60977451D0+X8*(.19636347D0+X8*.00002458D0)))+X8*
     +       (171.36272133D0+X8*(5.65539121D0+X8*.00309699D0))
C
C  AMS 55 - 9.11.4
      KEI =-DLOG(X/2)*BEIX-PID4*BERX+(X*X*D2)*(6.76454936D0+X8*(
     +      124.2356965D0+X8*(1.17509064D0+X8*.00029532D0)))-(X*X*D2)*
     +      SQX8*(142.91827687D0+X8*(21.30060904D0+X8*.02695875D0))
C
C  AMS 55 - 9.11.7
      DKER =-DLOG(X/2)*DBERX-(BERX/X)+PID4*DBEIX+(X*X*X*D2)*(
     + -3.69113734D0-X8*(11.36433272D0+X8*(.06136358D0+X8*.00001075D0
     + )))+(X*X*X*
     +  D2)*(SQX8*(21.42034017D0+X8*(1.4138478D0+X8*.00116137D0)))
C
C  AMS 55 - 9.11.8
      DKEI=-DLOG(X/2)*DBEIX-(BEIX/X)-PID4*DBERX+X*.21139217D0-X*SQX8*(
     +     13.39858846D0+X8*(4.65950823D0+X8*.00926707D0))+X8*X*
     +     (19.41182758D0+X8*(.33049424D0+X8*.00011997D0))
C
C  AMS 55 - 9.9.2
      KK0 =   KER + CI*KEI
C
C  AMS 55 - 9.9.2 , 9.9.17
      KK1 =-RTIN * (DKER + CI*DKEI)
C
      GO TO 40
   20 IF(X.GE.120.0D0) GO TO 30
      X8DX = 8.D0/X
C
C  AMS 55 - 9.11.9
      KK0    = FF(X,X8DX)
C
C
C     AMS 55 - 9.9.2, 9.9.17, 9.11.12
      KK1 =RTIN*KK0*PHI(-X8DX)

      GO TO 40
30    KK0 =(0.0D0,0.0D0)
      KK1 =(0.0D0,0.0D0)
C
40    RETURN
      END
```

```
C     ------------------------------------------------------
      SUBROUTINE BESCOF(K0,K1,HI,DI,THE1,THEM,UPS1,UPSM,YGRID,IY
     1,MD,mdz)
C     ------------------------------------------------------
c     called by SURF.....contains functions THETA and UPSLN
C     subroutine to set up initial integral coefficients for
C     the integral boundary condition at E(Y,0+) and B(Y,0+)
C     -GET COEFFS: K0(m,j),HI(m,j),K1(m,j),THE(M),THE(1),UPS(M),UPS(1)
C     and values DI(m)

      COMMON /LIMITS/NY,NZ
      COMPLEX*16 K0(200),K1(200),HI(200),Z
      COMPLEX*16 K0TEMP,K1TEMP,HHTEMP,IITEMP,THE1,THEM,UPS1,UPSM
      COMPLEX*16 RTI,RTIN,ARTI,CI,THETA,UPSLN
      REAL*8 YGRID(MD),X,ALPHA,D,DI(200)
      COMMON/CPLX/CI,RTI,RTIN,ARTI
      COMMON/ALPHA/ALPHA
C ****
      D= (YGRID(IY)-YGRID(1))
      X= ALPHA*D
      DI(1)=X
      Z= RTI*X
      CALL MODBES(K0TEMP,K1TEMP,X)
      CALL INTK0(X,Z,HHTEMP,IITEMP)
      K0(1)=K0TEMP
      K1(1)=K1TEMP
      HI(1)=HHTEMP
C ****
      IF(YGRID(IY).EQ.0.0D0) THEN
          UPS1=UPSLN(X,HHTEMP)
      ELSE
          THE1= THETA(X,-YGRID(IY)*ALPHA,HHTEMP)
      END IF
C ****
      DO 20 I=2,IY-1
         D=(YGRID(IY)-YGRID(I))
         X=ALPHA*D
         DI(I)=X
         Z=RTI*X
         CALL MODBES(K0TEMP,K1TEMP,X)
         CALL INTK0(X,Z,HHTEMP,IITEMP)
         K0(I)=K0TEMP
         K1(I)=K1TEMP
         HI(I)=HHTEMP
 20   CONTINUE
      D= (YGRID(NY)-YGRID(IY))
      X= ALPHA*D
      DI(NY)=X
      Z= RTI*X
      CALL MODBES(K0TEMP,K1TEMP,X)
      CALL INTK0(X,Z,HHTEMP,IITEMP)
      K0(NY)=K0TEMP
      K1(NY)=K1TEMP
      HI(NY)=HHTEMP

      IF(YGRID(IY).EQ.0.0D0) THEN
          UPSM=UPSLN(X,HHTEMP)
      ELSE
          THEM=THETA(X,YGRID(IY)*ALPHA,HHTEMP)
      ENDIF
C ****
      DO 30 I=NY-1,IY+1,-1
         D=(YGRID(I) -YGRID(IY))
         X=ALPHA*D
         DI(I)=X
         Z=RTI*X
```

```
            CALL MODBES(K0TEMP,K1TEMP,X)
            CALL INTK0(X,Z,HHTEMP,IITEMP)
            K0(I)=K0TEMP
            K1(I)=K1TEMP
            HI(I)=HHTEMP
   30       CONTINUE
C ****
         RETURN
         END
C ***************************************************************
         FUNCTION THETA(X,A,HHD)
C ***************************************************************
         COMPLEX*16 THETA,HHTEMP,HHD,HH,II,ARTI,CI,RTI,RTIN
         REAL*8 RSQ,RSQTEM,X,A,ALPHA,INC,S
         COMMON/CPLX/CI,RTI,RTIN,ARTI
         COMMON/ALPHA/ALPHA
         M=400
         THETA=(0.0D0,0.0D0)
         IF(100.D0-X)40,40,20
20       INC=100.0D0/M
         N=INT((100.0D0-X)/INC+1)
         HHTEMP=HHD
         RSQTEM =  (1.0D0/(X+A))**2
         DO 25 I=1,N
            S =X+I*(100.0D0-X)/N
            RSQ =  (1.0D0/(S+A))**2
            CALL INTK0(S,S*RTI ,HH,II)
            THETA=THETA + (RSQ+RSQTEM)*(HH-HHTEMP)
            HHTEMP=HH
            RSQTEM=RSQ
25       CONTINUE
         THETA=-CI*THETA*0.5D0
40       RETURN
         END
C ***************************************************************
         FUNCTION UPSLN(X,HHD)
C ***************************************************************
         COMPLEX*16 UPSLN,HHTEMP,HHD,HH,II,ARTI,CI,RTI,RTIN
         REAL*8 CUBE,CUBTEM,X,ALPHA,INC,S
         COMMON/CPLX/CI,RTI,RTIN,ARTI
         COMMON/ALPHA/ALPHA
         UPSLN=(0.0D0,0.0D0)
         M=400
         IF(100.D0-X)40,40,20
20       INC=1000.0D0/M
         N=INT((100.0D0-X)/INC+1)
         HHTEMP=HHD
         CUBTEM=1.0D0/X**3
         DO 25 I=1,N
            S =X+I*(100.0D0-X)/N
            CUBE=1.0D0/S**3
            CALL INTK0(S,S*RTI,HH,II)
            UPSLN=UPSLN + (CUBE +CUBTEM)*(HH-HHTEMP)
            HHTEMP=HH
            CUBTEM=CUBE
25       CONTINUE
         UPSLN = -CI*UPSLN*0.5D0*RTIN
40       RETURN
         END
```

```
C     ------------------------------------
      SUBROUTINE INTK0(X,Z,HH,II)
C     ------------------------------------
C     SUBROUTINE TO CALCULATE THE INTEGRAL OVER THE MODIFIED BESSEL
C     FUNCTION ,K0 .....called by BESCOF
      IMPLICIT COMPLEX*16(E,F,G,I,Y,Z),REAL*8(A-D,K,O-X)
      REAL*8 Y,X
      COMPLEX*16 CDEXP,W,HH
      COMMON/PI/PI,PID2,PID4,D2
      COMMON/SV/ AA(23),PP(23),Q(23),P(23),B(11),C(11),Q0,P00
      COMMON/SV1/NQ
C
C
C     AMS 55 - 11.1.18
      ZF(G) = 1.25331414D0+G*(.11190289D0+G*(.02576646D0+G*(.00933994D0+
     +     G*(.00417454D0+G*(.00163271D0+G*.00033934D0)))))
C
      IF(NQ.NE.0) GO TO 1
      W=(1.0D0,0.0D0)
      NQ = 1
      P00 = W - .57721566490153D0 + DLOG(2.0D0)
      R = (0.0D0,0.0D0)
      Q0 = -PID4
      AA(1) = 32.D0/3.D0
      Q(1) = AA(1)*Q0
      PP(1) = AA(1)*(P00+W/3.D0)
      DO 2 N = 2,23
      A = W*N
      AA(N) = 32.D0*(A+A-W)/((A+A+W)*A*A)*AA(N-1)
      Q(N) = AA(N)*Q0
      R = R + W/A
    2 PP(N) = AA(N)*(P00+R+W/(W+A+A))
C
    1 IF(X.GE.8.D0) GOTO 5
C
C     AMS - 55  11.1.9
      DL = DLOG(X)
      DO 3 N = 1,23
    3 P(N) = PP(N) - AA(N)*DL
      DD = X*X*D2/2.0D0
      B0 = P00 - DL - DD*Q(1)
      C0 = Q0 + DD*P(1)
      DO 4 N = 1,11
      B(N) = P(N+N) - DD*Q(N+N+1)
    4 C(N) = Q(N+N) + DD*P(N+N+1)
      D4 = -DD*DD
      R = B0+D4*(B(1)+D4*(B(2)+D4*(B(3)+D4*(B(4)+D4*(B(5)+D4*(B(6)+D4*
     1     (B(7)+D4*(B(8)+D4*(B(9)+D4*(B(10)+D4*B(11))))))))))
      S = C0+D4*(C(1)+D4*(C(2)+D4*(C(3)+D4*(C(4)+D4*(C(5)+D4*(C(6)+D4*
     +     (C(7)+D4*(C(8)+D4*(C(9)+D4*(C(10)+D4*C(11))))))))))
      HH = X*((R-S) + (0.0D0,1.0D0)*(R+S))/dsqrt(2.0d0)
      II = PID2 - HH
C
      GOTO 6
C
    5 IF(  X .GE.60.0D0) GO TO 7  !this can be ge.120.0e0 on IBM
      GG = -7.D0/Z
      II = ZF(GG)/(CDSQRT(Z)*CDEXP(Z))
      HH = PID2 - II
    6 GO TO 8
C
    7 II=0.0D0
      HH=PID2
    8 RETURN
      END
```

```
      SUBROUTINE GAUSSJF(A,RHS,C,DIYM1,IZ,IY,TA,TC,B,MD1,MD2,npol)
C*** Gauss-Jordan based elimination (line-by line forward ***
C*** elimination for one sub-block of the matrix) ***
c*** called from MATRIX.FOR ***
      COMMON /BAND/NSM,KSTART,KFLAG,KEND,KFIRST
      COMPLEX*16 ZDUM,TA(MD1,MD2),TC(MD1,MD2),B(MD1)
     1,DIYM1,A(MD1),C(MD1),RHS
      INTEGER IZ,IY
      INTEGER NSM,KSTART,KFLAG,KEND,KFIRST

      IF(NPOL.EQ.0.AND.IZ.EQ.2) GOTO 30
      IF(IZ.NE.1) THEN
       IF(DIYM1.EQ.(0.D0,0.D0)) GOTO 30
       IF(KEND.NE.1) THEN
         IF(IY.NE.1) A(IY-1)=A(IY-1)/DIYM1
         A(IY)=A(IY)/DIYM1
         A(IY+1)=A(IY+1)/DIYM1
         C(IY)=C(IY)/DIYM1
       ELSE
         DO 10 I=1,NSM
   10    A(I)=A(I)/DIYM1
       END IF
        RHS=RHS/DIYM1
        do 20 I=1,NSM
c*** eliminating lower diagonal (DIYM1 coefficients) by ***
c*** combination with previous sub-block ***
            A(I)=A(I)-TC(I,IY)
            TC(I,IY)=(0.D0,0.D0)
   20   CONTINUE
            RHS=RHS-B(IY)
            B(IY)=(0.D0,0.D0)
      END IF

C*** commencing regular forward Gaussian elimination ***
   30 NFIN=4*INT(NSM/4)
      NREM=NSM-NFIN
      IF(IY.NE.1) THEN
      DO 31 I=1,IY-1
        ZDUM=A(I)
        A(I)=(0.D0,0.D0)
          DO 40 J=I+1,NSM
   40     A(J)=A(J)-TA(J,I)*ZDUM
        IF(KEND.EQ.1) GOTO 55
          DO 50 J=1,NFIN,4
          C(J)=C(J)-TC(J,I)*ZDUM
          C(J+1)=C(J+1)-TC(J+1,I)*ZDUM
          C(J+2)=C(J+2)-TC(J+2,I)*ZDUM
          C(J+3)=C(J+3)-TC(J+3,I)*ZDUM
   50     CONTINUE
          DO 51 J=NFIN+1,NFIN+NREM
   51     C(J)=C(J)-TC(J,I)*ZDUM
   55     RHS=RHS-B(I)*ZDUM
   31 CONTINUE
      END IF
C*** checking for singularity ****
      IF(A(IY).EQ.(0.D0,0.D0)) GO TO 99

C*** adding line into sub-block arrays ***
      ZDUM=(1.D0,0.D0)/A(IY)
      TA(IY,IY)=(0.D0,0.D0)
        DO 60 J=IY+1,NSM
   60   TA(J,IY)=A(J)*ZDUM
      IF(KEND.EQ.1) GOTO 75
        DO 70 J=1,nfin,4
        TC(J,IY)=C(J)*ZDUM
        TC(J+1,IY)=C(J+1)*ZDUM
```

```
      TC(J+2,IY)=C(J+2)*ZDUM
      TC(J+3,IY)=C(J+3)*ZDUM
       C(J)=(0.D0,0.D0)
       C(J+1)=(0.D0,0.D0)
       C(J+2)=(0.D0,0.D0)
70     C(J+3)=(0.D0,0.D0)
       DO 71 J=NFIN+1,NFIN+NREM
       TC(J,IY)=C(J)*ZDUM
71     C(J)=(0.D0,0.D0)
75  B(IY)=RHS*ZDUM
    RETURN

99  PRINT *,'THIS MATRIX IS SINGULAR!!! (too bad)'
    PRINT *,A(IY),IY,IZ
    STOP
    END
```

```
      SUBROUTINE GAUSSJB(TA,B,TC,IZ,MD1,MD2)
C*** Gauss-Jordan based elimination (backelimination for ***
C*** one sub-block of the matrix) called from MATRIX.FOR ***
      COMMON /BAND/NSM,KSTART,KFLAG,KEND,KFIRST
      COMPLEX*16 ZDUM,TA(MD1,MD2),TC(MD1,MD2),B(MD1)
      INTEGER NSM,KSTART,KFLAG,KEND,KFIRST,IREC,ISTART,IZ

      NFIN=4*INT(NSM/4)
      NREM=NSM-NFIN
      DO 10 J=NSM,2,-1
        DO 20 K=J-1,1,-1
          ZDUM=TA(J,K)
          TA(J,K)=(0.D0,0.D0)
          IF(KEND.EQ.1) GOTO 26
            DO 25 L=1,Nfin,4
            TC(L,K)=TC(L,K)-TC(L,J)*ZDUM
            TC(L+1,K)=TC(L+1,K)-TC(L+1,J)*ZDUM
            TC(L+2,K)=TC(L+2,K)-TC(L+2,J)*ZDUM
            TC(L+3,K)=TC(L+3,K)-TC(L+3,J)*ZDUM
 25         CONTINUE
          DO 27 L=NFIN+1,NFIN+NREM
 27       TC(L,K)=TC(L,K)-TC(L,J)*ZDUM
 26       B(K)=B(K)-B(J)*ZDUM
 20     CONTINUE
 10   CONTINUE
      IF(KEND.EQ.1) RETURN
C*** Storing C matrix in temporary file ***
      ISTART=(IZ-1)*NSM
      DO 80 I=1,NSM
      IREC=ISTART+I
      WRITE(13'IREC) (TC(j,i),J=1,NSM),B(i)
 80   CONTINUE
      RETURN
      END
```

```
      SUBROUTINE BACKSUB(A,B,FIELD,NPOL,MD,MDZ,MD1,MD2)
c this subroutine does the backsubstitution in the matrix
c elimintaion...called from MATRIX  (H.Poll 1988)
      COMMON /BAND/NSM,KSTART,KFLAG,KEND,KFIRST
      COMMON /LIMITS/NY,NZ
      COMPLEX*16 A(MD1,MD2),B(MD1),FIELD(MD,MDZ)
      INTEGER NZB,NSM,IREC,NPOL,KSTART,KFLAG,KEND,KFIRST
C*** LAST RECORD WRITTEN WAS FOR NZ=NZ-1  ***
C*** SO IREC(LAST) WAS ((NZ-1)-1)*NSM+NSM ***
      IREC=NZ*NSM-NSM
      NZB=1
      DO 10 I=2,NY-1
        FIELD(I,NZ)=B(I-1)
   10 CONTINUE
      IF(NPOL.EQ.0) NZB=2
      DO 100 IZ=NZ-1,NZB,-1
      DO 20 K=NSM,1,-1
        READ(13'IREC) (A(J,K),J=1,NSM),B(K)
        IREC=IREC-1
   20 CONTINUE
      DO 30 I=1,NSM
        DO 40 J=1,NSM
          B(I)=B(I)-A(J,I)*FIELD(j+1,IZ+1)
   40   CONTINUE
   30 CONTINUE
      DO 50 I=2,NY-1
        FIELD(I,IZ)=B(I-1)
   50 CONTINUE
  100 CONTINUE
      RETURN
      END
```

```
      SUBROUTINE WRITE(YGRID,ZGRID,FIELD,MD,MDZ,NPOL)
c***  writes out the calculated fields...called by MATRIX  ****
      COMMON /LIMITS/NY,NZ
      COMMON /PER/T
      common /eone/fone
      COMMON /GROPT/NUN,YMIN,YMAX,ZMAX,GRAP
      COMPLEX*16 FIELD(MD,MDZ),FL1
      REAL*8 YGRID(MD),ZGRID(MDZ)
      REAL T
      CHARACTER*8 CHARPOL
      CHARACTER*6 GRAP
      INTEGER NUN,YMIN,YMAX,ZMAX

      DO 100 J=1,NZ
      FL1=FIELD(1,J)
      DO 200 I=1,NY
      FIELD(I,J)=FIELD(I,J)+FL1
  200 CONTINUE
  100 CONTINUE

      IF(NPOL.EQ.1) CHARPOL='ELECTRIC'
      IF(NPOL.EQ.0) CHARPOL='MAGNETIC'
      IF(ZMAX.NE.0) WRITE(14,400) CHARPOL
  400 FORMAT(///35X,'REAL PART X-COMPONENT ',A8,' FIELD'/)

      KK=YMIN
      KJ=YMIN+7
      print *,'field in write',field(ny,2)
   10 IF(ZMAX.NE.0) WRITE(14,222) (YGRID(I)/1000,I=KK,KJ)
  222 FORMAT(/1X,'Z/Y',11X,8(G13.6,1X))
      do 230 J=1,ZMAX
        ZGR= ZGRID(J)/1000
        WRITE(14,220) ZGR,(DREAL(FIELD(I,j)),I=KK,KJ)
  230 continue
      IF(KJ.EQ.YMAX) GOTO 15
      KK=KJ+1
      KJ=KK+7
      IF(KJ.GT.YMAX) KJ=YMAX
      GOTO 10

   15 IF(ZMAX.NE.0) WRITE(14,410) CHARPOL
  410 FORMAT(//35X,'IMAG PART X-COMPONENT ',A8,' FIELD'/)

      KK=YMIN
      KJ=YMIN+7
   20 IF(ZMAX.NE.0) WRITE(14,222) (YGRID(I)/1000,I=KK,KJ)
      do 240 J=1,ZMAX
        ZGR= ZGRID(J)/1000
        WRITE(14,220) ZGR,(DIMAG(FIELD(I,J)),I=KK,KJ)
  240 CONTINUE
      IF(KJ.EQ.YMAX) GOTO 221
      KK=KJ+1
      KJ=KK+7
      IF(KJ.GT.YMAX) KJ=YMAX
      GOTO 20
  221 CONTINUE
  220 FORMAT(4X,F7.3,2X,8(F13.6,1X))
      RETURN
      END
```

```
      SUBROUTINE BDERIV(FIELD,YGRID,ZGRID,RESGR,T,STNUM,NSTS
     1,STS,MD,MDZ,IFLAG)
C 2-D H-POLARISATION VERTICAL AND HORIZONTAL ELECTRIC FIELDS
C FORMULAE : 8 DIFFERENT CASES FROM I TO VIII, DEPENDING ON
C RESISTIVITY IN EACH QUADRANT .
C AT EACH NODE ON AN INTERNAL BOUNDARY THERE ARE 2 DIFFERENT RESULTS
C V- (LEFT) OR V+ (RIGHT) AND W- (UP) OR W+ (DOWN).
C IFLAG = 0 : CHOOSE V- AND W- FOR "DERIV" VALUES
C       = 1 : CHOOSE V+ AND W+
c
c       called from FR2D
c       purpose:
c               to compute the electric field at the nodes of the grid
c               and to calculate the apparent resistivities and phases.
c
c       parameters:
c deriv will contain calculated electric field
c       deriv(1) contains Ey
c       deriv(2) contains Ez
c field contains magnetic field
c ygrid and zgrid contain the node locations
c resgr contains the resistivity values IN EACH RECTANGLE
c
c
       IMPLICIT  REAL*8 (A-H,O-Z), LOGICAL (K)
       INTEGER MD,MDZ
       COMPLEX*16         FIELD(MD,MDZ)
      1,          DERIV(2,200,200)
      1,          sMN,tMN,AJYPLUS,AJYMINUS,AJZPLUS,AJZMINUS
      1,          AJY,AJZ,VM,VP,WM,WP,ap1,ap2,ap3,ap4
       REAL*8     YGRID(MD)
      1,          ZGRID(MDZ)
      1,          RESGR(MD,MDZ)
      1,          PI,OMEGA,RMU,PRCOND,PRINSUL,A1,A2
      1,          PANG(200,100),ARES(200,100),STS(30)
       REAL T
       INTEGER IFLAG,NY,NZ,YMIN,YMAX,ZMAX,STNUM(30),kk,kj
       CHARACTER*8 CHARPOL
       CHARACTER*6 GRAP
       CHARACTER*1 HEAD
       COMMON /LIMITS/NY,NZ
       COMMON /CONST/ PI, OMEGA, RMU, PRCOND, PRINSUL
       COMMON /GROPT/NUN,YMIN,YMAX,ZMAX,GRAP


         const = (omega*rmu)
C        IFLAG = 0  ! SELECT V- (LEFT) AND W- (UP) AT BOUNDARY
C        IFLAG = 1  ! SELECT V+ (RIGHT) AND W+ (DOWN)

         DO 77   IZ = 2, NZ - 1
                 AKN = ZGRID(IZ+1) - ZGRID(IZ)
                 AKN1 = ZGRID(IZ) - ZGRID(IZ-1)
                 AKPLUS = AKN + AKN1

         DO 78   IY = 2, ny - 1
                 HM = YGRID(IY+1) - YGRID(IY)
                 HM1 = YGRID(IY) - YGRID(IY-1)
                 HPLUS = HM + HM1

c  definitions of terms containing resistivities
         resmn   = resgr(iy,iz) / CONST
         resmn1  = resgr(iy,iz-1) / CONST
         resm1n  = resgr(iy-1,iz) / CONST
         resm1n1 = resgr(iy-1,iz-1) / CONST
         RMn     = hm*AKN*resmn
         RM1n    = hm1*AKN*resm1n
```

```
      RM1n1 = hm1*AKN1*resm1n1
      RMn1  = hm*AKN1*resmn1
      rhomn = (Rmn + Rm1n + Rmn1 + Rm1n1) / (hplus*AKPLUS)

c     definitions of several coefficients
      dMN = HM*HM1/(akn*akn1*akplus) * ((akn1*rM1N-akn*rM1N1)/
     .      (RM1N+RM1N1) - (akn1*rMN - akn*rMN1)/(rMN+rMN1) )
      cMN = akn*akn1/(HM*HM1*HPLUS) * ((HM1*rMN1 - HM*rM1N1) /
     .      (rMN1+rM1N1) - (HM1*rMN-HM*rM1N)/(rMN+rM1N) )

      sMN = -HM1/HM*FIELD(IY+1,IZ) + HM/HM1*FIELD(IY-1,IZ)
     .     + dMN*(akn1/akn*FIELD(IY,IZ+1) - akn/akn1*FIELD(IY,IZ-1) )
     .     + FIELD(IY,IZ)*(HM1/HM-HM/HM1-dMN*(akn1/akn-akn/akn1)
     .   + (0.D0,0.5d0)*HM*HM1*akplus*(HM/(rMN+rMN1)-HM1/(rM1N+rM1N1)))

      tMN = akn1/akn*FIELD(IY,IZ+1) - akn/akn1*FIELD(IY,IZ-1)
     .      - cMN*(HM1/HM*FIELD(IY+1,IZ) - HM/HM1*FIELD(IY-1,IZ) )
     .      + FIELD(IY,IZ)*(akn/akn1-akn1/akn+cMN*(HM1/HM-HM/HM1)
     .      + (0.D0,0.5D0)*akn*akn1*HPLUS*(akn1/(rMN1+rM1N1)
     .                                     - akn/(rMN+rM1N) ) )

c     definitions of currents
      AJYPFAC  = (rMN1+rM1N1)/(RMU*akn1*HPLUS*akplus*RHOMN)
      AJYMFAC  = (rMN+rM1N)/(RMU*akn*HPLUS*akplus*RHOMN)
      AJYPLUS  = AJYPFAC * tMN
      AJYMINUS = AJYMFAC * tMN
      AJZPFAC  = (rM1N+rM1N1)/(RMU*HM1*HPLUS*akplus*RHOMN)
      AJZMFAC  = (rMN+rMN1)/(RMU*HM*HPLUS*akplus*RHOMN)
      AJZPLUS  = AJZPFAC * sMN
      AJZMINUS = AJZMFAC * sMN
      AJY = AJYPFAC*AJYMFAC*RMU*akplus*       tMN
      AJZ = AJZPFAC*AJZMFAC*RMU*HPLUS*sMN

c     definitions of logical terms showing which region is homogeneous
            KUP    = RESM1N1 .EQ. RESMN1
            KDOWN  = RESM1N  .eQ. RESMN
            KLEFT  = RESM1N1 .EQ. RESM1N
            KRIGHT = RESMN1  .eQ. RESMN
c     choose FROM CASES IV TO VIII
      if ( (kleft.or.kright) .and. (kup.or.kdown) ) then  ! case VIII
            VM = CONST/(HM1*AKPLUS)*(RM1N+RM1N1) * AJY
            VP = CONST/(HM*AKPLUS)*(RMN+RMN1) * ajy
            wm = const/(AKN1*hplus)*(Rmn1+Rm1n1) * ajz
            wp = const/(AKN*hplus)*(Rmn+Rm1n) * ajz
      else if (kup)    then     ! case IV
            vm = const*Rm1n/(hm1*AKN) * ajyplus
            vp = const*Rmn/(hm*AKN) * ajyplus
            wm = const/(AKN1*hplus)*(Rmn1+Rm1n1) * ajz
            wp = const/(AKN*hplus)*(Rmn+Rm1n) * ajz
      else if (kdown)  then     ! case V
            vm = const*Rm1n1/(hm1*AKN1) * ajyminus
            vp = const*Rmn1/(hm*AKN1) * ajyminus
            wm = const/(AKN1*hplus)*(Rmn1+Rm1n1) * ajz
            wp = const/(AKN*hplus)*(Rmn+Rm1n) * ajz
      else if (kleft)  then     ! CAse VI
            VM = CONST/(HM1*AKPLUS)*(RM1N+RM1N1) * AJY
            VP = CONST/(HM*AKPLUS)*(RMN+RMN1) * ajy
            wm = const*Rmn1/(hm*AKN1) * ajzplus
            wp = const*Rmn/(hm*AKN) * ajzplus
      else if (kright) then     ! CAse VII
            VM = CONST/(HM1*AKPLUS)*(RM1N+RM1N1) * AJY
            VP = CONST/(HM*AKPLUS)*(RMN+RMN1) * ajy
            WM = CONST*RM1N1/(HM1*AKN1) * AjzMINUS
            WP = const*Rm1n/(hm1*AKN) * ajzminus
      else                      ! Case VIII
            VM = CONST/(HM1*AKPLUS)*(RM1N+RM1N1) * AJY
```

```
                VP = CONST/(HM*AKPLUS)*(RMN+RMN1) * AJY
                WM = CONST/(akn1*HPLUS)*(rMN1+rM1N1) * AJZ
                WP = CONST/(akn*HPLUS)*(rMN+rM1N) * AJZ
        end if ! (cases)

c  select between 2 possible values at each node.
        IF (IFLAG.EQ.0) THEN
                DERIV (1,IY,IZ) = VM
                DERIV (2,IY,IZ) = WM
        ELSE
                DERIV (1,IY,IZ) = VP
                DERIV (2,IY,IZ) = WP
        END IF ! (IFLAG)
78              CONTINUE        !       END DO
77      CONTINUE        !       END DO


! deal with the top/bottom of the grid
        AKN = ZGRID(2) - ZGRID(1)
        AKN2 = ZGRID(3) - ZGRID(2)
        AKPLUS = AKN+AKN2
        DO 79   IY=2,NY-1
                ! TOP
        HM = YGRID(IY+1) - YGRID(IY)
        HM1 = YGRID(IY) - YGRID(IY-1)
        HPLUS = HM + HM1
        RESMN   = RESGR(IY,1) / CONST
        RESM1N  = RESGR(IY-1,1) / CONST
        RMN   = HM*akn*RESMN
        RM1N  = HM1*akn*RESM1N
        VM = OMEGA*RESM1N*(FIELD(IY,2)*AKPLUS/(AKN*AKN2)
     +      -AKN*FIELD(IY,3)/(AKN2*AKPLUS)-(AKN2+2*AKN)/(AKN*AKPLUS))
        VP = VM * RESMN/RESM1N
        DERIV(2,IY,1) = (0.D0,0.D0)
                IF (IFLAG.EQ.0) THEN
                DERIV (1,IY,1) = VM
                ELSE
                DERIV (1,IY,1) = VP
                END IF

                ! bottom
        IF (RESGR(iy,NZ) .GE. PRCOND) THEN
        DERIV(1,IY,NZ) = DERIV(1,IY,NZ-1)
        DERIV(2,IY,NZ) = DERIV(2,IY,NZ-1)
        ELSE
        DERIV(1,iy,NZ)   = (0.D0 , 0.D0)
        DERIV(1,iy,NZ-1) = (0.D0 , 0.D0)
        DERIV(2,iy,NZ)   = (0.D0 , 0.D0)
        END IF
79      CONTINUE        !       end do

! and with the edges
        DO 80   IZ=1,NZ
                ! left
                DERIV(1,1,IZ) = DERIV(1,2,IZ)
                DERIV(2,1,IZ) = DERIV(2,2,IZ)
                ! right
                DERIV(1,NY,IZ) = DERIV(1,NY-1,IZ)
80              DERIV(2,NY,IZ) = DERIV(2,NY-1,IZ)
C
C**** writing out the derivative fields ****
C*********************************
c
      HEAD='Y'
      LL=1
```

```
      CHARPOL='ELECTRIC'

   99 IF(ZMAX.NE.0) WRITE(14,400) HEAD,CHARPOL
  400 FORMAT(//35X,'REAL PART ',A1,'-COMPONENT ',A8,' FIELD'/)

      KK=YMIN
      KJ=YMIN+7
  100 IF(ZMAX.NE.0) WRITE(14,222) (YGRID(I)/1000,I=KK,KJ)
  222 FORMAT(/1X,'Z/Y',11X,8(G13.6,1X))
      do 230 J=1,ZMAX
        ZGR= ZGRID(J)/1000
        WRITE(14,220) ZGR,(DREAL(DERIV(LL,I,J)),I=KK,KJ)
  230 CONTINUE
      IF(KJ.EQ.YMAX) GOTO 150
      KK=KJ+1
      KJ=KK+7
      IF(KJ.GT.YMAX) KJ=YMAX
      GOTO 100

  150 IF(ZMAX.NE.0) WRITE(14,410) HEAD,CHARPOL
  410 FORMAT(//35X,'IMAG PART ',A1,'-COMPONENT ',A8,' FIELD'/)

      KK=YMIN
      KJ=YMIN+7
  200 IF(ZMAX.NE.0) WRITE(14,222) (YGRID(I)/1000,I=KK,KJ)
      do 240 J=1,ZMAX
        ZGR= ZGRID(J)/1000
        WRITE(14,220) ZGR,(DIMAG(DERIV(LL,I,J)),I=KK,KJ)
  240 CONTINUE
      IF(KJ.EQ.YMAX) GOTO 221
      KK=KJ+1
      KJ=KK+7
      IF(KJ.GT.YMAX) KJ=YMAX
      GOTO 200
  221 CONTINUE
  220 FORMAT(4X,F7.3,2X,8(G13.6,1X))
      IF(LL.NE.2) THEN
        LL=2
        HEAD='Z'
        GO TO 99
      END IF

      A1=RMU/OMEGA
      A2=180.D0/PI
      DO 300 IZ=1,ZMAX
        DO 310 IY=YMIN,YMAX
          CALL APRES2(ARES(IY,IZ),PANG(IY,IZ)
     +,               FIELD(IY,IZ),DERIV(1,IY,IZ),A1,A2)
        IF(DREAL(DERIV(1,IY,IZ)).GT.0.AND.DIMAG(DERIV(1,IY,IZ)).GT.0)
     +               PANG(IY,IZ)=PANG(IY,IZ)-180
        IF(DREAL(DERIV(1,IY,IZ)).GT.0.AND.DIMAG(DERIV(1,IY,IZ)).LT.0)
     +               PANG(IY,IZ)=PANG(IY,IZ)+180
  310   CONTINUE
  300 CONTINUE

  160 IF(ZMAX.NE.0) WRITE(14,420)
  420 FORMAT(//35X,'APPARENT RESISTIVITY (MAGNITUDE)'/)

      KK=YMIN
      KJ=YMIN+7
  170 IF(ZMAX.NE.0) WRITE(14,222) (YGRID(I)/1000,I=KK,KJ)
      do 250 J=1,ZMAX
        ZGR= ZGRID(J)/1000
        WRITE(14,223) ZGR,(ARES(I,J),I=KK,KJ)
  223 FORMAT(4X,F7.3,2X,8(G13.6,1X))
  250 CONTINUE
```

```
      IF(KJ.EQ.YMAX) GOTO 180
      KK=KJ+1
      KJ=KK+7
      IF(KJ.GT.YMAX) KJ=YMAX
      GOTO 170

  180 IF(ZMAX.NE.0) WRITE(14,430)
  430 FORMAT(//35X,'APPARENT RESISTIVITY - PHASE ANGLE (DEGREES)'/)

      KK=YMIN
      KJ=YMIN+7
  190 IF(ZMAX.NE.0) WRITE(14,222) (YGRID(I)/1000,I=KK,KJ)
      do 260 J=1,ZMAX
        ZGR= ZGRID(J)/1000
        WRITE(14,224) ZGR,(PANG(I,J),I=KK,KJ)
  224 FORMAT(4X,F7.3,2X,8(G13.6,1X))
  260 CONTINUE
      IF(KJ.EQ.YMAX) GOTO 999
      KK=KJ+1
      KJ=KK+7
      IF(KJ.GT.YMAX) KJ=YMAX
      GOTO 190

  999 CONTINUE
C*** WRITING OUT DATA FILES FOR GRAPHING PROGRAM ***
      IF(GRAP.LT.'NOGRAP') THEN
        WRITE(NUN,500) T
  500   FORMAT(' Resistivities and Phases for period = ',f10.3)
        WRITE(NUN,501)
  501   FORMAT('  No       Y          Res          Phase       BPOL')

        DO 503 I=1,NSTS
          JKL=STNUM(I)
          IF(STS(I)*1000.LT.YGRID(1)) JKL=1
          IF(STS(I)*1000.GT.YGRID(NY)) JKL=NY
          CALL APRES2(ARES(JKL,1),PANG(JKL,1)
     +,               FIELD(JKL,1),DERIV(1,JKL,1),A1,A2)
        WRITE(NUN,505) I,STS(I),ARES(JKL,1),PANG(JKL,1)
  505   FORMAT(I4,F12.4,2(1X,g13.6))
  503   CONTINUE
      END IF
      RETURN
      END
```

```
C     ------------------------------------------------------------
      SUBROUTINE EDERIV(FIELD,YGRID,ZGRID,RESGR,T,STNUM,NSTS
     1,STS,MD,MDZ)
C       ------------------- DERIVATIVE CALCULATION.
C
C       called from FR2D
C       PURPOSE:
C         TO COMPUTE THE MAGNETIC FIELD AT THE NODES OF THE GRID
C         AND CALCULATE THE APPARENT RESISTIVITIES AND PHASES
C
C       PARAMETERS:
C DERIV       WILL CONTAIN CALCULATED MAGNETIC FIELD
C       DERIV(1) CONTAINS BY
C       DERIV(2) CONTAINS BZ
C FIELD       CONTAINS ELECTRIC FIELD
C YGRID AND ZGRID CONTAIN THE NODE LOCATIONS
C RESGR       CONTAINS THE RESISTIVITY VALUES IN EACH RECTANGLE
C
C       METHOD:
C  A NUMBER OF COEFFICIENTS ARE COMPUTED TO EVALUATE
C  THE TWO FIELD COMPONENTS.
C
C
       IMPLICIT
      +         REAL*8 (A,B,D-H,O-Z)
      +,        LOGICAL*1 (C,K)
       COMMON /LIMITS/NY,NZ
       COMMON /GROPT/NUN,YMIN,YMAX,ZMAX,GRAP
       common /eone/fone
       INTEGER MD,MDZ,YMIN,YMAX,ZMAX,STNUM(30),KK,KJ,stsenter
       CHARACTER*1 HEAD
       CHARACTER*6 GRAP
       CHARACTER*8 CHARPOL
       COMPLEX*16  FIELD(MD,MDZ)
      +,         fone(2,200)
      +,         fhold,dholdl,DHOLD2,e3
      +,         DERIV(2,200,200)
      +,         D1
      +,         D2
      +,         CONST
      +,         CONST1
      +,         E
      +,         EZ1
      +,         EZ2
      +,         EY1
      +,         EY2
      +,         WY,WZ
      +,         E1,E2,EM1,EM2
      +,         EY12,EY11,EY13
      +,         EZ11,EZ12,EZ13,EZ14
      +,         EN,EN1,EN2
       REAL*8    YGRID(MD)
      +,         ZGRID(MDZ)
      +,         RESGR(MD,MDZ)
      +,         PI,OMEGA,RMU,PRCOND,PRINSUL,A1,A2
      +,         ARES(200,200),PANG(200,200),STS(30)
      +,         DIFF,DELTA
       REAL T
       INTEGER NY,NZ
       COMMON    /CONST/
      +          PI
      +,         OMEGA
      +,         RMU
      +,         PRCOND
      +,         RRINSUL
C************************************
```

```
C     WRITE (6,*) '*** START DERIVE...'
C************************************
C
      CONST  = DCMPLX(0.D0, 1.D0/OMEGA)
      CONST1 = DCMPLX(0.D0, 0.5D0*OMEGA*RMU)
      DO 77  IZ = 2, NZ - 1
        ZN = ZGRID(IZ+1) - ZGRID(IZ)
        ZN1 = ZGRID(IZ) - ZGRID(IZ-1)
        Z2 = ZN + ZN1
        ZN$2 = ZN * ZN
        ZN1$2 = ZN1 * ZN1
        AY = ZN * ZN1 / Z2

        DO 78  IY = 2, NY - 1
C         ! NORMAL CALCULATION
          YM = YGRID(IY+1) - YGRID(IY)
          YM1 = YGRID(IY) - YGRID(IY-1)
          Y2 = YM + YM1
          YM$2 = YM * YM
          YM1$2 = YM1 * YM1
          AZ = YM * YM1 / Y2

          E = FIELD(IY,IZ)
          EZ1 = FIELD (IY,IZ+1) / ZN$2
          EZ2 = FIELD (IY,IZ-1) / ZN1$2
          IF (RESGR(IY,IZ).GE.PRCOND)
     +          THEN
C       !NORMAL CALCULATION
            WY1 = (YM/RESGR(IY,IZ))
     +            + (YM1/RESGR(IY-1,IZ))
            WY2 = (YM/RESGR(IY,IZ-1))
     +             + (YM1/RESGR(IY-1,IZ-1))
            WY = (1.D0/ZN$2) - (1.D0/ZN1$2)
     +           + CONST1*(WY1-WY2) / Y2
            DERIV(1,IY,IZ) = CONST*AY*(EZ1 - EZ2 - WY*E)
          ELSE
            ZN2 = ZGRID(IZ-1) - ZGRID(IZ-2)
            AY1 = ZN1/(ZN1+ZN2)
         DERIV(1,IY,IZ)=CONST*(FIELD(IY,IZ-2)*AY1-FIELD(IY,IZ-1)/AY1)/ZN2
          END IF

          EY1 = FIELD (IY+1,IZ) / YM$2
          EY2 = FIELD (IY-1,IZ) / YM1$2
          IF (RESGR(IY,IZ).GE.PRCOND)
     +          THEN
C       !NORMAL CALCULATION
            WZ1 = (ZN/RESGR(IY,IZ))
     +            + (ZN1/RESGR(IY,IZ-1))
            WZ2 = (ZN/RESGR(IY-1,IZ))
     +            + (ZN1/RESGR(IY-1,IZ-1))
            WZ = (1.D0/YM$2) - (1.D0/YM1$2) + CONST1*(WZ1-WZ2) / Z2
            DERIV(2,IY,IZ) = - CONST*AZ*(EY1 - EY2 - WZ*E)
          ELSE
            DERIV(2,IY,IZ) = (0.D0,0.D0)
          END IF

78        CONTINUE
77      CONTINUE
C  !DEAL WITH THE TOP/BOTTOM OF THE GRID
C       !TOP
C       !INTEGRAL OPTION
      DO 790 IY=2,NY-1
        ZN=ZGRID(2)-ZGRID(1)
        ZN1=ZGRID(3)-ZGRID(2)
        Z2=ZN+ZN1
        E1=FIELD (IY,1)
```

```
            E2=FIELD (IY,2)
            EM1=FIELD (IY+1,1)
            EM2=FIELD (IY-1,1)
            YM=YGRID (IY+1)-YGRID(IY)
            YM1=YGRID(IY)-YGRID(IY-1)
            Y2=YM+YM1
            AZ = YM * YM1 / Y2
            YM$2=YM*YM
            YM1$2=YM1*YM1
                WY1 = (YM/RESGR(IY,1))
                WY2 = (YM1/RESGR(IY-1,1))
                WY3 = (1/RESGR(IY,1))
                WY4 = (1/RESGR(IY-1,1))
                WY=(WY1+WY2)/Y2
                EY12=(E2-E1)/ZN
                EY11=WY*CONST1*ZN*E1
                EY13=ZN*((EM1/(YM*Y2))+(EM2/(YM1*Y2))
     +              -(E1/(YM*YM1)))
                DERIV(1,IY,1)=CONST*(EY12-EY11+EY13)

                EZ11=(YM/(YM1*Y2))*EM2
                EZ12=(YM1/(YM*Y2))*EM1
                EZ13=((YM1-YM)/(YM1*YM))*E1
                EZ14=CONST1*(WY3-WY4)*
     +             ((YM*YM1)/Y2)*E1
                DERIV(2,IY,1)=CONST*(EZ11-EZ12+EZ13+EZ14)
790         CONTINUE
C            !BOTTOM
               ZN1=ZGRID(NZ)-ZGRID(NZ-1)
               ZN2=ZGRID(NZ-1)-ZGRID(NZ-2)
               Z2=ZN1+ZN2
           DO 791 I=2,NY-1
               EN=FIELD(I,NZ)
               EN1=FIELD(I,NZ-1)
               EN2=FIELD(I,NZ-2)
             IF (RESGR(1,NZ) .GE. PRCOND) THEN
               EM1=FIELD(I+1,NZ)
               EM2=FIELD(I-1,NZ)
               YM=YGRID (I+1)-YGRID(I)
               YM1=YGRID(I)-YGRID(I-1)
               Y2=YM+YM1
               YMD=YM*Y2
               YM1D=YM1*Y2
               SN1=(YM/RESGR(I,NZ-1) + YM1/RESGR(I-1,NZ-1))/Y2
               DERIV(1,I,NZ) = -CONST*(EN1/ZN1 - (1/ZN1 + ZN1/(YM*YM1)
     1         + CONST1*SN1*ZN1)*EN + ZN1*EM1/YMD + ZN1*EM2/YM1D)
               WY3 = (1/RESGR(I,NZ-1))
               WY4 = (1/RESGR(I-1,NZ-1))
               WY=(WY3-WY4)/Y2
               DERIV(2,I,NZ) = -CONST*(YM1*EM1/YMD - YM*EM2/YM1D
     1         - (YM1/YMD - YM/YM1D + CONST1*WY*YM*YM1)*EN)
             ELSE
               DERIV(1,I,NZ) = CONST*(ZN1*EN2/(ZN2*Z2) - Z2*EN1/(ZN1*ZN2))
     1         +EN*(Z2/(ZN1*ZN2)-ZN1/(ZN2*Z2))
               DERIV(2,I,NZ) = (0.D0 , 0.D0)
             END IF
791         CONTINUE
C   !AND WITH THE EDGES
          DO 80  I=2,NZ-1
               ZN=ZGRID(I+1)-ZGRID(I)
               ZN1=ZGRID(I)-ZGRID(I-1)
               Z2=ZN1+ZN
               EZ11=ZN1/(ZN*Z2)
               EZ12=ZN/(ZN1*Z2)
               Y1=YGRID(2)-YGRID(1)
               YM1=YGRID(NY)-YGRID(NY-1)
```

```
C  !LEFT
           SM=(ZN/RESGR(1,I) + ZN1/RESGR(1,I-1))/Z2
           DERIV(1,1,I) = CONST*(EZ11*FIELD(1,I+1)
     1     - EZ12*FIELD(1,I-1) - (EZ11 - EZ12 +(0.d0,1.d0)*omega*rmu
     2     zn*zn1*(1/resgr(1,i)-1/resgr(1,i-1))/2)*FIELD(1,I))
           DERIV(2,1,I) = -CONST*(FONE(1,I)-FIELD(1,I))/YGRID(1)
C  !RIGHT
           SM1=(ZN/RESGR(NY-1,I) + ZN1/RESGR(NY-1,I-1))/Z2
           DERIV(1,NY;I) = CONST*(EZ11*FIELD(NY,I+1)
     1     - EZ12*FIELD(NY,I-1) - (EZ11 - EZ12+(0.d0,1.d0)*omega*rmu
     2     zn*zn1*(1/resgr(ny,i)-1/resgr(ny,i-1))/2)*FIELD(NY,I))
           DERIV(2,NY,I) = -CONST*(FONE(2,I)-FIELD(NY,I))/YGRID(NY)
80       CONTINUE
C  !CORNERS
         Z1=ZGRID(2)-ZGRID(1)
         Z2=ZGRID(3)-ZGRID(2)
         Z12=Z1/((Z1+Z2)*Z2)
         Z21=(Z1+Z2)/(Z1*Z2)
         DERIV(1,1,1) = CONST*(Z21*FIELD(1,2) - Z12*FIELD(1,3)
     1   - (Z21 - Z12)*FIELD(1,1))
         DERIV(2,1,1) = -CONST*(FONE(1,1)-FIELD(1,1))/YGRID(1)
         DERIV(1,NY,1) = CONST*(Z21*FIELD(NY,2) - Z12*FIELD(NY,3)
     1   - (Z21 - Z12)*FIELD(NY,1))
         DERIV(2,NY,1) = -CONST*(FONE(2,1)-FIELD(NY,1))/YGRID(NY)
         ZN1=ZGRID(NZ)-ZGRID(NZ-1)
         ZN2=ZGRID(NZ-1)-ZGRID(NZ-2)
         Z12=ZN1/((ZN1+ZN2)*ZN2)
         Z21=(ZN1+ZN2)/(ZN1*ZN2)
         DERIV(1,1,NZ) = -CONST*(Z21*FIELD(1,NZ-1) - Z12*FIELD(1,NZ-2)
     1   - (Z21 - Z12)*FIELD(1,NZ))
         DERIV(2,1,NZ) = -CONST*(FONE(1,NZ)-FIELD(1,NZ))/YGRID(1)
         DERIV(1,NY,NZ) = -CONST*(Z21*FIELD(NY,NZ-1) - Z12*FIELD(NY,NZ-2)
     1   - (Z21 - Z12)*FIELD(NY,NZ))
         DERIV(2,NY,NZ) = -CONST*(FONE(2,NZ)-FIELD(NY,NZ))/YGRID(NY)
C*********************************
C      WRITE (6,*) '*** END DERIVE'
C*********************************
C***  writing out the derivative fields****
C
       HEAD='Y'
       LL=1
       CHARPOL='MAGNETIC'

    99 IF(ZMAX.NE.0) WRITE(14,400) HEAD,CHARPOL
   400 FORMAT(//35X,'REAL PART ',A1,'-COMPONENT ',A8,' FIELD'/)

       KK=YMIN
       KJ=YMIN+7
   100 IF(ZMAX.NE.0) WRITE(14,222) (YGRID(I)/1000,I=KK,KJ)
   222 FORMAT(/1X,'Z/Y',11X,8(G13.6,1X))
       do 230 J=1,ZMAX
         ZGR= ZGRID(J)/1000
         WRITE(14,220) ZGR,(DREAL(DERIV(LL,I,J)),I=KK,KJ)
   230 CONTINUE
       IF(KJ.EQ.YMAX) GOTO 150
       KK=KJ+1
       KJ=KK+7
       IF(KJ.GT.YMAx) KJ=YMAX
       GOTO 100

   150 IF(ZMAX.NE.0) WRITE(14,410) HEAD,CHARPOL
   410 FORMAT(//35X,'IMAG PART ',A1,'-COMPONENT ',A8,' FIELD'/)

       KK=YMIN
       KJ=YMIN+7
   200 IF(ZMAX.NE.0) WRITE(14,222) (YGRID(I)/1000,I=KK,KJ)
```

```
      do 240 J=1,ZMAX
        ZGR= ZGRID(J)/1000
        WRITE(14,220) ZGR,(DIMAG(DERIV(LL,I,J)),I=KK,KJ)
  240 CONTINUE
      IF(KJ.EQ.YMAX) GOTO 221
      KK=KJ+1
      KJ=KK+7
      IF(KJ.GT.YMAX) KJ=YMAX
      GOTO 200
  221 CONTINUE
  220 FORMAT(4X,F7.3,2X,8(G13.6,1X))
      IF(LL.NE.2) THEN
        LL=2
        HEAD='Z'
        GO TO 99
      END IF

      A1=RMU/OMEGA
      A2=180.D0/PI
      DO 300 IZ=1,ZMAX
        DO 310 IY=YMIN,YMAX
          CALL APRES2(ARES(IY,IZ),PANG(IY,IZ),DERIV(1,IY,IZ)
     +,               FIELD(IY,IZ),A1,A2)
  310   CONTINUE
  300 CONTINUE

  160 IF(ZMAX.NE.0) WRITE(14,420)
  420 FORMAT(//35X,'APPARENT RESISTIVITY (MAGNITUDE)'/)

      KK=YMIN
      KJ=YMIN+7
  170 IF(ZMAX.NE.0) WRITE(14,222) (YGRID(I)/1000,I=KK,KJ)
      do 250 J=1,ZMAX
        ZGR= ZGRID(J)/1000
        WRITE(14,223) ZGR,(ARES(I,J),I=KK,KJ)
  223 FORMAT(4X,F7.3,2X,8(G13.6,1X))
  250 CONTINUE
      IF(KJ.EQ.YMAX) GOTO 180
      KK=KJ+1
      KJ=KK+7
      IF(KJ.GT.YMAX) KJ=YMAX
      GOTO 170

  180 IF(ZMAX.NE.0) WRITE(14,430)
  430 FORMAT(//35X,'APPARENT RESISTIVITY - PHASE ANGLE (DEGREES)'/)

      KK=YMIN
      KJ=YMIN+7
  190 IF(ZMAX.NE.0) WRITE(14,222) (YGRID(I)/1000,I=KK,KJ)
      do 260 J=1,ZMAX
        ZGR= ZGRID(J)/1000
        WRITE(14,224) ZGR,(PANG(I,J),I=KK,KJ)
  224 FORMAT(4X,F7.3,2X,8(G13.6,1X))
  260 CONTINUE
      IF(KJ.EQ.YMAX) GOTO 999
      KK=KJ+1
      KJ=KK+7
      IF(KJ.GT.YMAX) KJ=YMAX
      GOTO 190

  999 CONTINUE
C*** WRITING OUT DATA FILES FOR GRAPHING PROGRAM ***
      IF(GRAP.LT.'NOGRAP') THEN
        WRITE(NUN,500) T
  500   FORMAT(' Resistivities and Phases for period = ',f10.3)
        WRITE(NUN,501)
```

```
  501   FORMAT('  No       Y          Res          Phase      EPOL')

        DO 503 I=1,NSTS
          JKL=STNUM(I)
          sts1=sts(i)*1000
          stsenter=0
          IF(STS1.LT.YGRID(1)) then
            stsenter=1
            JKL=1
            FHOLD=FIELD(1,1)
            DHOLD1=DERIV(1,1,1)
            DHOLD2=DERIV(2,1,1)
            FIELD(1,1)=FONE(1,1)+YGRID(1)*
     +       (FHOLD-FONE(1,1))/(STS1)
            E1=FIELD (1,1)
            E2=FONE(1,2)+YGRID(1)*
     +       (FIELD(1,2)-FONE(1,2))/(STS1)
            E3=FONE(1,3)+YGRID(1)*
     +       (FIELD(1,3)-FONE(1,3))/(STS1)
            EY12=(E2-E1)/ZN
            EY11=E2/ZN1
            EY13=ZN*( E1/(ZN*Z2) + E3/(ZN1*Z2) )
            DERIV(1,1,1)=CONST*(EY12-EY13+EY11)
C TO CALCULATE DERIV(2,JKL,1)
            DIFF=YGRID(1)-STS1
            DELTA=DMIN1(DIFF,10000.D0)
C            IF(DELTA.EQ.STS1) DELTA=8000.E0
            IF(DABS(DELTA).EQ.DABS(STS1)) DELTA=DELTA+1000.e0
            E1=FONE(1,1)+YGRID(1)*
     +       (FHOLD-FONE(1,1))/(STS1+DELTA)
            E2=FONE(1,1)+YGRID(1)*
     +       (FHOLD-FONE(1,1))/(STS1-DELTA)
            DERIV(2,1,1)=(E1-E2)/(DCMPLX(0.D0,1.D0)*OMEGA*2*DELTA)
          END IF
          IF(STS1.GT.YGRID(NY)) then
            stsenter=1
            JKL=NY
            FHOLD=FIELD(NY,1)
            DHOLD1=DERIV(1,NY,1)
            DHOLD2=DERIV(2,NY,1)
            FIELD(NY,1)=FONE(2,1)-YGRID(NY)*
     +       (FONE(2,1)-FHOLD)/(STS1)
            E1=FIELD (NY,1)
            E2=FONE(2,2)-YGRID(NY)*
     +       (FONE(2,2)-FIELD(NY,2))/STS1
            E3=FONE(2,3)-YGRID(NY)*
     +       (FONE(2,3)-FIELD(NY,3))/STS1
            EY12=(E2-E1)/ZN
            EY11=E2/ZN1
            EY13=ZN*( E1/(ZN*Z2) + E3/(ZN1*Z2) )
            DERIV(1,ny,1)=CONST*(EY12-EY13+EY11)
C TO CALCULATE DERIV(2,JKL,1)
            DIFF=STS1-YGRID(NY)
            DELTA=DMIN1(DIFF,10000.D0)
            IF(DABS(DELTA).EQ.DABS(STS1)) DELTA=DELTA+1000.e0
            E1=FONE(2,1)-YGRID(NY)*
     +       (FONE(2,1)-FHOLD)/(STS1+DELTA)
            E2=FONE(2,1)-YGRID(NY)*
     +       (FONE(2,1)-FHOLD)/(STS1-DELTA)
            DERIV(2,NY,1)=(E1-E2)/(DCMPLX(0.D0,1.D0)*OMEGA*2*DELTA)
          END IF

          CALL APRES2(ARES(JKL,1),PANG(JKL,1),DERIV(1,JKL,1)
     +,               FIELD(JKL,1),A1,A2)
          WRITE(NUN,505) I,STS(I),ARES(JKL,1),PANG(JKL,1)
c          WRITE(NUN,505) I,STS(I),t,dreal(deriv(2,jkl,1)
```

```
c     +,   dimag(deriv(2,jkl,1)),dreal(deriv(1,jkl,1))
c     +,   dimag(deriv(1,jkl,1)),dreal(field(jkl,1))
c     +,   dimag(field(jkl,1))
          if(stsenter.eq.1) then
           FIELD(JKL,1)=FHOLD
           DERIV(1,JKL,1)=DHOLD1
           DERIV(2,JKL,1)=DHOLD2
          end if
  505     FORMAT(I4,FI2.4,2(1X,G13.6))
c  505     FORMAT(I4,F12.4,7(1X,G13.6))
c  505     FORMAT(I4,F7.2,F7.2,F7.2)
  503   CONTINUE
      END IF
      RETURN
      END
```

```
SUBROUTINE      APRES2 (RESM1,PHANG,B,E,A1,A2)
IMPLICIT        REAL*8  (A-Z)
COMPLEX*16      B,E,R

IF (E .EQ. (0.D0,0.D0)) THEN
   RESM1 = 0.D0
   PHANG = 0.D0
ELSE
   IF (CDABS(B).GE.1.D-20) THEN
      R = E/B
      RESM1 = A1 * ABS(R)*ABS(R)
      R1 = DIMAG(R)
      R2 = DREAL(R)
      R3 = R1 / R2
      IF (ABS(R3).LT.1.D30) THEN
         PHANG = A2 * ATAN( R3 )
      ELSE   !AVOID ZERO DIVIDE
         PHANG = 90.D0
      END IF
   ELSE   !AVOID ZERO DIVIDE
      RESM1 = 1.D20
      PHANG = 0.D0
   END IF
END IF
RETURN
END
```